LBL-5634

MOLECULAR SIEVING ACTION OF THE CELL MEMBRANE DURING GRADUAL OSMOTIC HEMOLYSIS

Roderick Dhu MacGregor, II

Ph. D. thesis

May 1977

Prepared for the U. S. Energy Research and Development Administration under Contract W-7405-ENG-48

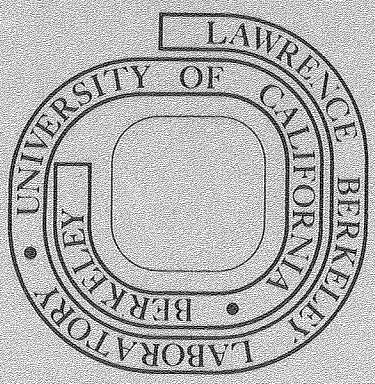

LBL-5634
c.1

LBL-5634

MOLECULAR SIEVING ACTION OF THE CELL MEMBRANE DURING GRADUAL OSMOTIC HEMOLYSIS

Roderick Dhu MacGregor, II

Group in Biophysics and
Radiation Biophysics Group
Division of Biology and Medicine
Lawrence Berkeley Laboratory
University of California
Berkeley, California 94720

May 1977

ABSTRACT

Rat erythrocytes restrained in either glass filters or a specially designed continuous-flow centrifuge were hemolyzed by exposing the cells to a flowing medium in which the concentration of NaCl, LiCl or dextrose was gradually decreased. This process was termed "controlled gradual osmotic hemolysis." The medium was collected in serial fractions after passing the erythrocytes, and the fractions were analyzed for ions (K^+) and proteins (adenylate kinase, hemoglobin (Hb), fumarase and catalase) of intracellular origin. Micrographs were taken of the cells in order to study cell morphology and hemoglobin loss from individual cells.

Intracellular solutes moved from the cells into the flowing medium for approximately one hour, and significant fine structure was observed

in the loss curves of centrifuge experiments. Centrifuge experiments gave better resolution than filter experiments. Individual cells lost their Hb over a period of at least six minutes, and concentration equilibrium was not obtained between intracellular and extracellular Hb.

The initial major loss of K^+ occurred at about the time that the cells became spherical, membrane flicker ceased, and the external solute concentration in all experiments was ~173 mOsm. The major loss of Hb started at ~167 mOsm in salt solutions but at ~151 mOsm in dextrose experiments. The loss curves of deoxy-, oxy- and met-Hb differed significantly. Incubation of red cells in saline prior to an experiment altered the loss curves. LiCl, in comparison to NaCl, appeared to increase the dissociation of catalase and to inhibit membrane resealing to small molecules at the conclusion of hemolysis.

The results suggest that each increase in the rate of loss of a protein from the cells during the initial phases of controlled gradual osmotic hemolysis is caused by the passage of a previously impermeable species across the stressed membrane. Similarly, during the final stages of controlled gradual osmotic hemolysis, each sharp decrease in the rate of loss of a protein corresponds to the termination of a molecular flow. If it is hypothesized that the first major loss of each protein is the loss of the monomer, the second is the loss of the dimer, and so forth for the other stable size units of each protein, the fine structure of all of the protein loss curves is explained by the passage of molecules of increasing size across the stressed membrane during the initial stages of controlled gradual osmotic hemolysis. Similarly, the maximum size of molecules that can cross the membrane decreases during the final phases

of the hemolytic process. Therefore, stressed rat red cell membranes appear to exhibit molecular sieving properties.

The stress-induced loss of K^+ is apparently caused by the insertion of foreign molecules into the membrane. The differences observed between salt and dextrose experiments are consistent with unspecific cation transport across the stressed membrane and negligible entrance of dextrose into the cells prior to Hb loss.

A theoretical model is described that predicts the molecular sieving of soluble globular proteins across the stressed red cell membrane. In the model, hydrophobic interactions occur between the soluble proteins and the lipid bilayer portion of the cell membrane. A spectrin network subdivides the bilayer into domains that restrict the insertion of large molecules into the membrane. Other membrane proteins affect soluble protein access to the membrane. Changes in the loss curves caused by incubation of red cells are discussed in terms of the model.

TABLE OF CONTENTS

ACKNOWLEDGMENTS

I wish to express my appreciation to my major professor, Dr. Cornelius A. Tobias, Department of Medical Physics, for giving me the freedom, trust, and support to pursue this study; I also wish to thank Dr. Robert I. Macey, Department of Physiology and Anatomy, who introduced me to red cell physiology, and Dr. Alexander V. Nichols, Department of Medical Physics, for their encouragement in this work. My sincere thanks also to Dr. Howard C. Mel for helpful discussion.

I am grateful to my parents, Mr. and Mrs. R. D. MacGregor, B. A. Barr, D. J. Mundy, J. R. Luce, Q. E. Gipson, and to F. E. Baca for their support, encouragement and assistance with various aspects of this work; to E. F. Dowling and H. L. Minasian for their able advice and assistance in constructing the continuous flow centrifuge and other apparatus; to D. E. Denney, M. H. Simpson, R. E. Kingsbury, and M. M. Drabkin for their help in obtaining references; and to K. S. Elam for editorial assistance and D. J. Olson for preparation of the manuscript.

I was a Teaching Assistant in the Department of Medical Physics, University of California, Berkeley. The experimental portion of this work was supported by Contract W-7405-eng-48 of the United States Energy and Research and Development Administration and by Ruth C. Hardison Memorial Scholarship Fund, Donner Laboratory, University of California, Berkeley.

To all, I wish to express my sincere thanks.

This work was done with support from the U.S.
Energy Research and Development Administration

INTRODUCTION

The osmotic hemolysis of red blood cells by hypotonic salt solutions was reported as early as 1873 (Malassez, 1873) and is employed today in the clinical osmotic fragility test (Wintrobe, 1967). Cells lysed under these drastic conditions have slits or tears with dimensions of 100 to 1000 Å localized in a 1μ-diameter region of their stressed membranes at the time of hemolysis (Huhn, Pauli and Grassmann, 1970; Seeman, Cheng and Iles, 1973) through which bulk flow of hemoglobin and other intracellular molecules occurs (Heedman, 1958; Davies, Marsden Östling and Zade-Oppen, 1968).

This work, a portion of which has been previously published (MacGregor and Tobias, 1972), presents a study of the process of gradual osmotic hemolysis (Danon, Nevo and Marikovsky, 1956) conducted within apparatus specially designed to minimize concentration inhomogeneities and variations in mechanical stress. The losses of intracellular molcules to the extracellular media were observed as a function of time from rat red cells restrained in the apparatus. The data suggest that, in contrast to drastic osmotic hemolysis, bulk flow does not occur during the initial or final stages of controlled gradual osmotic hemolysis. Rather, the stressed cell membranes appear to exhibit molecular sieving properties for molecules ranging in size from monovalent cations to at least fumarase (MW = 194,000) and catalase (MW = 232,400). Previous observations of red cell molecular losses (Hjelm, Östling and Persson, 1966) and gains (Marsden and Östling, 1959; Ihler, Glew and Schnure, 1973) following osmotic hemolysis and recovery of impermeability following

osmotic hemolysis (Colombe and Macey, 1974) have suggested molecular sieving during the hemolytic process, but, as noted particularly by Hjelm et al. (1966), the interpretation of results obtained only after the completion of hemolysis is fraught with difficulty.

The data are presented with few comments in the Results section and are subsequently interpreted in terms of the hypothesized molecular sieving by stressed rat red cell membranes. The process of controlled gradual osmotic hemolysis is considered in some detail from a biological viewpoint in the Discussion section. Consideration of the physical properties of red cell membranes and of lipid and protein systems then leads to a domain model of osmotic hemolysis. In this model, most of the membrane lipid is structured as a lipid bilayer, which is subdivided into domains on the inner membrane surface by the protein spectrin. Other membrane proteins are partially embedded in the lipid. It is shown that this model predicts the molecular sieving of soluble globular proteins across the stressed cell membrane and accounts for the observed stress-induced increase in cation permeability. Changes in the pattern of controlled gradual osmotic hemolysis and changes in membrane deformability, such as occur during incubation of red cells, are interpreted by the model in terms of changes in soluble protein access to the bilayer portion of the membrane, which can be influenced by aggregation of membrane proteins, and changes in soluble protein (primarily hemoglobin) distribution between subunits, intact protein, and aggregates. Finally, the model is extended to include bulk flow during the hemolytic process. Under suitable conditions, the domains apparently limit the size of isolated holes that develop statistically in the stressed membrane

and also limit the width of slits formed by coalescence of adjacent holes without disruption of the spectrin network. Under other conditions, especially in the absence of extracellular macromolecular solutes, which apparently increase the rate of pore nucleation in the outer membrane leaflet, and at moderate and rapid rates of decrease of the extracellular osmotic concentration, the spectrin network fails, and a single large hole (~1μ) develops in the stressed membrane.

MATERIALS AND METHODS

GENERAL EXPERIMENTAL PROCEDURE

Washed rat red blood cells were placed in either a filter device or a specially constructed centrifuge that served to restrain the cells with respect to a continual flowing solution. The composition of the solution was controlled before contact with the cells so as to wash the cells with isotonic solution first and then to decrease the concentration gradually and continually in order to slowly swell and then osmotically stress the cell membranes. The loss of intracellular molecules to the flowing extracellular solution as a function of time was determined by collecting the solution in serial fractions after it had passed the cells and assaying the fractions for the intracellular molecules. The molecules chosen for analysis ranged in size from K^+ to catalase. It was anticipated that, if the osmotically stressed red cell membrane suddenly failed through the production of a hole, all sizes of intracellular molecules would be lost simultaneously by the cell. If, instead, the failure involved a molecular sieving mechanism, the molecules would be lost in the order of increasing molecular weight.

Because this method allows for the experimental control of the time dependence of the external solute concentration and because concentration inhomogeneities in the vicinity of the cells are reduced to a minimum by adjustment of the solution concentration prior to contact with the cells, this method is termed "controlled gradual osmotic hemolysis" (see Discussion section).

CELL PREPARATION

Blood was obtained from the posterior *vena cava* of ether-anesthetized female Sprague-Dawley rats weighing in excess of 250g. The blood was withdrawn without the use of an anticoagulant through a No. 19 needle into a glass syringe that had been previously wetted with isotonic solution. The needle was removed and the blood was immediately added to at least five volumes of isotonic solution and centrifuged at 1,000 × g for 3 min in a fixed angle rotor (Sorvall SS-1). The supernatant and buffy coat were removed by aspiration, and the cells were washed an additional four times with 30- to 40-ml portions of isotonic solution. The cells were resuspended in isotonic solution at approximately a 30% hematocrit and were maintained at room temperature prior to being placed in the cell-holding device with the exception of one experiment in which the cells were maintained at 4°C for approximately one day (Table I).

$^{42}K^+$-LABELED RED CELLS

Approximately 1 mC $^{42}K^+$ (specific activity 170 mC/g K^+, ISO/SERVE) was administered to a rat by stomach tube. Ten hours later the blood was withdrawn from the posterior *vena cava* and washed as described above.

FLOW SOLUTIONS

Two solutions, which differed in the concentration of the major solute, were prepared for each experiment and were termed "isotonic" and "dilate." The major solutes employed in different experiments were NaCl, LiCl and dextrose. The composition of the solutions and other experimental parameters are listed in Table I. Prior to the start of an experiment,

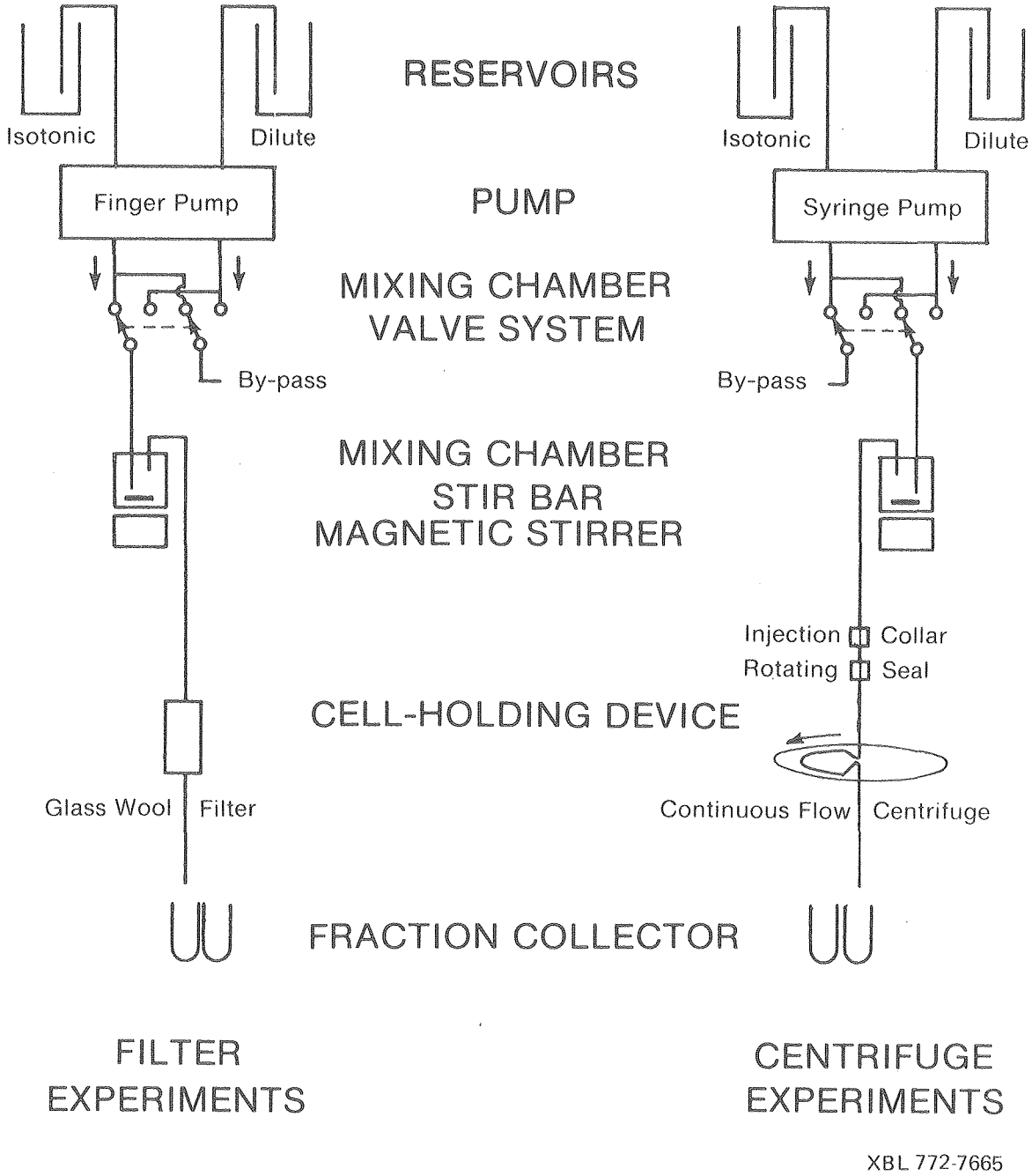

Figure 1. Sketch of the two experimental arrangements used to produce the controlled gradual osmotic hemolysis of rat red cells and to collect the flow solution in serial fractions.

TABLE I. Parameters and assays for controlled gradual osmotic hemolysis experiments.

Figure	Solution Composition: Isotonic	Solution Composition: Dilute	Cell-holding device	Incubation[a] (hr)	Expt. temp. (°C)	Fraction Collection: Interval (min)	Fraction Collection: Volume (ml)	Mixing chamber volume (ml)	Fluid delay[b] (ml)	Assay	Method[c]	Estimated maximum analytical error (%)[d]
5	150mM NaCl 1mM Tris[e] pH 7.4	30mM NaCl 1mM Tris pH 7.4	centrifuge	0	29	1.0	8.5	129.6	6.8	K Hb Cat	atomic absorp. OD-414	4. 2. 3.
6	150mM LiCl 1mM Tris pH 7.4	30mM LiCl 1mM Tris pH 7.4	centrifuge	3	29	1.0	8.5	129.6	6.8	K AK Hb Fum Cat	atomic absorp. OD-414	3. 13.[f] 1. 3.[g] 3.
7	150mM NaCl 1mM Tris pH 7.4	30mM NaCl 1mM Tris pH 7.4	centrifuge	5	29	1.0	8.5	129.6	6.8	K Hb Cat	atomic absorp. OD-414	6. 2. 3.
10	150mM NaCl 1mM Tris pH 7.4	30mM NaCl 1mM Tris pH 7.4	centrifuge	29	29	1.0	8.5	129.6	6.8	Hb	OD-401,417 and 433 (Deoxy-, Oxy-, and Met-)	--
11	150mM NaCl 5mM dextrose 1mM Tris pH 7.4	30mM NaCl 5mM dextrose 1mM Tris pH 7.4	filter	7	22	5.0	7.5	108.0	8.8	K Hb	^{42}K Cyanomet-Hb at OD-540	2. 1.
12	240mM dextrose 38mM NaCl 1mM Tris pH 7.2	-- 35mM NaCl 1mM Tris pH 7.2	filter	--	22	6.0	9.0	108.0	35.3	K Hb	flame emission OD-540	5. 3.
13	240mM dextrose 38mM NaCl 1mM Tris pH 7.2	-- 35mM NaCl 1mM Tris pH 7.2	filter	--	22	6.0	10.0	108.0	30.0	K Hb	flame emission OD-540	3. 1.

References:

[a] Time between preparation of cells and their injection into the cell-holding device.

[b] Volume of experimental apparatus between inlet valve of mixing chamber and outlet of fraction collector, less volume of mixing chamber.

[c] Specific assay employed when two or more methods were used during the course of this study.

[d] Based on the maximum difference observed between duplicate samples and referred to as the maximum sample value, which is plotted as full scale in the Results section.

[e] Tris = Tris(hydroxymethyl)aminomethane.

[f] There is a high probability that one AK sample became contaminated. If this is true, a more representative maximum error would be 5%.

[g] See text for discussion of the probable contamination of one Fum sample.

a fixed-volume mixing chamber containing a magnetic stir bar was completely filled with the isotonic solution. The mixing chamber was connected to a cell-holding device (see below), and isotonic solution was pumped into and through the mixing chamber and then into the cell-holding device to further wash the cells. After the cells had been washed for approximately 20 min for centrifuge experiments, or 1 hr for filter experiments, the experiment was initiated by switching the solution pumped into the mixing chamber from isotonic to dilute (Fig. 1). This resulted in an exponential decrease in solution concentration so that the concentration of the solution that flowed from the mixing chamber to the cells, C, was found experimentally to follow the theoretical equation:

$$C = C_d + (C_i - C_d)e^{-v/V}$$

where C_d = concentration of dilute solution, C_i = concentration of isotonic solution, v = total volume flow since start of dilute flow, and V = volume of mixing chamber.

After passing the cells, the solution was collected in serial fractions. The volume and collection times were constant within each experiment but varied between experiments (Table I). The approximate milliosmolar concentration was calculated at the midpoint of the collected fractions by assuming plug flow through the experimental apparatus and osmotic coefficients of 1.00 for dextrose and 0.94 for NaCl and LiCl. Thus, a 300 mM dextrose solution would be 300 mOsm, but, because NaCl and LiCl do not completely dissociate into osmotically active anions plus cations, a 150-mM NaCl or LiCl solution would be 282 mOsm, not 300 mOsm. The concentration profile used in centrifuge experiments is shown in Fig. 2. Typical concentration profiles used in filter experiments are

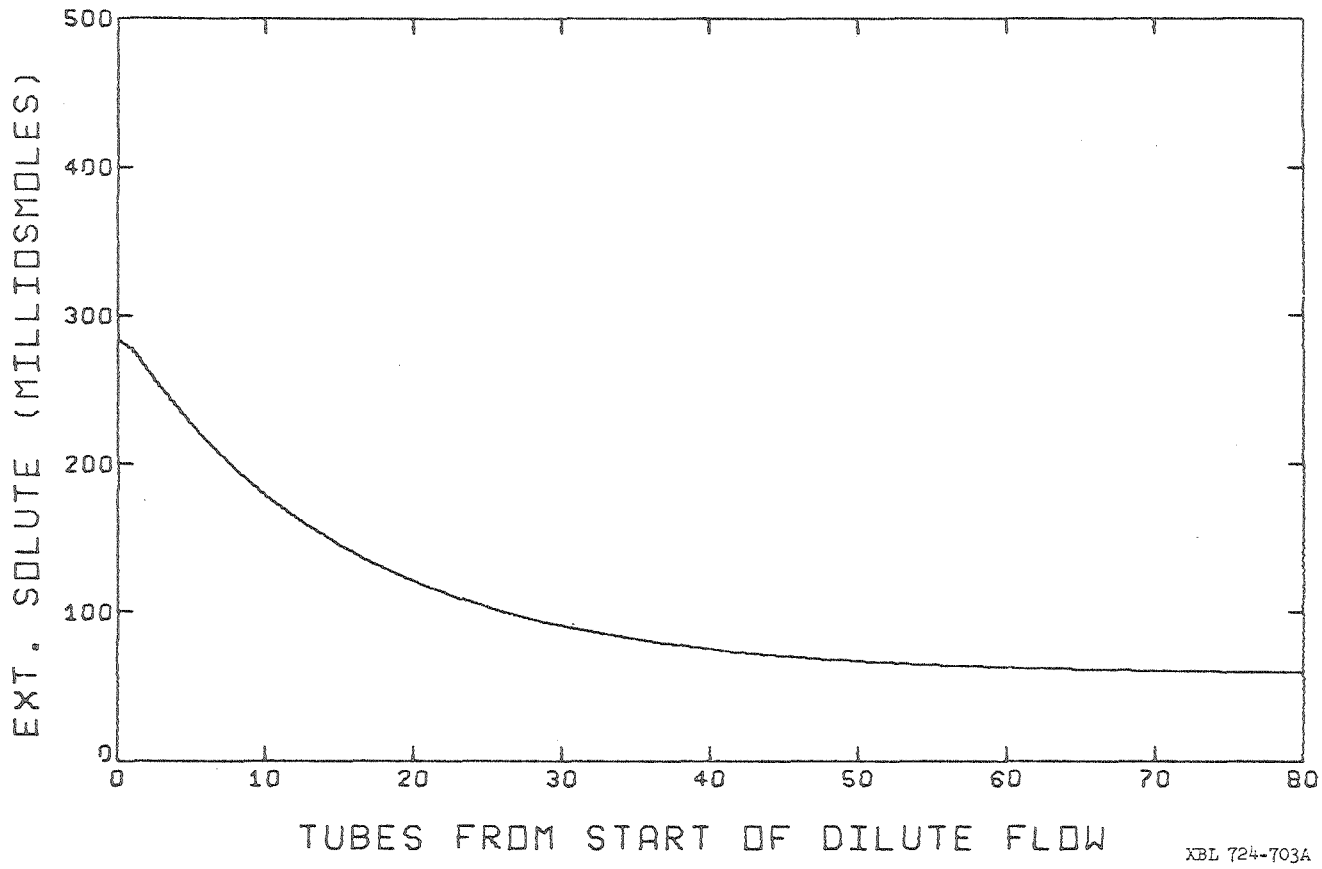

Figure 2. Concentration of flow solution in collected fractions after a centrifuge experiment was initiated by switching the solution pumped into the mixing chamber from saline to dilute.

shown on appropriate figures in the Results section.

CELL-HOLDING DEVICES

The red cells were restrained against the flowing solution by the use of either a continuous-flow centrifuge or a glass-wool filter (Fig. 1).

Centrifuge

A continuous-flow centrifuge was constructed to restrain cells against a flowing solution with a minimal and as uniform as possible restraining force (Fig. 3). It utilized a Bridgeport milling machine head as the drive for a rotor machined from lucite (Fig. 4). The rotor contained milled grooves through which Intramedic PE-260 polyethylene tubing ran from the center of the rotor to a radius of 5.250 inches around a circumferential groove for an adjustable distance and back to the center of the rotor. A valve system (which controlled the solution flow into the mixing chamber) and the mixing chamber were mounted above the centrifuge and were connected by PE-260 tubing to a rotating seal. This piece of tubing was covered by a tightly fitting, rubber injection collar 1¼ inches long through which the red cells were injected into the centrifuge. The rotating seal forced teflon disks against a length of #15 stainless steel needle tubing, which spun with the rotor. The polyethylene tubing that ran through the rotor was connected to this stainless steel tube just above the rotor. The other end of the polyethylene tube was connected to a short length of stainless steel tubing that protruded from the bottom of the rotor assembly and spun inside a ¼-inch diameter hole in a lucite block. This hole led directly to the fraction collector. The entire apparatus was located in a temperature-controlled room.

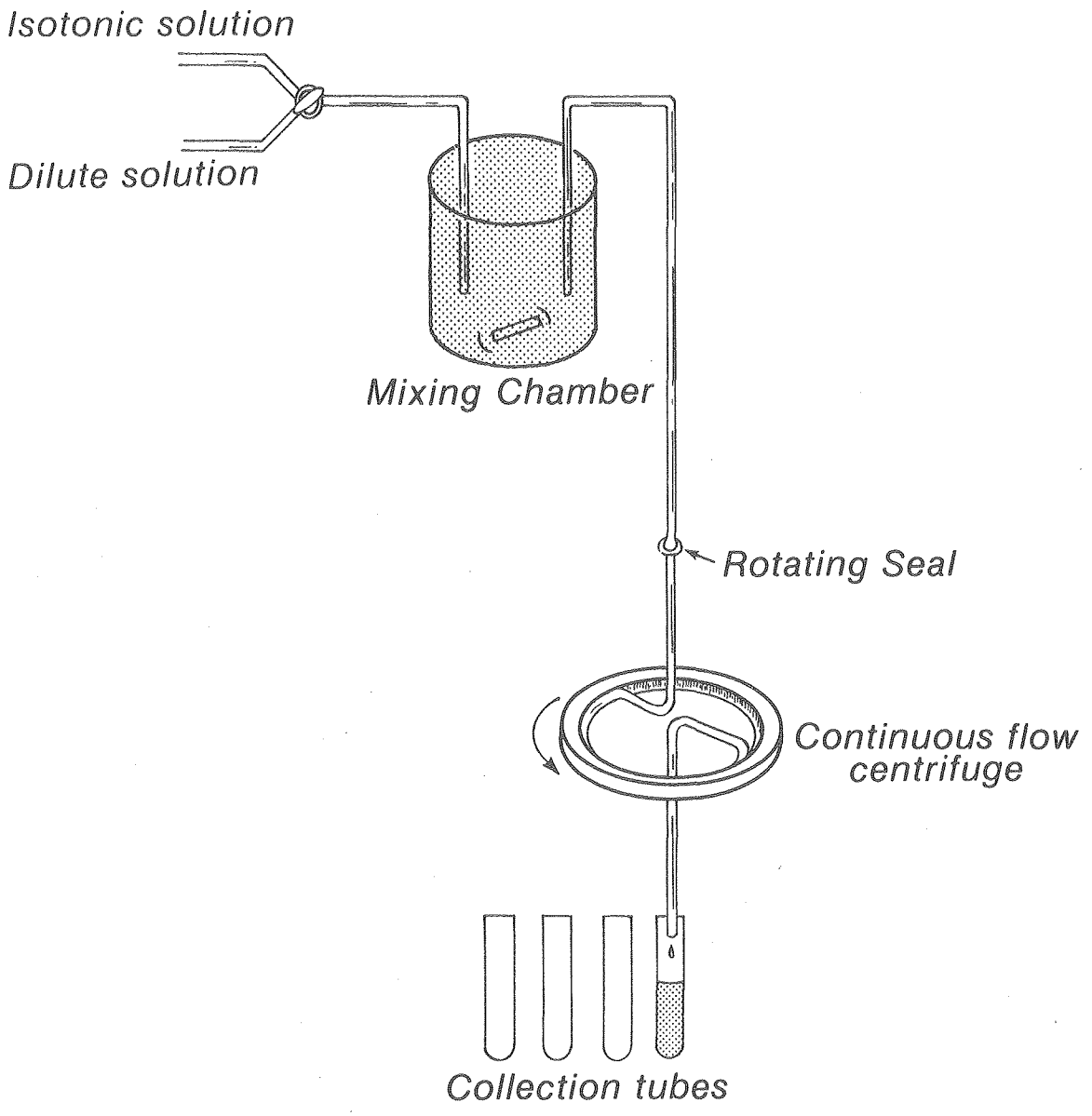

Figure 3. Schematic diagram of apparatus employed in centrifuge experiments.

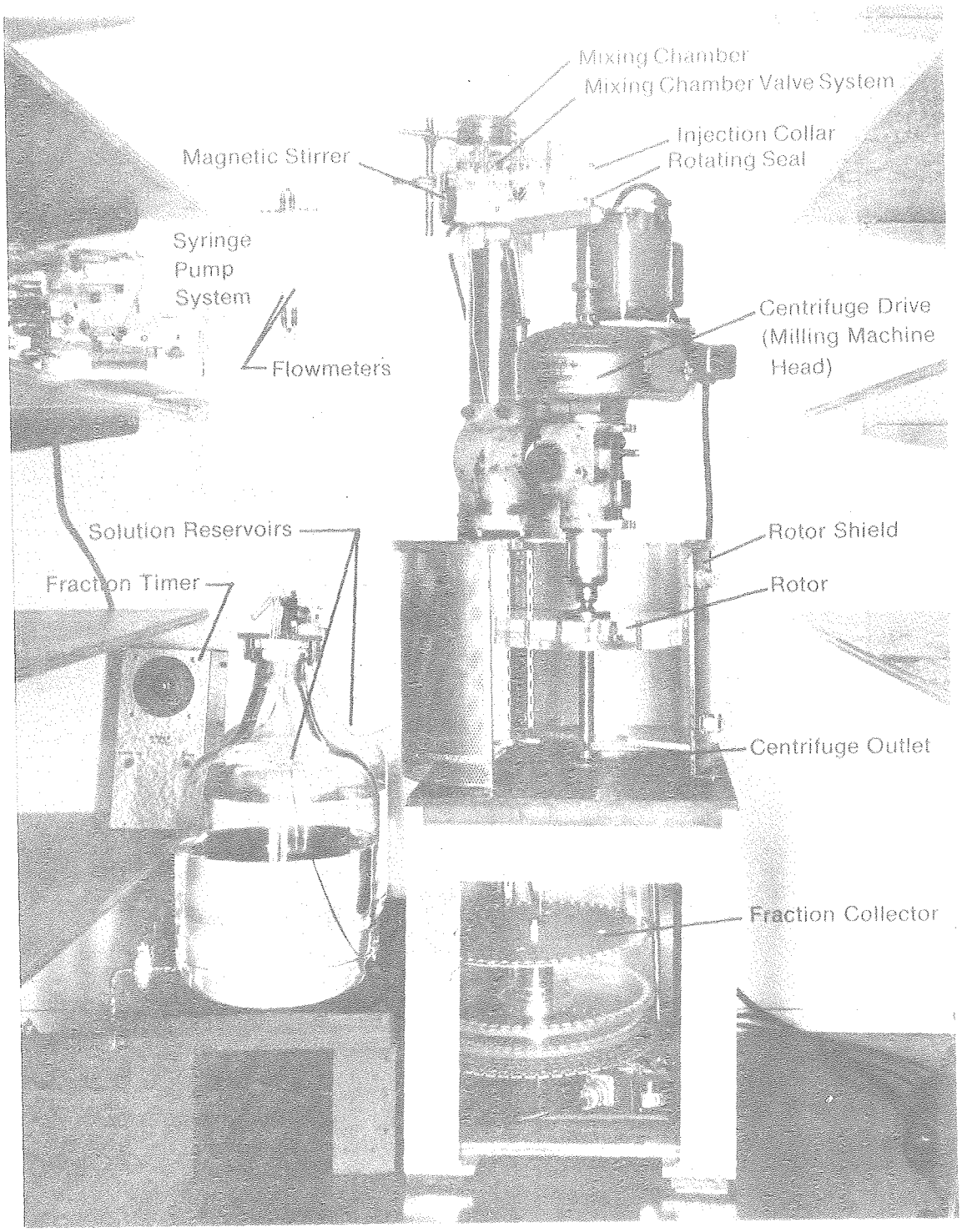

Figure 4. Continuous flow centrifuge. The flow solution concentration was adjusted, with the mixing chamber, prior to contact with the cells which were restrained against the flowing solution in the rotor. The flowing solution was collected as a function of time after it passed the cells and was subsequently analyzed for intracellular molecules lost to the flowing solution.

Figure 4a. Overall view of experimental apparatus.

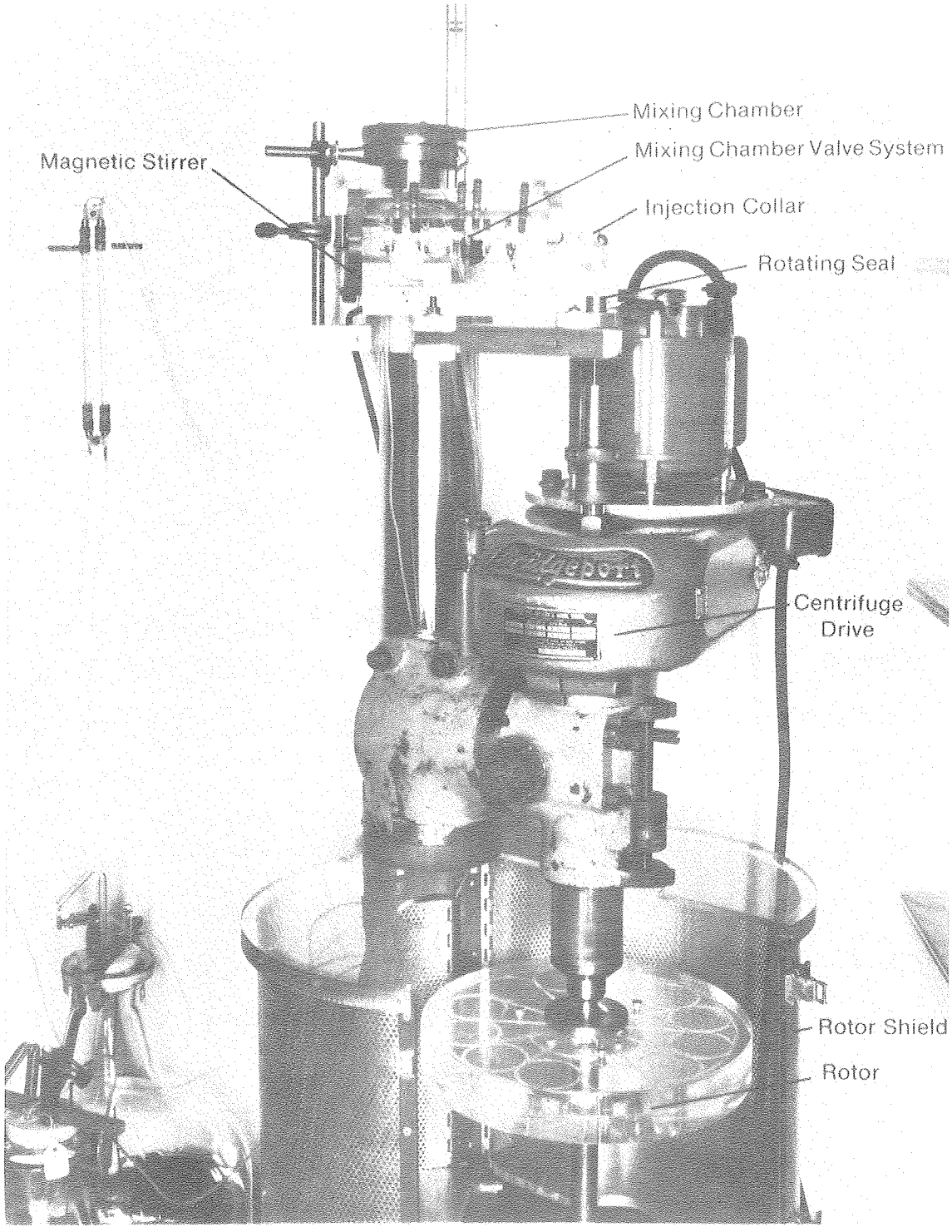

Figure 4b. Detailed view of the centrifuge.

Before use, the mixing chamber and centrifuge tubing were completely filled with isotonic solution. With a flow of about 3 ml/min of isotonic solution through the mixing chamber and centrifuge, approximately 0.2 ml of 30% hematocrit red cells were slowly injected through the injection collar with a No. 27 needle and 1-cc syringe. After the cells had been carried to the circumferential section of the rotor tube, the centrifuge was started, and the flow rate was increased. It was found that a force of about 1,500 G was required to restrain the ghosts in the centrifuge at the conclusion of the hemolytic experiment, and this force was used throughout the centrifuge experiments. A strobe light was used to determine whether the cells were evenly distributed in the tube. If they were bunched together, the centrifuge was stopped, the cells were discarded, and new cells were injected into the apparatus. An experiment was initiated by switching the solution pumped into the mixing chamber from isotonic to dilute.

Filters

Glass-wool filters were constructed by packing approximately 3-cm^3 chambers with glass wool. When the red cells were allowed to sediment into intimate contact with the glass fibers, they became attached to the glass and were restrained against the fluid flow.

CHEMICAL ASSAYS

The intracellular ion and molecules chosen for analysis were potassium (MW = 39), adenylate kinase (MW = 22,028), hemoglobin (MW = 64,459), fumarase (MW = 194,000), and catalase (MW = 232,400). These substances will be abbreviated K^+, AK, Hb, Fum, and Cat, respectively. The collected

fractions were stored at 4°C until the analyses could be completed.

Potassium

Total K^+ was determined by flame emission with a Beckman DU spectrophotometer with flame attachment and oxy-acetylene flame at 766 nm or by atomic absorption with a modified Jarrell-Ash 82-360 spectrophotometer with hydrogen-air flame at 7,655 Å. The atomic absorption data were corrected for drift by a computerized comparison to a reference solution.

$^{42}K^+$ was counted in a Nuclear Chicago C 120-1 well counter and the counts obtained corrected for background and decay.

Hemoglobin

Total Hb was estimated as oxy-Hb at 540 or 414 nm (MacFate, 1964; Martinek, 1966) or as cyano-met-Hb at 540 nm (Austin and Drabkin, 1935). The concentrations of deoxy-, oxy- and met-Hb were determined simultaneously by measuring the optical density at 401, 417 and 433 nm with a Cary 14 spectrophotometer and flow cuvette and then solving a set of three simultaneous equations, one for each wavelength, using the micromolar extinction coefficients listed in Table II. The approximate optical density at 414 nm was then calculated from the data in Table II.

Adenylate Kinase

Adenylate kinase was determined by the method of Kuby and Noda (Kuby, Noda and Lardy, 1954; Noda and Kuby, 1957) in which the formation of ATP from ADP by adenylate kinase is coupled to the formation of creatine phosphate with creatine phosphokinase. The creatine ~P was determined as inorganic phosphate following mild acid hydrolysis (King, 1932).

TABLE II. Approximate micromolar extinction coefficients for hemoglobin derivatives[a] at pH 7.2.[b]

Hemoglobin derivative[c]	Wavelength in nm			
	401	417	433	414
deoxy	0.4014	0.3560	0.5247	0.3173
oxy	0.2986	0.4927	0.1691	0.5081
met	0.5151	0.3300	0.0825	0.4253

References:

[a] Based upon Fe determination and assuming 4 Fe/Hb (Williams and Zak, 1957; Connerty and Briggs, 1962).

[b] The met-Hb spectrum is a strong function of pH at pH 7.2. Micromolar extinction coefficients at 414 nm are significant to 2 to 3 figures.

[c] Derivatives of unpurified rat hemoglobin were prepared from stroma-free red cell lysate as follows:

deoxy-Hb: 25-ml 50-mM phosphate buffer was added to a tube containing 0.125g dry sodium dithionite. The dithionite was dissolved and this solution was immediately used to dilute 1 ml of hemoglobin stock solution to 10 ml.

oxy-Hb: 1 ml hemoglobin stock solution was diluted with air or O_2-saturated buffer to 10 ml. Some samples were additionally shaken under an O_2 atmosphere.

met-Hb: 1 ml hemoglobin stock solution was diluted to 10 ml with 50 mM phosphate buffer containing $K_3Fe(CN)_6$ such that a 10-fold excess of $K_3Fe(CN)_6$ was present.

Fumarase

Fumarase was assayed after the fractions had been maintained at 4°C for at least one day by the method of Hill and Bradshaw (1969) in which the conversion of L-malate to fumarate is monitored by the optical density change at 250 nm.

Catalase

Catalase was assayed after the fractions had been maintained at 4°C for at least one day by the method of Werner and Heider (1963) in which the initial rate of disappearance of H_2O_2 is monitored at 240 nm. The rate of the catalase reaction was approximated by using the first term of an expansion of a log term as follows:

$$K = \frac{0.43429}{\Delta t} \ln_e \left(1 - \frac{\Delta OD}{OD_c}\right)$$

$$K \simeq \frac{0.43429}{\Delta t} \frac{\Delta OD}{OD_c}$$

where Δt = time for OD change, ΔOD, in min; ΔOD = optical density change in time Δt; and OD_c = initial optical density due to absorption of H_2O_2 (from control).

Analytical Errors

The analytical errors estimated for the assays are based on the maximum difference between duplicate samples and are referred to as the percentage of the maximum sample value (which is plotted full scale in the Results section). These values are listed in Table I.

PHOTOMICROGRAPHY

Photomicrography was used to study the morphology and Hb loss of individual cells during the hemolytic process. Red cells were allowed to sediment onto the inside surface of a glass microelectrophoresis cell. The cell was inverted and placed in series with a glass-filter, cell-holding device so that the solution first flowed past the cells in the electrophoresis cell and then past additional cells in the filter. The cells attached to the upper glass wall of the electrophoresis cell were observed through a microscope at 400×, and photographs were taken with 2-sec exposures on Eastman Kodak Tri-X film at intervals during the hemolytic process. The 790 cells in each photographs were categorized as unsphered, sphered except for contacts with other cells, sphered completely, or ghosts. The approximate time period over which Hg was lost from individual cells was estimated by eye from photographs taken at 2-min intervals. These observations of individual cell morphology and Hb loss were then compared with the population K^+ and Hb losses from the more numerous cells in the glass filter.

RESULTS

LOSSES OF K^+, Hb, Cat, AK, AND Fum IN NaCl AND LiCl CENTRIFUGE EXPERIMENTS

The concentrations of intracellular molecules in the collected fractions when a salt solution of continually decreasing concentration was flowed past rat red cells restrained in the centrifuge are shown in Figs. 5, 6 and 7. In overall appearance, the concentration of an originally intracellular molecule rises during the initial stages of the hemolytic process and falls again during the later stages of the process. Superimposed on this general pattern however, is a complex fine structure that differs for the different solutes assayed in a given experiment and to some extent for the same solute in different experiments. Because the flow rate of the external solution was constant during each experiment, the concentration of an originally intracellular molecule in each of the collected fractions is a measure of the transmembrane flow of that solute during the fraction collection period. Thus, when averaged over all the cells present and over the fraction collection period, the transmembrane flow of each solute is a complex function of time during controlled gradual osmotic hemolysis.

The presentation of data that follows notes various features of the molecular loss curves and of additional data; however, comments concerning the significance of these features and their implications are largely withheld until the Interpretation and Discussion sections.

The initial major K^+ loss began in tubes 11 and 12 (arrows, Figs. 5a, 6a, and 7a) when the external solute concentrations at the midpoint of the fractions were approximately 177 and 169 mOsm respectively.

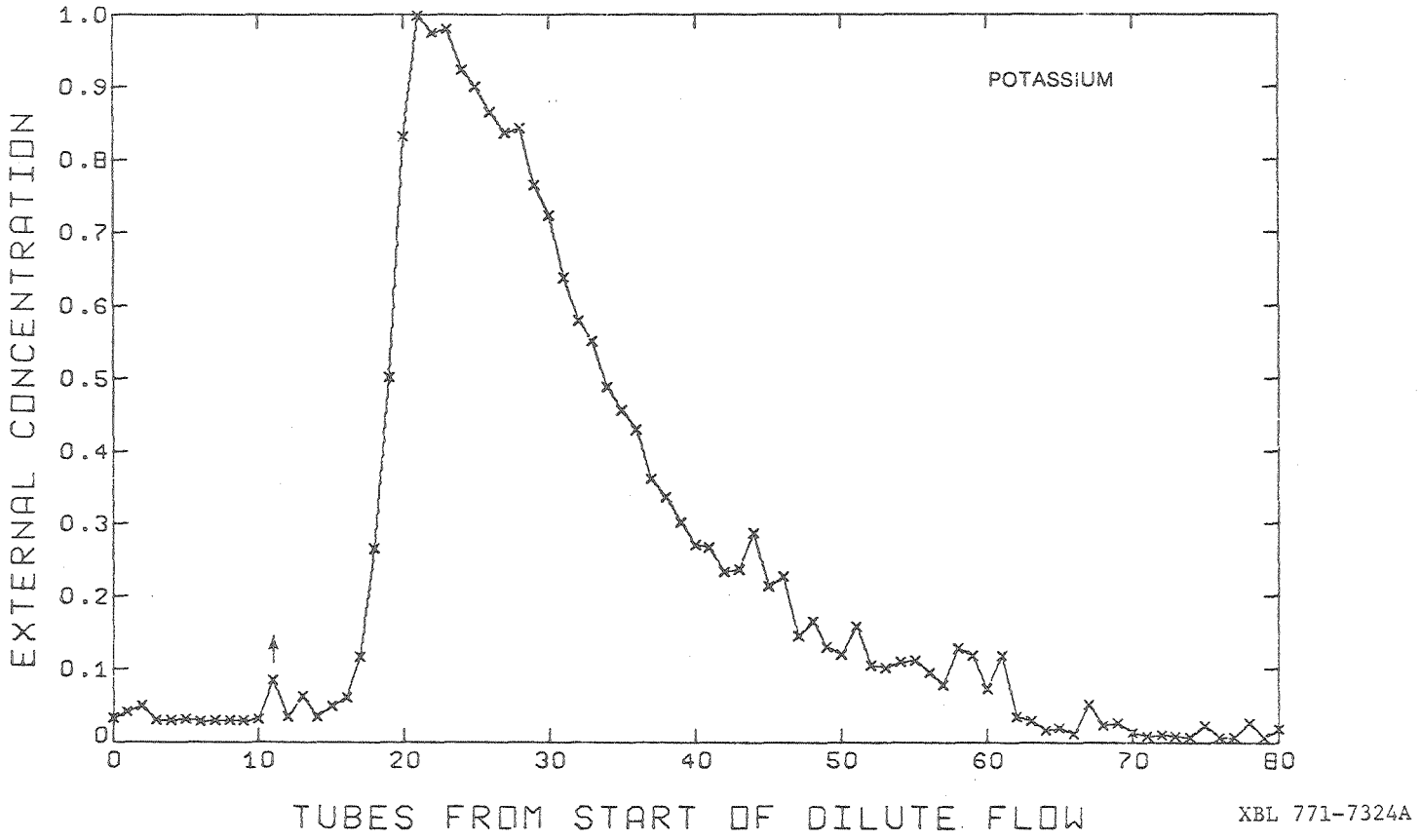

Figure 5. Concentrations of K^+, Hb, and Cat in a NaCl solution of gradually decreasing concentration that was flowed past rat red cells restrained in a centrifuge. The concentrations of the intracellular molecules in this and the following figures have been normalized to facilitate comparisons.

Figure 5a. Potassium (full scale = 63.9 μM).

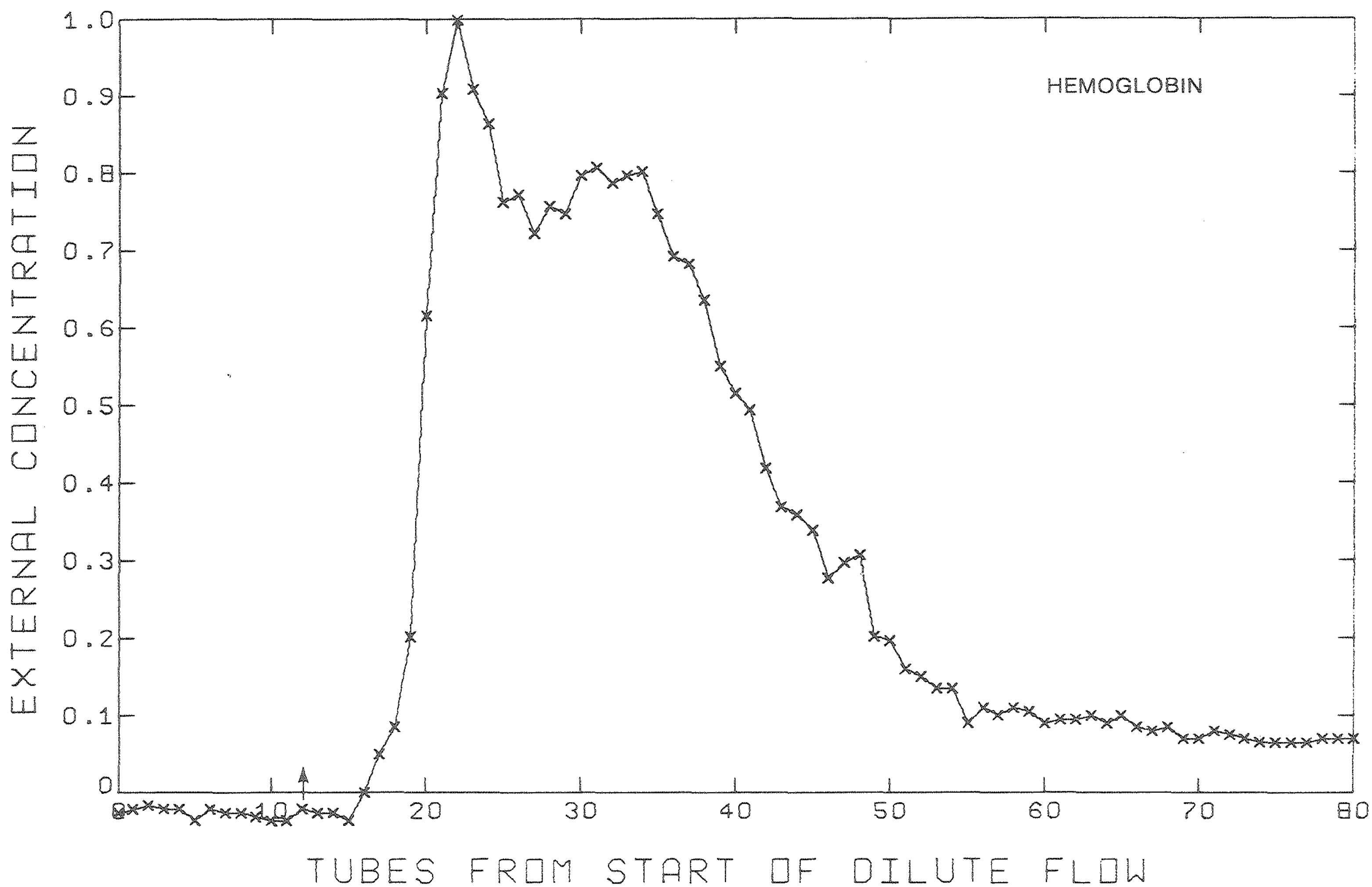

XBL 771-7325 A

Figure 5b. Hemoglobin (full scale = 0.198 OD).

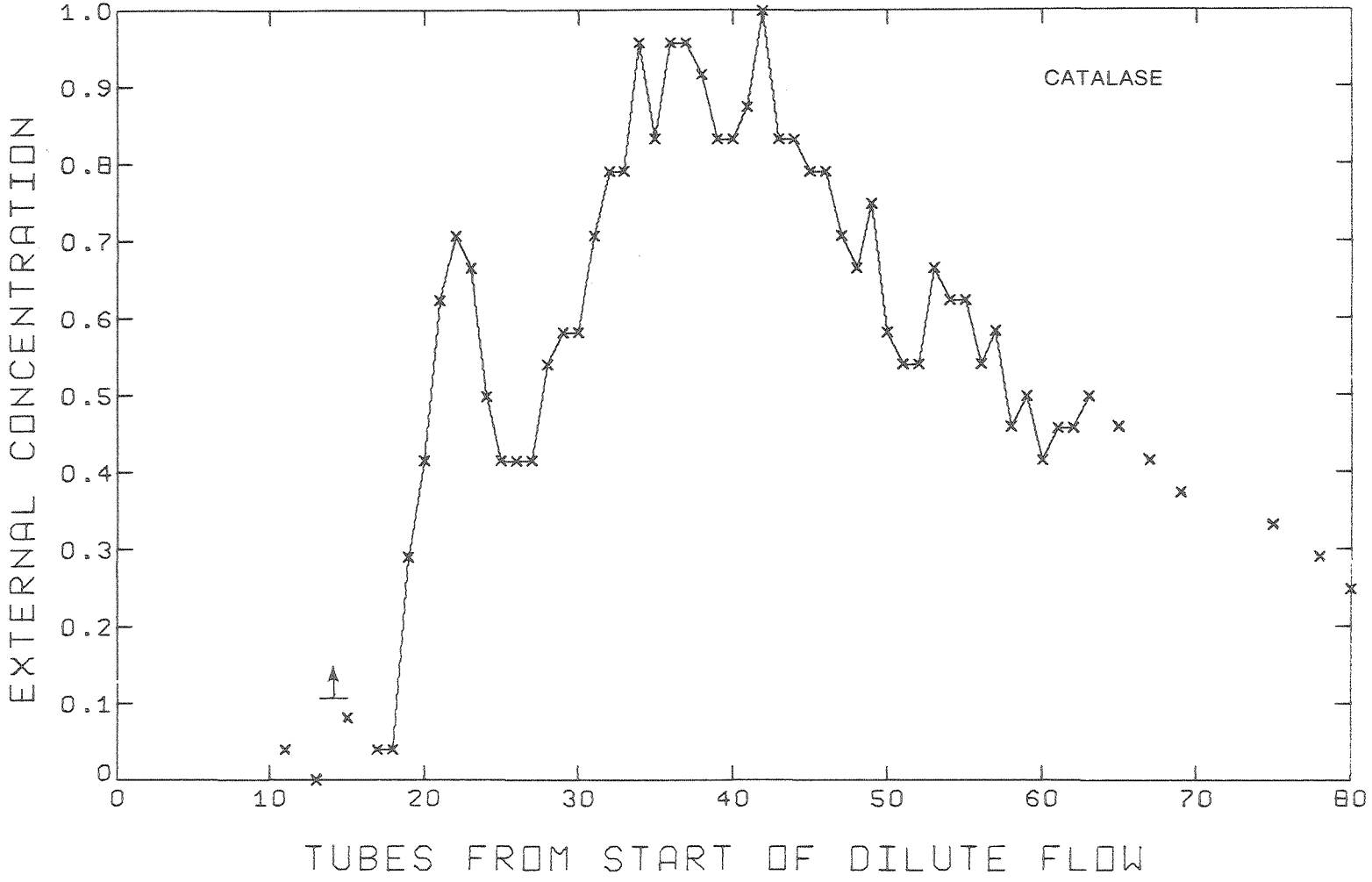

XBL 771-7326 A

Figure 5c. Catalase (full scale = 3.90×10^{-8} M).

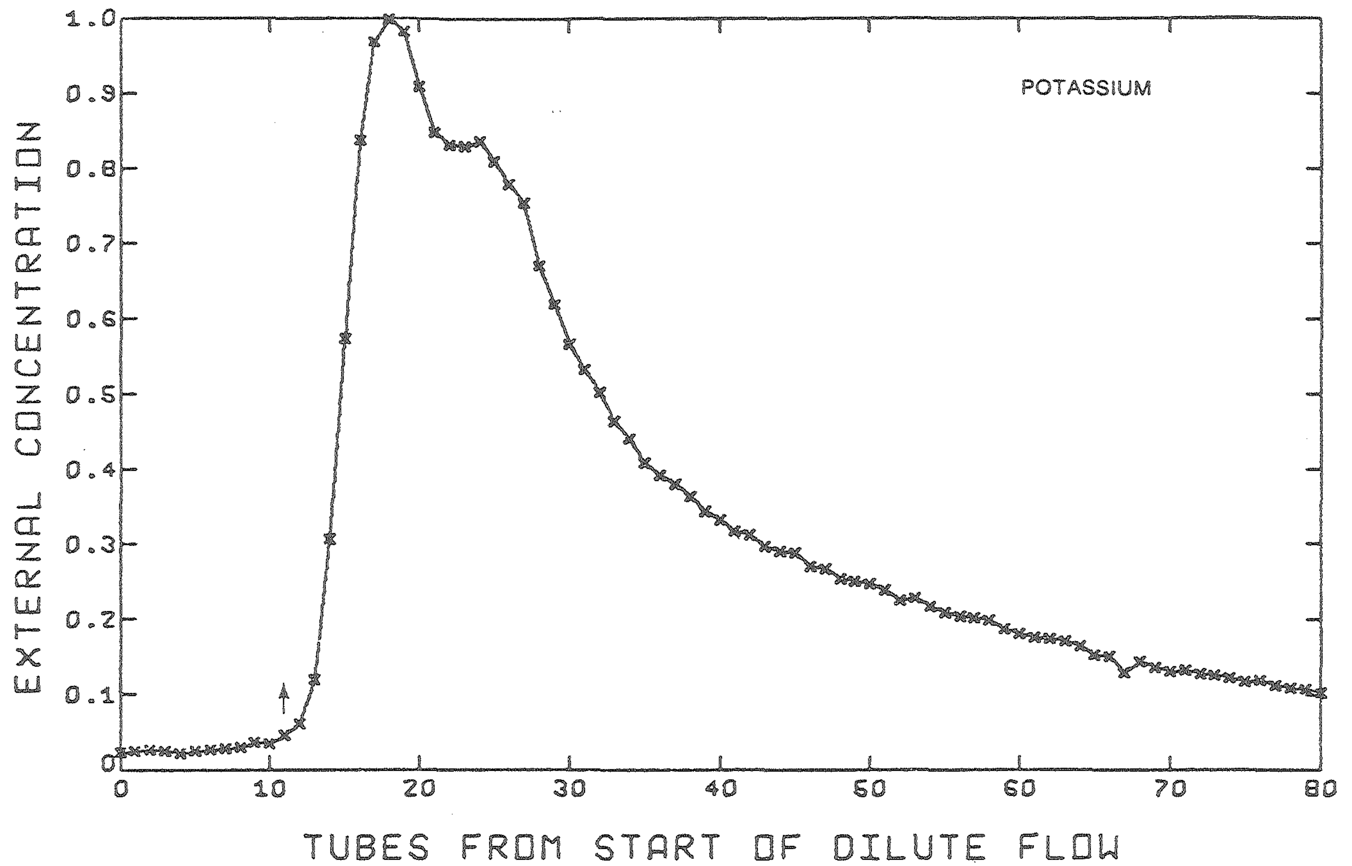

XBL 771-7327 A

Figure 6. Concentrations of K^+, Hb, Cat, AK, and Fum in a LiCl solution of gradually decreasing concentration that was flowed past rat red blood cells restrained in a centrifuge.

Figure 6a. Potassium (full scale = 82.8 μM).

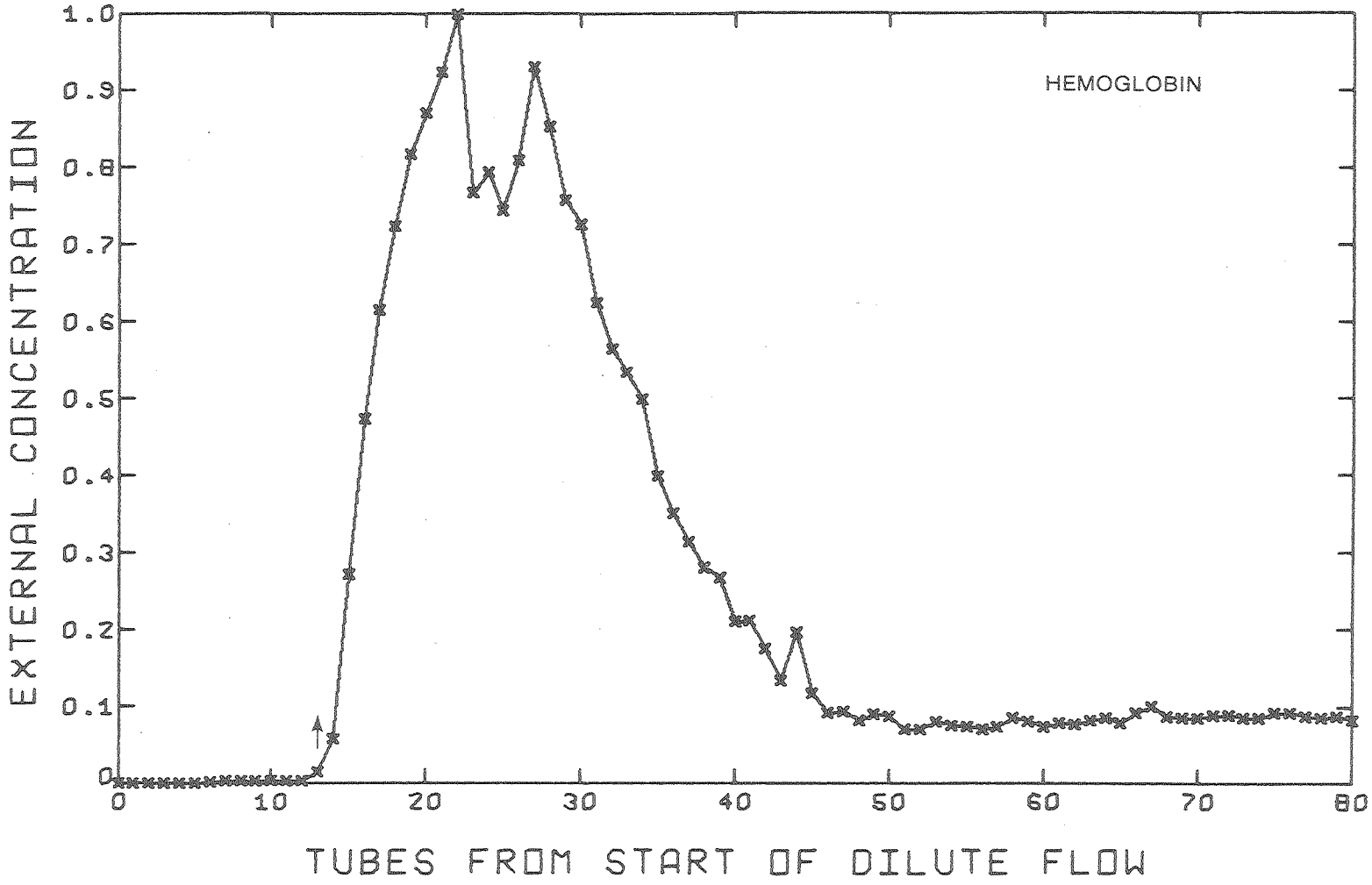

XBL 771-7328A

Figure 6b. Hemoglobin (full scale = 0.517 OD).

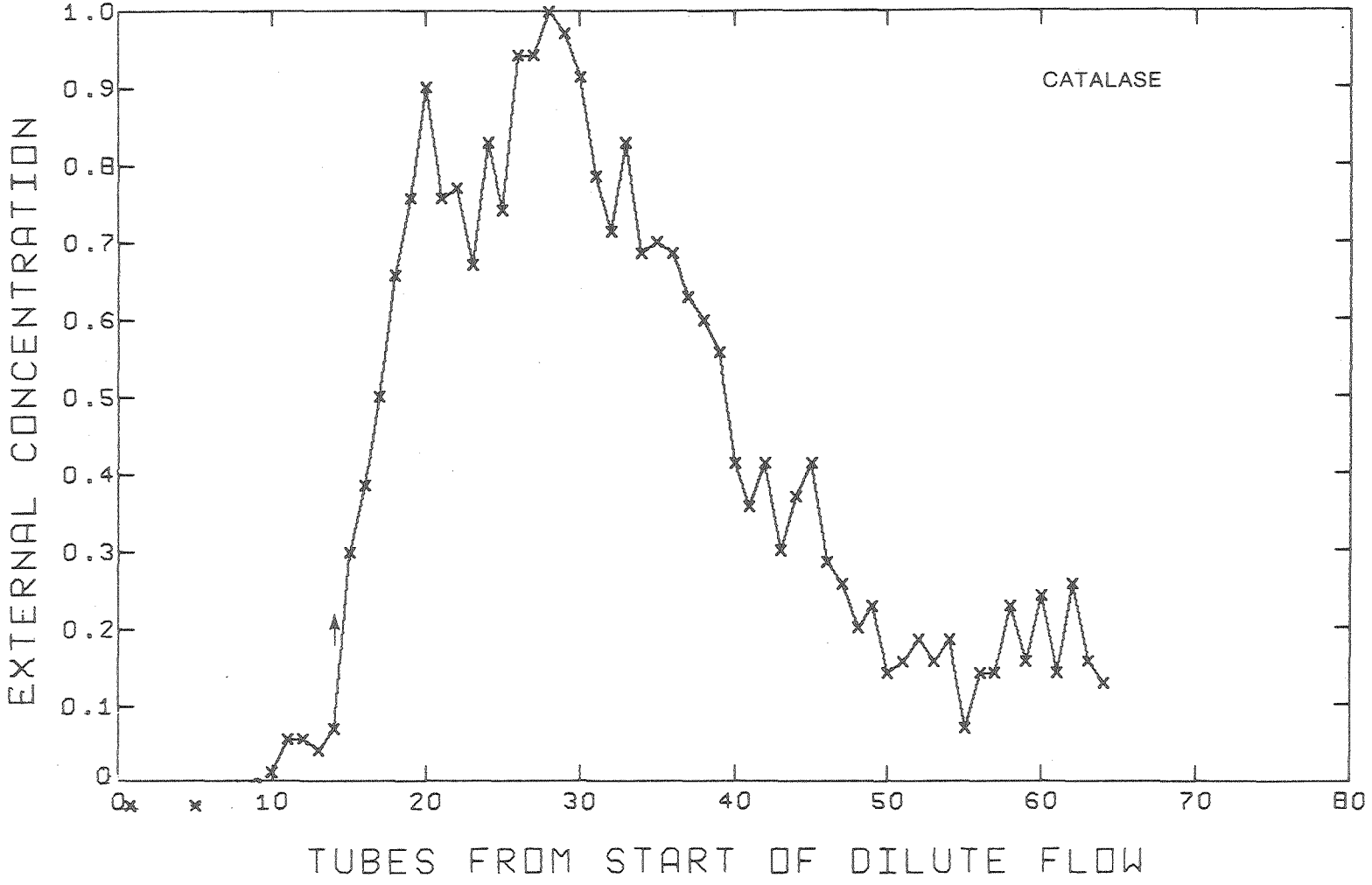

Figure 6c. Catalase (full scale = 2.14×10^{-8} M).

XBL 771-7329A

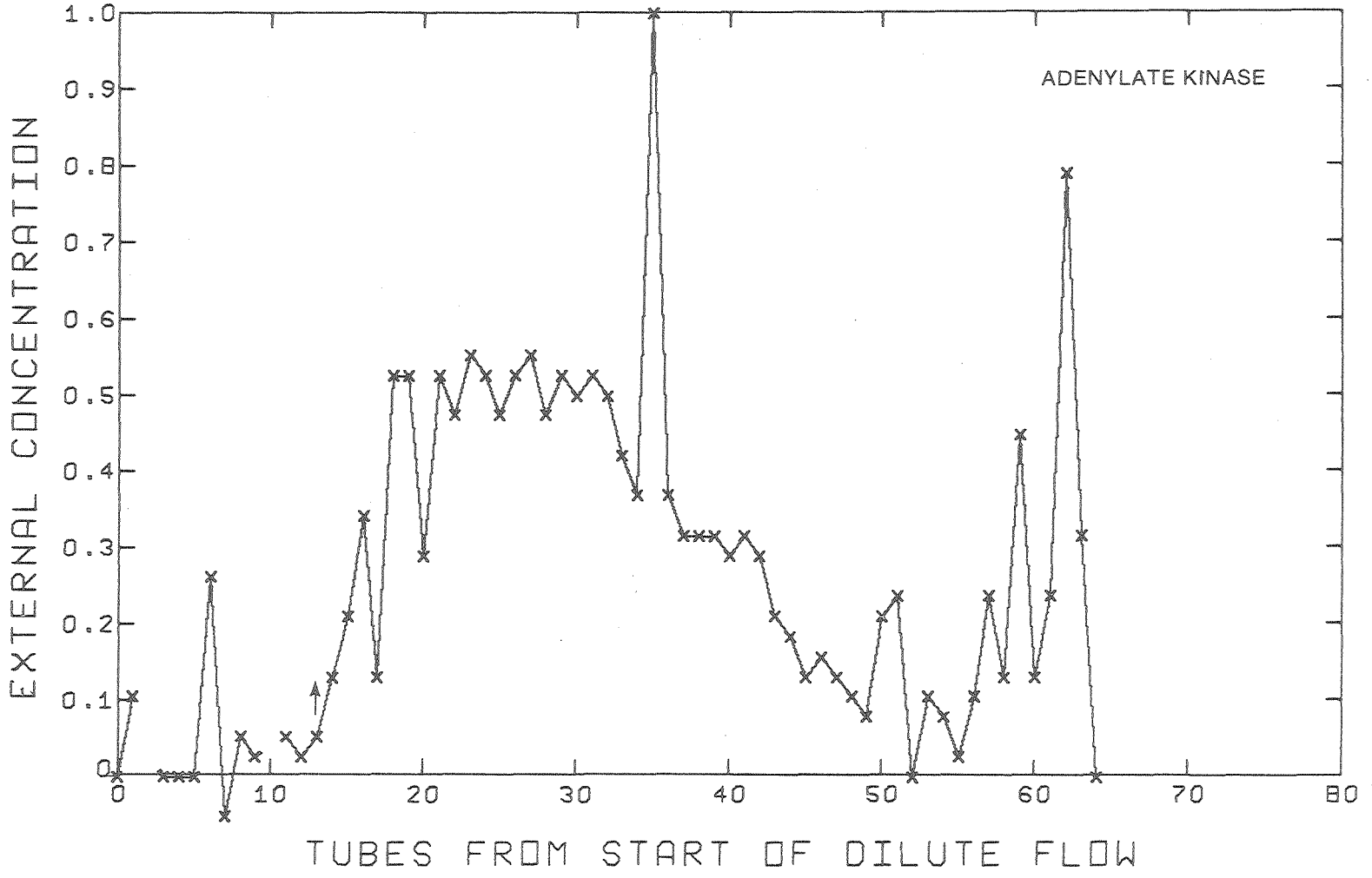

Figure 6d. Adenylate kinase (full scale = 0.038 OD).

XBL 771-7330 A

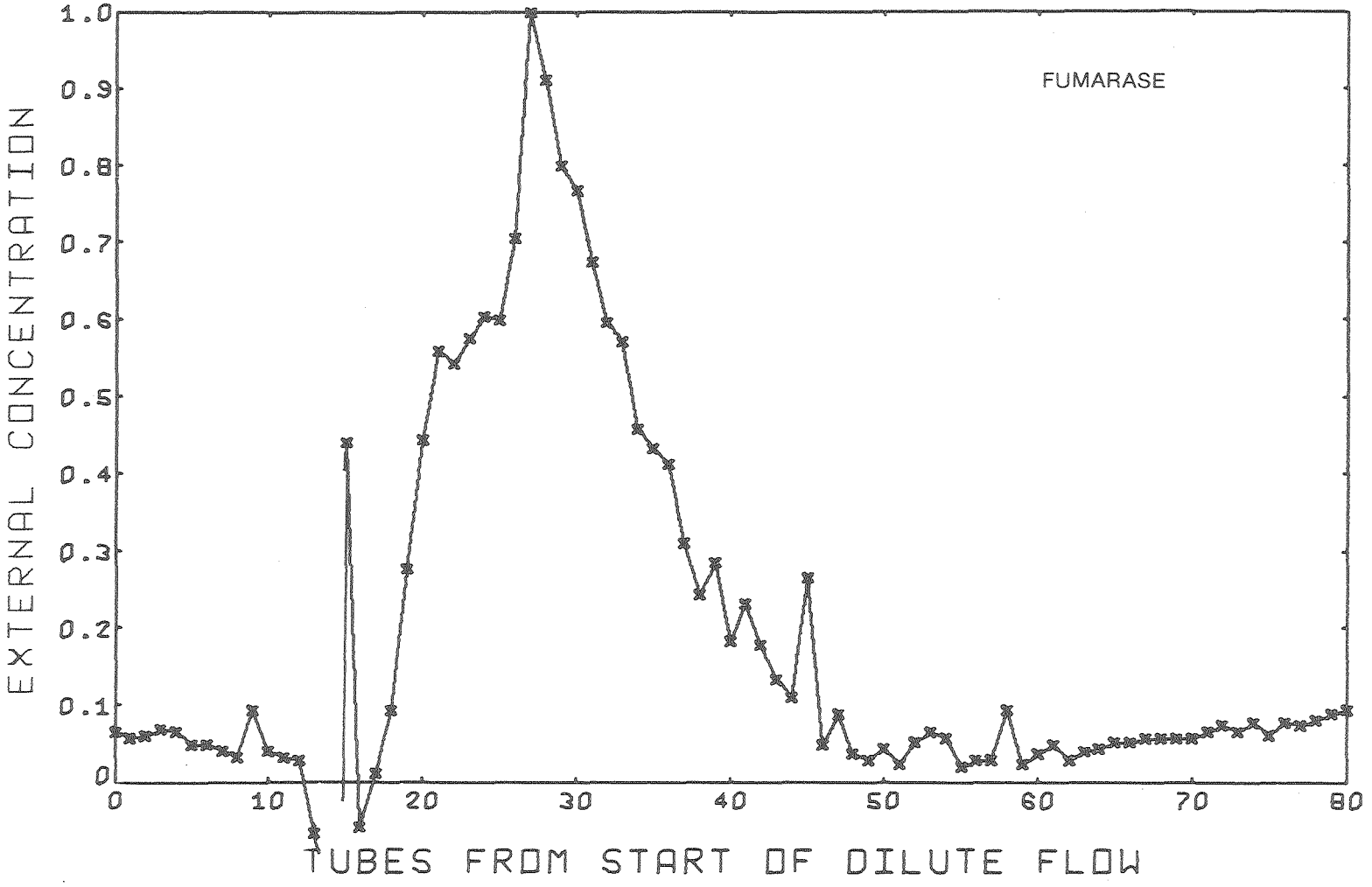

Figure 6e. Fumarase (full scale = 0.245 OD).

XBL 771-7331-A

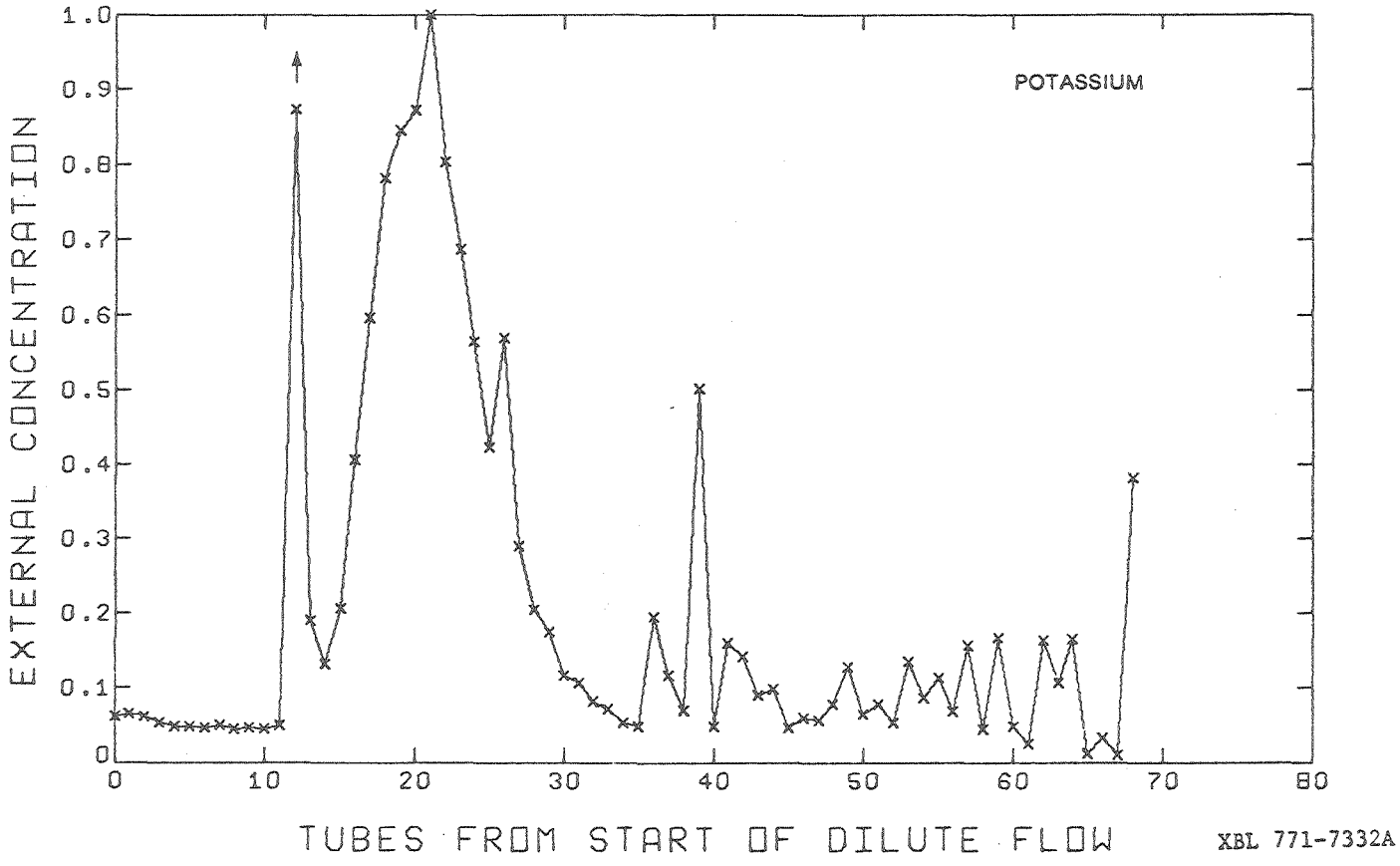

Figure 7a. Potassium (full scale = 41.2 μM).

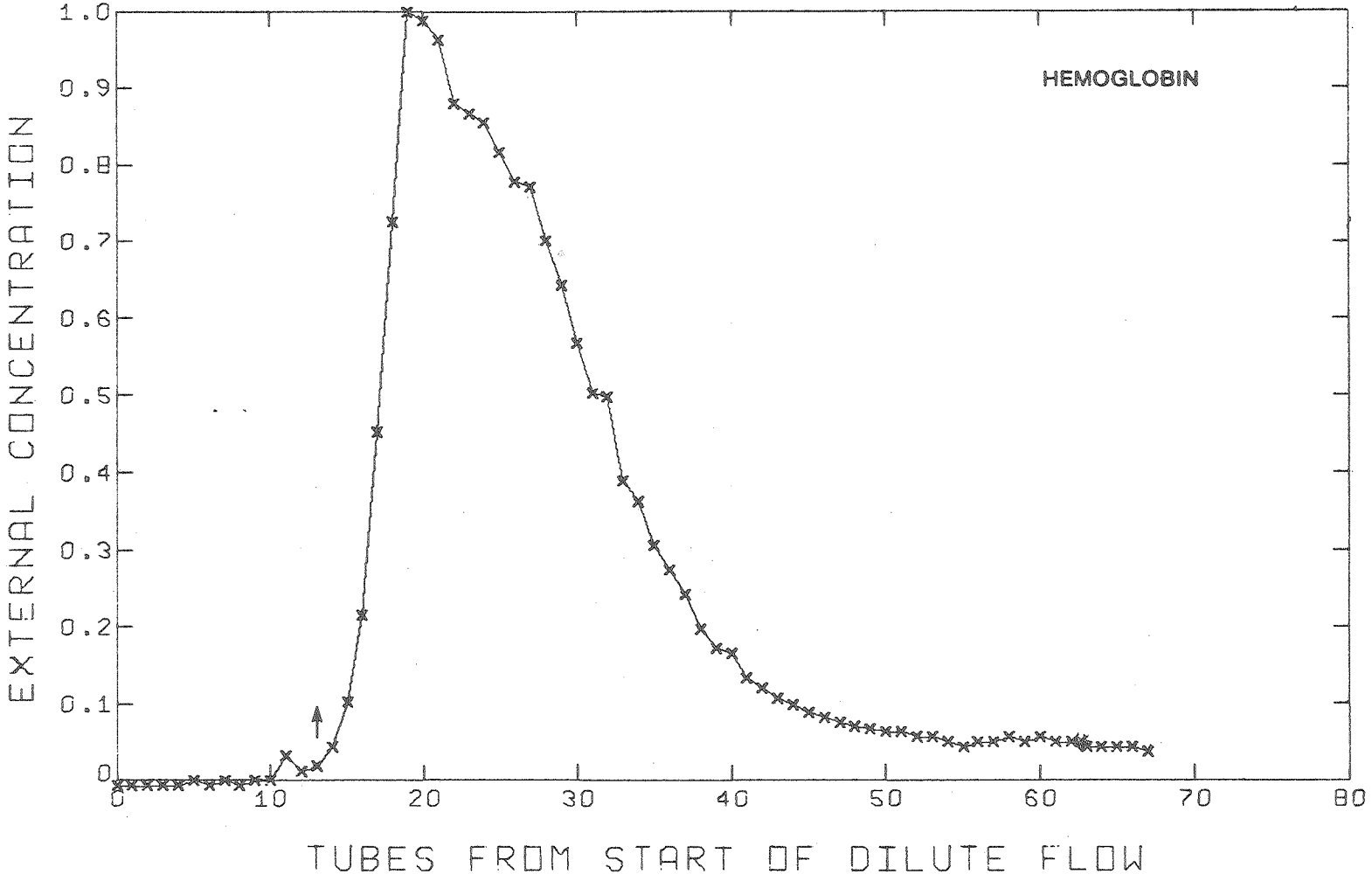

Figure 7b. Hemoglobin (full scale = 0.157 OD).

XBL 771-7333 A

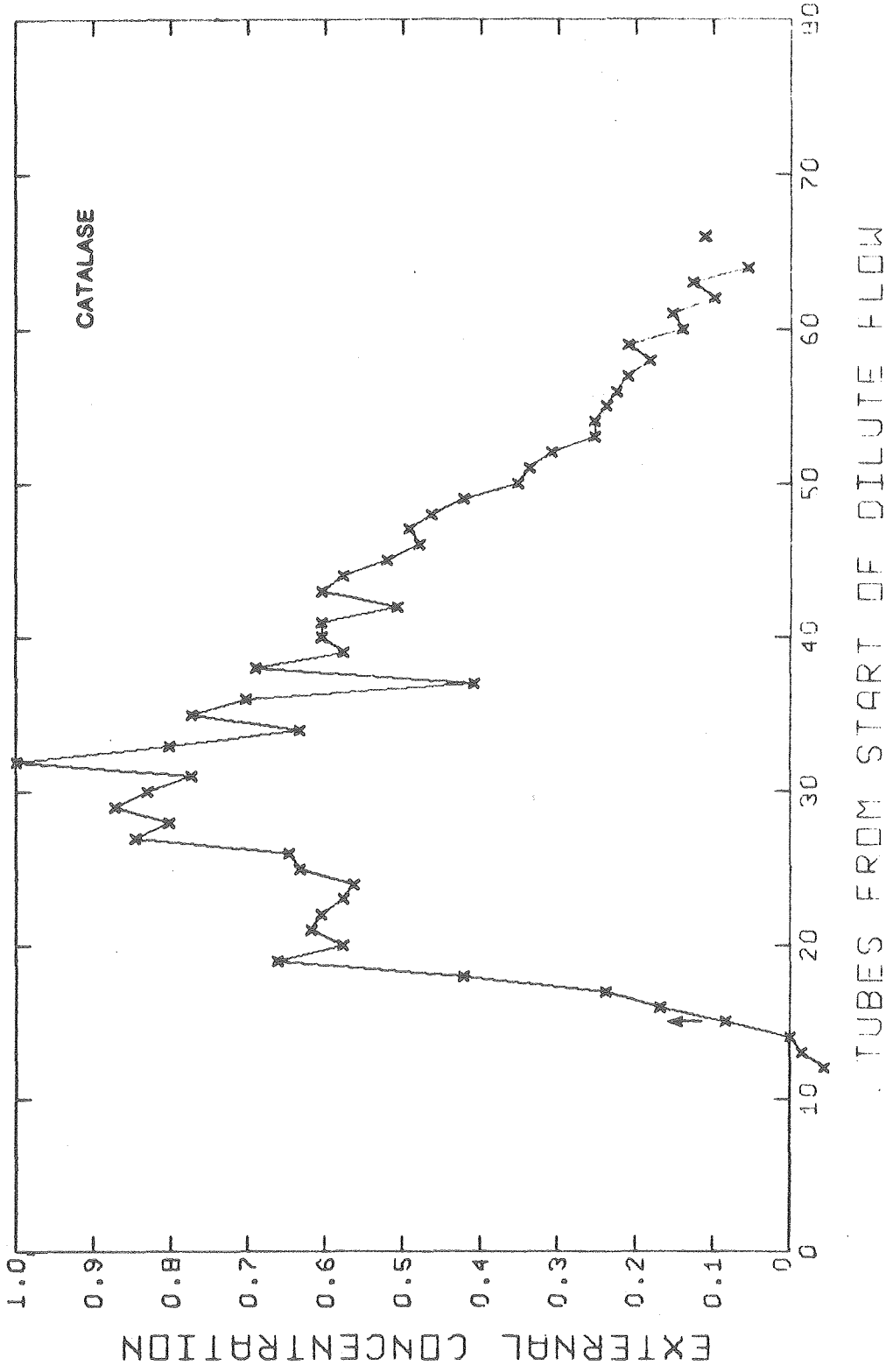

XBL 771-7334 A

Figure 7c. Catalase (full scale = 2.16×10^{-8} M).

Incubation of the cells in saline apparently increased the fine structure of the K^+ loss curve (compare the 0- and 3-hr cells in Figs. 5a and 6a, respectively, with the 5-hr cells in Fig. 7a) and caused minor Hb losses prior to and at the time of the initial K^+ loss (tube 11, Fig. 7b). Minor Hb losses were occasionally observed about tube 6, but the major Hb loss began in tubes 12 and 13 when the external solute concentrations were approximately 169 and 162 mOsm, respectively (arrows, Figs. 5b, 6b and 7b). The major Hb losses were observed in both fresh and incubated RBC and occurred after the start of the initial major K^+ loss. In contrast, "minor" Hb losses were not always observed (Fig. 6b) and occurred before or at the time of the initial major K^+ loss.

There appeared to be a minor Cat loss about the time of the initial K^+ loss, but the major Cat loss began in tubes 14 and 15 when the external solute concentrations were approximately 155 and 149 mOsm, respectively. An AK loss was observed at tube 6 and perhaps at tubes 10 or 11. The initial major loss of AK began in about tube 13 (Fig. 6d), and the initial major loss of Fum appeared to begin in tube 15 (Fig. 6e). An interference in the Fum assay, however, resulted in a net negative calculated Fum concentration in tubes 13, 14 and 16, but tube 15 was calculated to have a high Fum concentration. This tube was read repeatedly in order to follow the course of the incubation in addition to the usual OD determinations preceding and following the incubation. The high Fum concentration in tube 15 probably resulted from contamination of the sample while being transferred to or from the cuvette so that the initial major loss of Fum might have occurred in a later tube.

There is less fine structure in the K^+ loss curves from fresh RBC's

than in the protein loss curves (Figs. 5 and 6). The magnitude of this structure is well above the maximum analytical errors observed in the data (Table I, the "X" symbol on the graphs is about 2% of full scale in height). The relationship between the fine structure of the various solutes in a single experiment (Fig. 6) is not obvious because the flow increases observed did not necessarily occur in the same fractions for the different solutes and because a repeated series of losses was not observed. Rather, the rises and falls in the fine structure appear to occur at random. As detailed in the Interpretation section, however, relationships do exist in the fine structures that are reproducible between experiments and that relate the various molecular loss curves.

If the loss curve of a solute is integrated by the fraction-by-fraction addition of each data point, the cumulative percent loss of each solute, of the solute lost, can be plotted against fraction number (Fig. 8). These curves resemble the common osmotic fragility tests in which the percentage of hemoglobin loss is plotted against the NaCl concentration of the dilution media (Wintrobe, 1967). The drastic hemolysis used in the osmotic fragility test differs significantly, however, from the gradual process employed in this work as will be discussed in more detail later. It should be noted that, during the hemolysis process as conducted in NaCl centrifuge experiments in this work, there was a greater percent release of smaller molecules (K^+) than of larger molecules (Hb, Cat) at any given time with the exception of the very early and very late stages. During the very early and very late stages, the amount of a solute released does not appear to be a simple function of the solute's molecular weight. The independence of the fine

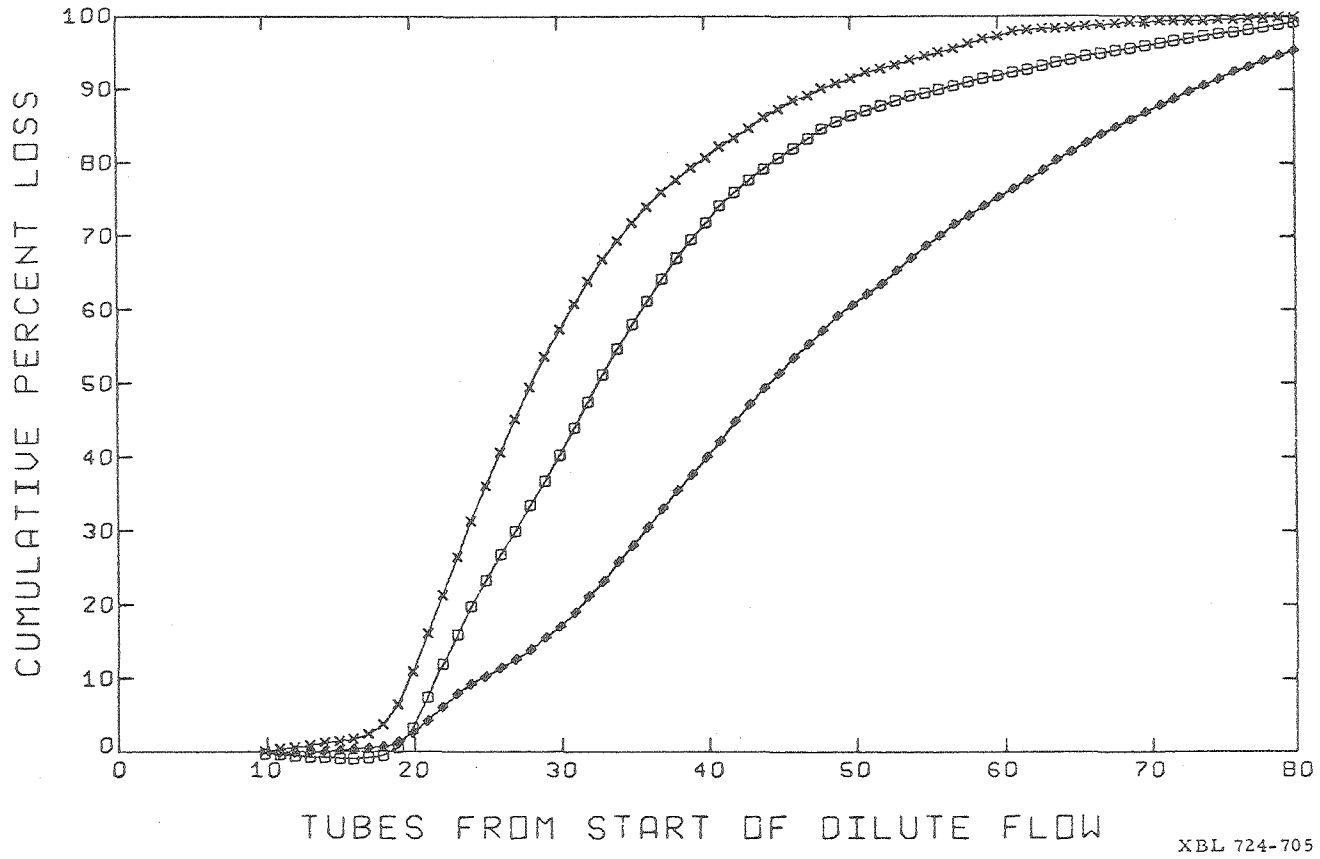

Figure 8. The loss curves of Fig. 5 have been added, point by point, to obtain an integrated curve of percent solute lost of the solute lost, prior to and including each collected fraction starting with fraction 10. At any time during controlled gradual osmotic hemolysis in a NaCl centrifuge experiment, with the exception of early and late fractions, a larger percentage of small molecules (K^+) were lost than of large molecules (Cat).

× Potassium □ Hemoglobin ◆ Catalase

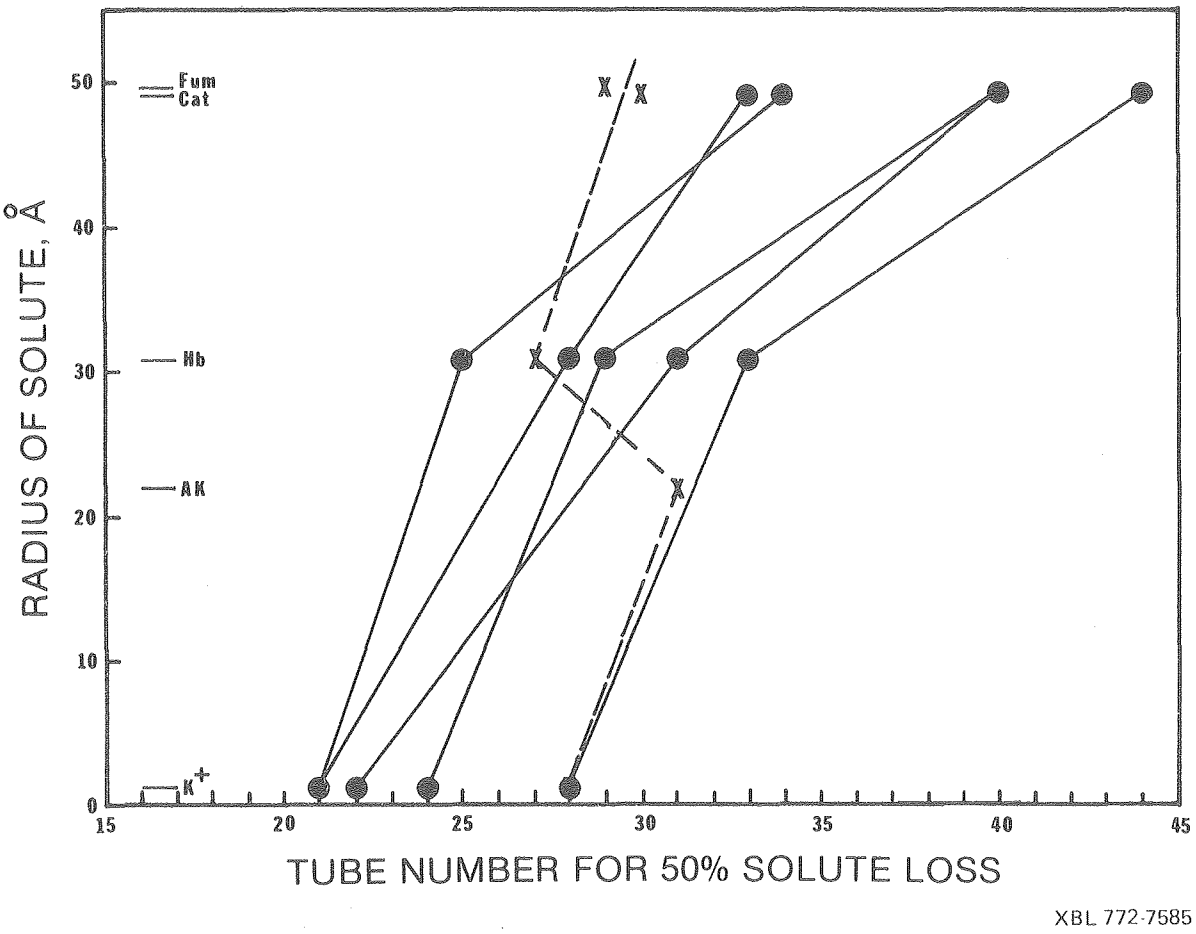

Figure 9. Times for 50% solute loss, of the total solute released, for representative centrifuge experiments. The times for 50% loss increased with the increasing size of the intact intracellular molecule in NaCl experiments (solid lines). This did not hold true for the LiCl experiment (dashed line, see text). The radii of the solutes are taken from Table V.

structure of the various solutes is again evident in Fig. 8 where a rapid increase in the percent loss of one solute is not evidenced in the losses of the other solutes (compare Cat loss with the losses of K^+ and Hb in Fig. 8).

Considering only the time at which 50% of a solute is lost from the cells of the total solute lost, the 50% loss times occurred in the order of increasing molecular size (K^+, Hb, Cat) in NaCl experiments (Fig. 9). In the LiCl experiment, however, the 50% loss times of the smaller molecules K^+ and AK occurred after the 50% loss times of the larger molecules Hb, Cat, and Fum.

The ghosts remaining at the conclusion of a centrifuge experiment utilizing salt flow solutions typically contained 10 to 25% of the initial cellular Hb and 0.5 to 4% of the initial cellular K^+. It is not known how much of this K^+ is free. Because the ratio of the intra- to extracellular Hb concentrations was at all times greater than 250, equilibrium was not reached during the course of the experiment between the intra- and extra-cellular compartments for Hb and may not have been reached for K^+.

LOSSES OF DEOXY-, OXY- AND MET-Hb FROM INCUBATED RBC's IN NaCl CENTRIFUGE EXPERIMENT

Figure 10a indicates the concentrations of deoxy-, oxy- and met-Hb in the collected fractions when a NaCl solution of continuously decreasing concentration was flowed past RBC's that had been incubated approximately 1 day at 4°C prior to the centrifuge experiment. The deoxy-Hb loss rose dramatically at tube 11 to form a narrow loss peak. The met-Hb loss increased in tube 11, but the oxy-Hb loss did not increase sharply until

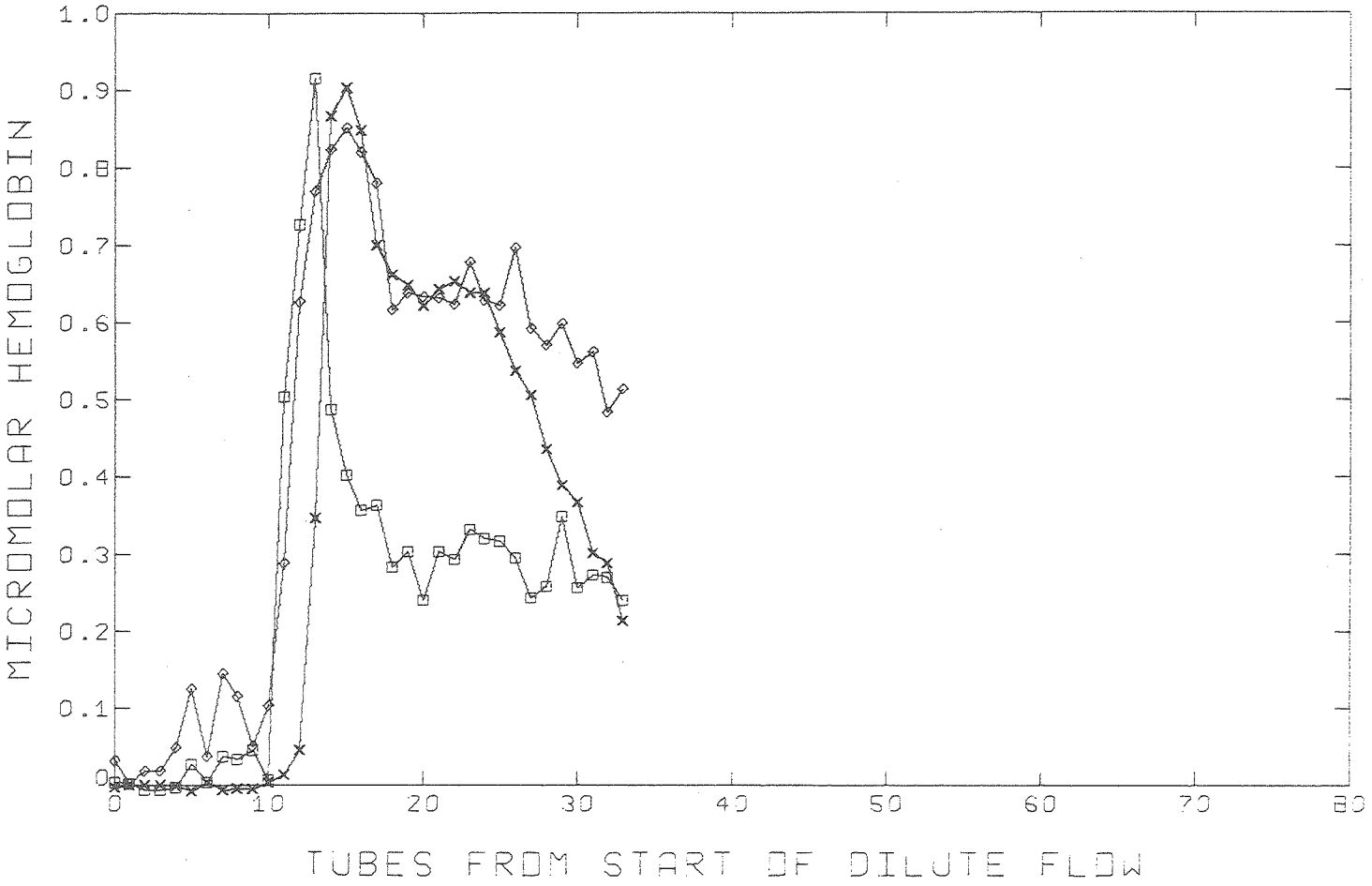

XBL 771-7335

Figure 10a. Concentrations of oxy-, deoxy- and met-Hb in a NaCl solution of gradually decreasing concentration that was flowed past rat red cells restrained in a centrifuge.

× Oxy-Hb □ Deoxy-Hb ◇ Met-Hb

The deoxy- and met-Hb concentrations have been multiplied by a factor of 10.

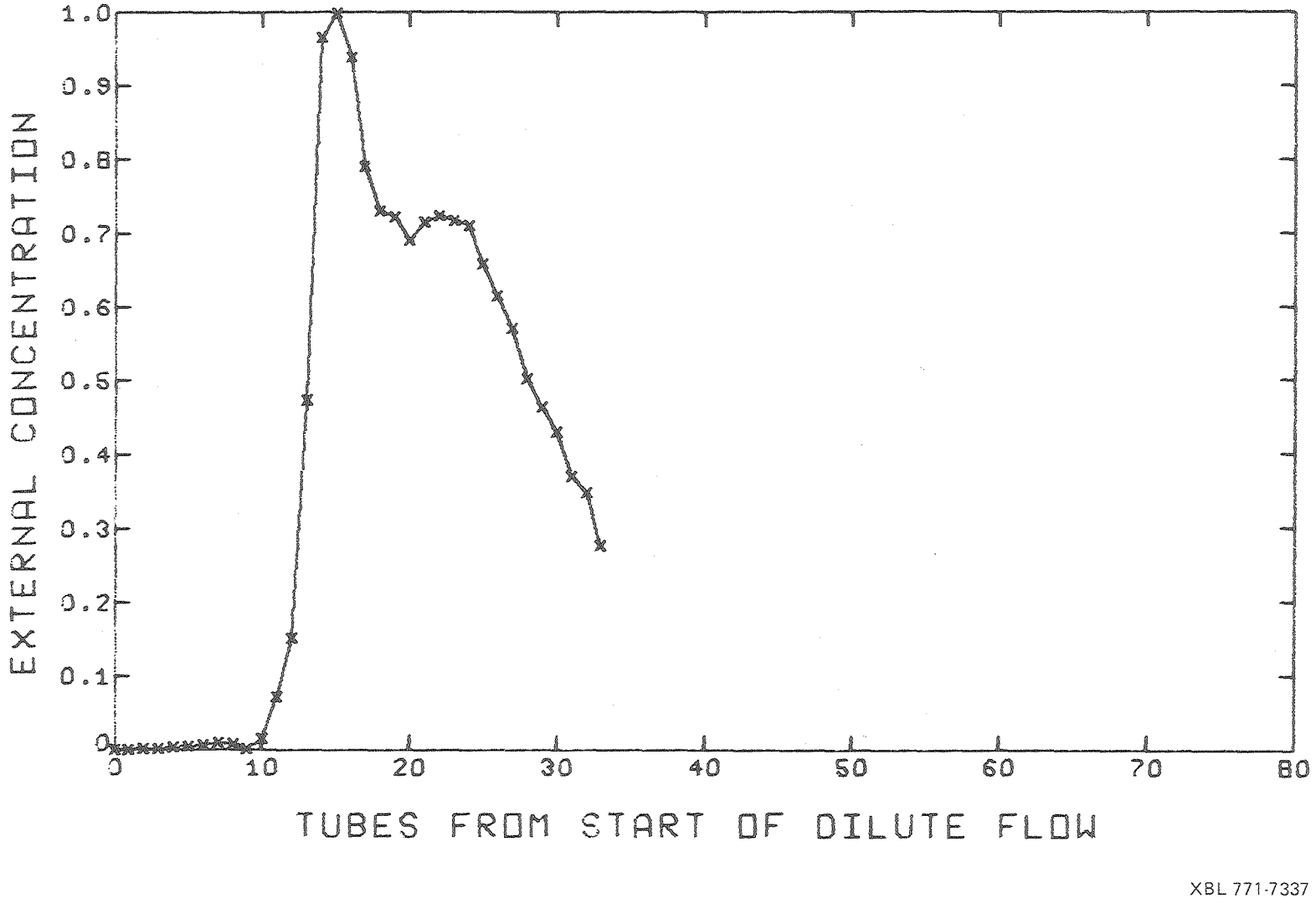

Figure 10b. Optical density at 414 mμ calculated from the data of Fig. 10a as described in the Methods section.

tube 13. The calculated OD at 414 nm (Fig. 10b) began to increase in tube 10, increased rapidly in tube 11, and obtained its maximum value at tube 15 whereas the maximum OD's at 414 nm were in tubes 22, 22 and 19 in the centrifuge experiments of Figs. 5, 6, and 7, respectively. The fine structure of the deoxy-, oxy- and met-Hb loss curves indicate that at all times there were differences in the loss patterns of these Hb's.

LOSSES OF K^+ AND Hb IN NaCl AND DEXTROSE FILTER EXPERIMENTS

The flows of K^+ and Hb from cells restrained in a glass filter into a NaCl solution of continuously decreasing concentration are indicated in Fig. 11. Data obtained with cells restrained in filters lacks the resolution obtainable with the centrifuge. Within the resolution of the data, the major K^+ and Hb losses started about 60 min after the start of the dilute flow when the external solute concentration was approximately 173 mOsm.

The flows of K^+ and Hb from cells restrained in glass filters into a dextrose solution of approximately constant ionic strength but continuously decreasing dextrose concentration are indicated in Figs. 12 and 13a.

The initial K^+ losses began at external solute concentrations of approximately 168 and 174 mOsm in Fig. 12 and 13a, respectively, but, in contrast to the salt experiments, the initial Hb loss occurred after a considerable delay in both dextrose experiments (Table III). In overall shape, the K^+ loss peak preceded the Hb loss in these dextrose experiments whereas in the salt experiments the overall shapes of the K^+ and Hb losses more nearly coincided.

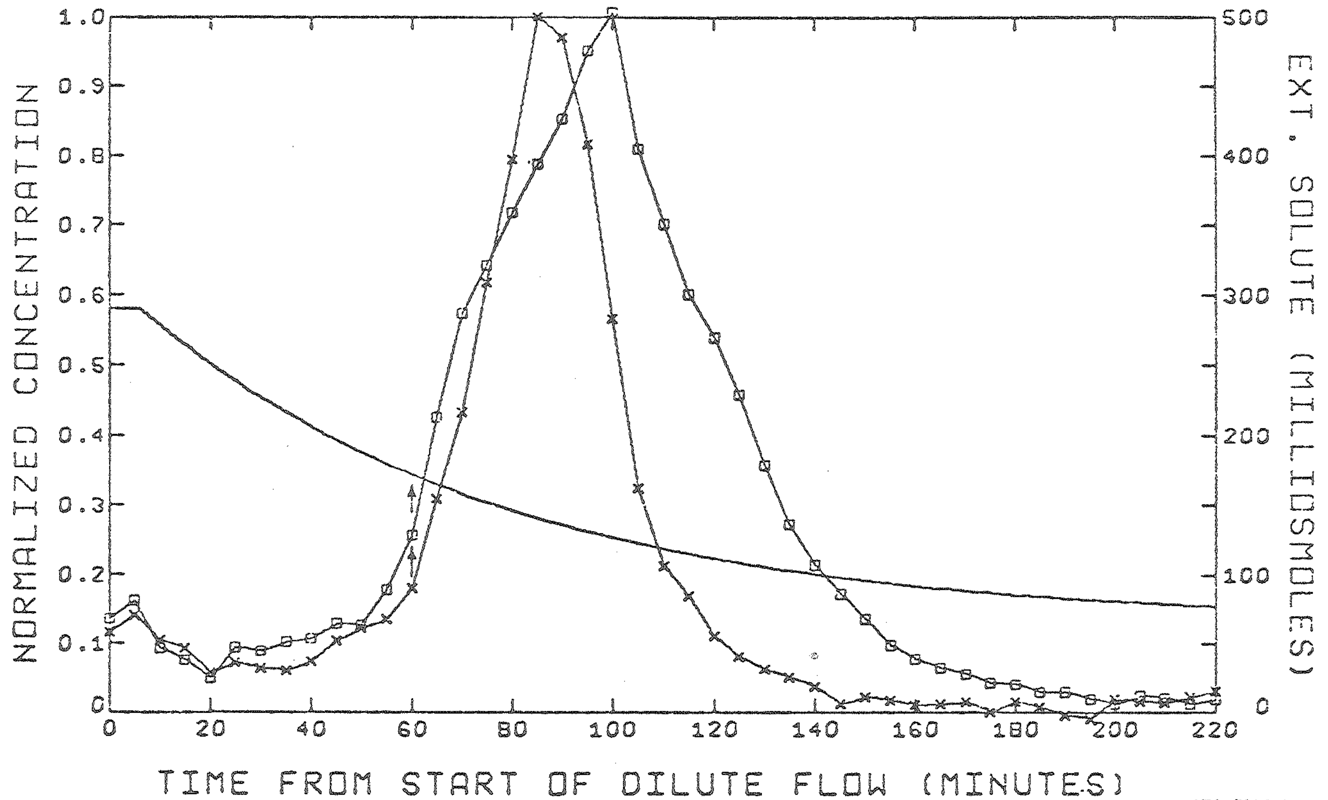

XBL 7210-1954A

Figure 11. Concentrations of K^+ and Hb in a NaCl solution of gradually decreasing concentration that was flowed past rat red cells restrained in a glass filter.

× Potassium (full scale = 5600 counts/5 min)

□ Hemoglobin (full scale = 0.369 OD)

The external solute concentration is indicated by the line and the scale on the left ordinate.

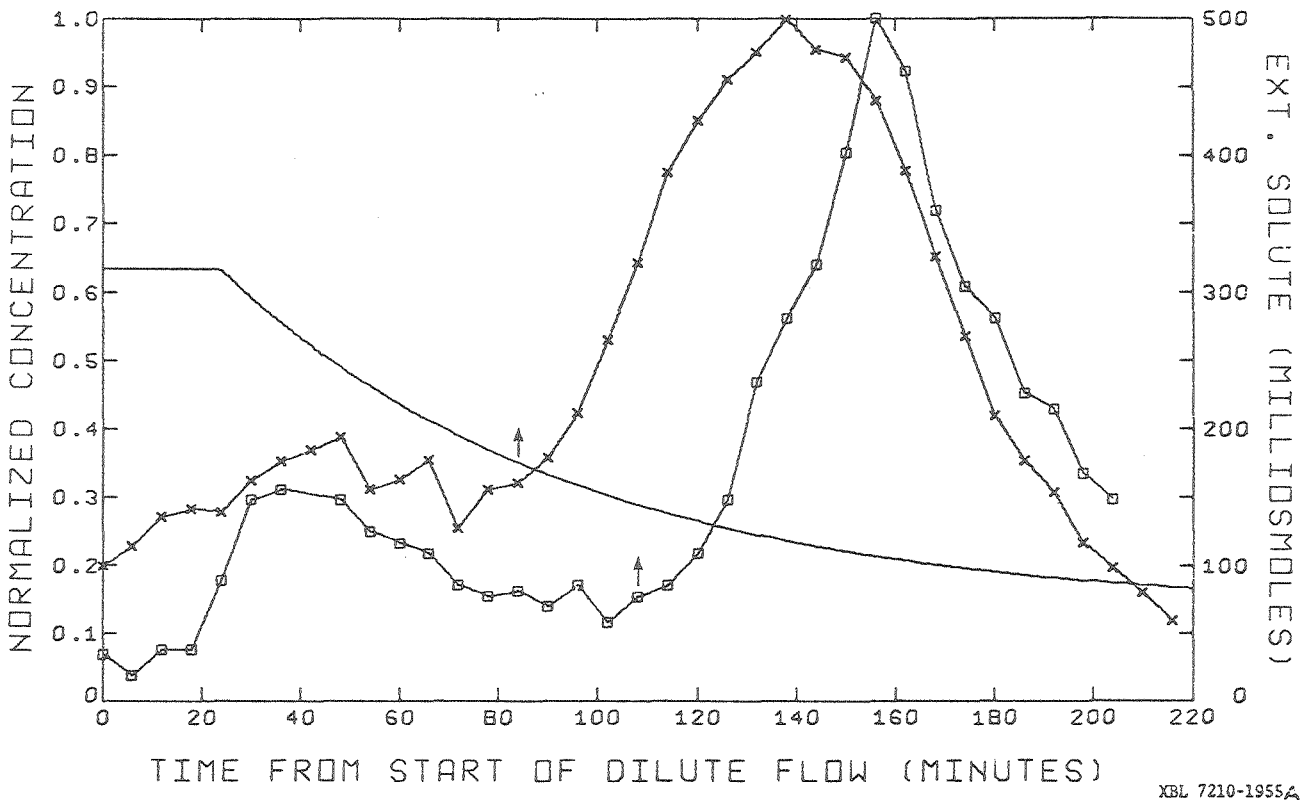

Figure 12. Concentrations of K^+ and Hb in a dextrose solution of gradually decreasing concentration that was flowed past rat red cells restrained in a glass filter.

× Potassium (full scale = 43.9 μM)

□ Hemoglobin (full scale = 0.128 OD)

The external solute concentration is indicated by the line and the scale on the left ordinate.

TABLE III. Flow solution concentration at start of major K^+ and Hb losses.

Figure	Major external solute	Cell-holding device	Milliosmolar Conc.		Start Major K^+ Loss		Start Major Hb Loss	
			Isotonic	Dilute	Tube No. or time	mOsm[a]	Tube No. or time	mOsm[a]
5	NaCl	centrifuge	283.0	57.4	#11	177.	#12	169.
6	LiCl	centrifuge	283.0	57.4	#11	177.	#13	162.
7	NaCl	centrifuge	283.0	57.4	#12	169.	#13	162.
11	NaCl	filter	288.0	62.4	60 min	173.	60 min	173.
					Average	174.	Average	167.
12	dextrose	filter	312.4	66.8	#15	168.	#18	146.
13	dextrose	filter	312.4	66.8	#12	174.	#14	155.
					Average	171.		151.

Reference:

[a]Milliosmolar concentration calculated at midpoint of fraction collection period.

MICROSCOPIC OBSERVATION OF INDIVIDUAL RBC's AND CORRELATION WITH POPULATION K^+ AND Hb LOSSES

When cells attached to glass were observed microscopically, they appeared to be uncrenated and usually appeared to be attached to the glass at distinct points, the details of which were beyond the resolution of the light microscope. When a cell was attached at only one such point and an isotonic solution flowed past it, it underwent a complex motion, which occasionally included moving more than 8μ from the point of attachment and springing back to the glass. When the cell was pulled away from the glass, it was slightly elongated but had a bioconcave shape except for a small protrusion from which a thread, observed only by its diffraction pattern, attached it to the glass. As the cell became osmotically swollen, the distance it moved from the glass was reduced. Cells attached at more than one point underwent less motion. This motion of the cells suggests that flowing a solution past cells attached to glass stresses the cell membranes regardless of the nature of the solution.

Major stress is not developed in a red cell membrane until an attempt is made to increase its membrane area (Rand and Burton, 1964a). In suspension, a cell does not suffer major osmotic stress until it becomes spherical. Similarly, in the monolayer of cells from which Fig. 13b was derived, under ideal conditions, nonspherical cells would be expected to have unstressed membranes, and completely spherical cells would be expected to have stressed membranes. Because there was insufficient space for all the cells to be spheres simultaneously, some of the cells that were spheres except for contacts with other cells would probably also have stressed membranes. The variable stresses exerted by the flowing solution and attachment of the cells to glass presumably modulated the osmotic stress nonuniformly.

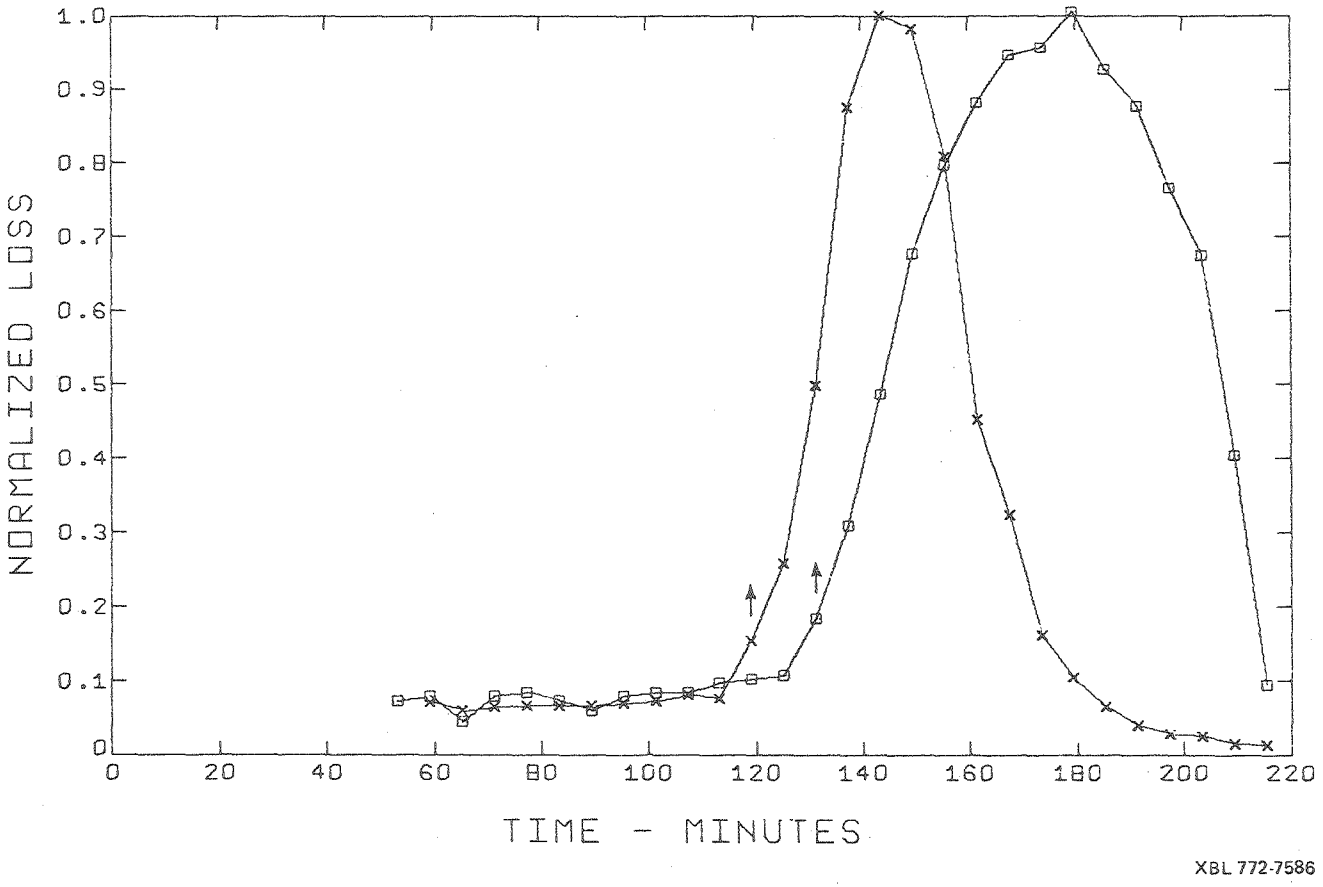

Figure 13a. Concentrations of K^+ and Hb in a dextrose solution of gradually decreasing concentration that was flowed past rat red cells restrained in a glass filter.

× Potassium (full scale = 305.0 μM)

□ Hemoglobin (full scale = 0.402 OD)

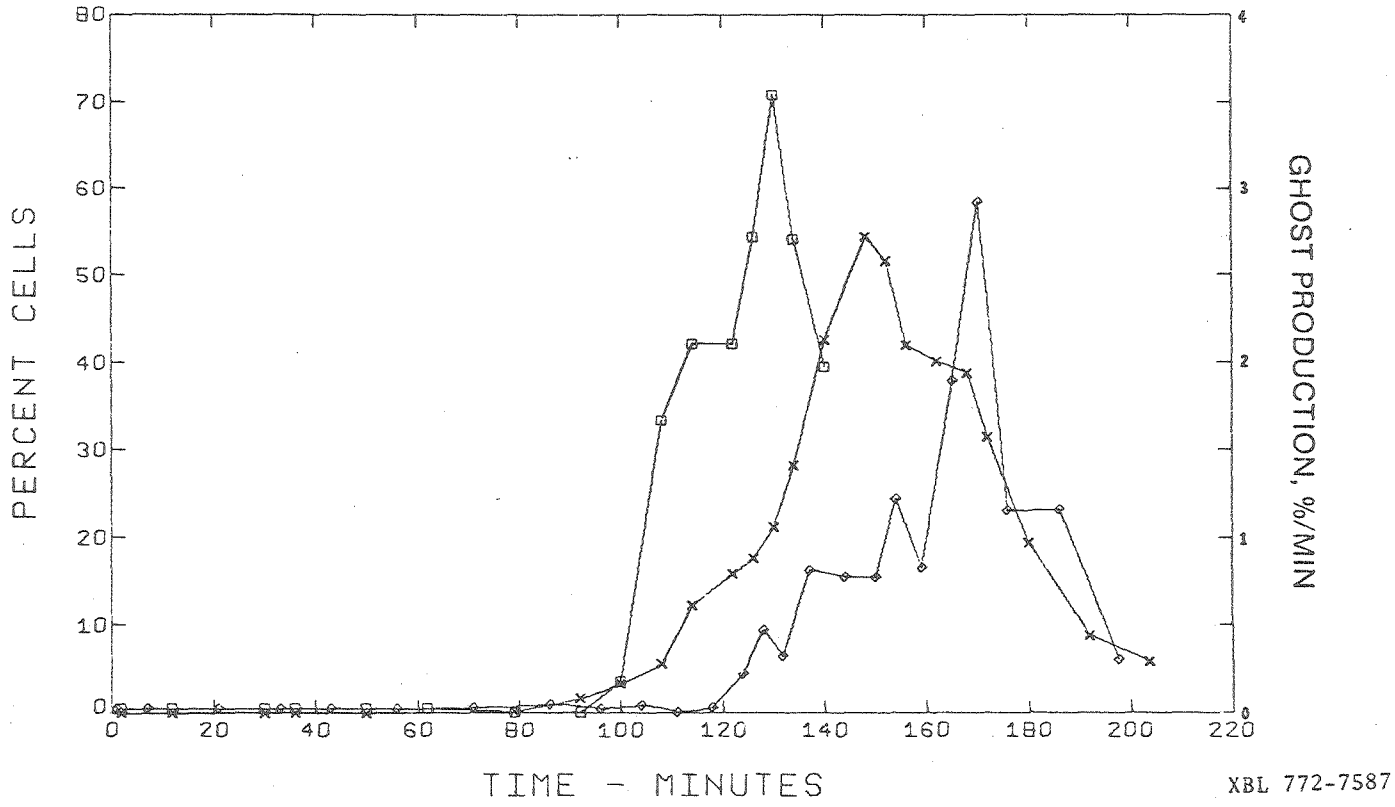

Figure 13b. Morphology of cells and the production of ghosts in a field of 790 cells when a dextrose solution of gradually decreasing concentration was flowed past rat red cells attached to glass. Note that the production-of-ghosts data are drawn to a different scale than that of the morphology data.

□ Cells sphered except for contacts with other cells
× Cells sphered completely
◇ Production of ghosts (full scale = 4%/min)

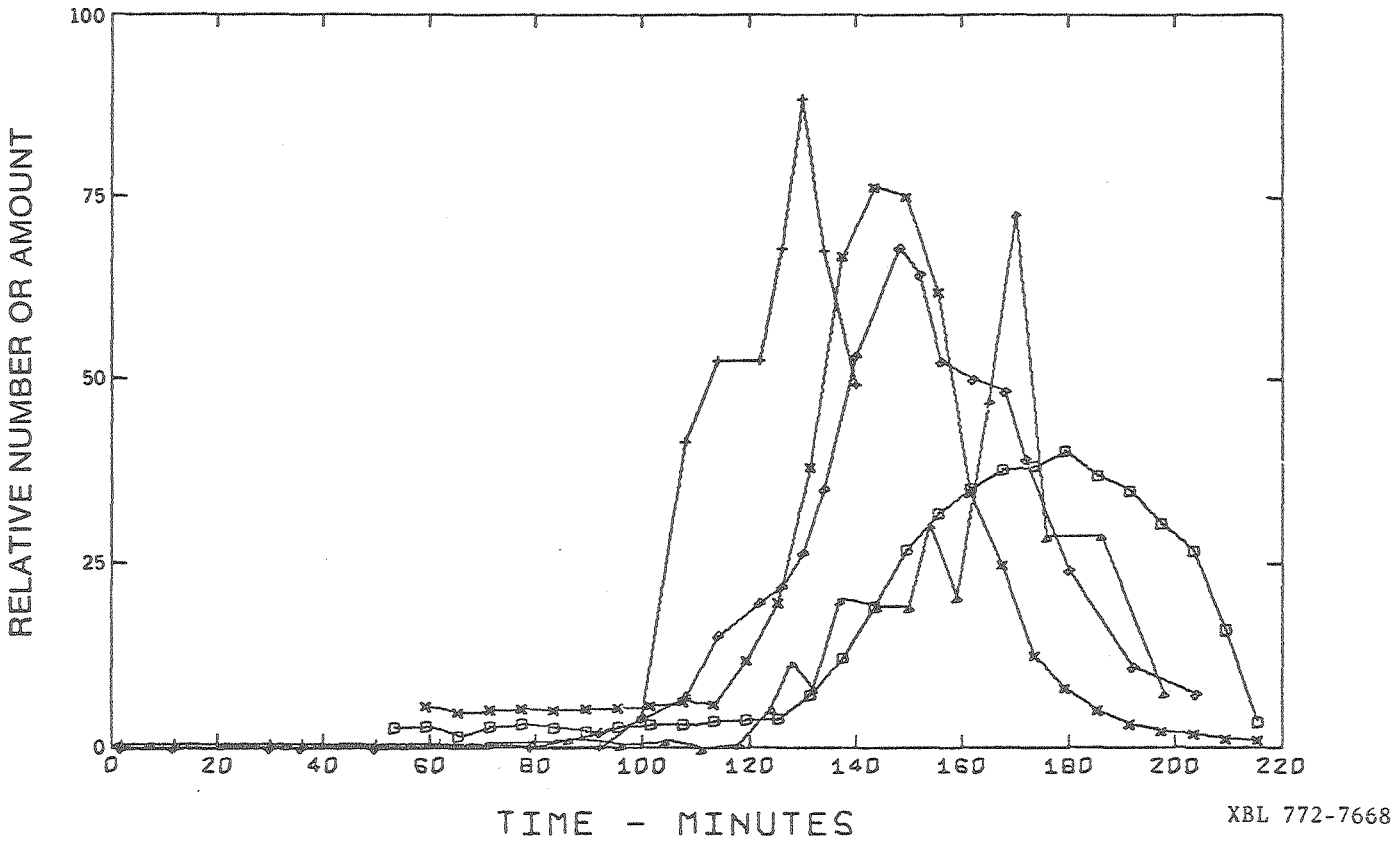

Figure 13c. Combined molecular-loss and cell-count data. The magnitudes of the loss data have been reduced to make the areas under their curves roughly equal to the areas under the cell-count curves.

× Potassium
□ Hemoglobin
\+ Cells sphered except for contacts with other cells
◇ Cells sphered completely
△ Production of ghosts

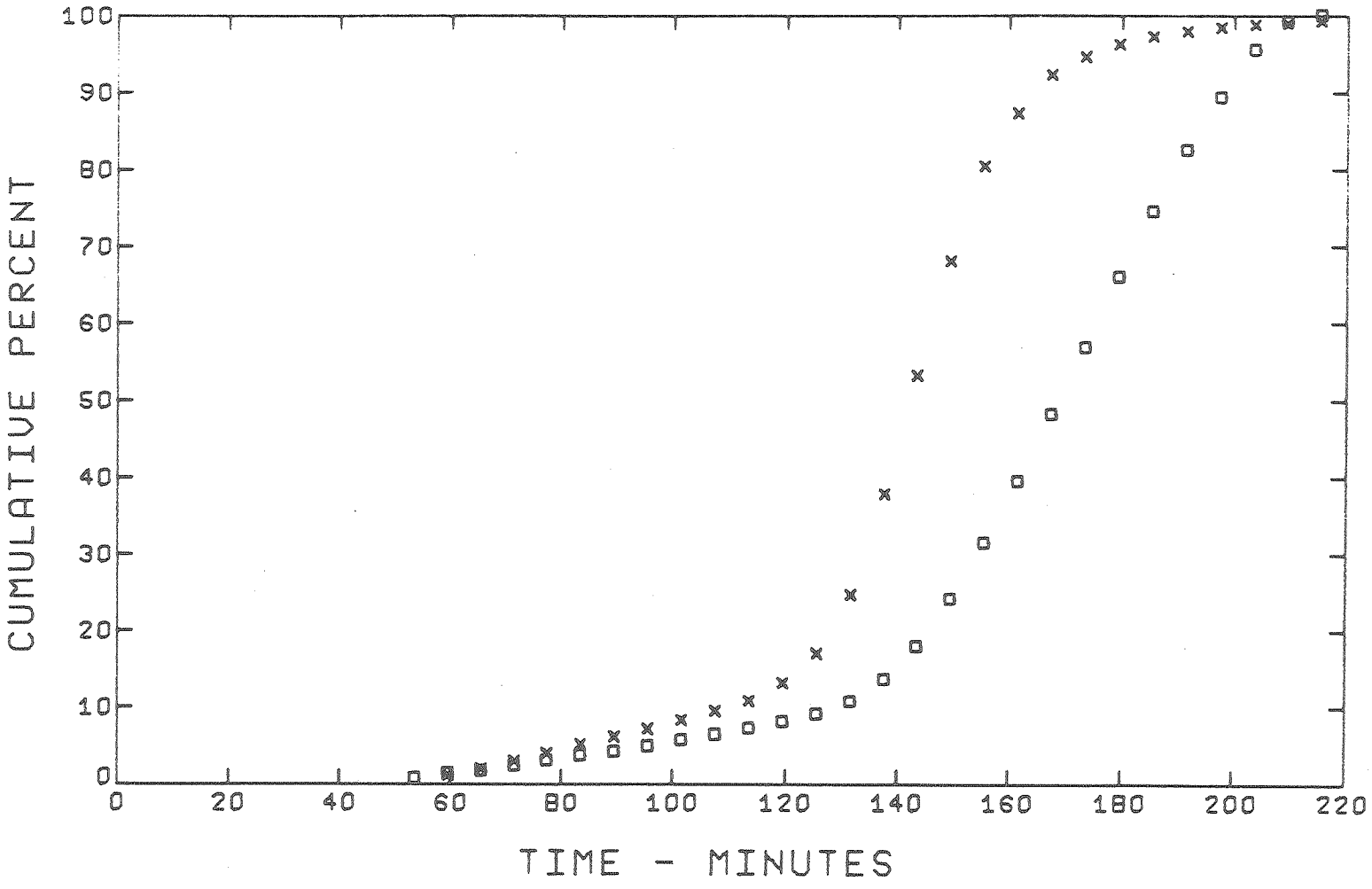

XBL 772-7589

Figure 13d. The K^+ and Hb loss data of Fig. 13a are represented here as the total cumulative percentage of solute that is lost to the flowing external solution.

× Potassium ▫ Hemoglobin

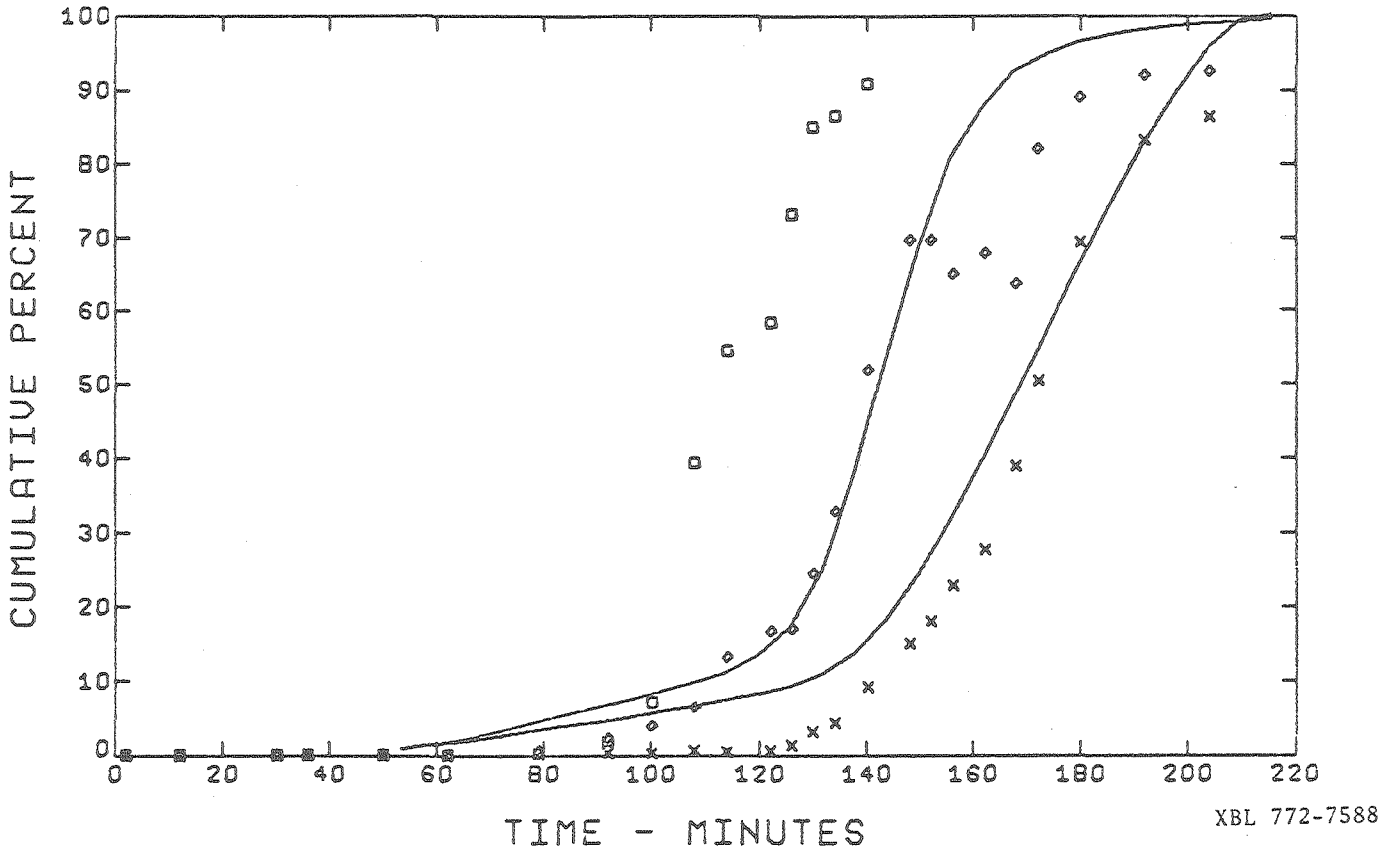

Figure 13e. The morphology and production of ghosts data of Fig. 13b are represented here as the percentage of cells that have progressed to or through a given morphological stage.

- □ Cells that have sphered except for contacts with other cells
- ◇ Cells sphered completely
- × Production of ghosts

The two lines are the cumulative percent losses of K^+ and Hb from Fig. 13d. Note that the K^+-loss data most nearly follow the complete-sphering-of-cells data.

Figure 13c correlates the morphological changes observed and the production of ghosts with the K^+ and Hb losses from the more numerous cells in the glass filter. The initial rise in the production of ghosts and the initial rise in Hb loss occur at about the same time, but the peak of ghost production precedes the peak of Hb loss. This may be due to the arbitrary decision of when a cell becomes a ghost. The K^+ loss peak occurs after the peak of cells that have sphered except for contacts with other cells but before the peak of cells that have sphered completely. Figure 13e indicates that the cumulative percent loss of K^+ closely follows the complete sphering of the cells during the initial stages of controlled gradual osmotic hemolysis. Thus, the loss of K^+ starts at about the time the membrane first suffers major stress.

No cells were observed to suddenly fade, to have an observable Hb loss in any local region of the membrane, or to be propelled owing to the loss of cellular constituents as occasionally observed by the author in drastic hemolysis and as reported by others (Comandon and De Fonbrant, 1929; Heedman, 1958; Danon, 1961; Kochen, 1964; Baker and Gillis, 1969). A cell that was sphered, with the possible exception of contacts with other cells, appeared sharper than either at earlier times or after the Hb loss was apparently completed, both in the microscope and in the photographs, probably reflecting reduced membrane motion in the stressed cell membranes. Examination of the photographs by eye indicated that individual cells faded, i.e., lost their cellular Hb, over a period of at least 6 min. The actual period of Hb loss was probably longer because it is unlikely that the entire loss period was detected.

At the conclusion of the experiment, all cells remained faintly

visible without the use of phase optics, implying that a portion of each cell's Hb remained within the cell at the conclusion of the experiment.

Uncertainty in the morphological classification of the cells prevented a detailed study of cell population heterogeneity; however, both the population K^+ and Hb losses (Fig. 13a) and cell morphology (Fig. 13b) appeared to be consistent with the presence of a single population distribution of red cells.

INTERPRETATION OF DATA

The molecular loss data presented in the Results section are more complex than might be expected if the red cell membrane simply ruptured during controlled gradual osmotic hemolysis. In this section, reproducible features of the data are discussed, and it is concluded that the rich fine structure of the loss curves results from a single population distribution in osmotic response of the majority of cells in the red cell population. Several explanations of the data are discussed, and it is found that, qualitatively, the initial and final phases of controlled gradual osmotic hemolysis can be explained by molecular sieving of the stressed cell membranes. Thus, it will be hypothesized that stressed rat red cell membranes exhibit molecular sieving properties.

SIGNIFICANT FEATURES OF THE DATA

In the experiments reported with freshly prepared rat red cells, a transition from relatively low K^+ permeability to higher K^+ permeability occurred at an external solute concentration of approximately 173 mOsm (Table III) regardless of the nature of the external solute (NaCl, LiCl or dextrose) and regardless of the method used to restrain the cells (glass filter or centrifuge). The transition occurred at about the time the cells became spherical and capable of deforming other cells (Fig. 13). Thus, the initial major K^+ loss started at about the time that major mechanical stress first developed in the membrane. This K^+ loss was not caused by low ionic strength (Davson, 1939; Donlon and Rothstein, 1969) because it occurred at about the same milliosmolar external solute

concentration regardless of whether the ionic strength was maintained at a constant value (Figs. 12 and 13) or varied during the experiment (Figs. 5, 6, 7 and 11). The K^+ loss observed was not significantly altered in filter experiments by the limited Cl^- for OH^- exchange that occurs when the NaCl solutions are replaced by dextrose solutions containing approximately 35 mM NaCl (Jacobs and Parpart, 1933) and was not dependent on the membrane potential in the manner observed by Donlon and Rothstein (1969). Thus, the initial major K^+ loss appeared to be caused by osmotic stress of the cell membrane. The course of the experiment after the initial K^+ loss depended, however, on the nature of the external solute; the loss of Hb occurred at approximately 167 mOsm in NaCl or LiCl solutions but was delayed to approximately 151 mOsm in dextrose solutions (Table III).

The reproducibility of the fine structure of the loss curves is perhaps best examined by first considering the losses of deoxy-, oxy- and met-Hb within a single experiment (Fig. 10a). When the calculated optical density at 414 mμ (Fig. 10b), the wavelength used to estimate the total Hb in other centrifuge experiments (Table I), is compared with the deoxy-, oxy- and met-Hb losses determined simultaneously by means of a three-wavelength assay (Fig. 10a), it is seen that the initial rise at tubes 10 and 11 is due to the losses of deoxy- and met-Hb whereas the rapid rise at tube 13 is due to the rapid loss of oxy-Hb at that tube. Thus, the transmembrane hemoglobin flow detected in the gross assays at 414 mμ appears to represent the sum of distinct molecular subflows. The sharpness of the deoxy-Hb peak suggests that each subflow loss occurs quickly. The breadth of the met-Hb initial peak might then be caused by the presence of multiple met-Hb subflows.

Similarly, the fine structure in the other protein assays might result from distinct molecular subflows of these other proteins. An attempt can be made to separate the suspected subflows, within the resolution of the data, by assuming that each protein subflow forms a sharp loss peak similar in shape to the initial deoxy-Hb peak. A rapid increase in flow rate would then signal the start of a new subflow. Because a rapidly decreasing flow rate occurs shortly after the start of a subflow (see Fig. 10a), subsequent flow starts might be totally obscured or represented only as a reduction in the rate of decrease of the net flow as indicated by the gross assay.

The loss curves can be characterized by the fraction numbers at which these apparent subflow starts occur. As an example of this procedure, consider the loss of Cat in Fig. 6c. This experiment is chosen because AK and Fum were assayed in addition to the routinely assayed K^+, Hb and Cat. The first subflow loss indicated in these incomplete data would occur at or before tube 11. The rate of loss decreases in tube 13, and a new subflow loss occurs in tube 14, which accounts for the increased rate of loss in tube 15. The rate of increase of the transmembrane Cat flow is less in tube 16 than in tube 15 but increases in tube 17 and so signals the start of another subflow loss. Similarly, hypothetical subflow losses start at tubes 20, 22, 24, 26 and 28 and probably at or near tube 30. Other subflow losses would occur at tubes 33, 35 and 38, and this procedure could be contained for the remainder of the data (Fig. 14a). This procedure allows the information contained in the molecular loss curves to be abstracted as the fraction numbers at which the hypothetical flow starts occur.

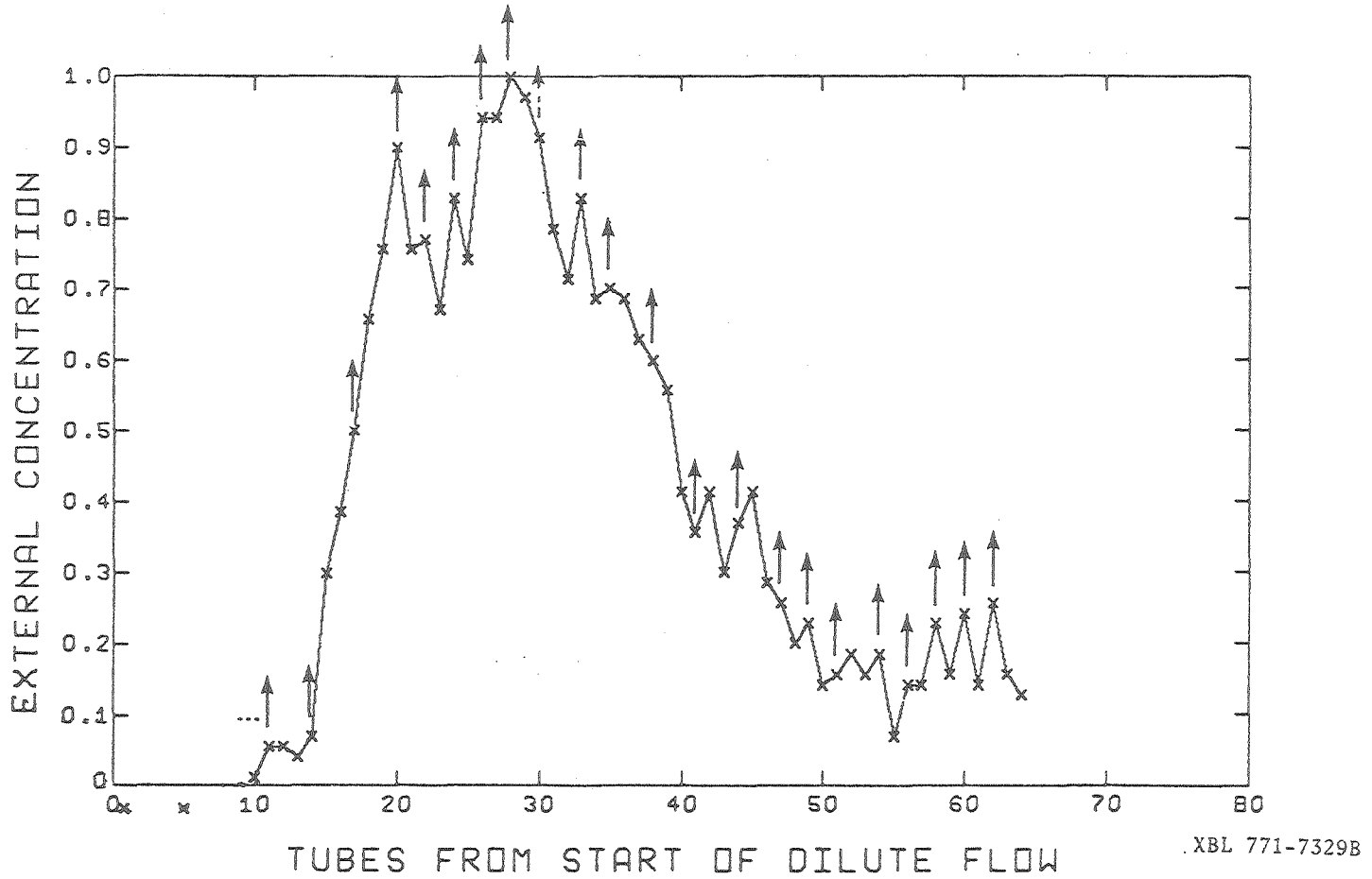

Figure 14. Resolution of molecular loss curves into hypothetical subflow increases and decreases. The Cat data of Fig. 6c are reproduced here with (a) upward-pointing arrows indicating the tube numbers at which hypothetical subflow increases occur, and (b) downward-pointing arrows indicating the tube numbers at which hypothetical subflow decreases occur. Using information contained in the molecular loss curve abstracted as the tube number at which the subflow increases and decreases occur, it is found that the upward-pointing arrows through tube 40 can be paired with downward-pointing arrows beyond tube 40 (see text and Figs. 15 and 16).

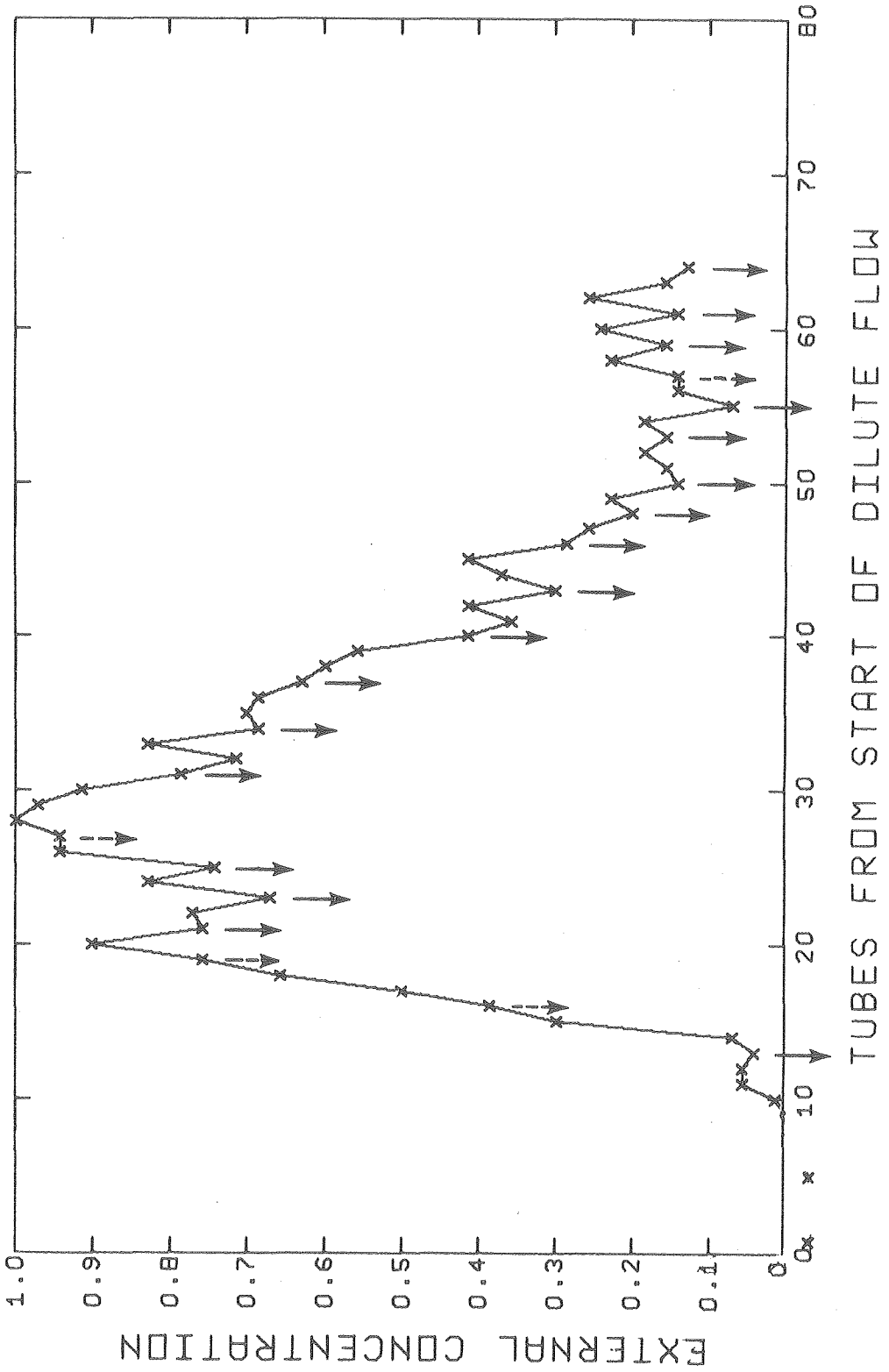

XBL 771-7329C

Figure 14b.

In a similar manner, it is possible to characterize the data by the rapid decreases in the transmembrane flow rate, which might be hypothesized to be the terminations of individual subflows. Continuing on from tube 38 in this manner (Figs. 6c and 14b), the rapid decreases occur in tubes 40, 43, 46, 48, 50, 53 and 55, probably in 57, and in 59, 61 and 63 or 64. It should be noted that, characteristically, there is a flow increase immediately preceding the rapid flow decrease. This will be considered in the Discussion section.

The primary concern at this point is the reproducibility of experiments; however, the relationships between the increases and decreases within a single experiment are examined first. Empirically, it is found that the increases in ascending order and decreases in descending order can be matched increase for decrease for each assay when the ascending and descending series are properly aligned. Furthermore, it is found that this alignment requires the reflection of the loss curves about the same tube number for each assay in a given experiment. This is demonstrated in Fig. 15 where the data of Figs. 5, 6 and 7 are reflected about tubes 39½, 40½ and 40½, respectively. The more certain alignments are indicated by ellipses with their major axes vertical whereas the more tentative alignments are indicated by ellipses with their major axes horizontal. Table IV lists the unmatched increases and decreases within the molecular loss curves. If each increase and decrease during the period of major solute loss is counted as a potential increase-decrease pair, there are 109 possible increases and/or decreases with the alignments shown in Fig. 15. If the alignments indicated by the ellipses about the data points in Fig. 15 are considered reasonable,

Figure 15. Flow increase-decrease alignment is demonstrated both within each molecular loss curve and between experiemnts. The original data from Figs. 5, 6, 7, and 10 have been redrawn so that the data through tube 39 or 40 are as originally presented and are referred to the lower abscissa. The original figures have been folded back upon themselves at tube 39½ or 40½, and tubes 40 or 41 and above are referred to the upper abscissa. Increase-decrease alignment is demonstrated by the vertical lines and ellipses. Ellipses with their major axes vertical encircle more certainly aligned data points whereas ellipses with their major axes horizontal encircle the more tentatively aligned data points. Aligned ellipses intersect the same vertical line.

(a) K^+, Hb and Cat alignments for the data of Figs. 5, 6, 7 and 10. Virtually complete agreement is seen in the tube numbers at which the flow increase-decrease pairs are seen in cells incubated for 3 hrs or less (bottom two rows). Differences become more apparent with longer incubation periods (top two rows; see text). The alignment of the Hb data from Fig. 10 is tentative (see text).

(b) Increase-decrease alignment of AK and Fum data of Fig. 6. See text concerning an interference and probable data error at tube 15 in Fum data.

Note that within a molecular loss curve the flow increases and decreases occur within one tube of each other as aligned in the figure and that similar flow increases-decreases in different experiments occur within one tube of the vertical lines drawn to indicate such similarities. Also note that the Hb loss at about tube 10 or 11 is not seen in fresh cells (bottom two rows) but increases rapidly with prolonged incubation (top two rows; see text). Finally, note that the aligned increases-decreases for K^+, Hb, Cat, AK and Fum do not necessarily occur at the same tube numbers.

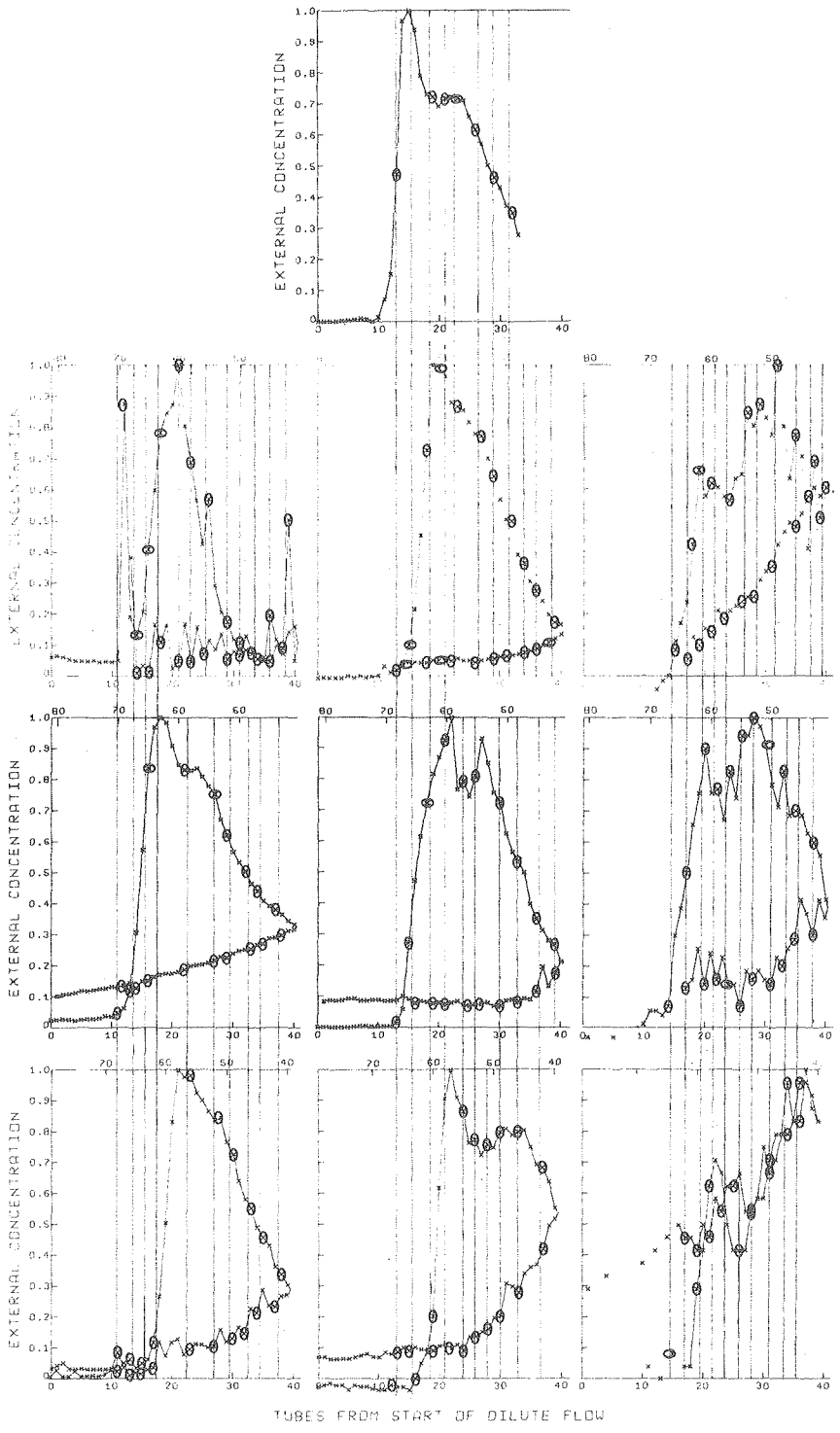

FIGURE 10

FIGURE 7

FIGURE 6

FIGURE 5

Figure 15a

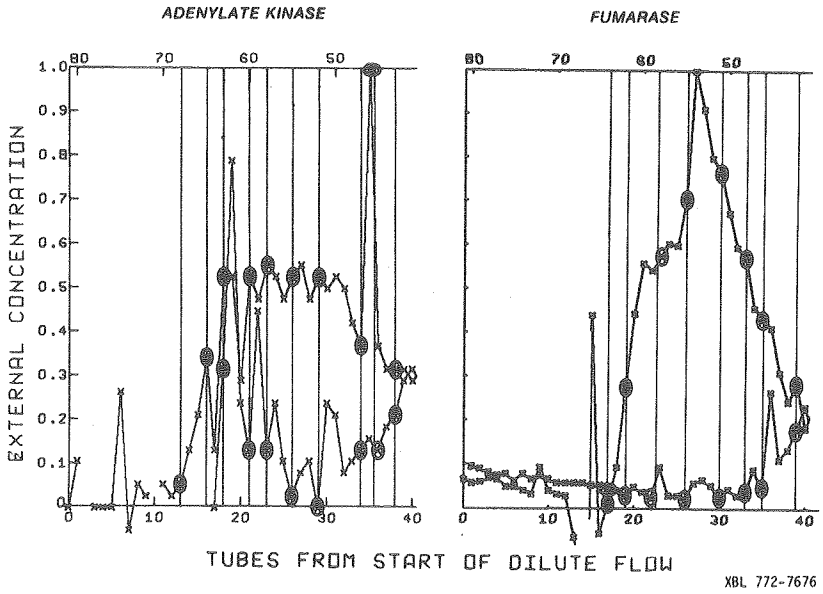
ADENYLATE KINASE
FUMARASE
EXTERNAL CONCENTRATION
TUBES FROM START OF DILUTE FLOW
XBL 772-7676

Figure 15b.

TABLE IV. Increase-decrease alignment within experiments during period of major solute loss.[a]

Figure	Assay	Matched increase-decrease pairs	Unmatched Increase or Decrease: Tube	Increase/decrease	Comment	Maximum number of increase-decrease pairs[b]
5	K^+	10	25	increase	--	12
			60	decrease	Possible matching increase at 19	
	Hb	9	57	decrease	Possible matching increase at 21	10
	Cat	7	56	decrease	Probable matching increase at 23	8
6	K^+	9	24	increase	May be part of increase at 22	10
	Hb	10	--			10
	Cat	10	--			10
	AK	8	31	increase	At limit of resolution of assay	9
	Fum	8	--			8
7	K^+	11	54	decrease	A matching increase at 27 may be obscured by the large increase at 26	12
	Hb	10	--			10
	Cat	10	--			10
Matched pairs		102				
Unmatched increases or decreases				7	Maximum pairs	109

References:

[a] Alignments as drawn in Fig. 15.

[b] With reflection points as indicated in Fig. 15. The maximum possible number of increase-decrease pairs is limited by the data available in 6 of the 11 loss curves (see Fig. 15).

seven increases or decreases are unpaired (Table IV). Of these seven unpaired points, five are consistent with a matching unresolved point, one is probably unpaired, and one is probably a data error (Table IV). Thus, the alignments appear to be significant. The reader interested in examining the data in detail is referred to Figs. 5, 6 and 7 where the original data are presented on a larger scale.

The reference tube numbers obtained from the increase-decrease alignments within each assay can be compared between experiments. This is demonstrated in Fig. 15a where a single vertical line has been drawn to connect similar points observed in the same assay (K^+, Hb or Cat) in independent experiments. Cells incubated for 0 and 3 hrs (Figs. 5 and 6; bottom and adjacent rows, Fig. 15a, respectively) show complete agreement with respect to the approximate tube numbers at which the flow increases-decreases occur in each of the K^+, Hb and Cat assays during the period of major solute loss up to the reflection point of Fig. 5 with two exceptions; the K^+ loss indicated by the line at tube 17½ is not present or is not resolved in the experiment of Fig. 6, and the Hb loss indicated by the line at tube 28 is not observed or is not resolved in Fig. 6. Cells incubated for 5 hrs (Fig. 7; top complete row, Fig. 15a) show complete agreement with the 0- and 3-hr cells during the initial and final stages of controlled gradual osmotic hemolysis. Increase-decrease alignment is observed throughout this experiment, but the tube numbers at which these occur differ from cells incubated shorter times above approximately tube 22 in the ascending series (Fig. 15a). Cells incubated for 29 hrs (Figs. 10 and 15a) appear to agree in alignment with fresh cells in Hb loss through approximately tube 21 although the loss at

approximately tube 15½ was not clearly resolved in the calculated optical density at 414 nm (but see deoxy-Hb in Fig. 10a). The alignment appears to agree with 5-hr-incubated cells through tube 32. This alignment is tentative because it is based only on the Hb assay (other experiments also compared K^+ and Cat) and differs from that assumed by MacGregor and Tobias (1972).

Thus, the tube numbers at which the flow increases-decreases occur are reproducible during the period of major solute loss extending through approximately tube 22 in all of the centrifuge experiments. In cells incubated for 3 hrs or less, there is nearly complete agreement throughout the experiment with the exception that the reflection point may vary (Fig. 15a). The magnitudes of the flow increases-decreases vary considerably, however, between the experiments. This will be treated in relation to the incubation of the cells in the Discussion section.

It should be emphasized from Figs. 15a and b that the flow increases-decreases for the different assays do not necessarily occur in the same collected fractions even within the same experiment.

RED CELL POPULATION HOMOGENEITY

The appearance of complex fine structures in the loss curves is unexpected. The fine structural variations vastly exceed the statistical analytical errors in the K^+, AK, Hb, Cat and Fum assays (Figs. 5, 6 and 7) and in the deoxy-, oxy- and met-Hb simultaneous determinations (Fig. 10; see Table I). The possible contamination of the Fum sample at tube 15 has been previously discussed. Because the K^+, Hb and Cat fine structures demonstrate reproducible subflow increases-decreases in

similar experiments utilizing red cells from different rats (Fig. 15a), the fine structure must result from the interaction of some property of rat red cell populations with the exponentially decreasing external osmolarity. The basic question is whether the fine structure results from the differential osmotic response of distinct subpopulations of red cells or whether it results from a single population distribution response of the majority of the red cells present.

Studies of the frequency distribution of cells lysed in the clinical osmotic fragility test indicate that a single population of cells is observed in the osmotic response of RBC's from a normal mammal (Ponder, 1948a,b). Because the osmotic fragility test lacks the resolution of the present system, however, a matter that will be considered in the Discussion section, further inquiry into the osmotic response of a population of rat RBC's is required.

If the loss of Hb from each red cell was observed to extend over the total time that the population of cells lost Hb, there would be some justification for assuming that a single, homogeneous population of cells was present. Technical difficulties, however, prevented the observation of individual cells while restrained in the centrifuge. Cells were observed while attached to glass and subjected to osmotic stress. Under these heterogeneous conditions where the osmotic stress is modulated by the attachment to glass and flow-induced stresses, individual cells were observed to lose Hb over an extended period of time, which would have included several hypothetical subflow increases-decreases in the high-resolution centrifuge experiments, but the population Hb loss extended over a longer time period than the Hb loss from an individual cell

(Fig. 13). Within the accuracy of the data, however, the osmotic response of the cell population, in terms of Hb loss from individual cells, could be represented as a single population response.

Evidence for the existence of two or more subpopulations in the osmotic response of a normal rat red cell population can be sought through an investigation of factors that are known to effect or might effect osmotic hemolysis. These factors would include, (1) the osmotically active constituents of the red cell, (2) the cell membrane area, (3) membrane area increase at hemolysis and viscoelastic properties of the membrane, (4) membrane permeability to the solutes present, and (5) any additional changes associated with aging of the cells in vivo.

The distribution of total osmotically active constituents of red cells can be investigated by observing the volume distribution of the cells (Jacobs and Stewart, 1947) whereas the distribution of specific molecules can be determined by physical or chemical assays. Because K^+ is the major cation in the rat RBC (Altman and Dittmer, 1974) and because the concentration-dependent behavior of intracellular Hb (Gary-Bobo and Solomon, 1968) and the related effects of pH (Jacobs and Parpart, 1931) and anion exchange (Jacobs and Parpart, 1933; Jacobs and Stewart, 1947; Coldman, Gent and Good, 1970; Wessels and Veerkamp, 1973) are responsible for the nonideal osmotic response of RBC's (Williams, Fordham, Hollander and Welt, 1959; Dick, 1966; Gary-Bobo and Solomon, 1968), these two solutes warrant particular attention.

Cell Surface-Area and Volume Distributions

Both the surface-area and volume distributions of a human's RBC's in isotonic solution are remarkably Gaussian and appear to represent

single population distributions (Canham and Burton, 1968; Canham and Parkinson, 1970; Evans and Fung, 1972; Groom and Anderson, 1972; Jay, 1975). In isotonic solution, RBC's often present a bimodal (Lushbaugh, Bassman and Glascock, 1962) or broad nonGaussian (Weed and Bowdler, 1967) Coulter frequency distribution. These effects arise from the orientation of the cells when flowing through the sensing aperture; the RBC volume itself is normally distributed (Grover, Naaman, Ben-Sasson and Doljanski, 1972), and the bimodal appearance of such distributions, when compared with distributions obtained under slow flow conditions, can be used to quantitate red cell deformability (Mel and Yee, 1975). Several different Coulter distributions can be observed in RBC's from young rats, but only one distribution is observed in the adult Sprague-Dawley rat (Valet et al., 1972). Thus in the adult human and probably in the adult rat, there is a single population distribution of total osmotically active cellular constituents and cell membrane area.

K^+ and Hb Distribution

Duprez and Vignes (1967) determined the K^+ content of individual human RBC's. A histogram of their data suggests that the K^+ content of individual red cells has a remarkably normal distribution.

The red cells from a normal human (Niemi, 1958; Bahr and Zeitler, 1962; Ponder and Barreto, 1955; Abms, 1956; James and Goldstein, 1974), a guinea pig (Gaffney, 1957), or a rat (Adams, 1964; Morselt and Tijmes, 1974) contain a single distribution of total Hb. Rats, however, contain multiple Hb species (Enoki, Tomita and Sato, 1966; Travnicek et al., 1967; Marinkovic and Smith, 1970; Stein, 1971; Stein, Cherian and Mazur, 1971; Travnicek, Borova and Sule, 1971), and a single amino-acid change in a

Hb polypeptide chain can greatly alter the degree of dissociation or aggregation, the oxidation state of the heme iron, and the oxygen affinity of the molecule (Perutz and Lehmann, 1968). The distribution of these multiple Hb's within the rat red cell population is not known. RBC's from human adults who are heterozygotes for Hb's A and F, S and F C and F, β-thalassemia and F (Shepard, Weatherall and Conley, 1962), A and S (Yakulis and Heller, 1964), or A and H (Rigas, Koler and Osgood, 1956) contain both Hb's in every cell, and the amount of each Hb appears to be normally distributed (Shepard, Weatherall and Conley, 1962). In the normal human adult, the minor Hb A_2 is uniformly distributed among all of the cells of the red-cell population as it is in patients with abnormally high levels of A_2 (Heller and Yakulis, 1969). Each stem cell appears to be capable of producing several Hb types with the proper stimulus as has been shown by Garrick et al. (1973) and Nienhuis and Bunn (1974) for the anemia-induced switch from Hb A to Hb C in goats and sheep and by Shepard, Weatherall and Conley (1962) and Dan and Hagiwara (1967) in the switch from human fetal to adult Hb. The apparent uniform distribution of Hb among mammalian red cells is not universal; red cells of the bullfrog *Rana catesbiana* have different Hb contents depending on the organ of origin (Broyles and Deutsch, 1975).

In contrast to the uniform distribution of genetically controlled mammalian Hb's, the presence of fetal Hb (Hb F) can be restricted to a subpopulation of red cells. This is true in the normal human adult (Shepard, Weatherall and Conley, 1962; Dan and Hagiwara, 1967; Boyer et al., 1975) and in individuals with abnormal adult Hb's other than persisting Hb F (Shepard, Weatherall and Conley, 1962). The normal

human adult has less than 0.7% Hb F (Boyer et al., 1975), an amount that would not account for the fine structure of the Hb loss curves.

To the extent that the cellular distribution of rat Hb's parallels that of human Hb's, only the fetal Hb's are likely to be restricted to a subpopulation of the red cells. Stein (1971) found that all fetal rat Hb's are replaced by adult Hb's by three days before birth in several rat species. In contrast, Shaw and MacLean (1971) found four Hb's present in both fetal and adult Wistar rats. In light of the disagreement concerning the presence of fetal Hb's in the adult rat, it is possible that fetal Hb's are present but not uniformly distributed among the red cells of the adult rat. In the normal rat, their quantity is, however, unlikely to be sufficient to account for the fine structure of the Hb loss curves. Thus, to the accuracy required for this work, it is reasonable to assume that both the total Hb and each of the multiple Hb's are uniformly distributed throughout the rat red cell population.

Distributions of Membrane Viscoelastic and Deformability Properties

The RBC membrane can undergo local strains of up to 400% for short durations and exhibits plastic flow resulting in permanent deformation with stresses of longer duration (Evans and La Celle, 1975). An attempt to increase the membrane area with forces greater than 2 dynes/cm^2 results in hemolysis of human RBC's with the duration of the stress required to produce hemolysis dependent on the magnitude of the stress (Rand, 1964). Rand (1964) gave histograms for the time to hemolyze human red cells at two different membrane tensions. The scatter of the data in these micropipette experiments is rather large, but the data are consistent with the presence of a single population in the viscoelastic response of the cells.

Jay (1973) gave a graph of pressures required to suck red cells into a pipette. A histogram of these data appears relatively normal, indicating that membrane deformability is a single population variable. Similarly, Leblond (1972) gave histograms of the pressures required to pull a 1μ tongue of RBC's into a 1.5μ-diameter pipette and the pressures required to pull a cell completely into a 2.8 - 3.0μ-diameter pipette. He found single population distributions for fresh biconcave human red cells (discocytes) and for crenated red cells (echinocytes) produced by the addition of oleate, increasing the pH to 8.5, or suspension in plasma that had been incubated 24 hrs. RBC's incubated for 20 hrs at 37°C in saline to reduce their ATP by 80% were crenated and had at least two distinct subpopulations in the larger forces required to pull the cells completely into the pipette. This effect is apparently partially determined by cellular ATP concentration (see Discussion section), and the ATP concentration of RBC's itself has a single population distribution in fresh RBC's (Lajeunie, 1974; Weed and Bessis, 1974). Thus, the viscoelastic and deformability properties of the membranes of fresh cells (Fig. 5) and cells incubated for short times (Figs. 6 and 7) would be expected to have single population distributions, but metabolically depleted cells might exhibit two or more distinct subpopulations in membrane deformability. The effects of metabolic depletion will be considered further in the Discussion section.

Membrane Area Increase at Hemolysis

The increase in membrane area at hemolysis was studied by Rand and Burton (1963) by photographing individual human RBC's. They found increases of 14 to 28% at hemolysis, depending on the initial shape of

the cell, but Canham and Parkinson (1970), utilizing similar but improved techniques, found no increase in surface area at hemolysis. The most definitive work to date on the area increase prior to hemolysis appears to be that of Evans and Fung (1972), who used interference microscopy to show that human RBC's swollen in 131-mOsm solution retain a single, normally distributed volume distribution but have a membrane area 7.5% greater than that in isotonic solution. The area increase, however, apparently resulted from a sampling error because the areas of individual cells in isotonic and 130-mOsm solutions are the same within the 2% accuracy of the method (Evans and Leblond, 1973). Canham and Parkinson (1970) found no area increase when individual RBC's were gradually swollen and hemolyzed, but the error in their method was larger. The swelling of the cells, however, theoretically limited the area increase to under 9%.

Thus, although only limited data are available concerning the viscoelastic response of the RBC membrane and the possible membrane area increase at hemolysis, these variables appear to be distributed as single population variables.

Membrane Permeability Distributions

The total osmotic contents of the cells might be changed by either loss of cellular molecules or gain of medium molecules prior to hemolysis so that the initial single population distribution of total osmotic constituents might become two or more distinct distributions during the washing and early phases of the experiment because of two or more permeability distributions in the cell population. This is unlikely, however, because Farmer and Macey (1972) found that the population membrane transport

parameters for glycerol and ethylene glycol are independent of cell volume in beef RBC's, and Evans and Fung (1972) found that human RBC's swollen in 131-mOsm Eagle-albumin solution have a single population distribution of cell volumes. Knowledge of permeability distributions appears to be limited to the work of Saari and Beck (1974) who determined the distribution of hemolysis times in solutions of several solutes. Because the time of Hb loss depends on the magnitude of the membrane stress (Rand, 1964) as recognized by Saari and Beck (1975) and because the time of Hb loss depends on the nature of the external solute in a manner different from the permeability pathway to be measured (MacGregor and Tobias, 1972), the permeability distributions of Saari and Beck (1974) must be regarded as tentative. They did, however, account for the entrance of ethylene glycol, propylene glycol, glycerol, and thiourea into human RBC's with log-normal permeability distribution functions. Similar data do not appear to be available for salts, dextrose, or small metabolites. The most that can be said at present is that there is no evidence for two or more permeability distributions for the same solute among the red cells from the same animal.

Summary: A Single Population Distribution in Osmotic Response of Rat RBC's in Controlled Gradual Osmotic Hemolysis

Because no evidence for two or more significant subpopulations was found in the total osmotically active cellular constituents, the cellular salt content, the total cellular Hb, the distribution of Hb species, the membrane area, the membrane area increase at hemolysis, or the visco-elastic and deformability properties of the cell membrane in fresh normal RBC's, it is most unlikely that a differential hemolysis of distinct

subpopulations of cells occurs. Rather, the rat has about 3% reticulocytes (Spector, 1956), and these young rat RBC's, which are osmotically resistant in the clinical osmotic fragility test (Sterling, Greenfield and Price, 1958), gradually become more osmotically sensitive with age.

Data are available that imply that a single population distribution is present; the prolonged loss of Hb observed from individual cells, which suggest that the molecular losses from a single cell spans at least several flow increases-decreases, has been mentioned previously. In NaCl solutions, the 50% loss times for the solutes occur in the order of increasing solute molecular weight (Fig. 9). Large population heterogeneity would tend to obscure such an observation. The separated K^+ and Hb losses in the dextrose experiments (Figs. 12 and 13) require a rather homogeneous cell response even in these filter experiments. The sharpness of the deoxy-, met- and oxy-Hb rises in Fig 10a suggest that one or more homogeneous populations are responsible for these losses but does not indicate that the rises result from the same entire RBC population. Thus, two or more subpopulations of cells do not appear to be present to account for the osmotic response of the cell population. The fine structure of the loss curves most likely arises from a similar response in the majority of cells present.

THE SOURCE OF THE FINE STRUCTURE

A hypothesis concerning the course of controlled gradual osmotic hemolysis must explain (1) the fine structure of each loss curve, (2) the relationships between the fine structures of the various loss curves, and (3) the delay in Hb loss in dextrose solutions over NaCl or LiCl solutions.

Several hypotheses can be advanced to explain the course of hemolysis and to compare hemolysis under different conditions. A number of these will be examined to see if they can explain the results obtained in this work.

It might be hypothesized that holes appear in the cell membrane, which result in bulk flow of all solutes from within the cell, and that the hemolysis of cells at different times causes the appearance of fine structure in the loss curves. The extended period of Hb loss from individual cells excludes the presence of membrane holes until after the completion of Hb loss in this system although holes are often observed in drastic hemolysis (see the Discussion section). In addition, it was previously argued that a differential osmotic response of discrete sub-populations of cells is unlikely. Thus, membrane holes are not consistent with the present data.

If oscillations of the membrane permeability, as a consequence of the viscoelastic properties of the membrane, were to account for the multiple flow starts of each solute, and if diffusion through the membrane and/or unstirred layer were to account for the differences in their times of arrival in the flowing solution, a repeated series of losses should be observed for the various solutes after each increase in membrane permeability. Such a repeated series of losses is not observed (Figs. 15 and 16 top). Thus, simple bulk flow through the membranes does not account for the shape of the loss curves.

The difference between the NaCl or LiCl experiments and the dextrose experiments might be explained by the anion exchange that occurs when the external Cl^- concentration is reduced from 150 mM to about 35 mM. This

change brings about a rapid change in the cellular ion content as the Donnan distribution is re-established (Jacobs and Parpart, 1933; Wessels and Veerkamp, 1973) and, according to the fixed-charge membrane theory, increases passive cation permeability (Passow, 1969). The initial loss of K^+, however, was observed at approximately the same external osmolarity in NaCl, LiCl, or dextrose solutions (Table III); the difference between the external solute concentrations at the time of the initial K^+ loss, 171 and 174 mOsm in dextrose and salts, respectively, is not significant in the filter experiments but is in the direction expected for excess K^+ loss in low ionic strength media. The cells must have had approximately the same critical hemolytic volumes and ion contents under these two conditions, in agreement with Jacobs and Parpart (1933) who found that 2 mM NaCl could reverse the anion shift observed in their work, with Ponder (1933, 1934) who found that RBC's hemolyze at the same critical volume in NaCl, LiCl and dextrose, with Simmons and Naftalin (1976) who found the same hemolytic volume in NaCl and dextrose solutions, and with Seeman, Sauks, Argent and Kwant (1969) who found that the critical hemolytic volume is independent of the rate of hemolysis. The lag in Hb loss in dextrose over NaCl or LiCl solutions, then, is apparently not explained by anion shifts.

Some molecules can physically enter the membrane and increase its surface area (Seeman and Kwant, 1969; Kwant and Seeman, 1969; McBride and Jacob, 1968) or affect membrane molecules, perhaps through an alteration in water structure (von Hipple and Schleich, 1969; Meryman, 1972,1973), and so increase the critical hemolytic volume. As mentioned above, however, the K^+ loss starts at approximately the same external solute

concentration in either dextrose or salt solutions, and the critical hemolytic volume is the same in NaCl, LiCl and dextrose solutions. Thus, the difference between salt and dextrose experiments does not appear to be caused by a difference in membrane structure, at least at the time of the initial K^+ loss. The possible insertion of molecules into the stressed membrane is considered in detail in the Discussion section.

An increase in the amount of K^+ lost by cells in slow versus fast osmotic hemolysis has been observed by Seeman, Sauks, Argent and Kwant (1969) and by Livne and Raz (1971). Both groups attribute the delay in Hb loss in slow osmotic hemolysis to the excess K^+ loss. A similar explanation might explain the difference between the dextrose and salt experiments in this work; however, the K^+ loss starts at the same osmolarity in both dextrose and salt experiments, and although it is true that more K^+ is lost before the start of the Hb loss in dextrose versus salt experiments, the difference is due to the delay in Hb loss, not to a drastic alteration of the K^+ loss. Attributing the difference to the amount of K^+ lost prior to the Hb loss would not answer the question nor would it explain the fine structure of the loss curves.

If dextrose entered the cells at a significant rate, the time to hemolysis in an isotonic solution of dextrose could be used as a measure of the membrane permeability to dextrose (Höber and Ørskov, 1933). Under the conditions of these experiments, rat RBC's did not hemolyze in isotonic solutions of dextrose (Table I), and, in fact, the Hb loss was delayed in dextrose versus NaCl experiments. Thus, the entrance of dextrose into the cells was not responsible, in this sense, for the experimental observations.

Seeman (1973) proposed that the reduction in the Hb diffusion coefficient observed in albumin solutions accounts for the differences in osmotic hemolysis observed in simple salt solutions and in solutions containing macromolecules (Marsden, Zade-Oppen and Johansson, 1957; Lowenstein, 1960; Davies, Marsden, Östling and Zade-Oppen, 1968). It is doubtful that dextrose causes an abrupt change in the Hb diffusion as observed at 7.5% albumin or that this hypothesis explains the difference between dextrose and salt experiments. It is possible, however, as will be subsequently discussed, that some features of osmotic hemolysis in macromolecular solutions result from a slowing in the mixing of the cells with the hypotonic solution owing to the increased viscosity of the macromolecular solutions. Macromolecules also apparently affect osmotic hemolysis through direct interaction with the stressed membrane (see Discussion section).

None of the aforementioned hypotheses explain the fine structure of the molecular loss curves, the relationships between the fine structures of the various loss curves, or the lag in Hb loss in dextrose versus NaCl and LiCl solutions. If, however, it is hypothesized that the stressed cell membranes exhibit molecular sieving properties, these observations are readily explained.

THE MOLECULAR SIEVING HYPOTHESIS

The Stokes-Einstein radii of the stable subunits and aggregates of the proteins studied in this work are summarized in Table V from the literature data compiled in Appendix A and accompanying estimates and calculations. If it is assumed that the initial major flow of a protein

TABLE V. Molecular sizes of ions and molecules employed by this work.

Ion	Crystal ionic radius[a] (Å)	Hydrated Radius[b] Average ± SD (Å)	Hydrated Radius[b] Range (Å)
Li^+	0.68	3.34 ± 2.06	1.74 - 10.03
Na^+	0.97	2.73 ± 1.59	1.49 - 7.90
K^+	1.33	2.19 ± 1.09	1.17 - 5.32

Molecule	Valence	Molecular weight	Estimated Stokes-Einstein radius[c], (Å)
Dextrose		180	3.5[d]
Adenylate kinase	*monomer	22028	22.1
	dimer	44056	27.1
	trimer	66084	31.1
	tetramer	88112	34.2
Hemoglobin	monomer	16115	19.4
	dimer	32230	25.0
	*tetramer	64459	30.8
	octamer	128918	41.7
Fumarase	monomer	48500	28.0
	dimer	97000	34.4
	*tetramer	194000	49.8
Catalase[e]	(Cat/12	19200-19800	20.6[f])
	(Cat/8	28800-29400	23.6[f])
	Cat/4	58100	29.7
	Cat/2	116200	36.4
	*Cat/1	232400	49.2

References:

[a] Weast 1965.

[b] From tabulation of Ling (1962).

[c] See Appendix A, Table A-VI for details concerning estimates of protein Stokes-Einstein radii.

[d] From D_{25} (Weast, 1965) with

$$R_{SE_{20}} = \frac{RT_{20}}{N} \frac{T_{20}}{6\pi D_{25} T_{25} \eta_{25}}$$

[e] Catalase dissociates readily into subunits one-fourth the size of the intact molecule. The size of the smallest subunit is uncertain (Appendix B).

[f] Possible catalase subunits. Polypeptide chains assumed to be of equal size, but fate of the 4 heme groups unknown. See Appendix B.

* equals size of intact protein.

corresponds to its monomer, the second to its dimer, and so forth for the other stable configurations of the protein, the consistent picture shown in Fig. 16 is obtained for all of the proteins studied. This figure interprets the fine structure of the individual protein loss curves as arising from the flow starts of successively larger molecular units of each protein during the initial stages of controlled gradual osmotic hemolysis. Similarly, the flow decreases during the final stages of the hemolytic process result from the successive stopping of these molecular flows. The initial major K^+ flow is indicated in Fig. 16, but the fine structure in the K^+ loss curves will be considered later (see Discussion section). The fine structure of the loss curves for the different proteins is then related by the sizes of the stable configurations of the proteins. The relatively greater stability of the intact protein is reflected in the correlation between the 50% loss times of the molecules in NaCl experiments with the molecular weight of the intact proteins (Fig. 9). Thus, during the initial and final stages of gradual osmotic hemolysis, the red cell membrane appears to be impermeable to molecules larger than a certain size, a size that is a function of time and is here termed the "effective hole size." The fine structure of the protein loss curves is interpreted as resulting from this hypothesized molecular sieving by the stressed rat RBC membranes and the dissociation-aggregation behavior of the intracellular proteins. This hypothesis is essentially that advanced by MacGregor and Tobias (1972).

The use of only a single parameter, the Stokes-Einstein radius, to characterize each protein size unit neglects possible conformational changes. In fact, the conformation of a membrane-associated molecule

Figure 16. Molecular-sieving interpretation of controlled gradual osmotic hemolysis data.

(Top) Flow increases for the data of Fig. 6 as shown in Fig. 15 are indicated by upward-pointing arrows and the lower abscissa. Flow decreases are indicated by downward-pointing arrows and the upper abscissa. In cases where the upward- and downward-pointing arrows do not occur at the same aligned tube number, the flow has been assumed to occur halfway between the increase and decrease as aligned and is indicated by a vertical line. Data are not available beyond the squares for the AK and Cat assays. Note that the flow increases-decreases for the various molecules do not necessarily occur at the same tube numbers.

(Bottom) The estimated Stokes-Einstein radii of the protein subunits and aggregates and the radius of K^+ are indicated by solid lines on the left side of the figure from the data tabulated in Table V. Additionally, tentative estimates of the Stokes-Einstein radii of 4 Hb, 6 Hb, 2 Fum, 1½ Cat and 2 Cat are indicated by dashed lines at 52.7, 60.3, 62.4, 55.8 and 61.5A, respectively. These have been calculated using the hydration of the largest protein size unit for which sedimentation-diffusion data are available (see Appendix A). The expected radius of Cat/8, if it exists (see Appendix B), is indicated by a dashed line. Only minor solute losses occur prior to tube 11 or after tube 70 (Figs. 6 and 15). The initial major loss of K^+ occurs at approximately tube 11½ (see arrows above) and is plotted as a bar extending between two estimates of the radius of K^+. This K^+ loss is accompanied by small losses of AK and Cat, which are interpreted to be the loss of membrane-associated protein (see the Discussion section). The initial major losses of AK and Hb at tube 13 (arrows above) are assumed to be the loss of AK and Hb monomers from the cells and are plotted at the size of the AK and Hb monomers. The Hb loss at tube 15½ is assumed to be the loss of the Hb dimer and is so plotted. Similarly, the other solid symbols correspond to the expected sizes of the proteins for which reasonable size estimates are available (Appendix A and Table V). This procedure is tentatively extended through tube 26 with open symbols using estimated radii of the protein aggregates.

AK aggregates larger than 3 AK are not indicated owing to uncertainty in aggregate size caused by uncertainty in the water of hydration. Aggregates of 4 Hb were not resolved in this experiment (tube 22 or 23) but are apparently resolved in cells incubated for longer times (Fig. 15). Note that the Cat increase at tube 14 would correspond to a protein approximately the size of Cat/8.

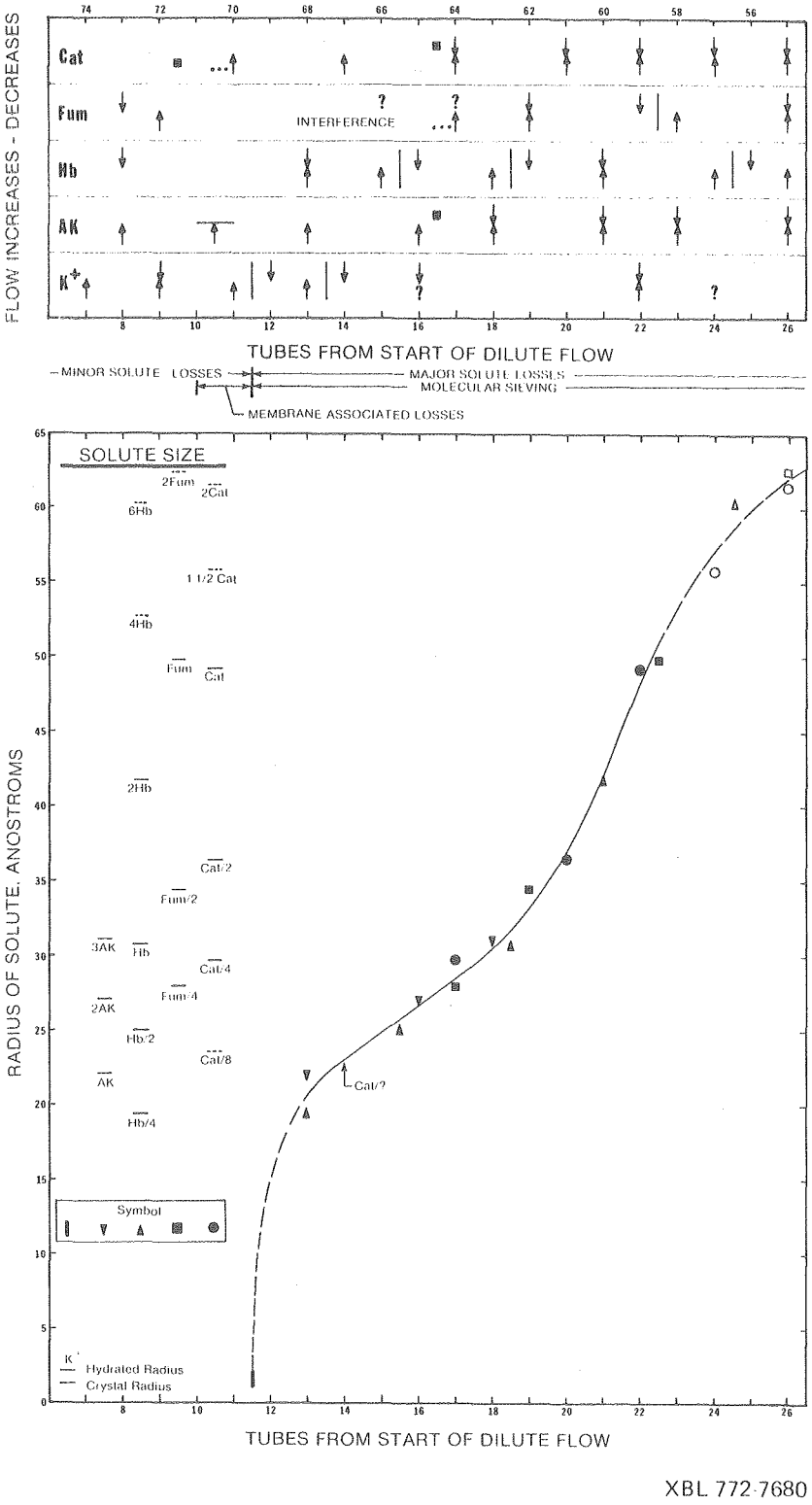

XBL 772-7680

Figure 16

undoubtedly differs from the conformation of the same molecule in aqueous solution (see the Discussion section) and is associated with a change in molecular hydration. The choice of the Stokes-Einstein radius to characterize the size of a protein is itself arbitrary. Other possible parameters include the molecular weight (proportional to mass of molecule), the one-third power of the molecular weight (proportional to the radius of spherical molecule of constant density), the one-half power of the molecular weight (proportional to radius of circular molecule of constant density and thickness), and an average of the crystallographic dimensions of the molecule in cases where such data is available. The selection of the Stokes-Einstein radius is based on its availability and accuracy for most of the protein size units of interest in this work (Appendix A) and on the belief that it reflects some of the conformational constraints that are applicable to both aqueous and nonpolar environments (see below).

Size assignments have not been extended past tube 26 in Fig. 16 owing to the difficulty in distinguishing the different possible conformations of one protein size unit from other possible size units of the same protein. It is possible that, under some conditions of controlled gradual osmotic hemolysis, oscillations in the effective hole size and/or bulk flow occur between the initial and final periods that involve molecular sieving.

DIFFERENCE BETWEEN SALT AND DEXTROSE EXPERIMENTS

The methods used in this work allowed the direct determination of the intracellular solutes lost to the flowing external solution. In contrast, the movement of extracellular solutes into the cells was not measured directly and can be inferred only from their effects on the

loss of intracellular solutes. Thus, the discussion of the differences between salt and dextrose experiments that follows and that will be expanded in the Discussion section will be partially speculative.

Molecular Movements and Osmotic Balance

It has been demonstrated that the loss of K^+ follows a similar course in salt or dextrose solutions but that the loss of Hb is delayed in dextrose solutions beyond its loss in NaCl and LiCl solutions. Table VI compares the composition of the medium and the cells at the time of the initial K^+ and Hb losses and notes the changes that have occurred in the time period between the initial losses of these solutes. The calculations presented are approximate and are based on literature values for the isotonic cell volume and intracellular K^+, Na^+ and dextrose concentrations (see footnotes to table). An isotonic solution was assumed to be 298 mOsm, and the cells were assumed to be perfect osmometers to the time of the initial K^+ loss, after which the critical hemolytic volume was assumed to be constant and equal in NaCl, LiCl and dextrose solutions. Active and passive movements of all solutes, except for passage of Li^+, Na^+, K^+ and dextrose via the stress-induced pathway(s), were neglected as were all metabolic changes. Additional details of the calculations are found in the footnotes to the table. Minor variations from these assumptions do not affect the conclusions to be drawn from the table.

At the time of the initial K^+ loss, the cells have swollen but have not changed in internal composition through gain or loss of solutes so their intracellular solute concentrations are computed on the basis of idealized volume increase of the cells. During the interval between the initial K^+ and initial Hb losses, approximately 1% of the intracellular

TABLE VI. Intracellular and extracellular concentrations in isotonic solutions at the time of initial K^+ and Hb losses, and changes occurring between the initial K^+ and Hb losses in NaCl, LiCl and dextrose solutions.

Time during experiment	Major external solute	Extracellular Concentration: Total (mOsm)	Extracellular Concentration: Na^+ or Li^+ (mM)	RBC volume (μ^3)	Intracellular Concentration: K^+ (mM)	Intracellular Concentration: $Na^+ + Li^+$ (mM)	Intracellular Concentration: Dextrose (mM)
Start: isotonic[a]	NaCl or LiCl	283.[d]	150.	61.[e]	105.[f]	34.[f]	1.2[f]
	Dextrose	312.	38.	61.[e]	105.[f]	34.[f]	1.2[f]
At initial major K^+ loss[b]	NaCl or LiCl	174.[g]	91.	104.[h]	61.[i]	20.[i]	0.7[i]
	Dextrose	171.[g]	36.	104.[h]	61.[i]	20.[i]	0.7[i]
At initial major Hb loss[c]	NaCl or LiCl	167.[e]	88.	104.[j]	61.[k]	$20+N_s$[m]	0.7
	Dextrose	151.[g]	36.	104.[j]	52.[l]	$20+N_d$[n]	0.7+D[o]

	Major external solute	Extracellular concen. (mOsm)	Intracellular Concentration[p]: K^+ (mM)	K^+ (mOsm)	$Na^+ + Li^+$ (mM)	$Na^+ + Li^+$ (mOsm)	Dextrose (mM=mOsm)	Osmotic stress increase[q] (mOsm)
Changes occurring between initial major losses of K^+ and Hb	NaCl or LiCl	7.	0.	0.	N_s	$1.88N_s$	0.	$7+1.88N_s$
	Dextrose	20.	-9.	-17.	N_d	$1.88N_d$	D	$3+1.88N_d+D$

References:

[a] The concentration at which rat RBC's are the same size as in rat plasma was not determined. In calculations, the average of the salt and dextrose concentrations, 298 mOsm, was used. An osmotic coefficient of 0.94 for NaCl and LiCl and 1.00 for dextrose was used throughout. The external K^+ concentration was less than 1 mM at all times in all experiments and is not tabulated (see Figure Captions).

TABLE VI (continued)

[b] Calculations at the time just prior to the stress-induced increase in cation permeability.

[c] Calculations at the time just prior to the initial major Hb loss.

[d] The solutions for the low resolution filter experiment of Fig. 11 contained, in addition, 5 mM dextrose (Table I), which raised its calculated osmotic pressure to 288 mOsm (Table III).

[e] Altman and Dittmer, 1974, p.1851.

[f] Coldman and Good, 1967.

[g] From Table III.

[h] Calculated from the isotonic volume (61 μ^3) assuming perfect osmometer behavior between isotonic solution (298 mOsm) and the initial K^+ loss in salt solutions (174 mOsm). The same volume has been used for the dextrose experiments since the critical hemolytic volume is the same in NaCl, LiCl, and dextrose.

[i] Calculated from isotonic cell volume and concentration, and cell volume at initial K^+ loss. Since the initial K^+ loss occurs at 171 mOsm in dextrose but at 174 mOsm in salt solutions, there may have been an additional loss of 1.5 mM cation, plus accompanying anion, in dextrose experiments.

[j] The critical hemolytic volume was assumed to be constant and equal to the volume calculated at the initial K^+ loss.

[k] In salt solutions, there was less than a 1% loss of K^+ prior to the initial Hb loss.

[l] In dextrose solutions, there was an approximate 15% loss of K^+ prior to the initial Hb loss.

[m] N_s is the net change in intracellular $Na^+ + Li^+$ in salt experiments between the initial flows of K^+ and Hb.

[n] N_d is the change in intracellular Na^+ in dextrose experiments between the initial flows of K^+ and Hb.

[o] D is the amount of dextrose to enter the cells in dextrose experiments between the initial flows of K^+ and Hb.

[p] Cation movements were assumed to be accompanied by anions and an osmotic coefficient of 0.94 was used for NaCl and LiCl.

[q] Critical hemolytic volume was assumed to be constant and equal in salt and dextrose solutions and only movements of Li^+, Na^+, and K^+, with accompanying anions, and dextrose were considered (see notes *h*-*p*).

K^+ was lost in salt experiments, but approximately 15% was lost in dextrose experiments. These changes are reflected in the reduced intracellular K^+ concentration at the time of the initial Hb loss (Table VI).

Just prior to the initial major K^+ loss, the cells contained approximately 20 mM Na^+ but virtually no Li^+. At this time, the external solute concentration was approximately 91 mM in Na^+ and Li^+ in the NaCl and LiCl experiments, respectively, but, because of the higher internal Na^+ concentration, the driving force on Li^+ was larger than on Na^+ at the same time in the separate experiments. The course of the experiment was, however, similar in LiCl and NaCl solutions during the initial stages. Thus, the net movement of salts across the stressed membrane must not be highly dependent on the concentrations of the individual salts but rather seems to depend on the total external monovalent cation concentration.

Between the initial K^+ and Hb losses in salt solutions, the external solute concentration decreased by 7 mOsm, the intracellular K^+ concentration changed little, and an unknown amount of Na^+ left the cell while an unknown amount of either Na^+ or Li^+ entered the cell. This net unknown movement of Na^+ or $(Na^+ + Li^+)$ into the cells is N_s. Because the total external cation concentration, approximately 91 mM, is larger than the total internal monovalent cation concentration, approximately 81 mM, because the external cation has a greater concentration than the same cation within the cell, approximately 20 mM for Na^+ and 0 mM for Li^+, and because, if the membrane were permeable to cations but not to Hb, the establishment of a Donnan equilibrium would lead to higher intracellular than extracellular concentrations, N_s is likely to be positive. Because only about 1% of the intracellular K^+ crossed the membrane between the

start of the initial K^+ and Hb losses, Ns is, however, likely to be a small positive value. Thus, under the conditions of the salt experiments, an increase of approximately 7 mOsm beyond the stress at the time of the initial K^+ loss was required to cause the initial Hb loss, provided the cell volume remained constant.

The experiments in dextrose involved the unknown movements of sodium, N_d, and dextrose, D, between the initial K^+ and Hb losses (Table VI). Because the external Na^+ concentration is 36 mM and the internal Na^+ concentration is 20 mM, it would be expected that Na^+ would enter the cell although the net cation movement ($K^+ + Na^+$) would be out of the cell. N_d is likely to be positive, but, because 15% of the intracellular K^+ is lost between the initial K^+ and Hb losses, its magnitude may be significant.

Comparison of the salt and dextrose experiments at the time of the initial Hb losses shows that the stress caused by the decrease in the external solute concentration during the interval between the initial K^+ and Hb losses was 7 mOsm in the salt experiments but 20 mOsm in dextrose experiments. The loss of intracellular K^+, together with an accompanying anion, reduced the stress by 17 mOsm in dextrose experiments but had no significant effect in salt experiments. Thus, the decrease in external solute concentration and loss of intracellular K^+ cause a net osmotic stress of 7 and 3 mOsm in salt and dextrose experiments, respectively.

If the same increase in membrane stress, beyond that required to cause the initial K^+ loss, is required to cause Hb loss in both salt and dextrose experiments, the following relationship is obtained between the unknown quantities N_s, N_d, and D (Table VI):

$$7 + 1.88\ N_s = 3 + 1.88\ N_d + D$$

where the factor 1.88 results from the assumed osmotic coefficient of 0.94 and an anion accompanying any cation movement. Because N_s is likely to be small, its value can be neglected and D is given by $D \simeq 4 - 1.88\ N_d$. It is unlikely that dextrose is lost to the extracellular solution because the external dextrose concentration varies from 103 to 83 mM between the initial K^+ and Hb losses in dextrose experiments but is only 0.7 mM within the cells. Thus $0 \leqslant D \simeq (4 - 1.88\ N_d)$. Because N_d is likely to have a significant positive value, we conclude that D has a small value; that is, little if any dextrose enters the cells prior to the initial Hb loss.

Unspecific Monovalent Cation Model

It is proposed that the basic difference between the salt and dextrose experiments is a lag in the entrance of dextrose into the cells compared to the entrance of monovalent cations. The exact nature of the delay and the kinetics of entry are not important to this argument, but it is useful to consider a specific model for the entrance of cations through the stressed cell membranes.

It is hypothesized that the monovalent cations Li^+, Na^+ and K^+ cross the stressed rat RBC membranes via the same pathway and with the same linear kinetics; that is, during a given time interval, the quantity of a cation that moves across the membrane from side A to side B is given by a constant multiplied by its initial concentration on side A, the constant being the same for all monovalent cations and for movement across the membrane in both directions. Table VII summarizes the predictions of this specific hypothesis. Because about 1% of the

TABLE VII. Calculated osmotic balance if cation transport is unspecific and is linearly related to cation concentration.[a]

Major external solute	$Li^+ + Na^+ + K^+$ Concentration at initial K^+ loss			K^+ loss between initial K^+ and Hb losses (%)	Net intracellular cation increase w/linear, unspecific transport (mM)	Increase in Osmotic Stress Between Initial Losses of K^+ and Hb			
	External (mM)	Internal (mM)	Ext-Int (mM)			External solute[b] (mOsm)	Internal salt[c] (mOsm)	Dextrose (mM=mOsm)	Net increase (mOsm)
NaCl or LiCl	91.	81.	10.	1.	+0.1	+7.	+0.2	0.	+7.2
Dextrose	36.	81.	-45.	15.	-7.	+20.	-13.	D	+7+D

References:

[a]The same assumptions regarding cell volume, intracellular concentrations, critical hemolytic volume, and solute losses that are made in Table VI are made here.

[b]From Table VI.

[c]An anion was assumed to accompany each cation and an osmotic coefficient of 0.94 was used.

intracellular K^+ was lost between the initial K^+ and Hb losses in salt experiments, it was assumed that $0.01[Na^+]$ or $0.01[Na^+ + Li^+]$ cross the membrane during this time period, causing an additional 0.2-mOsm stress across the membrane (N_s = 0.1 mM) and a total membrane stress of 7.2 mOsm. A similar calculation for the dextrose experiments, using the 15% K^+ loss, yields a total stress of (7 + D) mOsm. If it is again assumed that the same increase in membrane stress is required beyond the initial K^+ loss to cause the initial Hb loss in both salt and dextrose experiments, this hypothesis leads to 7.2 = 7 + D or $D \simeq 0$; that is, dextrose does not significantly enter the cells prior to the initial Hb loss.

Under this hypothesis, the cells in NaCl or LiCl experiments lose K^+ but gain a slightly greater quantity of the external cation owing to the higher external than internal monovalent cation concentrations. The cells in dextrose experiments have an intracellular monovalent cation concentration higher than the external solution and lose a total of 7 mOsm by salt loss between the initial K^+ and Hb losses. Because the K^+ loss causes a 17-mOsm decrease in intracellular concentration (Table VI), there was, however, a net gain of 10 mOsm owing to the entrance of Na^+ into the cells. Under this hypothesis, $1.88\ N_d = 10$, or $N_d = 5.3$, which confirms that N_d has a significant positive value in this model. Thus a simple, nonspecific, cation-transport model can explain the similarity between NaCl and LiCl experiments and the difference between NaCl or LiCl and dextrose experiments and leads to the calculation that little, if any, dextrose enters the cells prior to the initial major Hb loss.

Salt and Dextrose Experiments

The difference between the course of the experiment in salt and dextrose solutions is seen to be due primarily to differences in the entrance of the external solutes, the loss of intracellular K^+, and the continually decreasing external solute concentration. The basic difference is, however, the difference in the time of entrance of the external solute; if the entrance of dextrose followed the kinetics of the entrance of Na^+ or Li^+, the experiments would have been identical except for anion movements. Instead, the entrance of dextrose was delayed compared to Na^+ and Li^+, which allows K^+ to escape and to partially compensate for the continuing decrease in external concentration.

The important point in this discussion is that, regardless of the details of the model, in some fashion the entrance of dextrose is delayed compared to monovalent cations. The reason for this delay is not evident from the data. The dextrose permeability may increase at the time of the stress-induced K^+ permeability increase, which presumably is approximately the time of the Na^+ and Li^+ permeability increases, but the magnitude of the dextrose permeability may be much smaller than the cation permeabilities, or dextrose might be totally excluded from the stress-induced pathway(s) at least until the time of the initial Hb loss.

Thus, it would appear that stressed rat RBC membranes are capable of molecularly sieving molecules covering the size range from monovalent cations through dextrose and at least through the proteins studied. The specific interactions that result in each solute crossing the membrane need not, however, be the same for all of the solutes, and care must be exercised in extending these results to other molecules. Specific models

of the stress-induced pathway(s) will be considered in the Discussion section.

SUMMARY

If it is hypothesized that stressed rat red blood cell membranes are capable of molecular sieving and that the effective hole size increases during the initial stages of controlled gradual osmotic hemolysis and decreases during the final stages of controlled gradual osmotic hemolysis, the fine structure of each protein loss curve and the relationship between the fine structure of the loss curves of the different proteins are explained by the size of the various subunits and aggregates of the intracellular proteins. The difference between experiments conducted in salt and dextrose is explained by the delayed entrance or reduced rate of entrance of dextrose compared to monovalent cations. Although the movement of monovalent cations and dextrose across the stressed cell membranes might be explained by the increase in effective hole size during the initial stages of controlled gradual osmotic hemolysis, the mechanisms involved and the question of whether the membrane is actually controlling the passage of these solutes by molecular sieving remain unanswered. These points will be considered further in the Discussion section.

DISCUSSION - EXPERIMENTAL RESULTS

OSMOTIC HEMOLYSIS SYSTEMS

In a study of osmotic hemolysis under ideal experimental conditions, the external solution concentration would be homogeneous throughout the system and would be changed in time in a known, controlled manner. This would reduce the experimental variations to those inherent in the cell population studied. In spite of this obvious consideration, traditional studies of osmotic hemolysis have employed grossly heterogeneous conditions.

When red cells in plasma or saline are added to a large volume of dilute medium as in the common osmotic fragility test (Fig. 17), the cells are exposed to large and varying concentration gradients during the process of mixing. Different cells see different time-varying, external solute concentrations. These heterogeneous conditions may partially account for the heterogeneous properties of ghosts obtained by such drastic procedures (Hoffman, 1962; Bodemann and Passow, 1972; Theodore and Robin, 1965).

If, instead of adding the cell suspension to the medium, the medium is added to the cell suspension (Fig. 17; Seeman, Sauks, Argent and Kwant, 1969; Livne and Raz, 1971), similar heterogeneous conditions are obtained, but improved control is possible over the gross rate of change of the external solute concentration.

The dialysis method of gradual osmotic hemolysis (Fig. 17; Danon, Nevo and Marikovsky, 1956) lowers the solute concentration by loss of solute over the larger area of a dialysis sac and so presumably has smaller local concentration gradients than either of the two previous

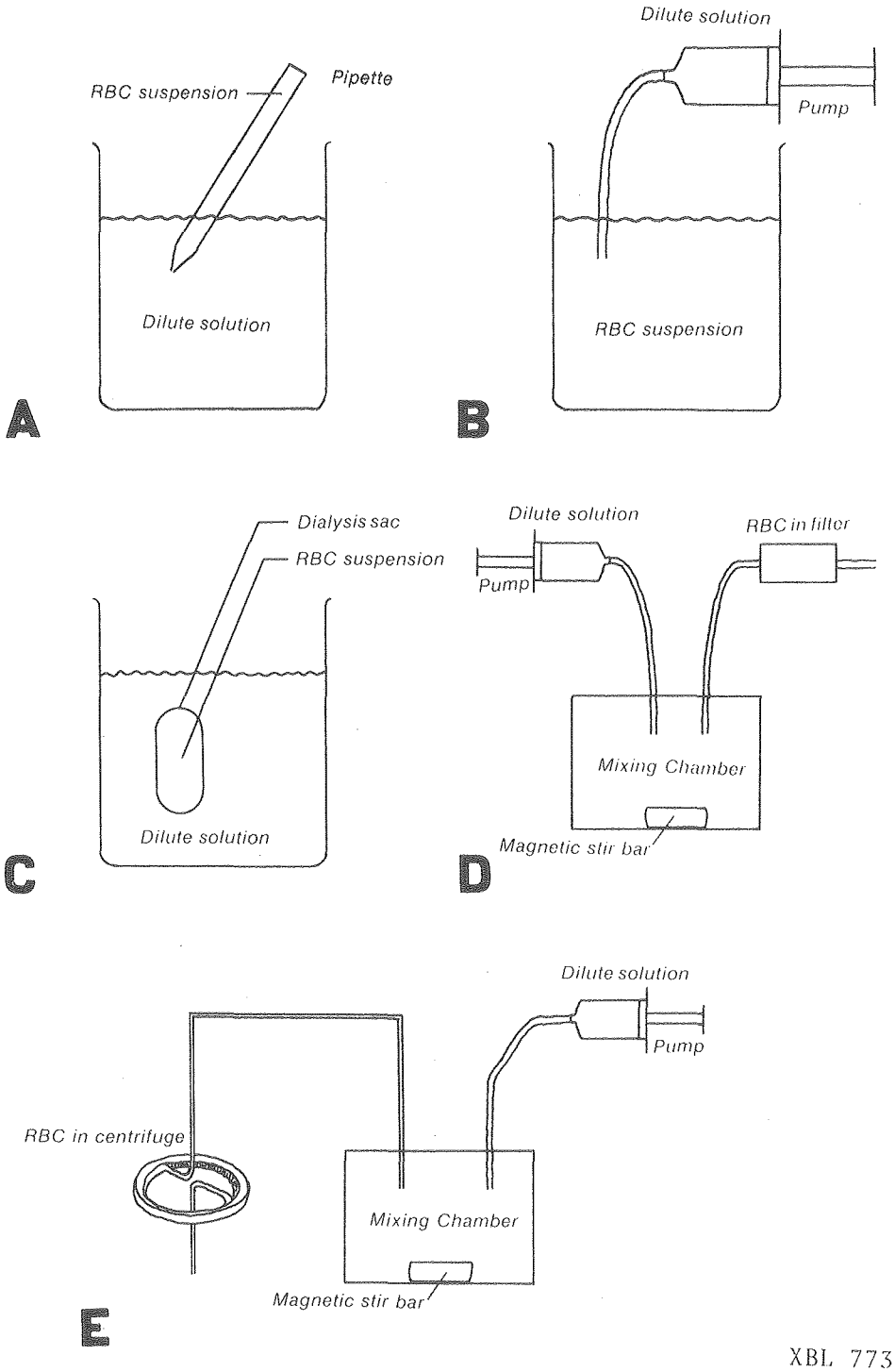

XBL 773-7920

Figure 17. Osmotic hemolysis systems.

A Drastic osmotic hemolysis
B Osmotic hemolysis by addition of dilute medium to cell suspension
C Dialysis method of gradual osmotic hemolysis
D Controlled gradual osmotic hemolysis using filters to restrain cells
E Controlled gradual osmotic hemolysis using centrifuge to restrain cells.

Drastic osmotic hemolysis exposes the cells to grossly heterogeneous conditions whereas controlled gradual osmotic hemolysis in the centrifuge exposes them to more uniform conditions. The heterogeneity of conditions and their effect on osmotic hemolysis are discussed in the text.

methods. Cells near the dialysis sac see different concentrations than cells near the center of the sac, and the cells tend to settle onto the bottom of the dialysis sac. If a stirrer is added, variable mechanical forces are imposed in addition to the osmotic stress.

If analysis of an osmotic experiment requires separation of the cells from the medium, additional stresses may be imposed on the cells. Davson and Danielli (1938) have shown that centrifugation of RBC's cause a K^+ leak from the cells of several species during the time of centrifugation. This observation has been confirmed by Sieberth (1971) for human RBC's and by the author for rat RBC's but conflicts with the observation of Savitz, Sidel and Solomon (1964) who found that centrifugation does not cause loss of K^+ from human RBC's. The observed K^+ loss presumably arises from membrane stress so that, if the progress of an osmotic experiment is followed by sampling as a function of time and this sampling involves centrifugation, an additional stress is applied at the sampling time. The effect of this pulse of separation stress is likely to vary during the course of the hemolytic procedure and thus complicate the interpretation of the experiment. It therefore seems prudent to avoid the use of a pulse-type separation force when studying the process of osmotic hemolysis.

In this work, methods were developed to osmotically stress each cell in the population in a manner as similar as possible to that for every other cell in the population and to have the stress across the entire cell membrane of each individual cell as uniform as possible. These ends were achieved primarily by pre-adjusting the flow solution composition prior to contact with the cells and by changing the composition gradually (Fig. 1).

The assays employed in this work required separation of the cells from the medium. A continuous rather than pulse-type separation force was used to restrain the cells throughout the experiment. The glass filters appeared to stress the cells at isolated membrane points, and the magnitude of the force appeared to vary with the varying local flow rate through the filters. This heterogeneous stress modulated the osmotic stress. The centrifuge applied a volume restraining force that varied gradually as the density of the medium and cells gradually changed. The increased fine structure of the centrifuge experiment loss curves over the filter experiment loss curves attests to the more uniform conditions within the centrifuge. This high degree of uniformity in the experimental conditions allowed the observation of fine structure in the loss curves obtained from a population of red cells. Because the effect of unstirred layers would be to obliterate this fine structure, a discussion of the effects of unstirred layers will not be presented in this report as it does not further elucidate the basic causes for the appearance of the fine structure.

The flow methods employed had the additional advantages of continuously removing the products of hemolysis so as to lessen their effects on the subsequent course of the hemolytic procedure (Paysant and Polonovski, 1971) and of permitting the direct measurement of the amount of solute that transverses the cell membranes into the external solution during each fraction collection period. Results from methods that measure only the total amount of solute liberated as a function of time must be differentiated to obtain data comparable with the present method. Ponder (1948a) and Suess et al. (1948) noted that data are more easily compared when plotted as obtained directly by the present method and that

sufficiently accurate data with the osmotic fragility test to permit its differentiation are difficult to obtain.

RED CELL RESPONSE AS A FUNCTION OF THE HEMOLYTIC SYSTEM

The results of an osmotic hemolysis experiment depend on the details of the experimental procedure used to lyse the cells because these details determine the external solute concentration(s) seen by each cell at every instant during the hemolytic experiment. Drastic hemolysis is characterized by large membrane defects (Seeman, 1967; Huhn, Pauli and Grassman, 1970; Seeman, Cheng and Iles, 1973), by bulk flow of Hb and other intracellular solutes from the cells, often from a single spot on the membrane with sufficient force to propel the cell in the opposite direction (Heedman, 1958; Danon, 1961; Kochen, 1964; Perk, 1966), and by equilibrium concentrations of Hb across the membrane at the conclusion of hemolysis (Hoffman, 1954; Hoffman, Eden, Barr and Bedell, 1958; Whitaker et al., 1974). At the conclusion of the hemolytic procedure, the membrane is impermeable to K^+ and Hb if the hemolysis has been conducted under proper conditions (Hoffman, 1958, 1962; Bodemann and Passow, 1972; Lepke and Passow, 1972).

This work has confirmed that, under the most gradual osmotic conditions, no local solute losses can be observed with a light microscope (Danon, 1961) and that, rather, the membrane exhibits molecular sieving properties (MacGregor and Tobias, 1972), and has demonstrated that equilibrium concentrations of Hb are not found across the membrane at the conclusion of the hemolytic procedure.

Intermediate conditions such as the dialysis method developed by Danon (Danon, Nevo and Marikovsky, 1956) produce cells with intermediate

properties; the cells apparently have smaller holes than under drastic hemolytic conditions (Seeman, 1967), but Hb equilibrium is still obtained between the intra- and extra-cellular compartments (Klibansky, De Vries and Katchalsky, 1960).

An intriguing result is obtained when cells are subjected to drastic hemolysis in the presence of the macromolecular solutes albumin, dextran, ficoll or polyethyleneglycol. At the conclusion of hemolysis, Hb equilibrium is not reached (Marsden, Zade-Oppen and Johansson, 1957; Lowenstein, 1960; Davies, Marsden, Östling and Zade-Oppen, 1968), a result that is characteristic of gradual conditions. Zade-Oppen and Laurent (1963) proposed that this alteration was caused by the precipitation of nonhemoglobin red cell proteins, and Seeman (1973,1974) suggested that the alteration is caused by a reduction in the rate of diffusion of Hb, which results from the extensive hydration of the macromolecules, and a resulting decrease in the solvent volume accessible to Hb. An alternative suggestion arising from this work is that the more viscous macromolecular solutions reduce the local rate of mixing of the cells and media so that the drastic procedure is slowed enough to produce gradual conditions. In addition, these macromolecules appear to interact directly with the membrane and to increase membrane stability through their influence on the solvent properties (structural properties) of water. These interactions are considered in detail in connection with a proposed mechanism for controlled gradual osmotic hemolysis (see below).

ASSAYS, MEMBRANE ASSOCIATION, AND SOLUTE EFFECTS

The fine structure of each of the protein loss curves has been interpreted as the flows of monomers, dimers and other stable configura-

tions of the protein through the stressed cell membranes into the flowing external solution. It has been tacitly assumed that the proteins within the cell are initially in solution and that various size units of the protein are present and are in a concentration equilibrium or at least a steady state. As will be noted in the discussion that follows, whereas the bulk of the proteins studied are probably in solution within the cells, a portion of most of the proteins appears to be associated with the cell membrane. It will be subsequently shown that these membrane-associated proteins show small losses before the start of their major loss from the cells and that the magnitude of these early losses increase with the duration of incubation of the cells prior to the experiment.

It has also been assumed that the assays detect all size units of the protein assayed; however, catalase and fumarase monomers and dimers are probably not detected if present at the time of the assay (see below). For this reason, the samples were maintained at 4°C for at least one day prior to these assays to permit re-association of these molecules. It was not determined whether concentration equilibriums had been obtained between these various subunits and aggregates of catalase and fumarase within this time period.

Adenylate Kinase

AK monomers and aggregates are catalytically active, but the relative activities of the different size units is not known (Sapico, Litwack and Criss, 1972). The rapid equilibrium between the various sizes of AK aggregates (Criss, Sapico and Litwack, 1970) suggest that all fractions would have had a similar aggregate distribution for each isozyme by the time of assay, although the distribution might be dependent on the total

AK concentration in each fraction (Klotz, Darnall and Langerman, 1975).

Some cellular AK (several percent) is associated with human, rabbit, bovine and porcine RBC membranes (Kashket and Denstedt, 1958; Ronquist, 1969; Heller and Hanahan, 1972) and is presumably similarly associated with rat RBC membrane. The enzyme is extracted with other membrane proteins from ghosts (Nilsson and Ronquist, 1969), is loosely bound in that all detectable activity can be removed from the membranes in 5 to 6 washes, and appears not to be specifically bound to the membrane (Cerletti and DeRitis, 1962). Klethi and Mandel (1968) have shown that multiple AK isozymes are present in rat RBC. If the RBC multiple AK isozymes have a distribution similar to that of rat liver AK isozymes (Criss, 1970), only one of the isozymes is highly membrane-associated.

Hemoglobin

In the centrifuge experiments, Hb was assayed by direct measurement of the optical density in the Soret band (Table I). Absorbing species other than Hb were not considered, and, when assayed at 414 mμ, errors introduced by variations in the amount of Hb in states other than oxy-Hb were not considered. The recombination of Hb subunits was probably sufficiently fast that equilibrium was established between Hb and its subunits by the time of the assay (Antonini et al., 1966; Antonini, Brunori and Anderson, 1968). If this were not the case, large errors would not be introduced by the presence of Hb monomers because the isolated oxy-monomers have the same absorption as the intact oxy-tetramer, and the absorption of the isolated deoxy-monomers differ from the deoxy-tetramer by a maximum of 15% in the Soret band on a heme basis (Antonini et al., 1965,1966; Brunori et al., 1968). Because of the high extinction coefficient of Hb

in the Soret band (Table II), and the high Hb concentration within the cells, the assays should have been relatively specific for heme-containing Hb. Heme-deficient Hb's would have been underestimated by these assays.

The multiple rat Hb types and their probable uniform distribution among the red cell population was previously discussed.

Hb appears not to be a structural constituent of the red cell membrane because ghosts can be prepared that contain less than 0.5% Hb on a dry weight basis with negligible loss of membrane lipid (Dodge, Mitchell and Hanahan, 1963; Weed and Reed, 1964; Hanahan, Ekholm and Luthra, 1974). Nevertheless, Hb is reversibly bound to the cell membrane (Dodge, Mitchell and Hanahan, 1963; Mitchell, Mitchell and Hanahan, 1965; Duchon and Collier, 1971). Klipstein and Ranney (1960) found that human red cell membranes preferentially bound the most basic Hb that the cells contained (Hb A_2 over A, S over A, and C over S) but that rabbit RBC's, which do not contain a basic Hb, do not preferentially bind a specific Hb. Mitchell, Mitchell and Hanahan (1965) could not confirm the selective binding of A_2 in human red cells that contained both Hb A_2 and A. This discrepancy was resolved by Fischer et al. (1975) who found similar binding for Hb A and S at low Hb concentrations but saturation levels that increased in the order Hb A, S, A_2 at more physiological concentrations. Wasemiller, Abrams and Bakerman (1968) isolated an Hb-binding protein from human red cell membranes. The direct interaction of Hb with membrane lipids is discussed below.

Some Hb pathologies result in the precipitation of Hb degradation products (Kusumoto and Nakajima, 1968) within the cell, their attachment to the cell membrane as Heinz bodies and hemolysis. Rentsch (1968)

argued that there is no correlation between the formation of met-Hb and the formation of Heinz bodies. Jacob (1970) argued persuasively, however, that the loss of heme from the β-chain of unstable Hb's (see Carrell and Lehmann, 1969) results in the precipitation of the denaturing β-chains as Heinz bodies and that this process is potentiated when the heme iron is oxidized to met-Hb (Jacob and Winterhalter, 1970). When the β-heme is lost, the β-93 sulfhydryl becomes more reactive, and Jacob (1970) suggested that mixed disulfide linkages might bind the denaturing Hb of Heinz bodies to the membrane. This binding of denaturing Hb would then be responsible for the hemolysis observed in individuals with an unstable Hb.

In this work, small but significant losses of Hb were observed near tubes 6 and 10 in the centrifuge experiments. The magnitudes of these losses tended to increase with the duration of incubation in saline (Fig. 15), and the loss observed at tube 6 with fresh cells (Fig. 5b) can be resolved into separate components at tubes 5 and 7 with cells incubated 5 hrs or longer (Figs. 7b and 10a). The losses at tubes 5 and 7 from cells incubated 29 hrs are enriched in met-Hb and to a lesser extent in deoxy-Hb compared to the total Hb composition (Fig. 10a). Similarly, the losses that start in tubes 10 and 11 are heavily enriched in met- and deoxy-Hb. It was previously argued that the minor Hb species are probably uniformly distributed among the rat red cells and that the osmotic response of a red cell population is quite uniform in centrifuge experiments. It will be argued below that the losses near tube 6 and at about the time of the initial K^+ loss, about tube 10 in this experiment (see Fig. 15), result from the loss of membrane-associated molecules.

If this is true, the rat RBC membrane appears to preferentially bind met- and deoxy-Hb components of the total rat Hb. Because one or more minor Hb components might be both more basic and have a larger percentage as met- and deoxy-Hb than the bulk of the Hb, these data do not elucidate the binding interactions between Hb and the membranes.

Catalase

Cat has been shown to be present in every RBC (Schedel, Fischer and Suter, 1974). Its subunits are present in normal red cells, and their amount increases during storage at 4°C (Aebi et al., 1974). Some, probably all, Cat subunits lack catalase activity (Shibata, Higashi, Hirai and Hamilton, 1967; Aebi, Scherz, Ben-Yoseph and Wyss, 1975), and the activity of the intact molecule appears to depend on the number of disulfide bonds present (Hermel and Havemann, 1966). In this work, incubation of the samples prior to assay presumably allowed the subunits to reassociate and to be assayed as intact molecules. Catalase also aggregates by the addition of successive Cat/4 subunits to the intact molecule (Diezel et al., 1970). Aggregates of two Cat molecules are readily apparent (Fig. 16) (Diezel et al., 1972).

Rodent (Davydova, Shapot and Drozdova, 1970; Holmes, 1972; Jones and Masters, 1972) and human (Krainev, 1970; Aebi, Moerikofer-Zwez and Vaon Wartburg, 1972) RBC's contain multiple forms of Cat, and a portion of the Cat is membrane-associated (Nisioka, 1969a,b; Davydova, Shapot and Drozdova, 1970; Krainev, 1970).

Cohen and Hochstein (1963) showed that, in normal RBC's, glutathione peroxidase rather than catalase was primarily responsible for decomposition of H_2O_2 when the extracellular H_2O_2 concentration was less than 1 μM.

In the catalase assay used in this work, the H_2O_2 concentration was 9 mM, and reduced glutathione was not added to the assay system. Therefore, it is unlikely that glutathione peroxidase would have been detected in this assay system. It should be noted that glutathione peroxidase is probably a tetramer with molecular weight 95,000 and monomer molecular weight 23,000 (Awasthi, Beutler and Srivastava, 1975).

Fumarase

Fum undergoes reversible dissociation in vitro and has a half time for reassociation on the order of 40 sec (Teipel and Hill, 1971). Its monomers and dimers are catalytically inactive (Kanarek et al., 1964; Teipel and Hill, 1971). Incubation of the samples prior to assay in this work presumably permitted the reassociation and detection of the subunits.

In most cells Fum, like other soluble citric acid cycle enzymes, is associated with the mitochondrial inner-membrane matrix fraction (Addink et al., 1972). It is present in both the particulate and soluble fractions of reticulocytes and appears not be to membrane-associated in the adult red cell (Rubinstein et al., 1956).

Sodium, Potassium, Lithium and Dextrose

Less than 0.2% of both the cellular Na^+ and K^+ are specifically bound by RBC membranes (Ginzburg, Friedlander and Pouchovsky, 1967; Spector, 1956). Neither interacts specifically with Hb (Morris and Wright, 1954; Pfister and Pauly, 1972; Bull et al., 1973; Yeh, Brinley and Becker, 1973), but they do increase the dissociation of Hb and other proteins in general (Appendix A) and function as counter ions to Hb and other molecules with

negative charge groups. In contrast, Li^+ appears to interact directly with Hb at concentrations above 0.1 M (Bull et al., 1973). The author is not aware of data concerning the effect of Li^+ on Hb dissociation, but its effect is probably equal to or greater than the effect of K^+ or Na^+ (von Hipple and Schleich, 1969). Duprez and Vignes (1967) found that the K^+ content of individual human RBC's was distributed approximately normal.

In contrast to salts, dextrose does not promote the dissociation of Hb and can be used as an energy source by RBC's. Thus, if the salts of an RBC were replaced by an osmotically equivalent amount of dextrose, Hb dissociation would be reduced, resulting in a shrinkage of the cell, and, if metabolic intermediates (2,3-diphosphoglycerate, ATP...) and glycolytic enzymes were still present in the cell, the cell might be in a more energized state than it would be in a salt solution. Additionally, dextrose specifically binds to a component of red cell membranes (Bobinski and Stein, 1966; Zala and Jones, 1974; Zimmer, Schirmer and Bastian, 1975). The binding is stereospecific (Taylor and Gagneja, 1975) and is associated with a glucose-binding protein that has been isolated from human RBC's (Kahlenberg and Walker, 1976). It should be noted, however, that phospholipids extracted from RBC's can carry sugars, including dextrose, into nonpolar solvents in the absence of water (LeFevre, Habich, Hess and Hudson, 1964).

Because the major differences observed between the low-resolution dextrose and salt experiments in this work appear to be adequately explained by the delayed entrance of dextrose into the cells, the more subtle effects of dextrose interaction with cellular molecules will not be considered further here.

The 50% loss of times of K^+, Hb and Cat occurred in the order of increasing molecular weight in the NaCl experiments, but the 50% loss times of K^+ and AK were later than those of Hb, Cat and Fum in the LiCl experiment (Fig. 9). The K^+ losses from fresh RBC's in NaCl centrifuge experiments typically appeared similar to Fig. 5a. The K^+ loss in the LiCl experiment, however, fell more like a washout curve at the higher fraction numbers (Fig. 6a). These observations suggest that the membranes did not reseal to K^+ and perhaps to AK as quickly in LiCl solutions as they did in NaCl solutions. The late loss of AK may, however, reflect the presence of AK aggregates and its slow dissolution from the membrane.

Thus, Li^+ appears to specifically effect the resealing of RBC membranes, at least to K^+. Rose and Lowenstein (1971) have observed specific effects of Li^+ on junctional membrane permeability. The mechanism(s) of these Li^+ effects on biological membranes is unknown but may be related to an alteration in protein structure that is observed in the specific Li^+-induced unfolding of ribosomal subunits and the release of RNA from the subunits (Belitsina, Rozenblat and Spirin, 1971; Arpin, Reboud and Reboud, 1972; Reboud, Buisson and Reboud, 1972).

THE PROCESS OF CONTROLLED GRADUAL OSMOTIC HEMOLYSIS

Early Events

A small, continuous K^+ loss was observed during the isotonic wash and was also evident after the start of the dilute flow prior to the major K^+ loss in high-resolution salt experiments (Figs. 5a, 6a and 7a). This loss was considerably increased in NaCl filter experiments and was accompanied by Hb loss (Fig. 11), presumably caused by the increased and non-uniform

filter-induced membrane stresses in this system. The K^+ loss in dextrose filter experiments during the isotonic wash and prior to the major K^+ loss was also accompanied by Hb loss (Figs. 12 and 13). The filter-induced losses tended to obscure the increased K^+ loss that occurred in low ionic strength medium (Davson, 1939; Donlon and Rothstein, 1969).

The optical apparatus employed to observe the morphology and Hb loss of individual cells attached to glass did not have sufficient resolution to permit a detailed study of cell morphology. The observed progression of shape changes corresponded to that observed by previous workers (Ponder, 1948b,1955; Danon, 1961; Rand, 1967) if the transitory, flow-induced shape changes are neglected. The cells were smooth biconcave disks in isotonic dextrose but gradually thickened as the external solute concentration decreased. Cup cells were rarely seen, and the cells were never crenated. The biconcavities were not observed to pop out; they apparently gradually moved outward, and the cells became ellipsoidal. Others have reported that the swollen ellipsoidal cell suddenly becomes a sphere or a spherical cell suddenly becomes a larger sphere and then hemolyzes. This sudden shape change was not observed in this system although it may have occurred. The cells, however, did suddenly appear sharper (less diffuse) at about the time of the initial major K^+ loss. The cells maintained this sharper appearance during Hb loss whereas in drastic hemolysis a localized buldge often develops from which Hb subsequently escapes (Kochen, 1964; Seeman, 1967; Danon, 1961) and the cells revert to their original diffuse appearance during the remaining period of Hb loss (Marsden and Hall, 1973). The shape change that occurs when the biconcavities of a red cell proceed to a convex configuration suggests

that the membrane is strained at this time, but the membrane does not suffer major osmotically-induced strain until about the time of the sudden shape change that involves the loss of K^+ and membrane flicker. The course of osmotic hemolysis after this point appears to depend on the hemolytic system; in drastic hemolysis, the flicker returns during the loss of Hb, which suggests that the bulk flow of intracellular molecules has reduced the membrane tension prior to the completion of hemolysis. In the gradual hemolysis studied here, the flicker was absent throughout the period of Hb loss, which suggests that membrane tension is high throughout the hemolytic process (Brochard and Lennon, 1975).

Small losses of Hb, especially from aged cells, occurred near tube 6 in centrifuge experiments (Figs. 7b and 10a). AK was also lost at this time (Fig. 6d), but K^+ (Figs. 5a, 6a and 7a) and Fum (Fig. 6e) showed little or no increased loss. Because both Hb and AK are membrane-associated molecules but K^+ and Fum are not, these results suggest that a membrane alteration occurred at about tube 6 in the high-resolution salt experiments. It is suggested that the basic alteration is the change in curvature of the membrane when the biconcave regions of the cell proceed to a planar or convex configuration. Because the sign of the radii describing these regions of the membrane changes during this shape change, it is not surprising that a rearrangement in the asymmetrically distributed membrane molecules might occur at this time (Bretscher, 1973; Singer, 1974; Verkleij et al., 1973). It should be noted that mixed lipid liposomes can have an asymmetric distribution of lipids between the inner and outer leaflets of their bilayer lipid membrane and that this asymmetry apparently results from the curved surface of the liposomes (Thompson, Huang and

Litman, 1974).

Evidence of a membrane alteration caused by swelling a red cell is obtained from the observations of Lankisch and Vogt (1972), who found that hypotonically-swollen washed RBC's are lysed by phospholipase A but that RBC's in isotonic saline are not lysed, and from the observations of Metz et al. (1971) who found deep pits and invaginations in the membranes of 10 to 15% of cells that had been hypotonically swollen and then returned to an isotonic medium. It is not known whether the changes caused by swelling a cell hypotonically to a point short of its becoming a sphere have any relationship to the shape changes that occur when red cells pass through capillaries. It is tempting to speculate, however, that these shape changes and the resulting membrane alterations might accumulate and partially account for the preferential removal of older red cells from circulation.

Losses at Time of Initial Major Osmotic Stress

Little force is required to deform the fresh RBC until it becomes spherical (Rand and Burton, 1964). In this work it was found that the K^+ loss is correlated with the loss of membrane flicker and the sphering of the cells and thus the time at which the membranes first suffer major osmotic stress. Minor losses of the membrane-associated proteins occurred at the time of the initial K^+ loss (Hb from aged cells, tube 11, Fig. 7b, and tubes 10 and 11, Fig. 10a; Cat, tube 11, Fig. 6c; and possibly AK, tube 10 or 11, Fig. 6d), but a loss of the cytoplasmic protein Fum was not evident (Fig. 6e). Minor losses of K^+ and Fum occurred at tube 9 when the external solute was LiCl (Figs. 6a and 6e); the cause of these losses of cytoplasmic molecules is not known.

The losses of membrane-associated proteins at the time of the initial major K^+ loss suggests that another alteration of membrane structure occurs at this time. In contrast to the alterations that occurred at about tube 6, this alteration permits a rapid increase in the passage of K^+ across the membrane. As previously discussed, this K^+ pathway is stress-induced because it occurs with fresh RBC's at an external solute concentration of approximately 173 mOsm when the major external solute is either an electrolyte (NaCl or LiCl) or a nonelectrolyte (dextrose) solution (Table III). Further strain of the membrane results in the losses of intracellular proteins by a molecular sieving mechanism, but the times of these losses depend on the nature of the external solute.

Mild stress of the red cell membrane, as in centrifugation (Davson and Danielli, 1938; Sieberth, 1971) or in the irreversible micropipette phase observed by Jay (1973) apparently causes the stress-induced loss of K^+, but the stress is of either a magnitude small enough or a duration short enough that it does not cause the loss of Hb (Rand, 1964). This stress-induced loss of K^+, however, is a part of the process of osmotic hemolysis. The use of terms such as "prelytic loss" (Ponder, 1948b; Seeman, Sauks, Argent and Kwant, 1969) to describe the K^+ loss that occurs prior to the loss of Hb in osmotic hemolysis obscures the fact that this K^+ loss is a part of the continuous process of osmotic hemolysis (see Models section below). It is recognized, however, that "prelytic loss" may be a useful term in other systems, particularly those containing a lysin (Ponder, 1948b).

Period of Major Solute Losses

Potassium

As mentioned in the Interpretation section, the techniques used in this work permitted detailed observation of the loss of intracellular solutes. The passage of extracellular solutes into the cells was not, however, measured directly and can be inferred only by their effects on the losses of intracellular solutes.

Little difference was observed during the initial stages of controlled gradual osmotic hemolysis between experiments conducted in NaCl solutions (Figs. 5 and 7) and those conducted in LiCl solutions (Fig. 6). This result is reasonable because the cations are of similar size (Table V) and charge and presumably could enter the cells by similar mechanisms. Because of the rapid decrease in external solute concentration at about the time of the initial major K^+ loss (tubes 11 and 12, Fig. 2), however, slight differences in the behavior of Na^+ and Li^+ would not have been resolved. K^+ is similar in both size and charge to Na^+ and Li^+, and it is reasonable to hypothesize that all three cations cross the membrane via similar stress-induced mechanisms but that the net movement of K^+ is in the opposite direction to that of the external cation and that there may be differences in their kinetics.

The loss of K^+ from cells aged 0 to 3 hrs in centrifuge experiments rises rapidly to a maximum rate of loss (Figs. 5a and 6a) but does not decline as rapidly as some of the protein losses (Fig. 10a). The loss of K^+ from cells aged 5 hrs (Fig. 7a) shows a rapid K^+ loss spike following its initial major loss and then a loss similar to that observed with fresher cells. The calculated K^+ permeability increases monotonically

during the initial stages of hemolysis with fresh cells (Fig. 5a) but shows more complexity as the cells age in saline (Figs. 6a and 7a) (unpublished observations). Because the intracellular K^+ appears to be free but subject to electrostatic interactions (Edzes and Berendsen, 1975) these observations suggest that the membrane remains relatively impermeable to K^+ throughout the initial stages of controlled gradual osmotic hemolysis although there is a transient permeability increase at the time of the initial K^+ loss in aged cells. The low permeability suggests that the reflection coefficient of K^+ and other monovalent cations remains near one throughout the initial stages of controlled gradual osmotic hemolysis, and the cations maintain their osmotic effectiveness on both sides of the stressed cell membranes. This was assumed in the Interpretation section. The reason for the slow loss of K^+ is not readily apparent from the data and will be discussed in the Model sections. The transient increase in K^+ permeability at the time of the initial K^+ loss in aged cells suggests that K^+ loss might not be limited by the net rate of anion loss (Harris and Pressman, 1967; Pressman, 1973). It appears, therefore, that the loss of K^+ is directly controlled by its interaction with the stressed membranes, but because its loss curves show considerably less fine structure than the protein loss curves, the mechanism by which K^+ and other monovalent cations cross the stressed cell membranes may differ from the mechanisms involved in protein transport.

Salt and Dextrose Experiments

The differences between experiments conducted in NaCl or LiCl solutions and those conducted in dextrose solutions were considered in some detail in the Interpretation section. The initial loss of K^+ is apparently caused

by osmotic stress. Its loss is independent of the nature of the major external solute and follows a similar course in salt and dextrose experiments during the initial stages of gradual osmotic hemolysis. The loss of Hb is also apparently caused by osmotic stress, but the course of the experiment is different in salt and dextrose. The lag in Hb loss in dextrose over NaCl or LiCl experiments can be explained by a delay in the entrance of dextrose over the entrance of NaCl or LiCl. The delay result from a lower dextrose permeability than that of NaCl and LiCl, or dextrose might be totally excluded from the stress-induced pathway(s) until at least the time of the initial major Hb loss. Hypothesizing that the entrance of Na^+ and Li^+ into the cells follows the same kinetics as K^+ loss from the cells, it was shown that the data are adequately explained by negligible entrance of dextrose into the cells prior to the major Hb loss. The lag in the entry of dextrose and similar losses of K^+ in dextrose and salt experiments allows the escape of approximately 15% of the intracellular K^+ to partially compensate for the continuing decrease in external solute concentration in dextrose experiments and thus to delay the loss of Hb. The mechanism of the delay in the entrance of dextrose will be considered in the Model sections.

Membrane Tension at Time of Hb Loss

The initial losses of K^+ and Hb were separated by about one fraction collection period in the high-resolution centrifuge experiments (Table III), limiting the resolution to about the 7 mOsm difference in external solute concentration between adjacent fractions at this time during the experiment (Fig. 2). If 7 mOsm is a true representation of the difference in external concentration required to cause Hb loss beyond that required to produce

K^+ loss under these experimental conditions, an osmotic pressure of 17.7×10^4 dynes/cm^2 is exerted across the membrane to cause the Hb loss beyond the stress required to produce the K^+ loss, assuming that cations are osmotically effective and the cell volume is constant. This osmotic pressure corresponds to a pressure head of about 180 cm of water inside the cells. In contrast, biconcave or partially swollen human red cells have an internal excess pressure of 0.23 cm of water (Rand and Burton, 1964a), and biconcave sheep red cells have an excess internal pressure of about 0.2 cm of water (Rand and Burton, 1964b).

Hoffman (1958) found that human RBC ghosts did not rehemolyze if the osmotic pressure of Hb within the ghost was 6370 dynes/cm^2 (6.5 cm of water) or less but did rehemolyze at about 10^4 dynes/cm^2 (10 cm of water). Rand (1964) found that membrane tensions of 2 dynes/cm caused hemolysis in about 2 hours. Applying Laplace's Law ($\Delta P = 2T/R$, where ΔP is the pressure differential across the membrane, T is the membrane tension, and R is the radius of the sphered cell), which is the model Rand employed to interpret his data, a pressure difference of 1.14×10^4 dynes/cm^2 (11.6 cm of water) across the human red cell membrane eventually causes hemolysis. Similarly, a pressure of about 7.15×10^4 dynes/cm^2 (73 cm of H_2O) causes human red cells to hemolyze in about 1 minute (Rand, 1964), the fraction collection period employed in the centrifuge experiments in this work. Thus, a pressure increase of roughly 17.7×10^4 dynes/cm^2 is required to produce Hb loss beyond the initial K^+ loss in rat RBC's, but 7.15×10^4 dynes/cm^2 are required to cause hemolysis in human RBC's in the same one-minute period. The membrane tensions for these cells at the time of Hb loss, calculated with Laplace's Law using Rand's value of 3.5×10^{-4} cm for the

radius of the sphered human red cell and 2.92×10^{-4} cm for the radius of the sphered rat red cell (from Table VI), are 12.5 and 25.8 dynes/cm for the human and rat red cell membranes, respectively. The difference of a factor of 2 between these values is within that expected from species variation and the limited resolution of the present work and suggests that the initial major K^+ loss starts at about the time major osmotic stress first occurs in the membranes, a conclusion previously reached by comparing K^+ loss with cell morphology.

Protein Losses

The erratic appearance of the protein loss curves has been shown to be reproducible and has been interpreted as the starting of flows of protein units of increasing size through the stressed cell membranes during the initial stages of controlled gradual osmotic hemolysis and the stopping of flows of decreasing protein size during the final stages of controlled gradual osmotic hemolysis. The presence of sufficient quantities of monomers and dimers of tetrameric proteins within the cells to allow their detection after reaching the external medium was not anticipated, but has precedence in the observed passage of Hb monomers and dimers through dialysis membranes (Guidotti and Craig, 1963). Similarly, the interpretation of the Hb loss curve includes Hb aggregates. Rodent Hb's have a marked tendency to aggregate, perhaps due to one additional cysteine residue on the α-chain (Chua and Carrell, 1974). The degree of aggregation is strain-dependent (Riggs and Rona, 1969) and is likely to be affected by oxygenation (Reynaers, 1966; Putzeys and Reijnaers, 1966; Bielen, 1967) and by the binding of organic phosphates, primarily 2,3-diphosphoglycerate and ATP (White, 1972; Adachi and Asakura, 1974), as are other mammalian

Hb's. The observation of Hb aggregates in this work is consistent with the properties of rat Hb. The relatively large flow increase of deoxy-Hb at tube 21 in Fig. 10a suggests that deoxy-Hb comprises a tionate share of the aggregated Hb octamers (Figs. 15 and 16). The relatively constant loss of deoxy-Hb between tubes 23 and 33 (Fig. 10a), compared to the rapid decrease in oxy-Hb, suggests that a greater proportion of deoxy-Hb than oxy-Hb is aggregated, in agreement with the behavior of other mammalian Hb's.

The Hb losses at tubes 5, 7 and 10 or 11 are enriched in met- and deoxy-Hb compared to the bulk of the Hb present (Fig. 10a). Figure 15 and comparison with the K^+, Hb, Cat, AK and Fum losses shown in Fig. 6 tentatively indicate that these Hb losses result from the loss of membrane-associated Hb's. As previously discussed, these membrane-associated Hb's are probably not typical of the bulk Hb present but are primarily restricted to a subset of the multiple Hb species present in the rat red cells.

The rapid increase in Hb loss at tube 13 (Fig. 15) is caused by the rapid loss of oxy-Hb (Fig. 10a). This loss is not resolved, may not be present in the deoxy-Hb loss, and is much less prominent in the met-Hb loss. Because this loss has been interpreted as the loss of Hb monomers (Figs. 15 and 16), rat oxy-Hb appears to dissociate substantially more than does rat deoxy-Hb. This result contrasts with the conclusion drawn by MacGregor and Tobias (1972) who assumed a different alignment between the data of Figs. 6 and 10. The present interpretation is in agreement with the properties of normal human Hb (A; $\alpha_2\beta_2$) wherein oxy-Hb dissociates substantially more than deoxy-Hb (Antonini, Brunori and Anderson, 1968;

Banerjee and Sagaert, 1967; Benesch, Benesch and Williamson, 1962; Kellett, 1971). This interpretation does not exclude the possibility that one or more of the Hb species present has a high oxygen affinity, dissociates substantially more than the other Hb species, and so forms the bulk of the Hb lost as monomers.

In this experiment, 10.3% of the total Hb recovered was assayed as met-Hb. Because 1.1% to 12.3% met-Hb was found in fresh rat blood obtained from other Sprague-Dawley rats maintained under similar conditions (MacGregor, unpublished), support is provided for the analytical methods used in the simultaneous determination of deoxy-, oxy- and met-Hb and for the presence of these species within the cells prior to the experiment. The sharpness of the individual species loss curves and the differences between them (Fig. 10a), when compared to the estimate of total Hb loss (Fig. 10b), originally suggested the presence of multiple Hb subflows. Because the net assay cannot discriminate between the individual species, some of which may be increasing in flow across the membranes at the time when others are decreasing (tube 14, Fig. 10a), the net assays may not detect with certainty all of the subflow starts such as the deoxy-Hb peak at tubes 16 and 17 (Figs. 10a and 10b). This inability to detect the individual species presumably accounts for the more tentative alignments in Fig. 15.

The AK data are subject to a 2- to 4-fold increase in error over the maximum analytical error of the other assays (3%) in the experiment of Fig. 6 (Table I). Its relatively flat-topped loss curve is, however, probably real and could be explained by the aggregation behavior of AK and/or its extensive membrane association.

The loss of Cat in the form of intact molecules or subunits with molecular weights one-half and one-fourth of that of intact Cat is evident in Fig. 16 and agrees with the generally accepted properties of Cat (Appendix A). The size of the Cat monomer(s) is uncertain however (Appendix A and B). A Cat loss was consistently observed at tube 14 or 15 in centrifuge salt experiments (Figs. 5c, 6c and 7c) and corresponds to a molecular weight between that of the Hb monomer and dimer (Fig. 16). This result suggests that a protein with a molecular weight of between 16,000 and 32,000 can increase the rate of H_2O_2 decomposition after the samples have been maintained at 4°C for one day. As previously discussed, it is unlikely that this is the glutathione peroxidase monomer (MW = 23,000; Awasthi, Beutler and Srivastava, 1975). Thus, if this protein is a subunit of Cat, it suggests the reversible dissociation of Cat to at least one-eighth of its intact molecular weight. It is therefore suggested that the molecular weight of an apo-catalase monomer is approximately 28,800 (based on the molecular weight of intact catalase of 232,400 and equal-sized monomers; see Appendix B). The aggregates of 1½ and 2 Cat molecules tentatively indicated in Fig. 16 are consistent with the aggregation behavior of Cat (Diezel et al., 1970,1972).

The intact Fum tetramer and its dimer are clearly represented at tubes 22½ and 19, respectively, in Figs. 6e and 16. The observation of the Fum monomer was obscured as previously discussed by an interference and probable contamination of tube 15. Figure 6e indicates that a flow start occurred at or prior to tube 17. Figure 16 supports this contention and suggests the monomer flow may have started as early as tube 16.

Red Cell Population Homogeneity in Controlled Gradual Osmotic Hemolysis

The complex fine structure of the individual protein loss curves and the relationships between the loss curves of the various proteins during the initial and final stages of controlled gradual osmotic hemolysis can be explained by the hypothesized molecular sieving properties of the stressed red cell membranes. The red cell population from each rat appears to have sufficient homogeneity to permit the observation of this fine structure in the loss curves. Although, as discussed in detail in the Interpretation section, there is no reason to expect two or more distinct subpopulations in the osmotic response of fresh rat red cells, a broad age-dependent distribution might be expected. Such a distribution is observed in the drastic osmotic hemolysis of rat red cells where it is found that young rat RBC's are osmotically resistant but gradually become more osmotically sensitive as they age in vivo (Sterling, Greenfield and Price, 1958). There appears to be less difference between young and old red cells in controlled gradual osmotic hemolysis, which suggests that rat red cells respond more homogeneously if their membranes are stressed slowly than if they are stressed rapidly. This contention is supported by the observation that rat red cells subjected to shear stresses of 325 dynes/cm^2 in a viscometer and suspended in plasma show a mechanical fragility independent of the age of the cell (Shapiro et al., 1969) even though suspensions of old red cells are more viscous than suspensions of young cells (Usami, Chien and Gregersen, 1969) and old red cells have less deformable membranes (La Celle, Kirkpatrick, Udkow and Arkin, 1972).

It is proposed that the apparent increase in population homogeneity in gradual versus drastic osmotic hemolysis results, in part, from changes

similar to those observed in metabolically depleted cells, which are described in the following section. ATP-depleted cells lose membrane lipid but not protein to the external medium and have internal vesicles (Bessis and Mandon, 1972). This loss of membrane lipid through myelin forms and microspheres probably partially accounts for the 5 to 10% reduction in lipid content of old RBC's (Wasterman, Pierce and Jensen, 1963; van Gastel et al., 1965). The slow application of stress might allow internal vesicles to rejoin the membrane and, if internal vesicles are more prevalent in old versus young RBC's, cause the osmotic response of old cells to be more similar to that of young cells under the conditions of controlled gradual osmotic hemolysis. In addition, the slow application of stress allows more time for a redistribution of membrane components to occur. This appears to be especially important in ATP-depleted cells, and presumably in old cells, because ATP depletion increases the aggregation of membrane proteins as will be discussed in detail below.

INCUBATION OF RBC's PRIOR TO CONTROLLED GRADUAL OSMOTIC HEMOLYSIS

Experimental Observations

Cells incubated in salt solutions prior to hemolysis were found to have increased fine structure in their K^+ loss curves (Fig. 7a) compared to fresh cells (Fig. 5a) and to have a large spike of K^+ loss at the time of initial K^+ loss (tube 12, Fig. 7a) as previously discussed. Incubation also increased the minor Hb losses prior to and at the time of the initial K^+ loss, and, as previously discussed, these losses appeared to be caused by the losses of a restricted subset of the Hb molecules present.
In addition, the tube of maximum Hb loss decreased from tube 22 in cells incubated 0 to 3 hrs to tube 15 in cells incubated 29 hrs (Fig. 18), and

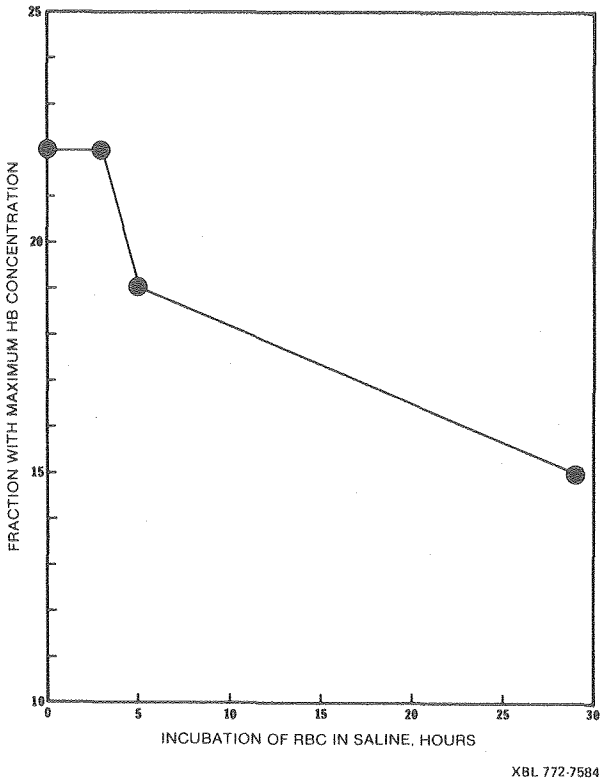

Figure 18. Tube of maximum Hb loss as a function of duration of incubation in salt solution prior to centrifuge experiments. The data are from Table I and Figs. 5b, 6b, 7b, and 10.

aggregates of 4Hb appeared to be more readily resolved in incubated cells (Figs. 15 and 16).

The shape of the individual Hb subunit loss curves is not known, but the deoxy-Hb loss in Fig. 10a suggests that each separate loss may rise rapidly over two or three tubes and then fall rapidly. A crude estimate of the amount of Hb lost as the dimer, for instance, can be obtained by summing the Hb loss between the losses of the dimer and the tetramer, using the size assignments of Fig. 15 and Fig. 16. Note that the size assignments for the data of Fig. 10 are based only on Hb losses whereas the other experiments also consider at least K^+ and Cat losses. Thus, the 29-hr incubation data, which are important in the following discussion, are less certain than the 0-, 3- and 5-hr data. The estimated Hb losses obtained by this procedure are plotted in Fig. 19.

Hb losses up to and including the initial monomer, dimer, tetramer and octamer losses appear to increase with the duration of incubation (Fig. 19a). Figure 19b suggests that the amounts of Hb lost as monomers, dimers or tetramers increase during the first 4 hrs of incubation. Between 4 and 29 hrs, the amount of Hb lost as the intact tetramer decreases somewhat, the Hb lost as the dimer increases somewhat, and the Hb lost as the monomer increases dramatically. The early Hb losses, which have been interpreted as losses of membrane-associated Hb, become significant only after prolonged incubation. This result suggests that the presence of Hb monomers may cause the increase in membrane-associated Hb. I interpret these data as incubation effects on both membrane properties and the distribution of Hb between its monomers, dimers, tetramers and variously sized aggregates. The increase in tetramer loss after about 4 hrs of incubation is most readily explained by a change in membrane

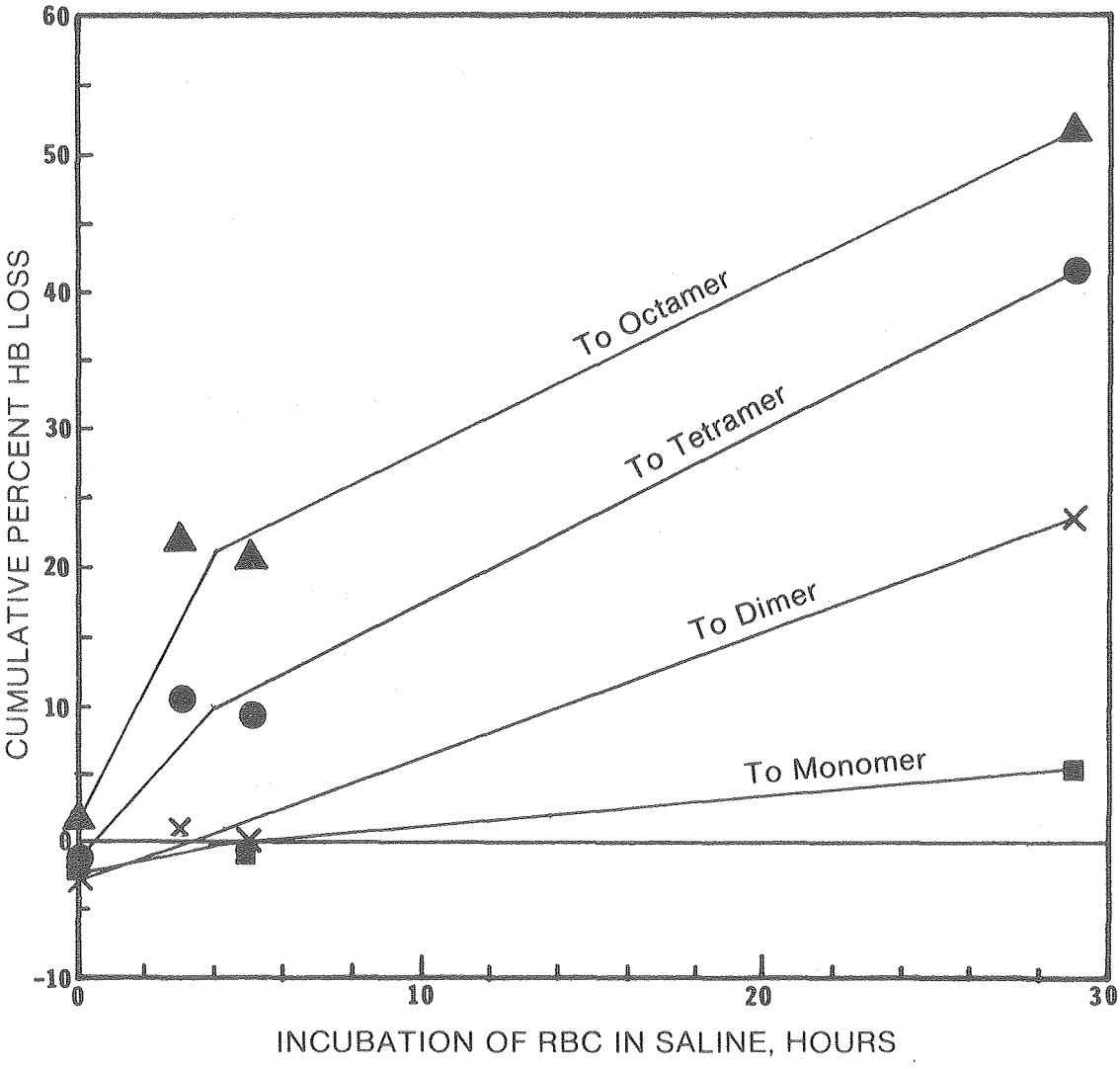

Figure 19a. Cumulative percent loss of Hb up to and including the first fraction assigned to each Hb subunit and aggregate as a function of the duration of incubation in salt solution prior to centrifuge experiments. Hb size assignments were obtained from Figs. 15 and 16. Because of the crude nature of these estimates, the raw data of Figs. 5b and 7b were not corrected for spectrophotometer zero, which results in the negative percentages shown in the figures.

- ■ To and including first monomer fraction
- × To and including first dimer fraction
- ● To and including first tetramer fraction
- ▲ To and including first octamer fraction

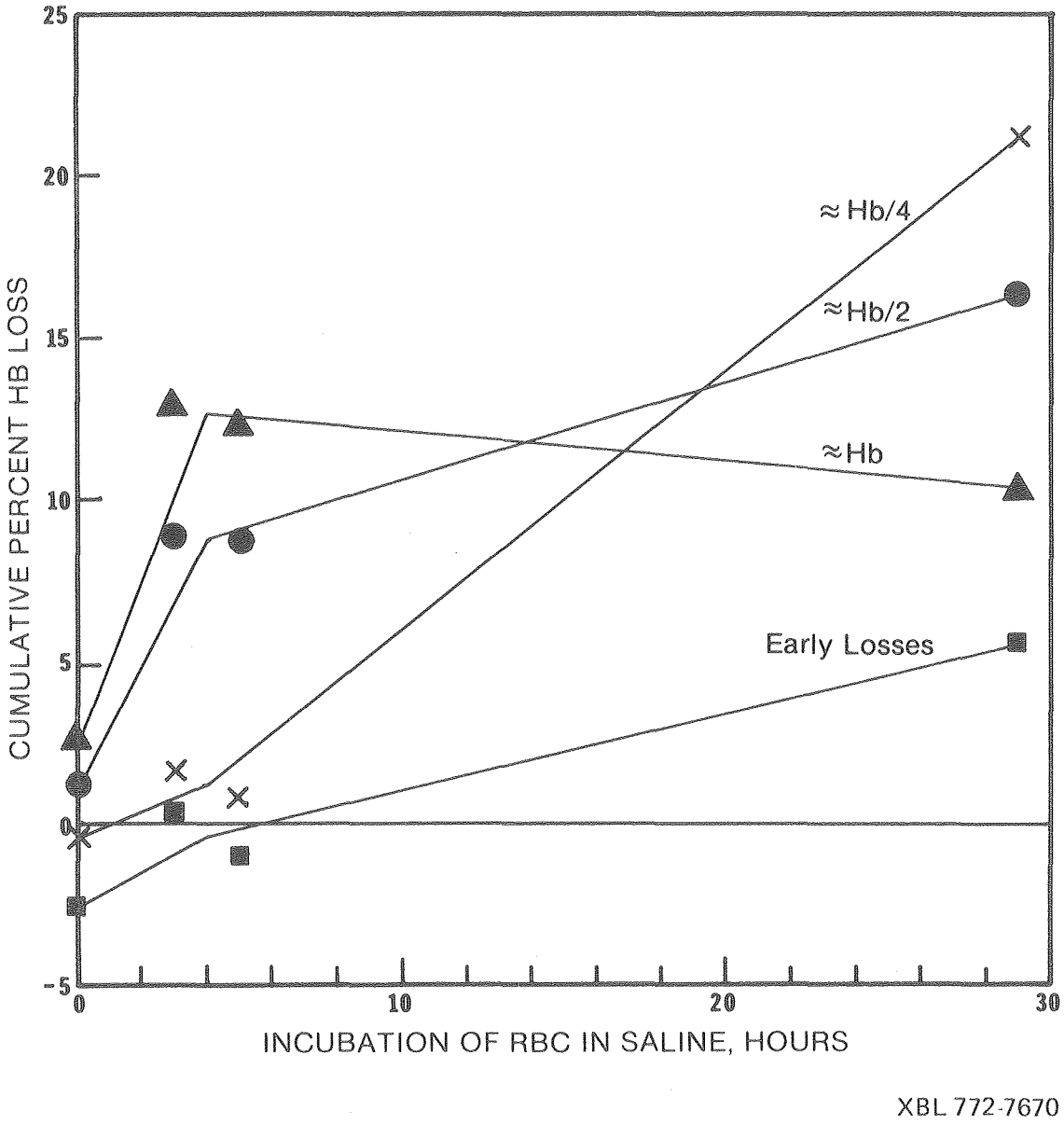

Figure 19b. The successive curves of Fig. 19a have been subtracted from one another to provide a crude estimate of the percent loss of each subunit or molecule as a function of the duration of incubation in salt solution.

- ■ Early losses prior to monomer ≈ membrane-associated losses
- × From monomer to dimer ≈ monomer
- ● From dimer to tetramer ≈ dimer
- ▲ From tetramer to octamer ≈ tetramer

properties. The large increase in Hb subunit losses is most easily explained by incubation-induced dissociation of Hb, which proceeds in the order tetramer ⇌ 2 dimer ⇌ 4 monomer. The dramatic increase in monomers after 29 hrs of incubation may reflect this dissociation (see below) or a chemical modification that stabilizes the monomer such as the -SH group reaction previously discussed. Possible incubation-induced effects on Hb and the membranes will be discussed in more detail below.

Incubation also appears to increase the loss of Cat subunits (Figs. 5c, 6c, 7c, 15 and 16). The greatly increased loss of Cat subunits in the LiCl experiment (Figs. 6c, 15 and 16) suggests that Li^+ specifically increases the dissociation of Cat to Cat/4 as it also specifically effects membrane resealing. The increase in Cat subunits found during incubation of rat RBC's in vitro in this work agrees with the increase in Cat subunits found during storage of human RBC's (Aebi et al., 1974). Thus, incubation of cells in saline causes increased fine structure in the K^+ loss curve, increased loss of specific Hb's prior to and at the time of the initial K^+ loss, increased Hb loss especially as monomers and dimers, and increased loss of Cat subunits. The basic cause of these alterations is probably the metabolic depletion of the cells caused by incubation in the absence of metabolic substrates. It is suggested that metabolic depletion of the cells causes changes in both the soluble proteins and the cell membrane that result in increased association of initially-soluble proteins with the membranes, and the combined effects of these two changes cause the observed incubation-induced alterations in the loss curves. Evidence for this view is discussed below.

Plasma-Induced Incubation Effects – Washing of RBC's

If whole blood is incubated, changes occur in both the cells and the plasma that effect cell morphology and osmotic fragility (Bessis and Brecher, 1971). A primary effect in the plasma is the removal of cholesterol from the red cells, causing them to become osmotically fragile, by the plasma enzyme lecithin-cholesterol acyltransferase, which forms a cholesteryl ester and so reduces the amount of unesterfied cholesterol present and in equilibrium with the red cells (Murphy, 1962; Cooper and Jandl, 1969). Lysolecithin is produced by the lecithin-cholesterol acyltransferase reaction and, if it is not metabolically removed, causes the red cells to become echinocytes (Féo, 1972; Shohet and Haley, 1972); it is lytic at high concentrations (Ponder, 1948b).

These plasma-caused alterations were avoided in the present work by thoroughly washing the cells and resuspending them in salt or dextrose media (Table I). Red cells in plasma are in a protein-rich environment and undergo rapid cholesterol (Porte and Havel, 1961) and phospholipid (Sakagami, Minari and Orii, 1965; Reed, 1968) exchange with plasma lipoproteins; phospholipids undergo additional turnover through reactions (Tarlov and Mulder, 1967; Cooper, 1970). The effects of washing and changing the extracellular environment on membrane structure are not known, but it should be noted that, in addition to any effects resulting from the removal of macromolecules, change in ionic interactions or other quasi-static effects, the membrane lipids are no longer subject to a dynamic exchange process, which might have promoted mixing and fluidization of the membrane lipids. The very slow disorder-to-order transitions observed in *E. coli* membranes, which extend over a period of tens of

minutes when the membranes are subjected to a temperature jump from 10°C above to 10°C below their transition temperatures (Dupont et al., 1972), strengthen this concern over the possible increased lipid order in washed red cell membranes over that present in vivo. The effects of extracellular macromolecules on the process of osmotic hemolysis are discussed in detail below.

Metabolic Effects of Incubation

When human red cells are incubated at 37°C in the absence of a metabolic substrate, ATP falls to 10% of its initial value in 15 to 20 hrs (Lionetti, McKay and Gendron, 1968; Weed, La Celle and Merrill, 1969; Lichtman and Weed, 1972; Shohet and Haley, 1972), and 2,3-diphosphoglycerate (2,3-DPG) falls to 5% of its initial value in 10 hrs (Schroeter and Bodemann, 1968). Incubation at room temperature leads to metabolic depletion in about 24 hrs (Weed, La Celle and Merrill, 1969). At about the time ATP is depleted, there is an increase in the rate of K^+ loss and Na^+ gain by the cells (Weed and Bowdler, 1966; Lionetti, McKay and Gendron, 1968; Cooper and Jandl, 1969) and an increase in intracellular Ca if the cells are in high Ca medium (Weed, La Celle and Merrill, 1969; Lichtman and Weed, 1972). The cells undergo a disc-to-sphere transformation independent of plasma factors (Lichtman and Weed, 1972), and, at about 48 hrs, cholesterol and phospholipid (Reed and Swisher, 1966; Langley and Axell, 1968; Cooper and Jandl, 1969) but not protein (Langley and Axell, 1968) are lost to the medium through the formation of microspherules and myelin forms (Weed and Bowdler, 1966; Bessis and Mandon, 1972). This lipid loss causes an increase in osmotic fragility (Weed and Bowdler, 1966; Cooper and Jandl, 1969). The presence of intracellular ATP prevents the

shape changes (Nakao, Nakao and Yamazoe, 1960; Nakao, Nakao, Yamazoe and Yoshikawa, 1961) and the increase in osmotic fragility (Gabrio et al., 1955) that otherwise occur during in vitro incubation.

The metabolic state of the rat red cells utilized in this work was not assayed; however, 0- to 5-hr cells appeared not to have undergone the disc-sphere transformation and thus probably had significant levels of ATP present (Lichtman and Weed, 1972). The 29-hr cells had increased osmotic fragility in the sense that there were increased Hb losses compared to the 0-, 3- and 5-hr cells (Figs. 15 and 19). These losses occurred, however, at approximately the same external solute concentration (tube number) in all centrifuge experiments (Fig. 15). It is therefore doubtful that these changes would correspond to the increase in osmotic fragility observed in drastic hemolysis and indicative of lipid loss and metabolic depletion. Rather, the 29-hr cells are likely to have had reduced, yet significant, levels of ATP because the incubation was at 4°C. Thus, it would be expected that the 0- to 5-hr rat RBC's would have had ATP and 2,3-DPG present but at concentrations that decreased with the duration of incubation. The 29-hr cells probably had ATP and 2,3-DPG present but were possibly metabolically depleted.

Membrane Effects of Incubation

It has been demonstrated that incubation causes an increase in membrane-associated protein; ghosts prepared from incubated cells have more non-Hb protein than do ghosts prepared from fresh cells (Weed, La Celle and Merrill, 1969; Lichtman and Weed, 1972; Sears, 1973), and the Hb content of ghosts prepared from cells incubated for 24 hrs at 37°C is greater than that of ghosts prepared from fresh cells (Weed, La Celle

and Merrill, 1969). Ghosts prepared from 48-hr cells, however, contain less Hb than the ghosts prepared from fresh cells (Lichtman and Weed, 1972). Incubation also causes increases in the viscosity of a cell suspension (Weed, La Celle and Merrill, 1969), in the filterability of a cell suspension (Teitel, 1969; Weed, La Celle and Merrill, 1969), in the negative pressure required to pull a hemispherical deformation of a cell into a 2.5- to 3.5-μ-diameter pipette (Weed, La Celle and Merrill, 1969), and in the negative pressure required to pull a red cell completely into a 3.0-μ pipette (Leblond, 1972). Weed et al. (1969) showed that similar incubation-induced results were obtained in the ghosts prepared from fresh and incubated red cells so that these incubation-induced mechanical changes are related to membrane alterations.

Causes of Incubation-Induced Changes in Membrane Properties and the Soluble Protein Size Distribution

The nature and causes of the incubation-induced alterations in membrane properties and the soluble protein size distribution are not resolved at the time of this writing. The following is a discussion of some of the interrelationships between intracellular Ca, ATP, 2,3-DPG, soluble proteins, and the cell membrane. It is hypothesized that previously unrecognized interactions of Hb subunits and aggregates with the cell membrane alter the properties of the membrane. This hypothesis is in accord with the incubation-induced changes in Hb loss observed in this work, with the above-mentioned incubation-induced changes in the mechanical properties of RBC membranes, with the effects of changing oxygen tension on membrane properties, and with the properties of RBC's that contain abnormal Hb's.

Calcium and ATP Membrane Effects

Weed et al. (1969) showed that intracellular Ca greatly decreased membrane deformability in ghosts and that the effect of 10^{-4} M Ca could be reversed by a 10-fold excess of ATP, EDTA or Mg. They also showed that ghosts prepared from old cells behaved like ghosts from fresh cells if ATP, EDTA or Mg was included in the lytic medium. They concluded that Ca was instrumental in causing a protein sol-to-gel transition at the inner membrane surface, that ATP and EDTA reversed the Ca effect by complexing the Ca, and that Mg reduced the Ca effect by competing for the same membrane site.

There is no doubt that Ca exerts a profound influence on membrane structure. The entrance of Ca into ghosts causes the immediate contraction of the ghosts by a process that does not require ATP (Palek, Curby and Lionetti, 1971); it also causes the appearance of protein aggregates in sodium dodecyl sulfate preparations of membrane proteins (Triplett, Wingate and Carraway, 1972). The membrane-binding of Ca is reduced by SH-blocking reagents (Tolberg and Macey, 1971) and ATP (Forstner and Manery, 1971; Chau-Wong and Seeman, 1971); the Ca-induced shape changes are prevented by SH-blocking reagents and by washing a water-soluble fibrous protein from the ghosts (Palek, Stewart and Lionetti, 1974). The Ca-induced stiffening of ghosts prepared by repeated hemolysis, which removes more Hb and other loosely bound proteins than a single-step hemolysis, is less than the Ca-induced stiffness of single-step ghosts (Weed, La Celle and Merrill, 1969). Thus, it is probable that abnormally high intracellular Ca concentrations exert an effect on membrane protein, and this effect is likely to involve the protein spectrin (Marchesi et al., 1969).

In the present work, however, the extracellular medium would have contained only that Ca present as impurity in the reagents employed (distilled de-ionized water was used to make the required salt solutions), which, according to the NaCl manufacturer's specifications, would have been less than 11 μM Ca in the isotonic NaCl solutions. This Ca would have been partially complexed by the 1 mM Tris present. Weed et al., (1969) found that 10^{-3} M ATP reversed the effect of 10^{-4} M Ca. If it is erroneously assumed that free Ca is the only important variable in this system and if the ATP-Ca association constant of approximately 5×10^{3} liter/mole (Sillén and Martell, 1964) is used, the free Ca concentration in this system is calculated to be 18 μM or more than the maximum Ca impurity of the NaCl solutions. Yet incubation appeared to cause increased protein-membrane interaction in controlled gradual osmotic hemolysis. Similarly, Weed et al. (1969) found that incubation in Ca-free medium reduced cell deformability and that incubation of cells in the presence of extracellular EDTA slowed but did not prevent the changes in cell morphology (Lichtman and Weed, 1972) and deformability (Weed, La Celle and Merrill, 1969) that occur during incubation. Thus, an increase in total cellular Ca is not necessary for the increased protein-membrane interaction or changes in membrane deformability.

Weed et al. (1969) explained this by suggesting that ATP chelates intracellular Ca. The decrease in intracellular ATP that occurs during incubation prior to the influx of Ca in high-Ca media, would increase the amount of free Ca, and this free Ca could then effect the sol-to-gel transformation. In the fresh cell, however, all measureable Ca is membrane-bound (Harrison and Long, 1968; Lichtman and Weed, 1972) so that

changes in the ATP concentration prior to an increase in cellular Ca would be expected to have little effect on the free Ca. The membranes of cells incubated from 0 to 48 hrs in high-Ca media show a constant amount of bound Ca even though the total cell Ca increases by 450% during the 48-hr incubation (Lichtman and Weed, 1972).

La Celle (1970) observed a marked decrease in cell deformability when the partial pressure of O_2 was reduced below 30 mm of Hg, which he interpreted in terms of the ATP-Ca chelation model. Hamasaki and Rose (1974), however, recently determined the dissociation constants of DPG, ATP, MgATP, ADP, 1,3-DPG, and glucose-1,6-diphosphate with oxy- and deoxy-Hb A. Their calculated equilibrium concentrations in oxygenated and deoxygenated cells, together with the maximum estimated intracellular Ca (1 μM, Schatzmann, 1973) suggests that the binding of ATP on complete deoxygenation of Hb could increase the intracellular Ca by a maximum of 4×10^{-8} M. It is not known experimentally if this change in Ca concentration could cause membrane alterations; 10^{-4} M Ca causes marked decrease in ghost deformability (Weed, La Celle and Merrill, 1969), 2×10^{-6} M causes contraction of ghosts (Palek, Curby and Lionetti, 1971), and 10^{-7} M Ca causes a detectable decrease in ghost deformability (La Celle and Kirkpatrick, 1975). It is doubtful that a change in free intracellular Ca is responsible for the decrease in deformability on deoxygenation. An alternate explanation is presented below.

Hemoglobin-Membrane Interaction

It is recognized that Ca-membrane interactions are the basic cause of decreased membrane deformability at abnormally high intracellular Ca concentrations. This high-Ca alteration is fully reversed following

short incubation periods by removal of the Ca (Teitel, 1969) and causes the aggregation of spectrin but is not itself bound to the spectrin (Carraway, Triplett and Anderson, 1975). The aggregation of spectrin might result from a Ca-induced aggregation of the negatively charged phosphatidylserine (Verkleij and Ververgaert, 1975; Papahadjopoulos and Poste, 1975), which is asymmetrically located on the inner surface of the RBC membrane (Bretscher, 1972; Verkleij et al., 1973).

It is also recognized that ATP effects the phosphorylation of spectrin (Greenquist and Shohet, 1975; Jacob, 1975) and that one cause of hereditary spherocytosis, in which membrane deformability is abnormal in that higher than normal concentrations of ATP are required to maintain a normal membrane deformability (La Celle and Weed, 1969), is the absence of one spectrin component (Kirkpatrick, Woods and La Celle, 1975). It seems reasonable to conclude that the reduction in ATP concentration that occurs during incubation effects phosphorylation of the membrane proteins and, through the membrane proteins, effects the process of controlled gradual osmotic hemolysis and membrane deformability. Membrane structure will be considered in more detail below.

It is proposed, however, that the direct effects of intracellular phosphates, primarily ATP and 2,3-DPG, on Hb stability are of importance in causing the membrane alterations that occur during incubation of RBC's. This hypothesis is in agreement with the work of Féo and Leblond (1974) who found that the extracellular phosphate concentration affected the discocyte-echinocyte transformation by other factors in addition to the intracellular ATP concentration. It is recognized that both Ca and ATP exert significant direct membrane effects, but the less appreciated

effects of dissociation and aggregation of normally soluble proteins and their possible membrane association will be stressed in the following discussion.

Basically, I suggest that the normal Hb tetramer is less membrane-active than either its subunits or its aggregates and that some of the altered properties of red cells that contain certain abnormal Hb's result from the increased Hb-membrane interaction of these Hb's. It was observed in this work that the multiple Hb's present within the cells apparently left the cells at different times. The Hb that was lost at about the time the biconcavities proceeded to a planar configuration was not typical of the bulk Hb, nor was the loss at the time of the (presumed) initial K^+ loss (Figs. 10 and 15). Because, in general, the surface activity of different Hb types is quite different, both for the intact tetramers and for the different monomers, and the surface activity also depends on the ligand (Elbaum, Harrington and Nagel, 1975a,b), the unrepresentative nature of these early Hb losses is expected if protein-membrane interactions are responsible for their loss.

During incubation, the ATP and 2,3-DPG concentrations would have decreased as previously discussed. ATP (Leyko and Jozwiak, 1970) and, to a limited extent, 2,3-DPG (White, 1972) stabilize the normal tetrameric configuration of oxy-Hb, which tends to dissociate (Appendix A). Normal human deoxy-Hb dissociates little (Thomas and Edelstein, 1972) but forms aggregates (Putzeys and Reijnaers, 1966; Reynaers, 1966; Bielen, 1967). The aggregation of deoxy-Hb is increased slightly by 2,3-DPG (White, 1972) and 2,3-DPG inhibits the precipitation of Hb A and S and their β chains (Adachi and Asakura, 1974). Calcium and Mg enhance the 2,3-DPG aggregation

of Hb (White, 1972), but Ca and Mg alone slightly increase the dissociation of deoxy-Hb and greatly increase the dissociation of oxy-Hb with complete dissociation to at least dimers of oxy-Hb at 1 M Mg^{2+} or Ca^{2+} concentrations (Kirshner and Tanford, 1964; Kawahara, Kirshner and Tanford, 1964; Guidotti, 1967). Ca^{2+} also causes the precipitation of concentrated oxy-Hb solutions (Teitel, 1969).

Thus, during incubation, the reduction in the concentrations of ATP and 2,3-DPG allow the increased dissociation of oxy-Hb. This increase in Hb dissociation during incubation is presumably the primary cause of the increase in the percentage of Hb lost as monomers and dimers and for the increased loss of membrane-associated Hb in incubated RBC's (Fig. 19).

In systems containing high extracellular Ca concentrations, the entry of Ca into the cells after metabolic depletion would cause additional dissociation of oxy-Hb. It is suggested (see below) that the increase in Hb dissociation is partially responsible for the observed changes in the mechanical properties of the cell membrane that occur during incubation. It is suggested that the increase in the aggregation of Hb, which occurs when Hb is deoxygenated, causes increased Hb-membrane association and that this increased protein-membrane association is responsible for the decreased membrane deformability observed at low pO_2.

Hb is a tetramer composed of two each of two different polypeptide chains. In the Hb tetramer these monomers are folded and nested together in a configuration with most of the polar residues on the outside of the molecule interacting with water (Perutz, 1969). Dissociation of the molecule into subunits without further conformational change exposes nonpolar residues from the contact regions of the subunits to an aqueous environment. If a

nonpolar environment such as membrane lipid were available, hydrophobic interactions between the subunits and the nonpolar phase might occur (Tanford, 1972) (see the discussion below). In addition, Wallach and Gordon (1968) noted that the H-helix of Hb has a nonpolar side that can bind one molecule of phosphatidyl ethanolamine.

Hb pathologies can be cited to support the contention that Hb subunits interact with the membrane to a greater extent than does the intact Hb tetramer. Hemolytic anemias are often caused by an abnormal Hb that dissociates more than normal (Perutz and Lehmann, 1968; Carrell and Lehmann, 1969) or by thalassemia, in which there is an unequal production of the Hb monomer polypeptides that result in an increase in Hb subunit concentration. As previously discussed, Jacob (1970) proposed sulfhydryl reactions of these subunits, which may be partially reversible (Srivastava and Beutler, 1974) and which lead to the formation of inclusion bodies. These bodies, the monomers and Hb degradation products, decrease the membrane deformability (Teitel, 1969) and lead to increased time-dependent permanent membrane deformations (La Celle, 1970; La Celle and Kirkpatrick, 1975). Treatment of normal RBC's with parachloromercuribenzoate, which increases the dissociation of human and rat Hb (Starodub and Shur'yan, 1973) causes increased Hb and globin retention in ghost membranes (Teitel, 1969) and decreases membrane deformability (Teitel, 1969; La Celle, 1970) in apparent mimicry of Hb dissociation effects.

Electron microscopy of cells containing an abnormal unstable Hb or thalassomic RBC's shows either diffuse or localized bodies in intimate contact with the cell membrane. These bodies can deform the membrane, alter the distribution of intramembranous particles, and interact with

filamentous structures on the inner surface of the red cell membrane (Lessin, Jensen and Klug, 1972; Lessin, 1972). Thus, it appears that an abnormally high concentration of Hb subunits can cause either Hb itself or its degradation products to have an abnormal increase in membrane association.

Hb C aggregates more readily than normal Hb (Charache et al., 1967), and Hb S polymerizes when deoxygenated (Murayama, 1966). Sickle cells containing oxygenated Hb S have normal membrane deformability, but partially deoxygenated cells have reduced membrane deformability (La Celle, 1973; see La Celle, 1970). Polymerized Hb S, in the form of 70Å-diameter filaments and 170Å-diameter helical rods composed of six of the filaments, are attached to the inner surface of the membranes (Jensen and Lessin, 1970). Cells containing Hb C have reduced membrane deformability (La Celle, 1970), and linear chains of Hb C can be observed adjacent to the membrane (Lessin, Jensen and Klug, 1972). Irreversibly sickled cells have vastly decreased deformability (La Celle, 1973), and numerous microbodies cover the inner membrane surface (Lessin, 1972). In contrast, normal Hb-A-containing cells do not show polymerized Hb, but the Hb is close packed adjacent to the membrane (Jensen and Lessin, 1970). Thus, it appears that an abnormal increase in Hb aggregation can cause increased Hb-membrane association. I propose that the increase in aggregation of intracellular Hb that occurs on deoxygenation is the basic cause of the reduction in membrane deformability, which also occurs on deoxygenation.

Thus, either an abnormal increase in Hb dissociation or an abnormal increase in Hb aggregation appears to cause increased Hb-membrane association or Hb degradation product-membrane association. The increase in Hb-

membrane association appears to be correlated with an increase in cation permeability as demonstrated in Heinz-body-containing cells (Parker and Welt, 1972) and mimicked by thio reagents (Parker and Welt, 1972) and as reversibly demonstrated when Hb-S-containing cells are deoxygenated (Tosteson, 1955; Tosteson, Carlsen and Dunham, 1955). In support of the proposed increase in Hb-membrane association in deoxygenated cells, deoxygenation also increases cation permeability (Nathan and Shohet, 1970). The cause of this increase in cation permeability and the cause of the increased fine structure in the K^+ loss curves in incubated cells will be discussed below.

In this work, I suggest that the incubation of the cells caused a decrease in ATP and 2,3-DPG and that this decrease caused an increase in Hb dissociation. The Hb subunits interacted with the membrane to a greater extent than the tetramer and caused the increase in early Hb losses at tubes 5, 7 and 10 or 11 in Fig. 10a. The increased oxy-subunit concentrations resulted in the observed increase in the percentage of Hb that was lost as the monomer and dimer near tubes 13 and 15 (Figs. 10a, 15 and 19).

DISCUSSION - A PROPOSED MOLECULAR MECHANISM FOR THE MOLECULAR SIEVING OBSERVED DURING CONTROLLED GRADUAL OSMOTIC HEMOLYSIS

In this section, selected physical and chemical properties of red blood cell membranes and model systems are briefly reviewed. It is hoped that this review will provide sufficient background for the model that is then presented. The review is not intended to be complete but rather stresses those papers that have been most influential in the development of the model.

The model of the process of controlled gradual osmotic hemolysis is presented in a qualitative manner. It is shown that gradual stress of the cell membrane is expected to cause the membrane to exhibit molecular sieving properties with certain classes of molecules and that, at any instant in time, there should be a sharp molecular weight cut-off. These properties result basically from hydrophobic interactions, which stabilize the membrane, and the presence of spectrin on the inner surface of the membrane. When the red cell membrane is stressed, it apparently exhibits permeability characteristics that are not typical of diffusion in polymer or lipid systems. This apparently new phenomenon reduces the cell's loss and gain of large molecules and may be important for the in vivo survival of the red cell.

A BRIEF REVIEW OF RED CELL MEMBRANE STRUCTURE

Lipids

The overall chemical composition of red blood cells is well known (Pennell, 1964). Cholesterol constitutes about 25% by weight of the total rat RBC lipid, glycolipid constitutes 2%, ganglioside 6%, and phospholipid 67% (Nelson, 1967). All of the red cell lipid is located in the cell

membrane (Weed and Reed, 1964). Of the phospholipid, about 11% is phosphatidyl serine, 22% is phosphatidyl ethanolamine, 48% is phosphatidyl choline, 13% is sphingomyelin, and the remainder is phosphatidyl inositol and lysophosphatidyl choline (Nelson, 1967). Most of the lipid is structured as a lipid bilayer (Wilkins, Blaurock and Engelman, 1971) with the cytoplasmic half of the bilayer containing all the phosphatidyl serine, 80% of the phosphatidyl ethanolamine, 25% of the phosphatidyl choline, and 15% of the sphingomyelin. The remaining phospholipid (van Deenen et al., 1976) and most of the cholesterol (Fisher, 1976) is located in the outer half of the bilayer in human RBC's and is presumably similarly distributed in rat RBC's.

The phospholipid hydrocarbon chain composition varies with diet in rat RBC's, but the head group composition is constant (de Gier and van Deenen, 1964). Because the fatty acids of phosphatidyl serine and phosphatidyl ethanolamine are generally more unsaturated than the fatty acids of phosphatidyl choline and sphingomyelin and because cholesterol moderates the fluidity of phospholipids (Jain, 1975), the inner membrane leaflet should be more fluid than the outer membrane leaflet (Emmelot and Van Hoeven, 1975). This conjecture is supported by two independent types of experiments. Tanaka and Ohnishi (1976) interpreted their phosphatidyl choline and phosphatidyl serine spin label data in terms of a more fluid inner than outer membrane leaflet, and Walter and Krob (1976) found that the outer membrane leaflet was more hydrophobic than the inner leaflet using right-side-out and inside-out RBC vesicles in a dextran-polyethylene glycol countercurrent distribution system.

Lipids extracted from human RBC's undergo a phase transition over a

broad temperature range, which includes the experimental temperatures of this work and normal body temperature (Ladbrooke and Chapman, 1969). Thus, regions of both crystalline and liquid crystalline hydrocarbon chains are present (see below). In model systems, phospholipids are found to cluster on the basis of fatty acid chain composition (Phillips, Hauser and Paltauf, 1972) and head group composition (Oldfield and Chapman, 1972). Cholesterol preferentially interacts with the lipid having the lowest transition temperature in a mixture of phosphatidyl cholines (De Kruyff et al., 1974) and regions of equimolar phosphatidyl choline: cholesterol separate from regions of excess phosphatidyl choline (Phillips and Finer, 1974). Similar separations would be expected in the bilayer regions of the RBC membrane, and, in fact, electron diffraction of wet RBC membranes suggests phase separation of the membrane lipids (Hui and Parsons, 1974).

In general, regions of both crystalline and liquid crystalline hydrocarbon chains are present in cell membranes at the growth temperature (McConnell, Wright and McFarland, 1972; Oldfield, 1973). The major phase transition in lipids appears to arise from cooperative gauche rotations, which occur in liquid-crystalline hydrocarbon chains but which are greatly reduced in crystalline hydrocarbon chains (Nagel, 1973; Rothman, 1973) although head group transitions also appear to influence the overall membrane transition (Chandrasekhar, Shashidhar and Tara, 1970; Scott, 1974, 1975; Chapman, Keough and Urbina, 1974). The presence of two hydrocarbon phases in the cell membrane indicates, on physical grounds, that large fluctuations are to be expected in the hydrocarbon density (Hill, 1956). Because the presence of cholesterol in phospholipid systems increases the hydrocarbon chain mobility in crystalline regions and reduces the hydrocarbon

chain mobility in liquid-crystalline regions (Chapman, 1975), the density fluctuations in a cholesterol-phospholipid system should be smaller than in a phospholipid system at temperatures at which two phases are present in the phospholipid system. Cell membranes, in general, probably require a portion of their lipid to be in the liquid-crystalline state so that density fluctuations are large enough to permit the entrance and movement of other molecules in the membrane (Blank, 1964; Blank and Britten, 1965; Linden et al., 1973; Phillips, Grahm and Hauser, 1975). It is probably significant that the red cell, which is a metabolically inactive cell, has a high cholesterol content in its outer membrane leaflet. The reduction of the magnitude of the density fluctuations caused by cholesterol would decrease the bilayer permeability compared to other cells with lower cholesterol contents (see below). The presence of multiple lipid phases and phase boundaries with protein suggests, however, that the density fluctuations will still be large compared to a pure lipid system that exists on a single phase at the growth temperature. Density fluctuations are discussed in more detail below.

Proteins

The surface pressure in each half of the lipid bilayer is calculated to be about 20 dynes/cm from the lipid hydrocarbon chain order parameter (Marčelja, 1974) and between 31 and 34.8 dynes/cm in the outer membrane leaflet of red cells from the action of several phospholipases (Demel et al., 1975). If the lipid of an RBC were spread as a bilayer over the entire surface area of the cell, its surface pressure would be on the order of 9 dynes/cm. Actually, some 23% of the membrane area is occupied by proteins, which are seen in freeze-fracture electron microscopy (Branton and Deamer,

1972). These tightly bound integral membrane proteins are unusually hydrophobic (Vanderkooi and Capaldi, 1972; Segrest and Feldmann, 1974). Less tightly bound peripheral membrane proteins are less hydrophobic and can be removed from the membranes by washing, removing divalent cations, or changes in ionic strength or pH. The peripheral protein with which we will be concerned is spectrin (Steers and Marchesi, 1969). It is a fibrous protein noncovalently bound on the inner surface of the RBC membrane (Nicolson, Marchesi and Singer, 1971). It normally exists as a dimer composed of monomers with molecular weights of about 220,000 and 240,000 (Clarke, 1971), but small amounts of higher aggregates are found in fresh RBC's (Gratzer and Beaven, 1975; Ralston, 1975). The isolated spectrin monomers are largely in a random coil configuration but become α-helical when reassociated to form the dimer (White and Ji, 1973). Spectrin exhibits Ca- and Mg-ATPases (Kirkpatrick, Woods, La Celle and Weed, 1975), and exposure of RBC membranes to γ^{32}P-labeled ATP causes the appearance of ^{32}P in the spectrin extracted from the membranes (Weidekamm and Brdiczka, 1975). It has been previously mentioned that phosphorylation of membrane proteins apparently affects membrane deformability. It is highly probable that spectrin is involved in this deformability change (see below). Ca causes the aggregation of spectrin in solution into fibers (Kirkpatrick, Woods, La Celle and Weed, 1975), but similar fibers are not seen in membranes under physiological conditions (Nicolson, Marchesi and Singer, 1971; Tilney and Detmers, 1975) although Ca induces the aggregation of spectrin and probably other proteins in membranes if present at the time of hemolysis at a concentration greater than 1 mM (Carraway, Triplett and Anderson, 1975).

Under some conditions spectrin promotes the polymerization of muscle actin (Pinder, Bray and Gratzer, 1975), and an actin that appears almost identical to muscle actin can be isolated from RBC membranes (Tilney and Detmers, 1975). The addition of spectrin to monomeric muscle actin (G-actin) reduces the polymerization observed when salts (1 mM $MgCl_2$ + 40 mM KCl) are subsequently added from that observed in a G-actin solution without spectrin. Thus, spectrin appears to inhibit the polymerization of muscle actin; however, it appears capable of crosslinking previously polymerized G-actin (F-actin). Salt-free solutions of actin plus spectrin show 250Å curved elements in negative-stained preparations, and the addition of salt causes the appearance of branching filamentous structure with filament diameters of from 40 to 120Å. In addition, Tilney and Detmers (1975) noted that spectrin and actin are present in the RBC membrane in approximately equal molar quantities; they suggest that the actin and spectrin mutually prevent each other from polymerizing. The red cell membrane would than have an unpolymerized branching network covering the cytoplasmic surface of the membrane. Each link in the network would be composed of a spectrin dimer plus actin.

Spectrin comprises about 20% of the membrane protein of mammalian RBC's when isolated by dialysis against 1 mM EDTA plus 5 mM β-mercaptoethanol at pH 7.5 for 48 hours at 4°C (Tillack, Marchesi, Marchesi and Steers, 1970). Trayer et al. (1971) stated, however, that the method used by Marchesi's group did not extract all of the spectrin and that spectrin comprises approximately 40% of the membrane protein.

A lower limit for the number of spectrin molecules per human RBC can be calculated from the following data:

0.69 pg of protein/RBC ghost (Lichtman and Weed, 1972)

spectrin = 0.2 of ghost protein (Tillack et al., 1970)

molecular weight of spectrin dimer $\cong 4.6 \times 10^5$ (Clarke, 1971)

Avogadro's number = 6.023×10^{23} molecules/mole.

Thus,

$$\frac{(0.69 \times 10^{-12})(0.2)}{4.6 \times 10^5} 6.023 \times 10^{23} = 1.8 \times 10^5 \text{ spectrin dimers/human RBC.}$$

The surface area of a human RBC is about 135 μ^2 but may increase up to 2% prior to hemolysis (Evans and Fung, 1972; Evans and Leblond, 1973). Thus, there would be one spectrin dimer per 7.5×10^4 $Å^2$ of unstressed membrane surface. If spectrin constitutes 40% of the ghost membrane protein, there would be one spectrin dimer per 3.8×10^4 $Å^2$ of membrane surface. If the first-order approximation is made that the membrane area influenced by a spectrin molecule is the membrane area per spectrin molecule, the area of influence of a spectrin molecule would correspond to a circular region with a radius of 155Å or 110Å or a square region with sides of 274Å or 195Å for the lower and higher spectrin estimates, respectively. These can be compared with the Stokes-Einstein radii of the Hb monomer (19.4Å) and intact Cat (49.2Å) (Table V), with the 250Å length elements observed in salt-free spectrin preparations, with the 2×10^3 Å by 30Å rods observed in millimolar Ca solutions (Clarke, 1971), and with the 30Å by 200Å fibers attached to the inner surface of the RBC membrane among amorphous material, all of which is removed when spectrin is extracted (Nicolson, Marchesi and Singer, 1971; Tilney and Detmers, 1975). It should be noted that the 2×10^3 Å rods are observed only under nonphysiological, high divalent-cation concentrations. These rods might be spectrin dimers because if a spectrin monomer were a single α-helix it would be approximately 2.4×10^3 Å

long (spectrin monomer MW = 2.3×10^5; amino acid MW = 142; 1.5Å translation per amino acid), and the 30Å width of the rod might result from two parallel α-helices, one from each subunit of the spectrin dimer (compare with Tilney and Detmers, 1975). This calculation also suggests that the 250Å elements represent only a portion of the spectrin dimer. Much of the amorphous material surrounding the extracted elements (Tilney and Detmers, 1975) and the fibers attached to the inner surface of red cell membranes must also be spectrin.

From the composition data for the human RBC's given by van Deenen and de Gier (1964), it can be calculated that there are about 1.9×10^8 molecules of cholesterol per cell and 2.05×10^8 molecules of phospholipid per cell. If the lower estimate of spectrin per human RBC is used, it is found that the maximum number of cholesterol molecules per spectrin dimer is 1,070 (most of which are located in the outer half of the bilayer) and that the maximum number of phospholipid molecules per spectrin dimer is 1,140. Because most of the lipid is in a bilayer structure, there is a maximum of roughly 10^3 lipid molecules per spectrin dimer on the inner side of the membrane. Because the lipid (Parpark and Dziemian, 1940) and spectrin (Tillack et al., 1970) contents per unit area of cell surface are about the same for human and rat red cells, these calculations should also apply to rat RBC's.

The proteins on the outer surface of the adult RBC have a diffusion coefficient of less than 3×10^{-12} cm^2/sec in the plane of the membrane, i.e., very slow translational diffusion (Peters et al., 1974), in contrast to the more rapid translational diffusion of proteins in most other cellular membranes (Edidin, 1974; Edidin, Zagyansky and Lardner, 1976).

Because treatments that remove spectrin allow the clustering of proteins on the external surface of the RBC that are normally prevented from clustering (Elgsaeter and Branton, 1974), because binding antispectrin antibodies to spectrin on the inner surface of the RBC membrane causes a redistribution of glycoproteins on the outer surface of the cell membrane (Nicolson and Painter, 1973), and because treatments that aggregate spectrin in solution cause the aggregation of intramembranous particles in partially spectrin-depleted cells (Elgsaeter, Shotton and Branton, 1976), it is generally accepted and has been stressed by Singer (1974) that spectrin inhibits the diffusion of other proteins in the RBC membrane.

Chemically crosslinking the proteins of the red cell membrane crosslinks spectrin to itself and to several other proteins (Steck, 1972; Wang and Richards, 1974). Presumably, the crosslinked spectrin molecules arise from a network of spectrin molecules normally present in the intact cell membrane. Molecules crosslinked to spectrin might normally be non-covalently bound to spectrin and so be relatively immobile. The glycoproteins are not crosslinked to other proteins and can be quantitatively extracted following a 1-hr exposure to 2% glutaraldehyde at 0°C (Capaldi, 1973). Band 3 in the notation of Fairbanks, Steck and Wallach (1971) is a membrane-spanning glycoprotein of the red cell membrane. When isolated, it binds glyceraldehyde-3-phosphate dehydrogenase and an inner membrane surface protein (band 4.2) (Yu and Steck, 1975), yet it is not crosslinked to these molecules in the membrane. If the glycoproteins in the intact membrane are limited in their diffusion by binding to other membrane proteins, they are unusually resistant to crosslinking reactions.

If they are not bound to other proteins, they are still protected from crosslinking reactions, perhaps by the bulk of their carbohydrate component on the external cell surface, by electrostatic effects or by tightly bound lipids. In this case, the diffusional motion of the glycoprotein might be limited to a small area (domain) by steric interference between the spectrin network and the cytoplasmic portion of the molecule. The area available for diffusion might be further reduced by the bulk of other bound proteins. Note, however, that there is little hard evidence that other proteins are bound to spectrin. If a molecule were confined by the spectrin network to a small area of the lipid bilayer, it could become crosslinked and permanently affixed to spectrin as the result of a rather improbable (time average) collision with the spectrin. Thus, it seems likely that at least some of the membrane proteins have their translational motions limited by steric interactions with the spectrin network, consistent with the proposed model for gradual osmotic hemolysis (see below).

Summary

For the purposes of this work, the red cell membrane is viewed as basically a lipid-protein system in which the bulk of the lipid is in the form of a bilayer. Integral membrane proteins interact with the lipid hydrocarbon chains and often penetrate the bilayer, being exposed on both the extracellular and intracellular membrane surfaces (Singer and Nicolson, 1972). The lipid is asymmetrically distributed between the inner and outer halves of the bilayer and is segregated in the plane of the membrane in each half of the bilayer both by molecular species and by physical state. Large fluctuations are to be expected in the local

hydrocarbon density. The inner membrane surface is covered with an unpolymerized protein netowrk. This network restricts the diffusion of other membrane proteins either by binding to them or by confining them to a small area of the lipid bilayer.

AQUEOUS LIPID AND PROTEIN SYSTEMS

In this section, some properties of aqueous systems containing lipids, proteins, or lipids plus proteins are discussed briefly. Because the red cell membrane exists in an aqueous environment, this discussion is restricted to systems containing excess water and is limited to a few topics that are directly relevant to the model which is subsequently developed.

Lipids

Hydrophobic Effects

The transfer of a hydrocarbon of sufficient size (C_3 for an alkane) from its vapor, or from an organic solvent, to water is often energetically favorable but is accompanied by a large decrease in entropy. This entropy decrease dominates the thermodynamic behavior and results from the formation of a transient cage-like structure of water molecules surrounding the hydrocarbon molecule. This ordering of water molecules by the presence of nonpolar solutes is the basis of the hydrophobic effect, i.e., the tendency of nonpolar solutes to associate with other nonpolar solutes so as to reduce their area of contact with water. The reduction in the area of hydrocarbon-water contact decreases the number of structured water molecules compared to dispersed hydrocarbons in water and so is entropically favored.

Water itself is a highly structured complex liquid for which a completely satisfactory structural model is not available. The reader interested in the structure of water and its solvent properties from a theoretical, chemical or physical viewpoint is referred to the reviews contained in the volumes edited by Horne (1972) and Franks (1972-1975). The more biologically oriented reader might consult the monograph by Tanford (1973), which stresses empirical relationships concerning hydrophobic phenomena and especially micelles, or the monograph by Lauffer (1975), which stresses the conformation of tobacco mosaic virus protein. A statistical mechanical treatment of water and solute interactions has been published recently (Ben-Naim, 1974).

Owing to the lack of an adequate theoretical model, in spite of recent theoretical work (Hermann, 1971; Ben-Naim, 1975), empirical correlations between the surface areas of hydrocarbon solutes and thermodynamic properties have been employed (Hermann, 1972; Harris, Higuchi and Rytting, 1973; Reynolds, Gilbert and Tanford, 1974; Amidon, Yalkowsky and Leung, 1974). Extrapolation of this work to biological membranes is uncertain for several reasons. The calculation of the hydrocarbon-water interface area requires knowledge of the location and conformation of all membrane molecules. Such information is not available, but the determination of the choline and ethanolamine head-group conformations in phospholipids (Phillips, Finer and Hauser, 1972) has allowed the development of models that include H-bonded water molecules (Forslind and Kjellander, 1975). Some groups such as the hydroxyl group can form hydrogen bonds with water molecules and so enter into the cage-like water structure surrounding a nonelectrolyte, rather than itself being surrounded by the cage. Finally, it is not obvious that the thermodynamic values

determined where a cage-like structure of relatively immobile water molecules completely surrounds a solute molecule would also apply to water molecules that enter crevices between other molecules such as in a micelle. Theoretically, this situation would appear to be rather different because it would be expected that steric interferences would increase the number of broken hydrogen bonds among the water molecules. The prediction of micelle size by Tanford (1974a,b) indicates that these values are at least approximately correct, and it might be appropriate to apply them to water molecules in a crevice between molecules in a lipid bilayer. I therefore conclude that spaces between lipid molecules in a bilayer that are large enough to allow the entrance of water and so increase the area of contact between water and hydrocarbon are entropically an unfavorable occurrence.

Lipid Structures

Lipids combine a polar head group with a hydrocarbon tail (or tails). For energetic reasons, the polar head group will almost invariably be hydrated provided that sufficient water is present. In a lipid-water system, the shape and size of the lipid structures that form are determined by the minimization of the total free energy of the system. In the case of charged amphipathic molecules, the structures observed generally have the polar group exposed to water, and a compromise is reached between the exposure of nonpolar groups to water and electrostatic repulsions. The two hydrocarbon chains of phospholipids are roughly the same size as the polar head group so that the overall shape of the molecule is roughly cylindrical. When uncharged, such molecules will pack in bilayers and so minimize water contact with the hydrocarbon portion of the molecule.

If, however, the pH is changed so that the polar head groups become charged, there will be repulsions between the head groups, and a micellular structure will form when the charge becomes approximately 1.25 |e| per phospholipid (Ohki and Aono, 1970). Similarly, if the shape of a phosphatidyl choline molecule (lecithin) is changed by removing one of the two hydrocarbon chains to form lysolecithin, the molecule is no longer cylindrical but has a larger polar group than hydrocarbon tail. Such molecules will pack together in spherical micelles. Lysolecithin is lytic and causes fusion of cells, both probably by disrupting the normal bilayer structure of the membrane (Lucy, 1975).

Permeability and Free-Volume Fluctuations

Because most of the lipid in the red cell membrane is in a bilayer, bilayer data are stressed in this discussion. Nevertheless, reference to monolayer data will be convenient although monolayers are significantly different from bilayers. A bilayer is formed in aqueous solutions, and hydrophobic effects lead to a dense packing of the hydrocarbon groups. In contrast, a monolayer spread at the air-water interface can have its polar groups in the aqueous solution and hydrocarbon groups in the air. This arrangement drastically reduces the hydrophobic effect, and such monolayers tend to spread rather than having densely packed hydrocarbon regions. Similarly, monolayers spread at an oil-water interface have drastically reduced hydrophobic effects and, additionally, increased configurational freedom from the possibilities of oil-monolayer hydrocarbon-chain interactions and oil-water (dispersion) interactions. The reader interested in pursuing the properties of monolayers is referred to the books by Davies and Rideal (1961) and Gaines (1966). Phillips

(1972) stresses the similarities of lipid monolayers and bilayers.

Monolayer gas permeability

The permeability of a hydrocarbon monolayer on water to gases is an exponential function of the permeant size (Blank, 1962; Princen and Mason, 1965) and a function of the physical properties of the monolayer molecules (Rosano and La Mer, 1956). It is correct to discuss the permeability barrier in terms of an energy barrier, but it will prove more useful to investigate briefly the molecular mechanisms involved in permeation through a monolayer. In a series of papers, Blank (1962,1964; Blank and Britten, 1965) developed the hypothesis that, in order for a gas molecule to permeate a monolayer, it must collide with an area of the monolayer surface that, at that instant, is clear of surfactant molecules in an area at least equal to the area of the permeant molecule. The small open areas between surfactant molecules fluctuate in size owing to the thermal motions of the surfactant molecules, and the probability of observing an open area of any given size can be estimated from the entropy change associated with forming the open area. This change is a function of the monolayer compressibility because the compressibility determines the amount of work required to clear an open area of a given size. Blank (1964) evaluated the entropy change theoretically from surface-pressure-molecular-area data, but Bockman (1969) showed that this procedure did not agree with the experimentally determined value of the entropy of extension of a monolayer. If the experimental value of the entropy of extension of a 1-eicosanol monolayer is used in the Blank theoretical calculation of the monolayer resistance to water evaporation, the calculation yields a rate constant of 0.274 cm/sec, which is in reasonable agreement with the experimentally

determined rate constant of 0.182 cm/sec (Bockman, 1969). Further qualitative support for the fluctuation hypothesis comes from the calculated self-diffusion coefficient of a liquid-crystalline stearic-acid monolayer at 20 dynes/cm, about 1×10^{-8} cm^2/sec (Blank and Britten, 1965), and its agreement with the experimentally determined lateral diffusion coefficient of lecithin in a bilayer, 1.8×10^{-8} cm^2/sec (McFarland, 1972). Further, Blank and Britten (1973) calculated a stearic-acid flip rate of 10^{-5}/sec in a monolayer from area considerations alone. Kornberg and McConnell (1971) measured a lecithin flip-flop rate of 2×10^{-5} in a lecithin bilayer, and Deamer and Branton (1967) measured a higher rate of flip-flop, 5×10^{-4}/sec, in a more expanded stearate film, which would be expected from the increased free volume in the film and thus the flip-flop rate. It should be noted, however, that transmembrane lipid exchange is much faster in RBC's with reported values for the half-time for the exchange being as long as 20 to 30 min (Huestis and McConnell, 1973) and as short as 3.5 min for the outward rate and 34 min for the inward rate (Hsia and Spera, 1972). Removal of the charged carbohydrate residues on the external cell surface with neuraminidase equalizes the inward and outward rates to 3 to 4 min. Similarly, the work required to clear an open area of sufficient size in a monolayer to accommodate an adsorbing solute molecule was utilized by Ward and Tordai (1952) in a theory of adsorption although they did not discuss the work in terms of monolayer fluctuations but rather as an additional energy required by the solute molecule in order for it to be adsorbed.

Further support for the Blank fluctuation hypothesis comes from the geometrical model of Barnes, Quickenden and Saylor (1970). They modeled

long-chain alcohols as noninteracting hard discs and obtained random distributions by photographing a vibrating tray of spheres. They then determined the number of water molecules, modeled by appropriately-sized spheres that could fit in the clear areas between the alcohol molecules. By assuming that the rate of water evaporation in the clear areas large enough to contain water molecules was the same as that from a pure water surface, they could reproduce the surfactant density effect on the rate of evaporation through the monolayer although the chain-length dependence of the rate of evaporation was not included in the model. It may be significant that as the density of the discs is increased, their packing changes at a volume fraction of 0.83 from random order to domains of close-packed order that increase in size up to a volume fraction of 0.906 where close-packed order is complete (Quickenden and Tan, 1974). The volume fraction 0.83 is close to the volume fraction at which many long-chain alcohol and acid monolayers undergo a liquid-crystalline to crystalline phase transition.

Penetration into an insoluble monolayer

The retardation of evaporation and gas permeability of a monolayer depends on the instantaneous configuration of the molecules. In a collision between a permeant molecule and the surface, the permeant either passes through the monolayer or is reflected. Penetration into a monolayer held at constant area is different in that when a hole of sufficient size opens due to a thermal fluctuation, a permeant molecule can enter but then remains in the monolayer. This reduces the free area in the monolayer, which reduces the probability of observing the same size fluctuation, but the process generally continues until little free area remains in the mono-

layer. A purely geometric model of the penetration of sodium dodecyl sulfate into a cholesterol monolayer (MacGregor and Barnes, 1974) successfully accounts for the experimentally determined surface concentration of sodium dodecyl sulfate as a function of the area per cholesterol molecule in the unpenetrated monolayer (Pethica, 1955).

Rate-limiting steps

The two cases discussed above, permeability of a monolayer to gases and penetration into an insoluble monolayer, are two extremes that pertain to biological membranes. We generally consider the passage of a permeant through a biological membrane in the following three separable steps:

- transfer of the solute from the aqueous solution on one side of the membrane into the membrane
- diffusion across the membrane
- transfer of the solute from the membrane into the aqueous solution on the other side of the membrane.

Solute movements in the reverse direction are also permitted. In the monolayer systems, the second aqueous solution is replaced by a gaseous phase. Any of these steps can be rate-limiting. For gases permeating the monolayer, diffusion through the monolayer and transfer from the monolayer to the gaseous phase are assumed to offer negligible resistance compared to the rate-limiting step of transfer from the aqueous phase into the membrane. Passage from the gas phase through the monolayer and into the aqueous phase is similarly limited by entrance into the monolayer. In contrast, the penetration of a solute into a monolayer is not accompanied by transfer into the gaseous phase; that is, dissolution from the membrane is the rate-limiting step in transfer across the monolayer. In the model

presented here to describe the molecular sieving observed in red cell membranes, the start of the flow of each size unit of a protein is associated with the time at which that molecular species can first fully enter the membrane. That is, the rate-limiting step is considered to be the entrance of the globular solute into the membrane at the time of each flow start.

Permeability of polymers, biological membranes, and lipid bilayers

The theory developed by Blank is a free-volume theory. Similar theories are successfully used to describe diffusion through polymers (Kumins and Kwei, 1968). In this case, free-volume fluctuations in the size of cavities between polymer chains effect the diffusion of permeants. If the permeant molecular size is small compared to the average cavity diameter in the polymer, its diffusion constant is proportional to $(MW)^{-\frac{1}{2}}$. If, however, the permeant is about the same size as the average cavity diameter or larger, its diffusion coefficient becomes a complex and roughly exponential function of its diameter (Lundstrom, 1973).

Stein (1967) reviewed a large body of cell membrane permeability data and noted similarities between permeation across cell membranes and permeation through soft polymers. This view was extended by Lieb and Stein (1969,1971) who suggested that a polymer diffusion model could account for the cell membrane permeability of most nonelectrolytes.

Träuble (1971) proposed a model for the permeation of small molecules such as water through a lipid bilayer. In this model, the molecules enter the free volumes of kinks formed by two gauche rotations in a hydrocarbon chain. The kinks move rapidly up and down the hydrocarbon chain, and the

permeant can diffuse in the cavity formed by the kink. Only one size of kink was considered, and the calculated water permeability is in agreement with experiment. Extension to larger molecules would require a more general development including larger cavities.

The permeability of lipid bilayer membrane vesicles (liposomes) to a series of solutes was determined by Cohen and Bangham (1972), who concluded that nonelectrolyte transfer through a lipid bilayer membrane is similar to that through a hydrophobic polymer or biological membrane. In an extension of this work, Cohen (1975a,b) demonstrated further similarities between permeation through liposomes and cell membranes, showed that cholesterol decreased the nonelectrolyte permeability of unsaturated phosphatidyl choline membranes by primarily effecting the dehydration of the solutes, and concluded, in agreement with Macey and Farmer (1970), that in the red cell membranes, water is the only non-electrolyte that crosses the membrane substantially through aqueous pores.

The permeability of phospholipid monolayers and bilayers is a function of both the hydrocarbon and polar portions of the molecule. A dipalmitoyl phosphatidyl choline monolayer has little effect on the rate of evaporation of water, yet dipalmitoyl phosphatidyl ethanolamine reduces the rate of evaporation with increasing effect at increasing surface pressures (Turner, Litt and Lynn, 1975). The area per molecule in the surface is, of course, a function of the surface pressure. At all surface pressures, including the collapse pressure, however, the area per molecule is larger for phosphatidyl choline than for phosphatidyl ethanolamine (van Deenen, Houtsmuller, de Haas and Mulder, 1962). This fact suggests that, qualitatively, the choline head groups prevent the close packing of the hydro-

carbon chains, thus increasing the free volume in the monolayer and permitting the rapid evaporation of water. The ethanolamine head group permits closer packing of the hydrocarbon chains, which reduces the free volume in the hydrocarbon phase, and results in fewer fluctuations large enough to permit the passage of a water molecule. The effect of the head group itself, however, is not yet fully understood. X-ray diffraction of closely opposed bilayers indicates that the choline head group is extended parallel to the hydrocarbon chains a distance of about 11Å and that there is an electrostatic repulsion between neighboring molecules. In contrast, the ethanolamine head group is bent over more parallel to the interface and occupies a larger surface area than the choline head group, and adjacent molecules electrostatically attract one another (Phillips, Fine and Hauser, 1972). If the orientations of the head groups in monolayers is the same as that in the closely opposed bilayers, the electrostatic effects limit the closest packing observable in saturated phosphatidyl choline monolayers, but whether the physical bulk of the ethanolamine head group effects the rate of evaporation is not known. Thus, the effect of changing the polar head group of saturated phospholipids agrees qualitatively with the predictions of the free-volume fluctuation model. Quantitative comparison with theory has not yet been presented, and it is possible that the polar head group effects water evaporation independently of its effect on free volume in the hydrocarbon phase.

If an unsaturated hydrocarbon chain replaces a saturated chain, the area per molecule at a fixed film pressure is increased (van Deenen et al., 1962), resulting in an increase in the free area in the membrane, and liposomes made from unsaturated lipids are more permeable than liposomes

made from saturated lipids of the same hydrocarbon chain lengths (Cohen, 1975a) as would be predicted by the free-volume fluctuation hypothesis. The addition of cholesterol to a monolayer (Phillips, Kamat and Chapman, 1970) or bilayer (Rand and Luzzati, 1968) of unsaturated phospholipids reduces the area per molecule, restricts the motion of the hydrocarbon chains (Darke et al., 1972), and decreases liposome permeability (Cohen, 1975b) as expected.

If liposomes are maintained at a temperature at which domains of crystalline and liquid-crystalline hydrocarbon coexist or if the temperature is changed so that such domains coexist, the liposomes have increased permeability compared to nearby temperatures where a single phase exists (Blok, van Deenen and De Gier, 1976). This is expected on the basis of the free-volume fluctuation hypothesis as previously mentioned because of the increased compressibility when two phases are present. Liposomes prepared by sonication of saturated phosphatidyl choline below the phase-transition temperature are leaky to ions and have their hydrocarbon chains organized in small, discontinuous but highly ordered domains. Annealing the liposomes at temperatures above the crystalline to liquid-crystalline phase-transition temperature causes the liposomes, when returned to the crystalline phase by lowering temperature, to be impermeable to ions and to have their hydrocarbon chains organized in larger domains (Lawaczeck et al., 1975). Thus, discontinuities between domains of the same phase also increase lipid-bilayer permeability, probably again by free-volume fluctuations.

The cation permeability of liposomes made from saturated phosphatidyl cholines with 14 or more carbon atoms per acyl chain is very low. Dilauryl

phosphatidyl choline (C 12) liposomes are, however, sufficiently permeable above the transition temperature to permit permeability studies to be conducted, and it is found that cation permeability decreases with increasing ion size (Blok, Van der Neut-Kok, van Deenen and De Gier, 1975) as is expected from the fluctuation hypothesis. In contrast to cations, the exchange of small anions across liposomes is very fast and proceeds primarily by an electrically silent, carrier-mediated process, which probably involves phospholipid flip-flop (Toyoshima and Thompson, 1975). Carrier-mediated anion transport is also present in red cells (Pressman, 1973; Gunn, Wieth and Tosteson, 1973), but it is generally accepted that anion transport in red cells involves a protein, specifically a band-3 protein (Cabantchik et al., 1975).

Summary

The thermodynamic properties of lipids are dominated by hydrophobic effects that tend to minimize the area of contact between hydrocarbon and water. In the case of lipid bilayers, this effect leads to a dense packing of the hydrocarbon chains, but the packing is dependent on the properties of both the polar and nonpolar portions of the molecules. The permeability properties of biological membranes and lipid bilayers to small nonelectrolytes are very similar and are typical of soft polymers. The mechanisms of transport into and/or through these membranes apparently involve fluctuations in free volume. Because the red cell membrane is largely a lipid bilayer, the process of controlled gradual osmotic hemolysis will be modeled as a process involving free-volume fluctuations in the lipid hydrocarbon chains under conditions that take into account hydrophobic interactions and the constraints of membrane proteins.

Proteins

Stability, Hydrophobic Effects, and α-Helix Content

Tanford (1970) noted that there is typically a free-energy difference of about 10 kcal/mole between the native configuration of a globular protein and its random-coil configuration. Because the transfer of a single aromatic amino-acid side chain from an aqueous environment to a site protected from water within the protein would contribute about 3 kcal/mole to the stability of the native conformation and because a protein monomer will generally have in excess of 100 amino-acid residues, a difference of 10 kcal/mole between conformational states is a remarkably low stability as noted by Tanford. In view of the marginal stability of the native conformation, fluctuations in the conformation would be expected to be significant. Experimentally, such fluctuations are observed, and it is found that significant concentrations of proteins are present in various unfolded states (Tanford, 1970). The reader is referred to Gō (1976) for a brief review of fluctuations in globular-protein conformation.

A general discussion of the factors involved in determining protein conformation is beyond the scope of this paper; however, hydrophobic effects are important and will be pursued briefly.

When increasing concentrations of nonpolar solute such as 2-chloroethanol, simple alcohols or dioxan are added to an aqueous solution containing a globular protein, the native configuration is stable to about 20% by volume of organic solvent. The protein then adopts a conformation that approximately maintains its native α-helix content but is otherwise partially unfolded. Further addition of organic solvent causes the appearance of a conformation characterized by a high helix

content (Weber and Tanford, 1959). Hb follows this typical globular-protein behavior (Ikai and Noda, 1968). The increase in helix content in less polar environments demonstrates that hydrophobic factors are important in maintaining the native conformation and that release from the hydrophobic constraints leads to a conformation with a higher helix content (Singer, 1971). In general, nonpolar solvents increase the helix content of proteins in which the native structure is a random coil or globular conformation but have little effect on fibrous proteins that are already in a high helix conformation (Tanford, 1968).

In a similar manner, the binding of detergents can project residues from water and so permit an increase in helix content (Jirgensons, 1966; Jirgensons and Capetillo, 1970). The apoproteins of serum lipoproteins, which normally bind phospholipids and cholesteryl ester, increase in helix content when these are bound (Luy et al., 1972). Apoproteins isolated from the red cell membrane bind lipid only in the α-helical conformation and generally do not retain a helical conformation if transferred to an aqueous medium unless they are stabilized by bound lipid (Zahler, 1972). It is therefore not surprising that one third to one half of the protein residues in red cell ghosts are in an α-helical conformation (Lippert, Gorczyca and Meiklejohn, 1975). Little or no β conformation is detected (Maddy and Malcolm, 1965) except during hydrolysis of ATP (Grahm and Wallach, 1971). Holzwarth, Yu and Steck (1976) recently established that the major integral membrane protein, band 3, had 38% of its amino acid residues in helical conformations, that the fibrous protein spectrin was 55% helical, and that an assortment of other peripheral proteins were 17% helical. Prior to extraction, the entire ghost protein was 37% helical. The value of 38%

for the helical form of the major integral protein may be misleading because this protein is accessible on both sides of the membrane to aqueous reagents. The portion within the membrane probably has a substantially higher percentage of helixes. Glycophorin is a membrane-spanning glycoprotein that carries the ABO and MN antigens that constitute about 10% of the human red cell ghost protein, and that carries almost all of the cell's sialic acid. It is a single polypeptide chain; the first 90 to 100 amino-terminal amino acids are on the outer surface of the cell and are associated with the carbohydrate. The next 23 nonpolar amino acids cross the membrane, and these amino acids are followed by a segment with a rather typical amino acid composition that is inside the cell (Marchesi, 1975). Thus, about 10% of its amino acid residues are probably involved in spanning the membrane, and all of these are nonpolar.

Helix Orientation and Aggregation

If a helical protein interacts with a lipid bilayer, the helix may be oriented specifically with respect to the bilayer plane. In the purple membrane of *Halobacterium halobium*, α-helical segments of protein transverse the membrane roughly perpendicular to its plane, and seven helices are formed into a super coil (Henderson, 1975; Henderson and Unwin, 1976). In contrast, a segment of an apoprotein of plasma lipoproteins has a line of negative charges in a narrow strip on the surface of the helix parallel to the axis of the helix. Positive charges alternate from one side of the line to the other. This side of the helix is polar but bears no net charge. The other side is nonpolar. Segrest et al. (1974) have suggested that the helix lies in the plane of the membrane with the phospholipid head groups interacting with the helix charges and the protein side chains

interacting hydrophobically with the lipid. Verdery and Nichols (1975) proposed a structure for high-density serum lipoproteins based on the amphiphathic protein helix.

Therefore, the α-helical conformation of proteins is often involved in lipid binding, lipids often stabilize the α-helical conformation, and different orientations of the helix with respect to the lipids exist. Not all helical proteins, however, strongly bind lipid: spectrin, which is 55% helical can be easily washed from red cell membranes.

Tanford (1968) noted that proteins in the highly helical conformation tended to precipitate and that HCl was usually added in order to increase the protein net charge and prevent precipitation. This precipitation is generally attributed to the lower dielectric constant of the nonpolar solvent but is probably partially caused by the alignment of the dipole moments of the peptide bonds in the helical segments, thus creating a large net dipole moment for the entire helix, as has been studied in poly-amino acids (Wada, 1976). This large dipole moment causes the aggregation of the helices, first head-to-tail and then randomly side-by-side, until large liquid crystals are formed. It is possible that spectrin, with its high α-helix content, might be similarly aggregated if its electric charge were altered.

Other Helical Conformations

Although most workers interpret their data in terms of α-helix, β-structure, and random-coil configurations, other helical structures are theoretically possible and, in fact, probable in the case of gramicidin A (Urry, 1972). The $\pi^{4}_{(L,D)}$ helix would have an ion-conducting 1.4Å pore, which would provide cation selectivity in the order $Na^{+} > K^{+} > Rb^{+} > Cs^{+}$;

the $\pi^{6}_{(L,D)}$ helix would have a 4Å pore, which would have cation selectivity in the reversed order; and the $\pi^{8}_{(L,D)}$ helix with a 6Å pore and the $\pi^{10}_{(L,D)}$ helix with an 8Å pore would have little selectivity. Urry believes that in lipid bilayers the $\pi^{6}_{(L,D)}$ conformation is the most probable conformation for gramicidin A.

Summary

The native configuration of a globular protein is marginally stable, and fluctuations to other conformations are probable. Hydrophobic effects are important in determining the native structure of proteins. If the hydrophobic effects are reduced or eliminated, globular proteins increase in helix content. In some proteins, a helical conformation is required to bind lipids, and bound lipids stabilize the helical conformation. The interaction of the helix with the lipid varies, however, with the amino acid sequences; examples are known in which the helices transverse a bilayer roughly perpendicular to its plane and in which the helix lies in the plane of the lipid head groups. Polypeptides can theoretically form helical structures other than the α-helix, and at least some of these structures can transport cations via a pore with a selectivity that is dependent on the helical conformation.

In the model to be presented, it will be assumed that globular cytoplasmic proteins fluctuate in their conformation and that suitable conformations are present to interact hydrophobically with lipids. These conformations may involve an increase in helix content. Because a lipid bilayer is only about 45Å thick (Rand, 1968), a portion of a protein interacting with a bilayer remains exposed to an aqueous environment so that the general prediction of an increase in α-helix content in a nonpolar

environment may not apply. The conformation of proteins interacting with lipid bilayers is considered further in the following section.

Protein Adsorption to Lipid Monolayers and Bilayers

Protein Conformation

It is to be expected from the properties of proteins and lipids that nonspecific interactions between lipids and proteins would involve, in general, both electrostatic and nonpolar interactions. In specific instances, one particular type of interaction may predominate, such as the electrostatic interaction between insulin and phospholipids.

X-ray diffraction can be used to determine the conformation of both lipids and proteins in a lipid-protein system. When insulin and phospholipid bilayers interact, it is found that insulin does not alter the lipid packing and that the insulin interacts with the polar head groups while maintaining a globular (but not spherical) conformation (Rand and Sen Gupta, 1972). Cytochrome-c interactions with lamellar lipid phases are predominantly electrostatic, and the protein maintains a globular conformation (Shipley, 1973). Lysozyme forms a similar phase with cardiolipins, but in addition, forms a phase in which the lipid bilayer is thinned from 35 to 27Å, in which the protein conformation is globular although circular dichroism suggests some change from the native conformation (Gulik-Krzywicki et al., 1969), and in which hydrophobic interactions occur between lipids and proteins as indicated by fluorescence studies (Shechter et al., 1971). Bovine serum albumin at pH 3.3 has a random-coil configuration. It initially interacts electrostatically with a lipid bilayer but then develops hydrophobic interactions that thin the bilayer. All of the positively charged groups at this pH appear to be able to bind to negatively

charged lipid head groups, which might suggest unfolding of the protein, but the overall protein configuration is a flattened glob rather than an extended monolayer (Rand, 1971). Thus, x-ray diffraction analysis of soluble globular proteins interacting with lipid bilayers and at least one soluble random-coil protein interacting with lipid bilayers indicate that the protein has a globular but not necessarily spherical conformation both in predominantly electrostatic interactions and in a combination of electrostatic and nonpolar interactions.

Segrest, Gulik-Krzywicki and Sardet (1974) showed that when the hydrophobic membrane-penetrating segment of the red cell MN-glycoprotein (glycophorin) was added to phospholipid vesicles, the segments aggregated within the membrane to form 80Å-diameter intramembranous particles composed of 10 to 20 segments each. Although this phenomenon may be specific to the MN-glycoprotein, it may be a general phenomenon resulting from reduced van der Waals forces between lipids and proteins compared to lipid-lipid interactions. Suitable energy differences could lead to a phase separation in an Ising model. Therefore, it appears reasonable to conclude that proteins, in general, have a globular conformation when interacting with bilayer lipid phases.

The number of residues of a protein in an interface can be determined by an investigation of the adsorption of the protein from bulk solution to an interface. It should be noted that spreading a protein at an interface often leads to an unfolding of the protein (denaturation) whereas adsorption of the protein to the interface generally retains more structure.

β-casein is a flexible hydrophobic protein with a random coil conformation in aqueous solution. When it absorbs to the air/water

interface, each amino acid lies in the interface at surface pressures below 7 dynes/cm, and the total thickness of the protein is less than 20Å. At higher surface pressures, some amino acid residues are squeezed out of the interface, and the protein layer thickness increases to about 50Å (Benjamins et al., 1975). In contrast, the more structured κ-casein (Benjamins et al., 1975) and lysozyme (Phillips, Evans, Grahm and Oldani, 1975) never have all of their amino acid residues in the interface at measurable surface pressures (>1 dyne/cm). This behavior is apparently typical for soluble globular proteins (Table VIII).

MacRitchie and Alexander (1963) interpreted the rate of adsorption of proteins in terms of the area that had to be clear of adsorbed molecules in order for adsorption to occur (Ward and Tordai, 1952). Joos (1968) interpreted the equilibrium surface pressure as a function of bulk protein concentration in terms of the number of residues in the interface (Frisch and Simha, 1957). Both approaches indicate that, with the exception of pepsin, only 6 to 16 amino acid residues are in the air/water interface or about 2% of the amino acids for bovine serum albumin (Table VIII). The single measurement at the heptane/water interface (bovine serum albumin) suggests that fewer residues reside in the organic/water interface than in the air/water interface.

Unfortunately, similar data concerning the number of amino-acid residues in the lipid/water interfacial region are not available. Other data are consistent with the view that soluble globular proteins retain a globular conformation and have a low percentage of their amino acid residues in the interfacial region when interacting with lamellar lipid phases (see below).

TABLE VIII. Number of amino acids and areas of proteins in interfaces.

Protein	Molecular weight[a]	pH	Salt	Interface	Number of Residues in Interface		Areas of Residues in Interface	
					Joos (1968)	MacRitchie & Alexander[b] (1963)	Joos[c] (1968) ($Å^2$)	MacRitchie & Alexander (1963) ($Å^2$)
Bovine serum albumin	66,200	--	--	air/water	--	9.6	--	135.
		4.9	0.1N NaCl	air/water	11.3	--	158.	--
		4.9	1mM HAc + 1mM NaAc	air/water	16.3	--	228.	--
		4.9	0.1N NaCl	heptane/water	4.0	--	56.	--
Human serum albumin	69,000	5.5	$\mu = 0.01$	air/water	--	7.1	--	100.
α-chymotrypsin	21,600	--	1mM HCl	air/water	6.5	--	91.	--
Lysozyme	13,930	5.5	$\mu = 0.01$	air/water	--	7.1	--	100.
Myosin	540,000	7.0	$\mu = 0.35$	air/water	--	10.4	--	145.
Ovalbumin	43,500	5.5	$\mu = 0.01$	air/water	--	12.5	--	175.
Pepsin	38,900	1.57	--	air/water	48.	--	672.	--
Trypsin	15,100	--	1mM HCl	air/water	15.	--	210.	--
Human γ-globulin	153,100	7.0	$\mu = 0.35$	air/water	--	9.3	--	130.

References:

[a] Average of molecular weights listed in Sober (1968).

[b] Calculated from their reported areas using 14 $Å^2$ per amino acid.

[c] Calculated from the number of amino acids in interface using 14 $Å^2$ per amino acid.

Bilayer Structure

The x-ray diffraction studies previously mentioned found that the bilayer structure is unperturbed by electrostatic interaction with proteins but that it becomes thinner and, on the average, the lipid head groups are spaced farther apart when both electrostatic and nonpolar interactions are involved.

All protein interactions with lipids appear to disrupt the cooperative head-group interactions responsible for the pretransition endotherm observed in differential scanning calorimetry (Chapman, Keough and Urbina, 1974; Papahadjopoulos, Moscarello, Eylar and Isac, 1975). In the red cell membrane, the motions of both the lipid head groups and hydrocarbon chains are restricted compared to the motions in lipids extracted from the membranes. If spectrin is removed from the membranes, the mobility of the choline group of phosphatidyl choline increases significantly, and there is a slight increase in the mobility of the lipid hydrocarbon chain methyl groups (Sheetz and Chan, 1972).

Proteins that interact electrostatically with the lipids have little effect on the enthalpy of the crystalline to liquid-crystalline phase transition of the lipid hydrocarbon chains (Papahadjopoulos et al., 1975). Proteins that interact electrostatically and hydrophobically (basic myelin protein A1, cytochrome c, and hemoglobin) reduce both the temperature at which the transition occurs and the enthalpy of the transition. These changes are perhaps best explained by a distortion of the bilayer by the protein, which alters the hydrocarbon chain conformations (Papahadjopoulos et al., 1975), because a distortion of the bilayer would explain the effects of proteins on liposome permeability (see below) and is in agreement with

the deviation from the normal parallel arrangement of lipid hydrocarbon chains caused by Folch-Lees protein (Butler, 1975). Other workers have interpreted calorimetric data with some of the same proteins but with different lipids predominantly in terms of protein-lipid head group interactions (Chapman et al., 1974).

Hydrophobic polypeptides such as the myelin proteolipid apoprotein N-2 and gramicidin A have little effect on the temperature of the transition but decrease its enthalpy (Papahadjopoulos et al., 1975). This is in accord with the observation on the hydrophobic membrane protein cytochrome oxidase by Jost et al. (1973). Phospholipids added to cytochrome oxidase first form a tightly bound layer of lipid over the protein, and only after this layer is complete does added lipid form a bilayer. This tightly bound lipid has severely restricted motion and is presumably removed from the lipid that undergoes the cooperative phase transition, thus reducing the enthalpy of the transition. The concept of a condensed monomolecular layer of egg phosphatidyl choline surrounding each hydrophobic β-casein molecule adsorbed to an egg phosphatidyl choline monolayer is consistent with the surface pressure increase caused by the penetration of β-casein into the phosphatidyl choline monolayer (Phillips, Evans and Hauser, 1975) and with the reduction of the enthalpy of the crystalline to liquid-crystalline phase transition caused by other proteins.

To summarize, proteins that interact primarily electrostatically with lamellar lipids effect the lipid head group motions but have little effect on the hydrocarbon portion of the lipid. In contrast, proteins that can interact hydrophobically often thin the bilayer and disorder the hydrocarbon chains. Very hydrophobic proteins can tightly bind a monolayer of lipid molecules and effectively remove them from cooperative motions.

Protein Penetration into Lipid Monolayers

If a solute in an aqueous solution adsorbs to an insoluble monolayer spread at the air/water interface of the solution and if it increases the surface pressure of the monolayer, the solute is said to penetrate the monolayer. This is an operational definition and, for the case under discussion, does not necessarily mean that protein amino acids interact with the lipid hydrocarbon chains.

The following paragraphs describe, in general, the penetration of a soluble globular protein into a lipid monolayer. The reader interested in pursuing a specific example is referred to the elegant work of Quinn and Dawson (1969a,b; Dawson and Quinn, 1971) with cytochrome c.

If a soluble protein is added to an aqueous solution below a lipid monolayer that is held at a constant area and that is initially at surface pressure π, the adsorption of the protein can cause an increase in the surface pressure of $\Delta\pi$. If a series of experiments are conducted with different initial surface pressures of the insoluble lipid monolayer but with a constant amount of protein injected under the monolayer, $\Delta\pi$, in general, is found to be a linearly decreasing function (or functions) of the initial surface pressure. At $\Delta\pi = 0$, a limiting surface pressure is reached. At surface pressures below this limiting surface pressure, the protein can penetrate the monolayer and cause an increase, $\Delta\pi$, in the surface pressure whereas above this surface pressure the protein does not penetrate the monolayer.

Electrostatic interactions are important in determining the limiting surface pressure. The change in surface pressure increases when the lipid head-group composition is changed to increase the protein-lipid electro-

static attraction (or when the pH is changed, although this effect is often more complex because it causes conformational changes) and decreases when salts are present in the subphase. Similarly, hydrophobic effects are generally important in determining the limiting surface pressure as indicated by the surface pressure increase that occurs when the lipid head groups remain unchanged but the hydrocarbon chains are lengthened. These effects are complex and only partially reversible; increasing the ionic strength under a penetrated monolayer in which electrostatic interactions are important generally does not remove penetrated protein from the interface; removal of protein from the subphase after penetration generally does not lead to a decrease in surface pressure; but increasing the surface pressure to well above the limiting value for penetration can reduce the amount of penetrated protein, especially at high ionic strengths. A similar behavior is observed in the amount of protein adsorbed to a monolayer held at a surface pressure above the limiting value. Here the amount of protein that can be desorbed by raising the ionic strength is found to decrease with time and reach a constant value after about 40 minutes (cytochrome c with phosphatidyl ethanolamine). It is generally believed that soluble globular proteins are first attracted to or repelled from a lamellar lipid system by electrostatic forces, but, after contacting the lipid, conformational changes occur that result in an increase in hydrophobic interactions (Quinn and Dawson, 1969b; Rand, 1971). The apparent irreversibility of protein-lipid-monolayer interactions is a severe handicap in the thermodynamic treatment of this system because most theoretical developments assume reversibility. A generally satisfactory treatment is not yet available although the nature of the interactions

between protein and lipid are becoming more evident (Hendrikx and Ter-Minassian-Saraga, 1975).

Whereas the limiting pressure is found to be determined primarily by electrostatic interactions and the length of the hydrocarbon chains, the amount of protein that penetrates the monolayer to cause a given $\Delta\pi$ increase is a strong function of the compressibility of the monolayer as expected if free-volume fluctuations are involved in the penetration. When the lipid of a monolayer undergoes a phase transition, the increase in monolayer compressibility causes a marked increase in the surface concentration of a protein (Phillips, Evans and Hauser, 1975). Similarly, when the compressibility of a monolayer is decreased by adding cholesterol, the amount of protein that penetrates the monolayer is reduced (Papahadjopoulos, Cowden and Kimelberg, 1973). The interaction also reflects specific interactions with the monolayer (Papahadjopoulos et al., 1973; Colacicco and Rapport, 1968) that presumably result from the formation of complexes and the separations in cholesterol-phospholipid systems that were previously discussed. Colacicco (1969,1970) has advanced the hypothesis that proteins enter the monolayer in a globular form between surface micelles formed from the monolayer components. This hypothesis is consistent with the generally globular shape of adsorbed proteins and is in agreement with the expected larger fluctuations at domain boundaries.

Protein-Liposome Interactions

Cation permeability

When proteins absorb to liposomes, there is sometimes a dramatic increase in cation permeability. Kimelberg and Papahadjopoulos (1971a) showed that proteins that could penetrate phosphatidyl serine monolayers

at pressures of up to about 40 dynes/cm (lysozyme and cytochrome c at pH 7.4, human serum albumin at pH 4.5) increased the $^{22}Na^{+}$ loss from phosphatidyl serine liposomes by a factor of 560 to 1,500. Proteins that could penetrate monolayers only to about 23 dynes/cm (ribonuclease and albumin at pH 7.4) increased the $^{22}Na^{+}$ loss by a factor of only 3 or 50. Thus, the dramatic increase in cation permeability is correlated with protein penetration of a monolayer. The signficance of a critical surface pressure between 23 and 40 dynes/cm was noted by Papahadjopoulos (1968); the area of a phospholipid molecule in a lipid dispersion is about 68Å^2, and in a monolayer this corresponds to a surface pressure of 20 to 25 dynes/cm. Proteins that could penetrate monolayers above this pressure presumably could also effect the hydrocarbon portion of a liposome. Subsequently, it was shown that these proteins altered the lipid crystalline to liquid-crystalline phase transition through distortion of the bilayer (Papahadjopoulos et al., 1975).

The activation energy for the cytochrome-c-induced loss of $^{22}Na^{+}$ from phosphotidyl serine liposomes is 29 kcal/mole, and the activation energy for the lysozyme-induced loss is about 16 kcal/mole (Kimelberg and Papahadjopoulos, 1971b). These high values indicate that this $^{22}Na^{+}$ loss is not by free aqueous diffusion.

Changes in the composition or compressibility of the lipid generally affect the $^{22}Na^{+}$ loss in a manner similar to protein penetration of a lipid monolayer. There is a large electrostatic effect for many globular proteins (Kimelberg and Papahadjopoulos, 1971b), and reducing the compressibility of the lipid by adding cholesterol or replacing an unsaturated hydrocarbon chain with a saturated chain reduces the protein-induced $^{22}Na^{+}$ loss. Thus,

it seems that the enhanced $^{22}Na^{+}$ loss from bilayer liposomes results from an interaction similar to the protein penetration of a lipid monolayer. The hypothesis that local fluctuations in lipid-free volume are important in lipid-protein interactions is strengthened by the observation that pancreatic phospholipase A_2 readily attacks pure phosphatidyl cholines and mixtures of phosphatidyl cholines at their crystalline to liquid-crystalline phase-transition temperature or when two phases are present in their mixtures but not, or at a much reduced rate, when only one phase is present (Op den Kamp, Kauerz and van Deenen, 1975). Addition of cholesterol inhibits the hydrolysis; however, filipin and amphotercin B increase the rate of hydrolysis, which agrees with the general prediction of increased free-volume fluctuations at the interface of dissimilar molecules due to steric interference and reduced van der Waals forces.

Lossen, Brennecke and Schubert (1973) found that if a mixture of tightly bound red cell proteins was added to one side of an oxidized cholesterol membrane, the electrical resistance of the membrane changed little, but if the protein mixture was added to both sides of the membrane, the resistance decreased 300-fold. Whereas an oxidized cholesterol membrane is quite different from a phospholipid membrane, this observation suggests that proteins that cannot produce an ion leak when on one side of the membrane can interact, perhaps indirectly, with a similar protein on the opposite side of the membrane to create an ion leak.

Mechanism of protein-induced permeability increase

The limited data available support Kimelberg and Papahadjopoulos' conjecture (1971a) that proteins that can penetrate a monolayer at a surface pressure on the order of 30 dynes/cm also cause an increase in the loss of

$^{22}Na^{+}$ from liposomes. If the same mechanism is involved in the permeability increase whenever it is caused by a soluble globular protein, this pathway apparently transports molecules of up to approximately the size of glucose. Lysozyme, cytochrome c, and Hb increase the cation permeability of liposomes (Kimelberg and Papahadjopoulos, 1971b; Papahadjopoulos, Cowden and Kimelberg, 1973) but do not increase the glucose permeability (Gould and London, 1972; Calissano, Alemà and Rusca, 1972), whereas unfolded bovine serum albumin (pH < 5.5) (Sweet and Zull, 1969), some RBC membrane proteins (Sweet and Zull, 1970; Lidgard and Jones, 1975) and the central nervous system basic A_1 protein (Gould and London, 1972) do increase glucose permeability.

The mechanism by which proteins increase the permeability of lipid bilayers is not known with certainty. It is possible that the protein forms a solute-conducting helix that transverses the membrane (Urry, 1972) or adopts some other conformation that constitutes a protein pore although it may fluctuate in size and exist only in a statistical sense. The calorimetric and spin-label data suggest, however, that proteins that increase liposome permeability also markedly alter the lipid hydrocarbon chain organization. Therefore, it seems more likely that the solute loss involves the disordered chains and is probably occurring through free-volume fluctuations near the lipid-protein interface.

Hb-lipid interactions — Comparison to RBC's

In view of the importance of hemoglobin and spectrin to the red cell, the interaction of these two proteins with lipids will be summarized. Hb at 0.1 mg/ml increases the rate of loss of $^{22}Na^{+}$ from liposomes from less than 0.1% per hour to 22% per hour with phosphatidyl serine liposomes and

to 17% per hour with phosphatidyl choline liposomes (Papahadjopoulos, Cowden and Kimelberg, 1973). Because Hb can increase the $^{22}Na^{+}$ loss from neutral phosphatidyl choline liposomes, hydrophobic interactions must be important in this system. The addition of cholesterol reduces the rate of $^{22}Na^{+}$ loss to 1.1% per hour for an equimolar mixture of phosphatidyl serine and cholesterol. Calissano, Alemà and Rusca (1972) showed that at 0.5 mg/ml and pH 7.5, Hb increased the $^{86}Rb^{+}$ loss from liposomes consisting of 75% phosphatidyl serine and 25% phosphatidyl choline from 0.41% per hour in the absence of protein to 38.7% per hour. Other soluble polypeptides at the same concentration (polyglutamic acid, pepsin, bovine serum albumin, pronase and ribonuclease) increased the $^{86}Rb^{+}$ loss to a maximum of 0.67% per hour except for cytochrome c, which increased the rate of loss to 1.90% per hour. Thus, Hb is very effective in increasing the cation loss from liposomes. Calorimetric data (Papahadjopoulos, Moscarello, Eylar and Isac, 1975) show that Hb decreases the crystalline to liquid-crystalline phase-transition temperature and the enthalpy of the transition in a dipalmitoyl phosphatidyl glycerol-Hb mixture, which suggests that Hb binds and disorders the hydrocarbon chains in a lipid bilayer. It is apparently this distortion of the bilayer that increases free-volume flucutations and results in the marked increase in cation loss from liposomes that occurs on Hb adsorption.

The Hb-induced permeability increase is apparently significant only for small ions and molecules because in liposomes consisting of 75% phosphatidyl serine and 25% phosphatidyl choline, 0.5 mg/ml Hb at pH 7.5 increases the rate of $^{86}Rb^{+}$ loss from 0.41 to 38% per hour, the rate of choline loss from 1 to 30% per hour, and the rate of 4-aminobutyric acid

loss from about 30 to about 40% per hour, but there is no detectable effect on the 60% per hour loss of glucose (Calissano, Alemà and Rusca, 1972).

Infrared spectra of Hb adsorbed to an arachidic acid monolayer at 30 dynes/cm indicate that the native Hb conformation is largely unaltered but that the lipid hydrocarbon chains have increased freedom. In contrast, if Hb is adsorbed onto a hydrophobic methylstearate monolayer, the Hb appears to unfold (Fromherz, Peters, Müldner and Otting, 1972). Unfortunately, experiments were not conducted at lower initial surface pressures, which would have allowed conformational studies when significant Hb monolayer penetration had occurred. Hb adsorbed to a monolayer does not desorb if Hb is removed from the subphase, but Hb can be at least partially desorbed by raising the surface pressure. If 10^{12} Hb molecules/cm^2 are adsorbed to a monolayer at 35 dynes/cm and the subphase is then cleared of Hb, an expansion of the monolayer to a surface pressure of 10 dynes/cm allows the adsorbed Hb to penetrate the monolayer. If the surface pressure is maintained at 10 dynes/cm and the increase in film area is measured two minutes after the expansion, the Hb adsorbed on an arachidic acid monolayer causes an area increase to 1.3 A_0. If, however, the subphase contains 5M urea, which would be expected to dissociate and unfold Hb, the film area is increased to 2.5 A_0. If the Hb is adsorbed to a methylstearate monolayer where it is at least partially unfolded and so presumably also dissociated, the film area is increased to 3.6 A_0 (Fromherz, 1971). Thus, conditions that tend to dissociate and/or unfold Hb lead to an increased rate of penetration into a monolayer as expected. It is probable that some of the effects of abnormal Hb's on the red cell membrane are related

to this increased rate of monolayer penetration by dissociated and/or unfolded Hb.

A rough estimate of the Hb-induced cation permeability in a liposome, which resembles a red cell, can be obtained as follows: From the data previously presented, it can be calculated that the inner membrane leaflet of the red cell membrane contains about 26% phosphatidyl serine and little if any cholesterol. The outer membrane leaflet has essentially no phosphatidyl serine but, on a molar basis, has more cholesterol than phospholipid. Data on protein-induced cation loss from asymmetric membranes or from membranes with the composition of either the inner or the outer red cell membrane leaflet are not available. Because the Hb-induced cation losses from phosphatidyl serine and phosphatidyl choline liposomes differ by about 30%, they can be used to obtain an estimate of the Hb-induced cation loss if the inner membrane leaflet controlled the loss. If the outer membrane leaflet controlled the loss, an appropriate model might be an equimolar phosphatidyl serine-cholesterol liposome.

Papahadjopoulos et al. (1973) have presented a graph of the percentage of $^{22}Na^{+}$ loss per hour as a function of Hb concentration from 0 to 0.2 mg Hb/ml. In the rat red cell, the Hb concentration is about 320 mg/ml. Extrapolation of the graphed data to higher concentrations for both phosphatidyl serine and phosphatidyl choline liposomes suggests that saturation might occur by 1 mg Hb/ml with a $^{22}Na^{+}$ loss in excess of 50% per hour. Data are presented for phosphatidyl serine-cholesterol (1:1) liposomes that suggest that the Hb-induced cation loss is saturated at about 0.4 mg Hb/ml at a $^{22}Na^{+}$ loss of about 3% per hour. Using the method of calculation employed by Kimelberg and Papahadjopoulos (1971a) for a

similar liposome preparation, the Hb-induced phosphatidyl serine liposome permeability is found to be in excess of 10^{-9} cm/sec for Na^+. The surface area of phosphatidyl serine-cholesterol liposomes has not been published, but from monolayer data (Papahadjopoulos et al., 1973) it can be estimated that the area per molecule is reduced from about 71Å^2 per molecule in a phosphatidyl serine monolayer at 25 dynes/cm to about 50Å^2 per molecule in a phosphatidyl serine-cholesterol monolayer at 25 dynes/cm. Using these areas, the Hb-induced permeability of phosphatidyl serine-cholesterol liposomes is found to be 9×10^{-11} cm/sec. Thus, the Hb-induced Na^+ permeability in a liposome with a lipid composition similar to that of RBC's might range from 9×10^{-11} cm/sec to more than 10^{-9} cm/sec.

In the red cell the mean Na^+ passive permeability is 4×10^{-10} cm/sec (Stein, 1967), and this passive leak is genetically associated with the Na^+-K^+ pump (Hoffman, 1975). Because a loss as small as the lower liposome permeability should be experimentally separable from the pump passive leak and because the larger estimate exceeds the total red cell passive Na^+ leak, the red cell must have some mechanism to prevent the Hb-induced cation loss that is observed in liposomes. Spectrin is primarily responsible for this inhibition of the Hb-induced increase in cation permeability that is observed in liposomes although other membrane proteins are also involved (see below).

Spectrin-lipid interactions

Spectrin, as a constituent of the red cell membrane, contains about 55% α-helices (Holzwarth, Yu and Steck, 1976). It penetrates monolayers of phosphatidyl serine at surface pressures up to 45 dynes/cm at pH 3.5, but at pH 7.4 it penetrates only below 30 dynes/cm. It penetrates mono-

layers of the neutral phosphatidyl choline to about 30 dynes/cm at either pH 3.5 or 7.4. Spectrin would therefore be expected to cause only a small increase in cation permeability of phosphatidyl choline liposomes at pH 3.5 or 7.4 or of phosphatidyl serine liposomes at pH 7.4. This has been found to be the case for protein concentrations of up to about 300 mg/ml (Juliano, Kimelberg and Papahadjopoulos, 1971). At a physiological pH (7.4), spectrin appears to cause a maximal $^{22}Na^{+}$ permeability of about 2×10^{-11} cm/sec in phosphatidyl serine liposomes during the first hour of incubation and a higher permeability in phosphatidyl choline liposomes by approximately a factor of 2, as calculated from the data of Juliano et al. (1971). At pH 7.4, the permeability appears to be independent of protein concentration above 70 mg/ml and independent of time, whereas at pH 3.5 the permeability is both protein-concentration and time-dependent. As suggested by Juliano et al., this finding is consistent with a conformational change in spectrin occurring at pH 3.5.

Sweet and Zull (1970) found that at pH 7.7 and a spectrin concentration of 1.3 mg/ml, the rate of glucose loss from negatively charged liposomes (12 mg phosphatidyl choline + 0.9 mg cholesterol + 2.3 mg dicetyl phosphate) increased from 2 or 3% per hour in the absence of protein, to 12 or 14% per hour with spectrin present. From positively charged liposomes (12 mg phosphatidyl choline + 0.9 mg cholesterol + 1.15 mg stearyl amine) the rate increased from 5 or 8 to 12 or 14% per hour. From the data presented, it could be calculated that at 1.3 mg spectrin/ml, the bound spectrin/lipid weight ratio was 0.02 for the negative liposomes. This value is lower than that calculated for the red cell where the spectrin/lipid weight ratio was calculated to be 0.4 from the composition data previously presented. In

contrast, Juliano et al. (1971), working at lower spectrin concentrations, found a much smaller $^{22}Na^{+}$ permeability increase (0.4 to 0.7% per hour) caused by spectrin binding to positively charged liposomes (10% steryl amine in phosphatidyl choline). The reason for the rapid glucose loss from the Sweet and Zull liposomes with or without added spectrin is not known, but the loss might result from the small domains present in liposomes sonicated below their crystalline to liquid-crystalline phase-transition temperature and/or the production of small domains on passage of liposomes through a Sephadex column (Lawaczeck et al., 1975).

In spite of the somewhat conflicting data, if the red cell lipid behaved as a lipid bilayer and the effect of cholesterol were neglected, it might be possible to experimentally resolve a permeability of 2×10^{-11} cm/sec caused by spectrin (which appears to be saturated and independent of the spectrin concentration at pH 7.4) from the pump lead that accounts for the major portion of the red cell passive Na^{+} permeability (4×10^{-10} cm/sec). Because both Sweet and Zull (1970) and Juliano et al. (1971) found that spectrin has an overall behavior similar to that of albumin and because cholesterol reduces the albumin-induced Na^{+} permeability of equimolar phosphatidyl serine-cholesterol liposomes 61-fold (Papahadjopoulos et al., 1973), it is doubtful that a spectrin-induced increase in Na^{+} or glucose permeability could be measured.

Therefore, the major effect of spectrin on the lipid molecules in the cell membrane is probably the limitation of the head-group motion (Sheetz and Chan, 1972). It will be shown that this can account for both the inhibition in Hb-induced cation loss compared to a spectrin-free bilayer and for the molecular sieving observed in stressed red cell membranes.

Summary

A soluble globular protein retains a generally globular conformation when interacting with a lipid bilayer. If the protein-lipid interaction is limited to electrostatic effects, the lipid-head-group motions are affected, but the hydrocarbon region of the bilayer is unperturbed. If the protein-lipid interaction involves hydrophobic interactions, a soluble globular protein generally thins the bilayer, increases the average distance between lipid molecules, and disorders the lipid hydrocarbon chains. Hydrophobic membrane proteins tightly bind a monolayer of lipid and effectively remove it from cooperative motions.

The adsorption of protein to lipid monolayers and bilayers often involves first, electrostatic attraction between the protein and the lipid, but later, conformational changes and hydrophobic interactions. These changes are often irreversible on the experimental time scale.

Free-volume fluctuations in the lipid appear to permit protein interaction with the hydrocarbon regions of lipid monolayers and bilayers. The large increase in cation permeability of liposomes caused by proteins that can penetrate a monolayer at about 30 dynes/cm also probably occurs through free-volume fluctuations in the disordered hydrocarbon chains near the protein. Hb is very effective in increasing the cation permeability of liposomes. The red cell membrane differs from a lipid bilayer in that this Hb-induced Na^+ permeability increase does not occur in the cell membrane. A major effect of spectrin in the red cell membrane is to reduce lipid-head-group motions.

MOLECULAR SIEVING MODEL

Lipids and Proteins in Hemolysis

Using different conditions, it can be shown that both membrane lipid and protein can be important in determining the point of hemolysis of red cells. If the lipid composition of the membrane is changed so that the stable configuration of the lipids is no longer a bilayer, hemolysis will result. This is a characteristic of many drugs (see below) and is typified by lysolecithin, which forms spherical micelles and causes hemolysis above a critical concentration (Ponder, 1948b).

Similarly, an alteration in protein conformation appears to cause hemolysis. Krizan and Williams (1973) studied shear-induced hemolysis as a function of temperature and fit their data to an Ising model. The data fit the model with a transition temperature of 49°C. Because this is the temperature at which many proteins undergo an α-helix to random-coil conformational transition and because the native red cell membrane protein has a high α-helix content, they suggest that the hemolysis was caused by a protein conformational phase transition.

In osmotic hemolysis, the cell can increase in volume at constant surface area by swelling until it becomes spherical. Once spherical, any further decrease in the external osmolarity will cause major membrane stress and hemolysis with a minimal increase in membrane area. The hemolytic volume can be experimentally varied by altering the lipid content of the cell membrane. Cooper (1970) demonstrated that when the cholesterol content of red cells is slowly changed, the osmotic fragility of the cells is a linear function of the change in cholesterol content and thus a linear function of the membrane surface area. Because membrane

lipid occupies about 77% of the surface area of the normal human red cell, it is primarily lipid that determines the hemolytic volume.

If the proteins of the cell membrane are lightly crosslinked by a brief exposure to glutaraldehyde, the cell remains flexible (Heusinkveld, 1973) and shrinks or swells to its spherical volume in response to changes in its osmotic environment, but it cannot be hemolyzed by osmotic hemolysis procedures (Baker and Gillis, 1969). Because the cell does respond osmotically, the membrane must sustain stress once the cell becomes spherical and can no longer increase its volume through shape change. It does this without a gross rupture of the membrane. Glutaraldehyde fixation has little effect on membrane lipid (Jost, Brooks and Griffith, 1973); therefore, hemolysis is presumably prevented because the crosslinking of proteins prevents the area increase necessary to cause hemolysis (see below). Unfortunately, membrane area measurements are not available for glutaraldehyde-fixed RBC's at various tonicities. Crosslinking of Hb, however, might prevent its loss even if small ruptures did occur in the cell membrane (Baker and Gillis, 1969) and so prevent the observation of hemolysis even though the membrane was breached.

Similarly, red cells crosslinked with 1,5-difluoro-2,4-dinitrobenzene can withstand an osmotic pressure gradient of at least 6×10^5 dynes/cm^2 across the membrane (Berg, Diamond and Marfey, 1966) although this reagent crosslinks proteins, phosphatidyl ethanolamine, and phosphatidyl serine (Marinetti and Love, 1974) and causes the cells to be rigid.

It should be mentioned that Jacob, Amsden and White (1972) and Saari, Jay and Beck (1972) observed that vinblastine, colchicin and strychnine decreased the osmotic fragility of red cells. Because these

drugs disrupt microtubual formation (Wilson and Bryan, 1974), these authors concluded that membrane protein was an important determinant in hemolysis. The concentration dependence of the vinblastine and strychnine protection against drastic osmotic hemolysis is typical of nonspecific drugs (Seeman, Chau-Wong and Moyyen, 1973), however, so it is doubtful that they interact specifically with membrane protein (see below).

Rand (1964) determined the length of time required to hemolyze red cells when membrane tension was caused by pulling a portion of a swollen red cell into a 2- to 3μ-diameter micropipette with various negative pressures. Under his conditions, the red cell suddenly lost its Hb and disappeared up the pipette. He found that larger membrane tensions caused hemolysis in shorter times and fit the data to a model that consisted of a parallel plus a series spring and dashpot, assuming that hemolysis occurred at a critical membrane strain (area increase). Seeman, Sauks, Argent and Kwant (1969) confirmed the existence of a critical membrane strain. Depending on the effective mechanical thickness of the membrane and the critical strain and its geometrical meaning in the membrane, he estimated the Young's modulus to be between 7.3×10^6 and 3.0×10^8 dynes/cm^2 for both springs and the viscosity to be between 5.8×10^7 and 2.4×10^9 poise for the parallel dashpot, but between 1.6×10^9 and 9×10^{10} poise for the series dashpot. Thus, the membrane is a tough viscoelastic material, not a simple liquid-liquid interface. The molecular interactions responsible for the viscoelastic properties are not yet known in detail but apparently involve both lipids and proteins. Makowski (1976a) showed that the Young's modulus is consistent with the expected properties of a lipid bilayer in which hydrocarbon residues are statistically exposed to

water when the membrane area is increased, provided that hemolysis occurs at a membrane area expansion of less than 2% (see below). The viscoelastic membrane properties require the presence of an additional membrane element which could be provided by a protein network (Evans, 1973a,b; Evans and La Celle, 1975).

Thus, both membrane lipid and protein appear to influence red cell hemolysis. It will be shown below that the membrane composition is not constant in controlled gradual osmotic hemolysis but that normally soluble molecules, under suitable conditions, can enter the stressed cell membrane. Such entry occurs at low membrane stresses, is physiologically relevant, and presumably occurs as an initial phase in processes in which larger stresses ultimately result in bulk flow of Hb and other solutes from the cell.

Controlled Gradual Osmotic Hemolysis

Previous Work

Hemolysis can apparently result from a phase change in membrane proteins (Krizan and Williams, 1973), and Makowski (1976b) has suggested that stress-induced hemolysis occurs owing to a phase separation of lipid head groups from water at the stressed-membrane-water interface. In contrast, Burton (1969) proposed that stressing the red cell membrane opened or increased the size of aqueous pores, and these pores allowed Hb to diffuse out of the cell. This phenomenon would be reminiscent of the increase in pore size caused by biaxial stress of cellophane membranes (Craig and Konigsberg, 1961). Neither of these mechanisms of hemolysis would readily explain the process of controlled gradual osmotic hemolysis because it is difficult to see how a phase change would lead to an effec-

tive hole size that increased gradually with time or why K^+ would be lost so slowly through aqueous pores large enough to pass globular proteins.

Based on the unpublished work of P. G. de Gennes and W. Helfrich and using the concept of an edge energy (Helfrich, 1974), Litster (1975) showed that if an aqueous pore appeared in a bilayer it would reseal if it had a radius smaller than a critical radius, which was calculated to be approximately 100Å. Pores with radii larger than this critical radius would be unstable and would tend to enlarge. Taupin, Dvolaitzky and Sauterey (1975) extended this model to account for the rate of solute loss caused by osmotic pressure gradients across phosphatidyl-choline-bilayer liposome membranes. They considered the formation of the pores to be a statistical process and, although not concerned with the mechanism of transfer across the membrane, employed formalisms based on the presence of aqueous pores. At concentration gradients larger than about 2M NaCl, the data fit the model for unstable pores, which caused the loss of the entire vesicle contents. In the low-stress region where the probability of occurrence of an unstable pore is negligible, they assumed that the vesicle permeability was proportional to the total area of all pores present and again found a good fit to the data.

In controlled gradual osmotic hemolysis, the passage of molecules across the cell membrane appears to be a statistical process that does not involve the formation of aqueous pores. This process appears to be more complex than that described by Taupin et al. (1975), but the passage of most molecules across both liposome and red cell membranes appears to involve basically the same mechanisms although additional restraints exist in red cell membranes (see below).

Entrance of Molecules into Stressed Membranes

Molecules such as cholesterol can enter the normal, unstressed red cell membrane and increase its surface area. Other molecules have a low solubility in the normal red cell membrane and do not increase its area but are more soluble in the stressed membrane. These molecules can increase the membrane area prior to hemolysis and so provide protection against osmotic hemolysis.

Two classes of molecules that can enter the stressed membrane and protect against osmotic hemolysis are discussed in the following sections. It is then proposed that intracellular proteins can enter the stressed membrane in controlled gradual osmotic hemolysis, but, because of the large size of these molecules, additional membrane constraints become important.

Amphipathic molecules soluble in stressed membranes

For the present purposes, the red cell membrane is viewed as basically a lipid plus protein system that can be conveniently treated by a lattice model (MacGregor, unpublished). The chosen lattice spacings are suitable for a lipid bilayer in aqueous solution, and proteins are represented as appropriate groups of lattice sites. When the membrane is stressed, its area will increase, and this increase is represented by an increase in the size of the lattice, but the lattice now contains more vacant sites. Because the polar-head-group size of the lipids is fixed, more hydrocarbon-containing sites are exposed to water. Configurational changes in the membrane proteins are not considered at this stage of the model. The exposure of hydrocarbon sites to water causes the ordering of adjacent water molecules, which is entropically unfavorable. If,

however, some amphipathic molecule were present in solution, it could enter the membrane and occupy one or more lattice sites, depending on its size, and have its polar group in the interface to reduce the hydrocarbon-water contact area. In so entering the membrane, simple molecules might eliminate their own nonpolar contacts with water and also decrease the nonpolar membrane-water contacts. For some molecules, the entropy increase resulting from the entrance of the molecule into the stressed membrane will be favorable enough to allow the membrane area to be increased without hemolysis. This entrance of molecules into the stressed membrane can be viewed in terms of an increased solubility (or partition coefficient) in the stressed membrane or in terms of an increased number of membrane sites for drug interaction. Because most molecules do not form stable bilayer structures, it is expected that as the mole fraction of the added component in the membrane increases, eventually the bilayer will become more unstable and the cell will hemolyze.

This phenomenon appears to account for the typical behavior of a large class of drugs such as lipid-soluble anesthetics (Seeman, Kwant, Sauks and Argent, 1969) and long-chain fatty acids and alcohols (Raz and Livne, 1973). Low concentrations of these drugs do not change the surface area of red cells in isotonic media but allow cells in hypotonic media to increase in area (and critical hemolytic volume) and thus to delay hemolysis to lower osmotic concentrations. As the concentration of the drug is increased, the cells are first increasingly protected against osmotic lysis, but at 10^{-5} to 10^{-4}M maximum protection is reached, and higher drug concentrations make the cells increasingly osmotically sensitive. The membrane expansion caused by drugs can exceed that expected from the

bulk of the drug alone (Kwant and Seeman, 1969). Such effects are not fully understood but in some cases appear to involve changes in membrane Ca^{++} binding, membrane proteins (Seeman, 1975), phase changes in the membrane lipid (Jain, Wu and Wray, 1975), and restriction in the motion of water molecules (Parrish and Kurland, 1975).

Extracellular macromolecule stabilizer plus lipid-soluble molecule

In the absence of an amphipathic molecule, it might be possible for a molecule that is not highly polar to occupy space in the expanded lattice, which might be thinned, provided that the membrane structure were stabilized by increasing the thermodynamic cost of exposing nonpolar residues to water. This mechanism is apparently the explanation for the increase in hemolytic volume observed in some instances by Meryman (1973). Red cells suspended in hypotonic solutions of Na_2SO_4, $MgSO_4$, citiate, phosphate, lactate, borate, D-sucrose, D-mannitol, L-xylose, L-glucose, α-melibiose, cellobiose, inositol, polyvinylpyrrolidone, or hydroxyethyl starch and containing the penetrating solute ammonium chloride or ammonium acetate (0.1M) had an increased volume at hemolysis compared to cells in NaCl and had an increased rate of K^+ loss prior to Hb loss. Table IX indicates the mean cell volumes at which Meryman found Hb loss just detectable. The sulfates have essentially no effect by themselves but increase the membrane area at hemolysis some 20 μ^2 in the presence of NH_4Cl. Sucrose increases the volume at hemolysis 15 μ^2 by itself and by another 15-μ^2 increment in the presence of NH_4Cl. Meryman also noted that ammonium acetate and trimethylammonium acetate could replace NH_4Cl in sucrose experiments but were not as effective in allowing the membrane area increase prior to Hb loss (cell volumes were 148 and 185 μ^3 with NH_4Ac

TABLE IX. Mean corpuscular volumes of human red blood cells in various hypotonic media at the concentration that causes detectable hemoglobin loss.

External solute	Mean corpuscular volume[a] (μ^3)	Cell surface area[b] (μ^2)	Increase in surface area over area in NaCl (μ^2)
NaCl	140.	130.4	--
NaCl + 0.1M NH_4Cl	140.	130.4	0.
Na_2SO_4	142.	131.6	+ 1.2
Na_2SO_4 + 0.1M NH_4Cl	172.	149.6	+19.2
$MgSO_4$	135.	127.4	- 3.0
$MgSO_4$ + 0.1M NH_4Cl	177.	152.4	+22.0
Sucrose	165.	145.4	+15.0
Sucrose + 0.1M NH_4Cl	190.	159.8	+29.4

References:

[a] Taken from Figs. 1 and 9 of Meryman (1973).

[b] Calculated from mean corpuscular volume assuming a spherical shape at hemolysis.

and NH_4Cl, respectively). He also found that the penetrating solute D-xylose (0.1M) with Na_2SO_4 had the same effect as NH_4Cl (0.1M) with Na_2SO_4.

My interpretation of this data differs from that of Meryman, but both interpretations recognize the importance of extracellular solutes affecting the membrane, presumably through changes in the equilibrium distribution of water molecules and therefore the solvent properties of water.

In Meryman's systems, membrane expansion at hemolysis appears to require the presence of a substance that can interact with the membrane to increase its area and a substance in the external medium that is known from other studies to stabilize the structured conformation of macromolecules. When NH_4Cl is present, NH_3 and possibly NH_4^+ could occupy membrane lattice sites. Similarly, acetate and trimethylammonium ions could occupy membrane sites, but, because the charged groups are expected to destabilize the bilayer structure, hemolysis might be expected at lesser volume increases than with NH_4Cl as is found experimentally. Xylose and sucrose could possibly occupy membrane sites also. The substances that Meryman found to cause membrane expansion upon hemolysis in the presence of NH_4Cl or NH_4Ac appear to have in common the property of increasing the stability of the structured conformation of macromolecules over the random-coil conformation (von Hippel and Schleich, 1969). These solutes appear to exert their influence on macromolecular structure by influencing the distribution of water molecules among various possible states. Because there is not as yet a completely satisfactory model of water, the distribution considered is a function of the model chosen to describe water

(Franks, 1972-1975). The overall effect appears to be an increased thermodynamic cost to expose nonpolar groups to the aqueous environment.

The case of sucrose is interesting in that it both promotes macromolecular structure and can presumably interact with the membrane to increase its area. The area increase caused by sucrose alone, which is also caused by fructose but not glucose (Simmons and Naftalin, 1976), probably rests on the spacings between the sugar hydroxyl groups. In glucose (and also in manose and galactose), these spacings are such that the sugar can fit into the bulky water lattice by replacing water molecules whereas the other sugars cannot have most of their hydroxyls H-bonded in the water lattice. This structure provides a very stable glucose hydration complex (Franks, 1973). Because at least partial dehydration would seem to be necessary for a sugar to interact with the membrane, sucrose and fructose would be more likely to enter the membrane than glucose. The entrance of sucrose into the stressed membrane probably explains the susceptibility of red cells swollen in hypotonic sucrose solutions to phospholipase C and A_2 compared to the resistance of cells in saline (Woodward and Zwaal, 1972). When sucrose is present with NH_4Cl, additional membrane sites could be occupied in the stressed membrane, and its area could be further expanded prior to hemolysis (Table IX).

Intracellular proteins

The major external solute in this work was dextrose (glucose), NaCl, or LiCl (Table I). These solutes would not permit membrane expansion by the mechanisms mentioned in the two previous sections. The intracellular compartment contains a large assortment of molecules, however, including the proteins assayed in this work. These molecules undergo conformation fluctuations and occasionally expose

normally buried apolar residues to the external environment. When hemolysis is conducted under the very slow and uniform conditions of the present work, I proposed that intracellular proteins interact with the membrane and occupy lattice sites in the model. This entrance of protein into the stressed membrane is similar to the protein penetration of lipid bilayers and monolayers previously discussed. Proteins would be expected to interact with the hydrocarbon phase of the membrane only when fluctuations separated the lipid polar head groups to provide a sufficient area for protein interaction, and interaction could then only occur if a protein-membrane collision occurred at the site of the fluctuation with a protein in a configuration and orientation that allowed hydrophobic interaction with the membrane. Obviously, the number of collisions would be increased if the protein were electrostatically attracted to the membrane. Because the probability of a fluctuation of a given size rises roughly exponentially with the total free area in the membrane, represented to first order by the number of unoccupied sites in the surface of the lattice, an increase in membrane area rapidly increases the probability of fluctuations opening a given sized area clear of head groups.

The order of insertion of protein residues into a lipid bilayer is not known. It was previously shown that globular proteins such as the proteins assayed in this work retain a globular conformation when interacting with lamellar lipid phases and that a low number of residues are in the air/water or oil/water interface when adsorbed to the interface. It was also shown that when suspended in a less polar medium than water, globular proteins generally increased in α-helix content, but it is not known if this increase also occurs when proteins penetrate a lamellar lipid

phase because the more polar residues are presumably restricted to the aqueous phase. In any case, it appears most probable that the initial hydrophobic interaction of a protein with a lipid bilayer involves the interaction of a small portion of the protein with a small open area between the lipid head groups as the probability of these occurrences is much greater than the probability that both protein and lipid have large nonpolar areas exposed for interaction. This mechanism might allow the insertion of residues from several different proteins into different areas of the bilayer. Because these globular proteins would not be expected to have regions selected through evolution to bind lipids, the lipid-protein interactions are expected to be weaker than lipid-lipid interactions. The differences between these interactions are likely to lead to an aggregation of protein subject to steric requirements. It appears that the result of such a process is to favor the insertion of several segments of a single protein into a bilayer, which leads to a reduction in the number of proteins with only small segments inserted into the bilayer.

Constraints Imposed by Spectrin

The red cell membrane is more complex than the bilayer just discussed. The presence of more than one hydrocarbon phase, the clustering of lipids, and the presence of integral membrane proteins will be neglected here, and attention will be focused on the influence of spectrin on a lipid bilayer. If appears that some 200 to 300Å of spectrin (plus actin) is in a rigid conformation under physiological conditions and that spectrin inhibits lipid head-group motions. This limitation of head-group motions apparently results from the presence of a network of spectrin. The presence of a

spectrin network is consistent with this work (MacGregor and Tobias, 1972) (see below), with the branching filamentous networks observed in extracted spectrin plus actin preparations (Tilney and Detmers, 1975), with the fibrous network observed in RBC membranes after lipid extraction (Yu, Fischman and Steck, 1973), with the deformation properties of ghosts (Blais and Geil, 1969; Wong and Geil, 1975), and with mechanical properties of the cell membrane (Evans, 1973b). The spectrin molecules may be capable of slow translational movements but would represent a nearly rigid boundary to lipid molecules colliding with them. Thus, the spectrin meshwork can be viewed as dividing the lipid bilayer into adjacent domains through rigid boundaries at the level of the lipid head groups. The domains need not be closed to diffusion of lipids, but for ease of discussion the domains are assumed to be closed. The total free area available for fluctuations that would allow protein insertion into the membrane is thus reduced to the total free area available in each domain. I contend that it is the presence of these domains that causes the molecular sieving observed during controlled gradual osmotic hemolysis and that prevents the Hb-induced cation leak observed in liposomes.

Mechanism of Stress-Induced K^+ Loss and Molecular Sieving of Proteins

In the unstressed red cell membrane, the domain size is such that the total free area available for fluctuations does not permit the entrance of a sufficiently large protein segment to cause the protein-induced cation leak observed in liposomes even though proteins are present within the red cell that would cause cation leaks from liposomes. When the membrane is stressed, the domain size is increased, and the resulting increase in

free volume allows protein penetration of the red cell membrane by normally soluble globular proteins. This leads to an increased cation permeability and is seen in this work as the initial major K^+ loss, which most likely results from diffusion through free-volume fluctuations in the disordered hydrocarbon phase near the newly inserted protein but which might occur through a protein pore as previously discussed.

As the membrane is further stressed, the domain area is further increased, and a larger area of protein can be inserted into the membrane. Although the mechanisms of insertion of the first protein segment into a bilayer and into the inner surface of the red cell membrane are quite similar, the insertion of subsequent segments is quite different. In the bilayer, free-volume fluctuations could allow the insertion of an additional segment nearby or adjacent to the first segment. In contrast, in the red cell membrane, if the domain size were sufficient to allow the penetration of only one protein segment, the additional segment would have to enter some other domain. Consequently, as the total free area in both membranes is increased, the probability of insertion of several segments of the same protein into the bilayer is finite whereas the probability of insertion of the same number of segments into a single domain of the inner red cell membrane leaflet is zero until the membrane has suffered sufficient strain to provide the required area within a single domain. Thereafter, the probability is finite.

It is not obvious how many segments or how large an area of a protein must be inserted into a lipid bilayer before the protein can dissociate from the opposite side of the membrane. The red cell membrane is about 55Å thick (Stamatoff, Krimm and Harvie, 1975), and the Stokes-Einstein

radii of the proteins assayed in this work range from 19.4Å for the Hb monomer to 49.8Å for the intact Fum tetramer to an estimated 61.5 and 62.4Å for aggregates of two Cat and Fum molecules, respectively. The relevance of the Stokes-Einstein radii determined in aqueous solution to the protein interactions with the membrane rests on the globular shape in both instances. It is to be expected that the Stokes-Einstein radius is only a first-order approximation of the radius of the area of protein (when treated as a circle) inserted into the membrane that permits the protein to transverse the membrane.

The mechanism by which the protein transverses the membrane is not known. This work indicates that globular proteins cross the membrane in globular form without dissociating although dissociated proteins can cross the membrane, also in globular form. The range of possible mechanisms would extend from each added protein segment completely penetrating the membrane with release of the protein into the extracellular solution, possible when the protein is roughly cylindrical (not a large globule on the inside of the cell), to each protein segment occupying sites only in the inner bilayer leaflet. In this case, lipid molecules would be expected to move from the inner to the outer leaflet via the flip-flop mechanism. Irregularities in the protein at its interface with the hydrocarbon of the outer leaflet would be expected to destabilize what would then be a lipid monolayer over the protein. Transfer across the membrane and into the extracellular solution might then be possible when the area of the protein in the interface was approximately equal to the cross-sectional area of the protein in the aqueous phase.

Regardless of the actual mechanism of transfer, if, in order to

transverse the red cell membrane, a protein must be inserted into a single domain of the membrane and must retain a globular conformation in transversing the membrane, the permeability of the membrane to a given protein should rise suddenly from zero to a finite value when the membrane is strained enough to allow the required insertion of the protein. Further, more strain would be required to insert larger proteins.

The data reported in this work are consistent with this scheme. As the membrane first suffers major osmotic stress and flicker is no longer observed owing to thermal membrane motions, K^+ loss occurs owing to the initial insertion of protein into the stressed membrane. As the experiment continues, increased membrane stress increases the domain area, and small proteins can transverse the membrane and are released to the flowing external medium. Continued membrane stress increases the area per domain, and proteins of increasing size are suddenly able to transverse the membrane. This increase in domain area accounts for the sudden increases in transmembrane flow that occur at different times for the different proteins analyzed. The increasing domain area thus causes the molecular sieving of the proteins, which is interpreted in terms of an effective hole size in Fig. 16.

During the later stages of the experiment, membrane stress is decreasing, and the effective hole size is decreasing. The membrane contains proteins that are suddenly too large for the domain area. As in monolayer experiments, significant quantities of these proteins can be squeezed out of the membrane, and the loss of these molecules results in the typical increase in protein released just prior to when their flow across the membranes stops. This typical "pump-out" effect is considered

to strongly support the loss mechanism proposed here in which normally soluble proteins structurally become parts of the stressed cell membrane.

At the conclusion of the experiment, there is a small, apparently continuous loss of Hb (Figs. 5, 6 and 7). Presumably, this partially arises from a process analogous to the time-dependent conformational changes observed on desorption of proteins inserted into lamellar lipid phases, which were previously discussed. It may also partially result from the viscoelastic properties of the membrane, but these properties will not be discussed in this paper.

The fine structure of the K^+ loss curves is interpreted to result from the insertion of different proteins into the membrane at different times during the hemolytic process. Because different proteins could disorder the lipid chains to different extents or have different pore properties, the fine structure does not elucidate the cation transfer mechanism.

Domain Size

An experimental estimate of the size of the domains might be obtained by aggregating intramembranous particles and observing their distribution. Pinto da Silva (1972) found that the intramembranous particles in human red cell ghosts aggregated reversibly between pH 6.2 and 4.8. His freeze-fracture micrographs at pH 5.5 and 5.0 suggest that the particles are aggregated along domain boundaries with an area clear of particles left in the center of the domain. Using this interpretation of the micrographs, each domain has an area of approximately 0.015 μ^2 so there would be approximately 9.3×10^3 domains per cell or about 20 spectrin dimers per domain. Similar measurements on phospholipase-C-treated, ATP-depleted rat RBC

membranes (Gazitt et al., 1976) suggest a domain area of 0.0047 μ^2 in the intact rat red cell membrane. If this domain area were applied to the human RBC, there would be approximately 3.1×10^4 domains per cell or about six spectrin dimers per domain.

In replicas of rat red cell membranes, I have observed raised bumps. The smaller bumps, about 550Å in diameter, are approximately round while the larger bumps tend to have straight sides with rounded corners and an overall square or rectangular appearance. A histogram of the diameters of the small bumps and the lengths and widths of the large, rectangular bumps gives a well resolved peak at about 550Å, a large peak at 1100Å which may be resolvable into separate peaks at about 1000 and 1200Å, and a small peak at 1500Å. Longer sides were not observed. A histogram of the areas of the bumps has peaks corresponding to the 550Å-diameter bumps ($2.4 \times 10^5 Å^2$) and peaks at about 9×10^5 and $15 \times 10^5 Å^2$, corresponding to the rectangular bumps (MacGregor, unpublished). The discrete dimensions of these bumps suggest that they might arise from an underlying pattern within the membrane. I suggest that they are similar to the bumps observed by Elgsaeter, Shotton and Branton (1976), which form when spectrin in human RBC's is caused to contract. If this is the case, the different-sized bumps might arise from different combinations of contraction of nearby spectrin molecules and so also give a measure of (contracted) domain size.

The arrangement of the spectrin molecules in the membrane is not known. They might form a random network or a regular lattice. If they form a rectangular lattice, the 550Å-diameter bump might result from the contraction of the smallest lattice square. Therefore, we can assume that the lattice sites are separated by sides of 550Å. The next largest bump

could arise from the contraction of molecules lying in a square having sides of two lattice dimensions or 900Å and thus an area of $8 \times 10^5 Å^2$. The largest bump might result from the contraction of a rectangle of (2×3) lattice sites $(900 \times 1650Å)$ and have an area of $15 \times 10^5 Å^2$. These areas agree reasonably well with the experimentally measured areas. The linear dimensions suggest that if this lattice does correspond to the spectrin network in the membrane, contraction of spectrin distorts the lattice to make the large bumps more square than rectangular and the small bumps circular.

These data suggest that the smallest domain size is a square with 550Å sides and an area of 3.0×10^{-3} μ^2, and the data would underestimate the uncontracted domain size. If the contracted domain size is applied to the human RBC, there would be a 4.8×10^4 domains per cell or four spectrin dimers per domain.

The three estimates of domain size are 15×10^{-3} μ^2 in human RBC's and 4.7×10^{-3} and the underestimate of 3.0×10^{-3} in rat RBC's. In the human RBC, these estimates lead to domains of 20, 6, and 4 spectrin dimers, respectively (which may be in error by a factor of 2 owing to uncertainty in the cell spectrin content alone). If one Hb tetramer were inserted into each domain, the area increase would be between 0.27 μ^2 and 1.4 μ^2, corresponding to increases in the membrane area of 0.2 and 1% for the high and low estimates of spectrin dimers per domain, respectively. These estimates are consistent with Evans and Leblond's (1973) area increase prior to hemolysis of less than 2%. Similarly, it is unlikely that they would have detected an area increase sufficient to insert a spherical Fum molecule into each domain (0.5 to 2.4%) although it is doubtful that their system was uniform enough to permit this area increase (see below).

In summary, domains probably consist of regions bounded by 4 to 20 spectrin dimers. If a spherical Hb or Fum tetramer is inserted into each domain, the total area increase of the cell membrane is less than the uncertainty in the possible membrane area increase prior to hemolysis measured by Evans and Leblond (1973). Therefore, the proposed mechanism of controlled gradual osmotic hemolysis is consistent with the available data on membrane-area increase at hemolysis, and it is possible but not proven, that proteins transverse the membrane in a spherical conformation.

Li^+, Na^+, K^+ and Dextrose Movements

The calculations presented in the Interpretation section concerning cation movements assumed that the critical hemolytic volume was the same in NaCl, LiCl and dextrose solutions and that the membrane area did not increase at hemolysis. The assumption that the membrane area does not increase at hemolysis was only an approximation but is of sufficient accuracy for the conclusions drawn from the calculations, provided that the same area increase occurred in both salt and dextrose experiments. Because the data obtained in this work are consistent with the same hemolytic volume in these three solutions; because the physical properties of dextrose that lead to its stable hydration predict that it would not increase the membrane area itself; and because red cells have the same hemolytic volume in drastic hemolysis in NaCl and dextrose solution — the assumption of the same hemolytic volume in controlled gradual osmotic hemolysis in NaCl, LiCl and dextrose solutions appears valid.

It was shown that the difference between salt and dextrose experiments could be explained by a negligible transfer of glucose across the cell membrane prior to Hb loss together with unspecific cation transfer.

The data do not, however, exclude other interpretations. Because the protein-induced permeability increase in liposomes has an apparent cut-off for molecules about the size of dextrose and because adsorbed Hb appears to have a negligible effect on the glucose permeability of liposomes, there is most likely a negligible entrance of dextrose into the cells prior to Hb loss. Either a lipid-fluctuation model or a protein-pore model could provide little selection between Li^+, Na^+ and K^+ and yet have a significantly lower dextrose permeability. The calculation presented is therefore consistent with the known properties of model systems. I believe that cation transfer via free-volume fluctuations in lipid hydrocarbon chains adjacent to and near inserted proteins is the most probable mechanism for the stress-induced cation loss both prior to Hb loss and during the remainder of the hemolytic process. Other mechanisms such as an increased stress-induced leak through the Na-K pump cannot, however, be excluded at this stage of the work.

Effect of RBC Incubation Prior to Controlled Gradual Osmotic Hemolysis

Domain Size

As demonstrated in Fig. 15a, the flow increases and (aligned) decreases occurred at approximately the same fraction numbers in fresh and incubated cells during the early and final stages of the experiments. Therefore, the basic osmotic response of the membrane is similar between 0 and 29 hrs of incubation. Because the protein losses observed depend on the domain size in the proposed model, the domain size must increase in a similar manner in both fresh and incubated cells; that is, the elastic or viscoelastic membrane properties that determine domain size were not affected by incubation up to 29 hrs.

The tube of maximum Hb loss (Fig. 18) is, however, the same at 0 and 3 hrs, falls by 5 hrs, and is further decreased at 29 hrs. Similar time-dependent changes are seen in the filterability and the negative pressure required to pull a hemispherical deformation of a human red cell into a 3μ-micropipette (Weed et al., 1969). Weed et al. showed that these changes could be reversed following approximately 24 hrs of incubation by adding 30-mM adenosine. Their extensive deformability data show that the deformability of human RBC's at room temperature is constant from 0 to 3 hrs, rises from 4 to 6 hrs to reach a new plateau, begins to rise again near 12 hrs, and reaches another plateau at about 24 hrs. It is therefore probable that at least two mechanism are involved in the reduction of human-red-cell-membrane deformability, both of which are influenced by ATP.

Membrane Access

After 3 and 5 hrs of incubation in this work, the amounts of Hb lost as the intact tetramer increased sharply over the losses from fresh cells (Fig. 19b). Because it is unlikely that the tetramer concentration had increased signficaintly and because the domain size increased in the same manner in the fresh and incubated cells, the Hb apparently had greater access to the membrane in incubated cells than in fresh cells. On the assumption that the Hb tetramer itself was not changed, the access to the lipid portion of the membrane could be changed by either a change in the electrostatic charge of some membrane component(s) and/or a physical rearrangement of membrane molecules. The data in the present work do not distinguish between these possibilities; however, Gazitt et al. (1976) observed that the intramembranous particles on the fracture surface of the inner membrane leaflet were randomly distributed in fresh rat RBC's but

aggregated in cells that had been incubated to deplete them of ATP. The aggregation left larger areas of smooth membrane (lipid) clear of particles, and they showed that these incubated cells were more susceptible to phospholipase C than were fresh cells. Thus, the random particle distribution apparently inhibited the phospholipase C hydrolysis of phospholipids by physically preventing sufficient enzyme access to the lipids. Aggregation of the particles would then allow enzyme access to the lipid in regions cleared of intramembranous particles. On this basis, I propose that the increase in Hb tetramer loss at about 4 hrs of incubation was caused by the aggregation of intramembranous particles. This aggregation increased the probability of Hb-membrane interaction by increasing the total membrane area where openings between the cytoplasmic portions of the intramembranous particles were of sufficient area to allow Hb access to the bilayer portion of the membrane. This increased-access area would partially account for the increased early losses of membrane-associated proteins observed from incubated cells (see below).

The reason for the particle aggregation during incubation is not yet known although it is probably related to phosphorylation of some membrane protein, possibly spectrin. Changes in electrostatic charge or conformation could cause particle aggregation either directly or through a phase change in the bilayer lipid.

Hb Dissociation and Aggregation

The increased loss of Hb subunits with duration of incubation is anticipated owing to the increased Hb dissociation caused by decreasing concentrations of ATP and 2,3-DPG during incubation. The increased loss of Cat subunits is consistent with the increase in Cat subunits that occurs

during storage of RBC's as previously discussed. The loss of the Hb monomer increases dramatically between 5 and 29 hrs of incubation (Fig. 19b). There is a similar although less dramatic increase in the early Hb losses, which have been interpreted as the loss of membrane-associated Hb. A dramatic decrease in membrane deformability also occurs at this time (Weed et al., 1969). I propose that the decrease in intracellular organic phosphates, primarily ATP and 2,3-DPG, after prolonged incubation causes a sharp increase in Hb dissociation to monomers. The monomers have exposed hydrophobic areas and thus can interact hydrophobically with the membrane without further unfolding, provided that they gain access to the bilayer and that a fluctuation in the bilayer occurs which clears an area of sufficient size between the head groups (or between head groups and protein). Because the Hb-monomer Stokes-Einstein radius is 19.4Å compared to 30.8Å for the tetramer (Table V), the total area of access to the membrane is larger for the monomer than for the tetramer because the monomer can fit between the cytoplasmic portions of membrane proteins that would prohibit membrane access to the larger tetramer. The combination of exposed hydrophobic areas and small size in the monomer leads to its insertion into the membrane even in the "unstressed" membrane as indicated by the losses that apparently result when the dimples of biconcave cells proceed to a convex configuration (tubes 5 and 7, Fig. 10a). I propose that it is this insertion of Hb monomers into the membrane that causes the decreased membrane deformability after prolonged incubation and that is responsible for the decreased deformability observed in cells that contain abnormal Hb's that dissociate to a greater extent than Hb A and in thalassemic cells.

In view of the apparent high membrane activity of Hb monomers and their ability to decrease the deformability of incubated but unstressed red cell membranes, it is probable that the initial membrane pathology in cells containing an abnormally high concentration of Hb monomers is the insertion of Hb into the membrane. Subsequent events could then include the deposition of Hb and its degradation products, either as a continuous layer over the cytoplasmic surface of the membrane or as Heinz bodies, and the formation of disulfide crosslinks as previously discussed. In general, treatments that increase Hb dissociation would be expected to decrease membrane deformability.

If the formation of an Hb aggregate deformed the tetramer so as to expose nonpolar residues to the external environment, the aggregate might be more membrane-active than the tetramer despite its larger size. Presumably, this accounts for the decreased membrane deformability that occurs when red cells are deoxygenated or when they contain an abnormal Hb that aggregates (see above).

The insertion of membrane-active protein into the unstressed membrane presumably involves only a small segment of the protein owing to the limited free volume available in each domain. The insertion of a small segment is consistent with the observation of Gazitt et al. (1976) that the number of intramembranous particles per unit area was the same in fresh and incubated cell membranes and with the observation that total membrane protein increases during incubation (see above). If the membrane is stressed, however, the model predicts that individual proteins will enter the membrane to a greater extent. A stress sufficient to enlarge the domain size would allow further Hb penetration, which might decrease

membrane deformability greatly. I believe this mechanism accounts for the observation that pulling a membrane fragment off of a red cell greatly decreases membrane deformability (La Celle et al., 1972) and is the mechanism involved in the production of irreversibly sickled (Hb-S-containing) cells.

Reversibility of Protein Insertion into Membrane

Because the decrease in membrane deformability after a 24-hr incubation is completely reversed by adding adenosine (Weed et al., 1969), the Hb monomers, which presumably penetrate the unstressed membrane to cause the dramatic decrease in deformability, can be removed from the membrane. In lipid monolayers and bilayers, however, protein adsorption is often irreversible or is reversed only by a large increase in surface pressure. If protein adsorption in a model system is initially reversible, it may become irreversible during incubation.

The binding of Hb to the stressed membrane appears to be partially reversible as evidenced by the pump-out effect when the domain size is decreasing but also involves a long time-constant loss as evidenced by the long, continuous loss of Hb following the conclusion of the molecular sieving process. Similarly, La Celle et al. (1972) found decreased deformability some time after pulling a membrane fragment off of a cell, and irreversibly sickled cells are, in fact, considered to be irreversibly sickled.

The result of a membrane stress in vivo that is sufficient to enlarge the domain size would depend on the properties of the molecules within that particular cell. The presence of an abnormal Hb, because of its high concentration, would be expected to have a significant effect on the

cell's response to stress. Abnormal cell metabolism affects both solute dissociation and membrane properties; changes in spectrin or the quantity of spectrin could affect domain size; changes in other membrane proteins could affect access to the membrane; and any change in the membrane activity of a soluble protein could alter the response to membrane stress. Because spectrin is altered in at least some cases of hereditary spherocytosis, I predict that in at least some cases of hereditary spherocytosis the domain size will be altered. In cases where the membrane is normal, the long-term effect of membrane stress would depend on the rates at which the normally soluble species entered and left the membrane. An alteration of protein charge or conformation could affect physical access to the membrane; a change in conformation that involved changes in the exposure of nonpolar groups would affect that probability of a hydrophobic interaction occurring given that a sufficient lipid fluctuation had occurred; alterations in the rate of conformational changes could affect the amount of irreversibly bound protein following a pulse of membrane stress; and alteration in the tightness of a reversibly bound protein and its dependence on surface pressure would affect the time-average membrane protein content. This view is consistent with the different membrane activities observed for deoxy-, oxy- and met-Hb in this work (Fig. 10a), with the ligand and Hb type-dependent, air/water surface activity of Hb (Elbaum, Harrington and Nagel, 1975a,b), with the apparently irreversible binding of Hb S, and with the more reversible binding of Hb A to stressed membranes.

Uniformity of Lipid Distribution

In cells incubated for 5 hrs, there was a large spike of K^+ loss at the time of the initial major K^+ loss and greatly increased fine structure

in the K^+ loss curve (Fig. 7a) compared to fresh cells (Fig. 5a). The general increase in fine structure probably resulted from the increased access to the membrane and greater protein penetration of the bilayer portion of the membrane. The initial spike is most interesting. Small losses of membrane-associated proteins also occurred at this time, especially from incubated cells. A probable explanation for these observations is that the membrane lipid is not uniformly distributed across the cell surface when major tension is first applied to the membrane. Some areas have more lipid, and some areas have less than the average content. This imbalance might result from aggregation of the intramembranous particles within domains creating a lipid-poor region within the aggregate while the area clear of particles is lipid-rich, or the domains in the unstressed membrane might be distorted compared to the stressed network, resulting in lipid density differences when the membrane is stressed. Because the mechanism is incubation-dependent, it is probably dependent on cellular ATP. The aggregation of the particles has been previously discussed. Distortion of domains might result from dephosphorylation of spectrin causing a conformational change that physically changes the domain shape in the unstressed membrane or from changes in the electrostatic charge or the large dipole moment of spectrin, altering spectrin-spectrin interactions and changing the domain shape in the unstressed membrane. In any case, stress would increase the membrane area and cause the appearance of regions of low lipid density. Such regions might allow the formation of an aqueous pore (see below) or, more likely, the insertion of proteins into the bilayer to cause the observed K^+ loss. Some membrane-associated proteins would also be lost from the low density regions in the

same manner that they are lost later during the hemolytic process as a function of their size. Diffusion of lipids would equalize the bilayer surface pressure throughout the membrane and proteins inserted into the low-lipid-density regions would be (partially) squeezed out of the bilayer. Because the K^+ spike and early protein losses last for approximately one fraction collection period (1 min), membrane reorganization takes on the order of a minute.

A similar process might account for the greater population homogeneity observed in controlled gradual osmotic hemolysis compared to drastic hemolysis. If old cells contain more aggregated protein than young cells, slow stress of the membrane might allow the membrane to become more homogenous and thus more similar to a young cell membrane than in drastic hemolysis, where the membrane might rupture at its weakest point without having had time to become more homogeneous. The "weakest point" may correspond to the region of lowest lipid density (see below). The possible entrance of internal lipid vesicles into the cell membrane of old cells has been previously discussed. Again, this process would be expected to be time-dependent.

Spectrin Aggregation

After prolonged incubation, RBC's lose membrane lipid but not protein. The mechanism has not been studied, but it may result from the contraction or aggregation of spectrin; a purse-string-like aggregation of spectrin causes the aggregation of the intramembranous particles to the spectrin purse string while the lipid, which bulges out from the purse string and aggregated particles, is left free of particles (Elgsaeter, Shotton and Branton, 1976). This process leads to the loss of protein-free lipid

vesicles from the cell membrane. Elgsaeter et al. used this as evidence for a linkage of the particles to spectrin. It is equally likely, however, that the proteins are less soluble in a bilayer of small radius or that a pressure-induced phase separation of protein from lipid occurs. In any case, the effect of prolonged incubation, which was not investigated in this work or that of Weed et al. (1969), is likely to result from the aggregation of spectrin.

BULK FLOW DURING HEMOLYSIS

The work reported in this paper considered hemolysis under conditions and at times when bulk flow did not occur from the cells. The mechanism proposed for controlled gradual osmotic hemolysis does appear, however, to be relevant to hemolysis involving bulk flow from the cell. In this section, some pertinent observations concerning bulk flow during hemolysis are summarized from the publications of other workers. The type of bulk flow that occurs appears to be a function of the magnitude and uniformity of the stress applied to the membrane and is dependent on the presence or absence of extracellular macromolecules.

I propose that (1) increasing the tension in the bilayer portion of the membrane decreases the critical radius above which a spontaneously formed pore is unstable and tends to enlarge (and permit bulk flow) rather than to reseal (Litster, 1975; Taupin, Dvolaitzky and Sauterey, 1975), (2) that the presence of extracellular macromolecules increases the probability of pore nucleation, and (3) that the spectrin network influences the pattern of Hb loss by limiting the loss to isolated pores, each having an area of less than 10% of the domain area when membrane stress is low

and multiple pore nucleation occurs. Under other conditions, pores can coalesce without disruption of the spectrin network, or the spectrin network can fail, and a large hole (~1μ diameter) can develop.

Experimental Observations

When washed human red cells in NaCl solution are lysed by dialysis against a glutaraldehyde solution, the initial membrane defect observed in electron microscopy is the lifting off of a flap of membrane with an area of a few hundred square Angstroms from an otherwise undistorted membrane. This defect then enlarges into a hole, which eventually has a maximum diameter of about 1μ, through which Hb diffuses out of the cell and can be fixed as a crown of Hb rising from the cell surface. There is only one such hole per cell, and it is located on the rim of the cell (Baker and Gillis, 1969).

If, instead of washed cells, unwashed human red cells are lysed by rapid mixing with hypotonic NaCl (drastic osmotic hemolysis), a single vesicle-like bulge is observed in the cell membrane about 12 sec after the mixing of cells and hypotonic medium (under the specific conditions of these experiments). At a later stage, numerous gaps are evident in the membrane. In thin sections, each gap is typically 200 to 500Å long and is bounded by the abrupt end of apparently normal membrane. These defects are confined to a 1μ-diameter region of the membrane (Seeman, 1967). Serial sections of this region show isolated holes with areas of a few hundred square Angstroms and interconnected slits, which appear to be typically 40 to 100Å wide extending for up to ½μ (Seeman, Cheng and Iles, 1973). Under these conditions of hemolysis, the holes open rapidly enough to allow 50% of the cells to contain added ferritin at 15 sec and then

close so that 50% of the cells are impermeable to ferritin at 25 sec. Because ferritin is a protein with a radius of about 61Å, its presence in cells cannot be used as proof of bulk flow because, presumably, it could also enter the cell by the molecular sieving mechanism. Colloidal gold particles of up to 300Å, the largest size used, were also found inside the cells if present at the time of hemolysis (Seeman, 1967).

When unwashed red cells are lysed by dialysis (gradual osmotic hemolysis), they are found to contain ferritin and colloidal gold particles of up to 150Å in diameter. Seeman (1967) did not know whether this indicated that the cells were impermeable to larger gold particles or whether the number of large gold particles present was so low as to preclude their observation.

When the time to hemolysis is less than 40 sec, some unwashed red cells lysed by an ion-exchange method, similar in principle to gradual osmotic hemolysis, will burst at one point on the cell membrane and will be propelled in the opposite direction. Apparently, the cells can burst before they become spherical, and a bulge often appears in the membrane before the cells burst (Danon, 1961). Similarly, Seeman (1967) found vesicle-like bulges in the membranes of nonspherical RBC's fixed prior to Hb loss during drastic osmotic hemolysis. A slower decrease in extracellular concentration causes hemolysis to occur at later times, and the cell becomes spherical prior to releasing its Hb in all directions and becoming increasingly pale (Danon, 1961).

If ferritin is present in the extracellular medium and unwashed human red cells in NaCl solution at pH 6 are hemolyzed by dialysis against a glutaraldehyde solution, Hb loss occurs through numerous 200Å gaps

($\sim 3 \times 10^4 \text{Å}^2$) apparently randomly distributed across the membrane surface during the early stages of Hb loss (Baker, 1967).

When drastic hemolysis is conducted in salt solutions that contain macromolecules, the amount of Hb lost from each cell is greatly reduced compared to lysis in the absence of the macromolecule (Marsden, Zade-Oppen and Johansson, 1957; Davies, Marsden, Östling and Zade-Oppen, 1968). This protective effect appears to be a general effect of macromolecules (albumin, ficoll, dextran, polyethyleneglycol). Dextran of molecular weight 1800 is effective in causing the effect, but raffinose of molecular weight 504 is not effective. The magnitude of the effect depends on the weight fraction of the macromolecule solute (not its molarity) and increases linearly with the macromolecule concentration up to a maximum protective effect at which about 20% of the Hb is lost (Davies et al., 1968). When dextran with a wide distribution of molecular weights is present in the hypotonic medium, the proportion of dextran that enters the cells during the hemolytic process decreases with increasing molecular weight with an apparent cut-off for entrance into the cell at ~300,000, which has a Stokes-Einstein radius of ~100Å (Marsden and Östling, 1959).

Estimation of Critical Pore Radius

In general, when stress is applied to the red cell membrane, the domain area is expected to increase. This increase in area will cause an increase in the tension in the bilayer portion of the membrane owing to exposure of hydrocarbon groups to water. The increase in area also increases the probability of a large fluctuation in lipid density, producing a large open area in the bilayer. In this section, the stability of such an open area is examined. The open area is not defined theoretically, but

experimental data are treated as if the area were a cylindrical hole (pore through the membrane. The energy associated with the formation of the pore is evaluated following the developments of Litster (1975) and Taupin, Dvolaitzky and Sauterey (1975). Several estimates of membrane tension at hemolysis are used to estimate the critical radius for unstable pore formation, which is found to be $2.5 < r_c < 33.$ Å in the stressed membrane.

An approximation of the energy required to open a hole in the membrane can be written in terms of the edge energy γ and the (bifacial) surface tension σ as a function of the pore radius r (Litster, 1975; Taupin, Dvolaitzky and Sauterey, 1975).

$$E(r) = 2\pi r\gamma - \pi r^2\sigma \tag{1}$$

This energy of pore formation has a maximum at a critical radius r_c given by

$$\frac{dE(r_c)}{dr} = 0 = 2\pi\gamma - 2\pi r_c\sigma \tag{2}$$

or

$$r_c = \gamma/\sigma \tag{3}$$

Pores with radii smaller than r_c will tend to reseal; pores with radii larger than r_c will tend to increase in size and so permit bulk flow from the cell.

Taupin et al. (1975) found the edge energy, γ, to be about 0.65×10^{-6} dyne for dipalmitoyl phosphatidyl choline and egg phosphatidyl choline liposomes. This value will be applied to the red cell lipids, and any dependence on pore radius will be neglected.

The tension in the red cell membrane is not constant but is a function of the available area per lipid molecule. In the biconcave cell it is less than 0.02 dyne/cm (Rand and Burton, 1964a). If the cell is treated as a simple bilayer, r_c is calculated to be greater than 0.33μ; that is, almost any conceivable pore will reseal.

In the following paragraphs, three estimates of the tension in the lipid portion of the membrane during hemolysis are used to estimate the critical pore radius at hemolysis. In addition, one possible experimental value of the critical radius is examined.

It was found in this work that a membrane tension of approximately 25.8 dyne/cm beyond that of the initial major K^+ loss was required to produce Hb loss. This tension is not necessarily applied to the bilayer because other cell components could support the stress. In view of the proposed domain structure of the membrane, it is likely that the spectrin network accepts a significant portion of the stress. If this stress were applied to the bilayer portion of the membrane, it is calculated from Eq. (3) that $r_c = 2.5$Å, and the critical pore area is 19.6Å^2. Thus, it is expected that the critical pore radius would be significantly larger than 2.5Å. In making this calculation, the decrease in surface tension that would occur as the pore increased in size is neglected in comparison to the probable error introduced by the crude nature of the tension estimate.

A membrane tension of about 2 dynes/cm eventually hemolyzes human red cells (Hoffman, 1958; Rand, 1964). Because hemolysis under this stress occurs after some hours, molecules not normally part of the membrane probably enter the membrane and could decrease its stability. Neglecting

this possibility and assuming that flow of the membrane allowed a significant fraction of the applied stress to be applied to the bilayer portions of the membrane, a critical radius for pore instability is calculated to be $r_c = 33$Å. The area of this critical pore is 3,400Å^2. Note that if one pore of this size were inserted into each of the estimated 9.3×10^3 to 4.8×10^4 domains per human red cell, the area increase would be between 0.2 and 1.1% and thus undetectable by the most accurate available means of measuring cell area increase (2%, Evans and Fung, 1972). The possibility of having one pore per domain with a radius less than the critical pore radius is therefore consistent with the experimental observation of no membrane area increase prior to hemolysis.

Figure 16 indicates that molecular sieving was observed in this work for proteins with a Stokes-Einstein radius in excess of 60Å. This observation suggests that the critical pore radius is greater than 60Å and so implies a membrane tension of about 1 dyne/cm or less. It seems more likely, however, that the proteins enter and leave the membrane in segments smaller than the cross sectional area of the protein, probably in segments closer to the area of single amino acid residues (Table VIII). The loss of small segments would permit other protein segments to enter the membrane and maintain the total free area in each domain low enough so that fluctuations that would expose a hydrocarbon region the size of a protein would have a vanishingly small probability of occurrence.

A final estimate of σ can be obtained from the observation that the membrane area increase is less than 2% at hemolysis. Makowski (1976a) provided a theoretical treatment of the water-hydrocarbon interaction as a function of the area per lipid molecule in a bilayer. If the red cell

membrane is treated as a lipid bilayer (the protein is neglected), a 2% area increase would require a tension on the order of 30 dynes/cm. Because this maximum estimate of the bilayer tension at hemolysis is larger than the previous experimental value of 25.8 dynes/cm, which is also an overestimate and is time-dependent (Rand, 1964), this estimate will not be pursued further.

Therefore, the critical radius for unstable pore formation is significantly greater than 2.5Å and substantially less than 33Å ($2.5 < r_c < 33$Å). The area of the critical pore $Å_c$ is $19.6 < Å_c < (3.4 \times 10^2)Å^2$.

Comparison of Theory and Experiment: Effect of Nucleation and Domain Size

Unstable pore formation

The critical-pore-radius estimates are now compared with the experimental data summarized above. When no macromolecules were present in the external medium and washed cells were subjected to low stress by gradual osmotic hemolysis, which caused hemolysis in about 4 min, the initial membrane defect was the lifting off of a membrane flap of a few hundred square Angstroms. Assuming an area of about 200Å and therefore a radius of about 8Å, this radius falls within the range of estimated critical pore radii ($2.5 < r_c < 33$Å) nd thus might reasonably be expected to result from the formation of an unstable pore in the stressed membrane.

I speculate that under these conditions, which involve both fixation and hypotonic stress, membrane lipid was not able to redistribute itself rapidly enough to provide a uniform density when the cell was sphered. Because the membrane lesion appeared on the site of the former rim of the cell, domains in the former rim region presumably have lower lipid density

in the sphered cell than other domains.

The consistent presence of roughly 8Å pores suggests, according to this model, that the bifacial lipid tension was on the order of 8 dynes/cm. I believe that only one large pore is observed at later times during the experiment because, in the absence of external macromolecules, the probability of pore nucleation in the outer membrane leaflet is low and the mean pore size is small. When an unstable pore does appear, membrane stress and bulk flow of cellular constituents lead to a disruption of the spectrin network in the region of the pore, and a rupture of about 1μ diameter develops.

Effects of macromolecules and multiple pore nucleation

Consider now the case in which macromolecules are present in the extracellular solution. Because of the increased viscosity of these solutions, the local rate of mixing about each individual cell in drastic hemolysis will be reduced compared to saline. In addition, as the membrane is osmotically stressed, the external macromolecules could interact with the external membrane surface and occupy lattice sites in a model of the membrane in a similar manner to the interactions that occur during controlled gradual osmotic hemolysis on the inner membrane surface. In the absence of membrane-active external molecules (salt and dextrose experiments), either the penetration of intracellular protein or lipid transfer from the inner to the outer leaflet is probably required to prevent membrane failure, and these processes may be slow even in the stressed membrane. If the macromolecules could fill vacant lattice sites at a rate faster than intracellular protein penetration and lipid transfer, drastic hemolysis in the presence of macromolecules would be even more

similar to controlled gradual osmotic hemolysis (Katchalsky et al., 1960). Drastic hemolysis in solutions containing macromolecules is thus similar to hemolysis in solutions that promote macromolecular structure and contain a lattice-filling species (Meryman, 1973). Alterations in the solvent properties of water are probably important in macromolecule effects.

When red cells were lysed by gradual osmotic hemolysis by dialysis against a glutaraldehyde solution as in the previous case except that ferritin was present in the extracellular solution, numerous holes with radii of about 100Å were observed in the membrane. The apparent molecular weight cut-off for dextran entrance into the red cell during drastic hemolysis in a dextran-containing solution also gave a pore radius of about 100Å.

The presence of multiple pores in each cell probably means that in the presence of external macromolecules, the probability of pore nucleation is greatly increased over that in the absence of external macromolecules. This would be consistent with the insertion of macromolecules into the stressed membrane and the expected increased free volume fluctuations in the hydrocarbon chains near the inserted molecule. The multiple nucleation can apparently cause loss of cellular constituents at a sufficient rate during gradual osmotic hemolysis that the domain network remains intact.

Limitation of size of unstable pores

The significance of the 100Å-radius holes is not clear. If this value corresponds to the critical radius for unstable pore formation, the bifacial tension would be 0.65 dyne/cm, a reasonable value. It might have resulted from fortuitous conditions in the two experiments noted above, which led to the development of similar sized pores. I suggest, however,

that the critical radius was less than 100Å and that the maximum pore size under these conditions is limited to an area within each domain that is free of integral membrane proteins; that is, the spectrin network is not disrupted. From the estimated domain areas, a 100Å radius hole in a domain would occupy between 2 and 10% of the domain area. A further increase might require compression of the proteins or a disruption of the spectrin network. In gradual osmotic hemolysis in the presence of a low macromolecule concentration and in drastic hemolysis in the presence of a higher macromolecule concentration, nucleation of a new pore is apparently thermodynamically and kinetically favored over the compression of the intramembranous particles or the disruption of the spectrin network. The presence of 100Å pores would also account for the absence of 300Å-diameter colloidal gold particles from unwashed cells hemolyzed by gradual osmotic hemolysis.

At high macromolecule concentrations, the entrance of the macromolecules into the membrane and their effect on water structure probably permit an increase in membrane area and a loss of K^+. The loss of about 20% of the Hb from the cells at maximum protection might then be due to the rapid application of stress, which does not allow the macromolecules to enter the membrane at a sufficient rate to prevent some loss of Hb during the initial stages of hemolysis, perhaps by the molecular-sieving mechanism of controlled gradual osmotic hemolysis.

Coalescence of Pores

Consider now the drastic hemolysis of unwashed red cells. In this case, macromolecules are present at low concentrations in the external media and are adsorbed to the membrane, but the application of membrane

stress is both rapid and very heterogeneous. The rapid stress probably allows only a partial equalization of lipid density in the membrane and the heterogeneous conditions stress some membrane regions more than others. The external macromolecules preferentially enter regions of low lipid density and high stress and provide nucleation sites for multiple pore formation. Some of these pores retain a radius of about 100Å as in drastic hemolysis in the presence of high concentrations of macromolecules or in gradual hemolysis in the presence of macromolecules. The characteristic 40 to 100Å width of the slits observed under these conditions might result from the joining of adjacent pores with the intramembranous particles pushed to the sides of the domains but with the spectrin network remaining intact. The intact network would then account for the unexpectedly uniform width of the slits. It may be fortuitous that the length of a 40Å rectangle having the same area as a 100A-radius pore ($3.1 \times 10^4 Å^2$) is 785Å, which falls within the range of diameters estimated for the human RBC domain (618 to 1382Å).

On geometrical grounds, this supports the view

(1) That the 100Å-radius pores represent the maximum available area for pore formations per domain without disruptions of the spectrin network.

(2) That slits can arise from the joining of two or more pores.

(3) That the spectrin network remains intact.

(4) That the 100Å slits probably arise from the coalescence of adjacent 40Å slits with the particles pushed to the outside and the spectrin network still intact.

Summary

Thus, according to this model, the molecular sieving of controlled gradual osmotic hemolysis occurs as an initial phase of stress-induced hemolysis in general. The course of hemolysis is influenced by the magnitude of membrane stress and its uniformity and by the presence of extracellular molecules. The extracellular molecules can influence the rate of application of membrane stress and its uniformity and additionally interact with the membrane and water to increase the membrane area and the number of pore nucleation sites.

For low membrane stress, molecular sieving without the formation of aqueous pores is observed. Soluble globular proteins enter the stressed cell membrane, occupy space, reduce the free volume in each domain, and thus prevent large fluctuations in lipid density, which could form an unstable pore. There may be a net movement of lipid from the inner to the outer membrane leaflet during this process.

Increased membrane stress in the presence of a macromolecule leads to the nucleation of many unstable pores. The maximum size of each pore is apparently limited to about a 100Å radius by the bulk of the membrane proteins and the spectrin network. Hemolysis in the absence of external macromolecules or other external pore-nucleating molecules, even when the external solute concentration is lowered over a period of several minutes, apparently results in one large pore per cell, probably because of a low rate of pore nucleation in the outer membrane leaflet. Rapid hemolysis in the presence of macromolecules leads to nucleation in a small region of the membrane, probably owing to a heterogeneous lipid distribution and heterogeneous stresses, and the coalescence of some of the resulting pores into slits. The formation of the slits need not disrupt the spectrin network.

PROPERTIES OF GHOST MEMBRANES

The proposed molecular sieving model of gradual osmotic hemolysis predicts that when red cells are made into ghosts by an osmotic hemolysis procedure, the resulting membrane will be different from the membrane of the intact red cell. The increase in membrane area required to cause hemolysis would increase the free area of the domains. The increased free area would be expected to increase the lipid flip-flop rate, would allow the insertion of cytoplasmic and extracellular molecules into the membrane, and might allow conformational changes and transmembrane movement of integral membrane proteins. The extent to which these changes would occur would depend on the details of the hemolytic procedure.

Experimental data support these predictions. Phospholipids are labeled to a greater extent with acetic anhydride in ghosts than in intact cells (Carraway et al., 1972); phospholipase C from *Bacillus cereus* and pancreatic phospholipase A_2 hydrolyze phospholipids in ghost but not in intact RBC's when suspended in saline (Zwaal et al., 1971; Woodward and Zwaal, 1972); and the differences observed with spin labels between the inner and outer membrane leaflet in intact cells are not present in ghosts unless the hemolysis medium contains Mg^{++} (Tanaka and Ohnishi, 1976).

Cytoplasmic proteins are expected to be inserted into the stressed membrane. The amount remaining after release of membrane stress is predicted to be a function of the duration and magnitude of the stress and of the properties of the protein. The marked difference in the enzyme activities associated with ghost membranes prepared under different conditions (Duchon and Collier, 1971; Bramley, Coleman and Finean, 1971; Bramley and Coleman, 1972) suggests that at least some enzymes normally

associated with ghosts have little or no association with the intact red cell membrane. Fujii and Sato (1975) have shown that this is the case for aldolase and glyceraldehyde 3-phosphate dehydrogenase.

Finally, whereas a similar pattern of protein crosslinks is observed in intact cells and ghosts (Wang and Richards, 1975), some proteins that are not labeled by reagents in the intact cell are labeled in ghosts (Carraway and Shin, 1972; Staros, Haley and Richards, 1974), and proteins not susceptible to trypsin in the intact cell are cleaved in the ghost (Carraway, Kobylka and Triplett, 1971). Ghost membranes are, therefore, significantly different from the membranes of intact red cells. These differences presumably result from the membrane stress applied to transform red cells into ghosts and are caused by the mechanisms proposed in this paper to describe the process of osmotic hemolysis.

CONCLUSION

The development of this paper has proceeded from the presentation of the experimental observations in the Results section, through the interpretation of the data in terms of molecular-sieving of variously sized subunits and aggregates of intracellular proteins by stressed rat red cell membranes, to the presentation of a molecular model that predicts the molecular sieving phase of osmotic hemolysis and the extension of this domain model to hemolysis under conditions which involve bulk flow from the cells.

The molecular-sieving interpretation of the experimental data is consistent with previous apparent observations of molecular sieving during osmotic hemolysis (Marsden and Östling, 1959; Östling and Persson, 1966; Ihler, Glew and Schnure, 1973; Colombe and Macey, 1974) and with the long times over which Hb loss can occur during osmotic hemolysis (Danon, 1961; Perk and Danon, 1965). The domain model which predicts the molecular sieving of soluble globular proteins (and other classes of molecules) across stressed RBC membranes is based on hydrophobic interactions occurring between normally soluble proteins and the lipid bilayer portion of the membrane, on the area constraints imposed by a spectrin network, and on the presence of other membrane proteins.

The existence of lipid bilayer areas in the RBC membrane and the presence of peripheral and integral membrane proteins are now readily accepted. Katchalsky et al. (1960) and MacGregor and Tobias (1972) suggested that a molecular network in the red cell membrane was important in determining the course of osmotic hemolysis. The existence of a spectrin network in the red cell membrane is strongly supported by the

data and model presented in this work, by the mesh-like appearance of lipid extracted RBC's (Yu, Fischman and Steck, 1973), and by the subchain molecular weight, $\sim 10^5$, in an elastomer network model of the membrane derived from the membrane shear modulus (Evans, 1973b; Evans and La Celle, 1975). The membrane model developed in this work is therefore consistent with the known properties of red cell membranes and is rather similar to the model proposed by Bechhold (1921) in which a protein framework was impregnated with lecithin and cholesterol.

In general, the mean square fluctuation in the volume per particle is expected to be inversely proportional to the square of the number of particles in a system (Landau and Lifschitz, 1958). The subdivision of a lipid bilayer by spectrin into domains might, therefore, increase the magnitude of volume fluctuations. The primary effect of spectrin, however, is to limit the area per domain. This subdivision prevents the passage of large molecules across the membrane and prevents the formation of unstable pores. Both of these restrictions appear necessary for the in vivo survival of the metabolically inactive red cell.

The unstressed RBC membrane, therefore, appears to prevent the passage of large molecules across the membrane owing to the spectrin constraints imposed on lipids of the inner membrane leaflet. The high cholesterol content of the outer membrane leaflet, however, reduces free volume fluctuations and causes this leaflet to present a greater resistance to the diffusion of small nonelectrolytes than the inner membrane leaflet. Thus, both the inner and outer red cell membrane leaflets are involved in limiting diffusion across the membrane.

Stress of the cell membrane during circulation is probably suffi-

cient to increase the domain area over that of the unstressed membrane. This area increase would allow the partial insertion of proteins into the inner and outer membrane leaflets and might increase the probability of loss of integral membrane proteins. The irreversible binding of some of the inserted proteins might partially account for the decreased deformability of old cells and the increased probability of removal of old cells from circulation.

The model views the membrane as a dynamic system in which some molecules enter and leave the membrane in a statistical manner, but in which membrane stress increases the quantity of foreign molecules in the membrane. Similarly, the organization of membrane molecules is not static, but changes with the metabolic state of the cell and affects the accessibility of membrane lipids to soluble molecules. Thus, whether a soluble protein, such as Hb, is a constituent of the cell membrane is not clear. In the normal unstressed red cell, there is probably always some Hb inserted into the membrane, and this amount is increased by aggregation (deoxygenation) or dissociation (metabolic depletion) of Hb. Most of this membrane-associated Hb is reversibly bound and is not required for the structural integrity of the membrane. When the membrane is stressed, however, Hb enters the membrane, stabilizes the bilayer structure, and prevents the formation of unstable pores. By this process, it is probably partially responsible for the in vivo survival of the red cell.

The limitation of diffusion of large molecules across the RBC membrane caused by the subdivision into domains, and the similarity of erythrocyte spectrin and actin to muscle proteins, suggest that a contrac-

tion of spectrin might be involved in the transfer of molecules and information across the membrane. The entrance of a newly synthesized protein into a membrane might result from the protein triggering a suitable contraction in the spectrin network that increases the domain area adjacent to the protein. A membrane protein contraction might also be involved in membrane fusion, permease control, release of neurotransmitters, and propagation of action potentials.

APPENDIX A
ESTIMATION OF THE SIZE OF ADENYLATE KINASE, HEMOGLOBIN, FUMARASE AND CATALASE FROM SEDIMENTATION AND/OR DIFFUSION DATA

Einstein (1926) showed that, in general, a diffusion coefficient can be written as

$$D = \frac{\mathcal{R}T}{N} \frac{1}{f} \qquad \text{(A-1)}$$

where f is the frictional resistance that a solute molecule experiences in moving through a solvent, $\mathcal{R}$ is the gas constant, T is the absolute temperature, and N is Avogadro's number. If the solute molecule is considered as a sphere that is large compared to the dimensions of the solvent molecule, the frictional resistance is given by Stokes law as $f = 6\pi\eta r$, where η is the viscosity of the solvent and r is the radius of the solute molecule. Thus, a Stokes-Einstein radius can be calculated from the diffusion coefficient of any solute as

$$R_{SE} = \frac{\mathcal{R}T}{N} \frac{1}{6\pi\eta D} \qquad \text{(A-2)}$$

Its value corresponds to the radius of the sphere that would have a diffusion coefficient equal to that of the solute.

A measure of the hydration and/or asymmetry of solute molecules can be obtained by considering the ratio of the observed frictional resistance f to the frictional resistance of an anhydrous spherical molecule with the same molecular weight and partial specific volume as the solute (Svedberg and Pedersen, 1940). The anhydrous volume of a solute molecule is given by $M\bar{v}/N$ where M is the anhydrous molecular weight (g/mole), $\bar{v}$ is the partial specific volume (cm^3/g), and N is Avogadro's number

(molecules/mole). If the molecule is spherical, its volume is also given by the volume of a sphere with the Stokes-Einstein radius, $\frac{4}{3} R_{SE}^3$. The radius of the anhydrous sphere is then

$$R_{SE} = \left(\frac{3M\bar{v}}{4\pi N}\right)^{1/3} \tag{A-3}$$

and, because $f_o = 6\pi\eta R_{SE}$,

$$f_o = 6\pi\eta \left(\frac{3M\bar{v}}{4\pi N}\right)^{1/3} \tag{A-4}$$

where f_o denotes the frictional resistance of a spherical molecule. Thus, the ratio of the observed frictional resistance to the frictional resistance of a spherical anhydrous molecule of the same molecular weight and partial specific volume is

$$\frac{f}{f_o} = \frac{RT}{N} \frac{1}{6\pi\eta D} \left(\frac{4\pi N}{3M\bar{v}}\right)^{1/3} . \tag{A-5}$$

If the measured f corresponds to an unhydrated spherical molecule, the ratio f/f_o will equal one. Hydration of the solute or the nonspherical shape of the solute will cause $f/f_o \neq 1$.

The f/f_o values encountered with the proteins used in this study and with proteins in general are greater than 1 (Table A-IV). The contributions to f/f_o due to hydration and to nonspherical molecular shape can be assessed separately only if additional information is available. The effects of multi-component systems as contrasted with the two-component system outlined will not be discussed. The contribution of hydration to f/f_o can be obtained by considering the frictional resistance due to a hydrated spherical molecule provided that the water of hydration has the density of bulk water. If the hydration is w grams of water per gram of

protein, the product of the effective molecular weight and the partial specific volume of the hydration complex is

$$M_h\bar{v}_h = M(\bar{v} + w\bar{v}_w) \qquad \text{(A-6)}$$

where the subscript h refers to the hydration complex and the subscript w refers to water. The frictional resistance experienced by this complex is found by analogy with f_o to be

$$f_h = 6\pi\eta \left(\frac{3M(\bar{v} + w\bar{v}_w)}{4\pi N} \right)^{1/3} \qquad \text{(A-7)}$$

Thus, the contribution of hydration to f/f_o is

$$\left(\frac{f}{f_o}\right)_h = \left(\frac{\bar{v} + w\bar{v}_w}{\bar{v}} \right)^{1/3} \qquad \text{(A-8)}$$

Table A-I presents the calculated contribution of hydration to the observed f/f_o for the partial specific volumes of the proteins used in this work.

If a molecule is represented as an ellipsoid of revolution rotated about the a axis and if the axes of the ellipsoids are randomly oriented in solution, Perrin (1936) has shown that the contribution of molecular asymmetry to f/f_o for an axial ratio $\gamma = b/a$ is

$$\frac{f}{f_o} = \frac{\gamma^{2/3}}{\sqrt{1 - \gamma^2}} \log_e \left(\frac{1 + \sqrt{1 - \gamma^2}}{\gamma} \right) \quad \text{for } \gamma < 1 \qquad \text{(A-9a)}$$

$$\frac{f}{f_o} = \frac{\gamma^{2/3}}{\sqrt{\gamma^2 - 1}} \arctan (\gamma^2 - 1) \quad \text{for } \gamma > 1 \qquad \text{(A-9b)}$$

It should be stressed that these equations apply only to molecules that can be considered ellipsoids of revolution; an extensively unfolded protein cannot be considered as a rigid ellipsoid. Table A-II presents the calcu-

HYDRATION[1]	PARTIAL SPECIFIC VOLUME[2] .730	.738	.740	.749
.01	1.005	1.005	1.004	1.004
.02	1.009	1.009	1.009	1.009
.03	1.014	1.013	1.013	1.013
.04	1.018	1.018	1.018	1.018
.05	1.022	1.022	1.022	1.022
.06	1.027	1.026	1.026	1.026
.07	1.031	1.031	1.031	1.030
.08	1.035	1.035	1.035	1.034
.09	1.040	1.039	1.039	1.039
.10	1.044	1.043	1.043	1.043
.11	1.048	1.047	1.047	1.047
.12	1.052	1.052	1.051	1.051
.13	1.056	1.056	1.056	1.055
.14	1.060	1.060	1.060	1.059
.15	1.064	1.064	1.064	1.063
.16	1.068	1.068	1.068	1.067
.17	1.072	1.072	1.071	1.071
.18	1.076	1.076	1.075	1.075
.19	1.080	1.079	1.079	1.078
.20	1.084	1.083	1.083	1.082
.21	1.088	1.087	1.087	1.086
.22	1.092	1.091	1.091	1.090
.23	1.096	1.095	1.095	1.094
.24	1.100	1.099	1.098	1.097
.25	1.103	1.102	1.102	1.101
.26	1.107	1.106	1.106	1.105
.27	1.111	1.110	1.109	1.108
.28	1.114	1.113	1.113	1.112
.29	1.118	1.117	1.117	1.115
.30	1.122	1.121	1.120	1.119
.31	1.125	1.124	1.124	1.123
.32	1.129	1.128	1.127	1.126
.33	1.133	1.131	1.131	1.130
.34	1.136	1.135	1.135	1.133
.35	1.140	1.139	1.138	1.137
.36	1.143	1.142	1.141	1.140
.37	1.147	1.145	1.145	1.143
.38	1.150	1.149	1.148	1.147
.39	1.154	1.152	1.152	1.150
.40	1.157	1.156	1.155	1.154
.41	1.160	1.159	1.159	1.157
.42	1.164	1.162	1.162	1.160
.43	1.167	1.166	1.165	1.164
.44	1.171	1.169	1.169	1.167
.45	1.174	1.172	1.172	1.170
.46	1.177	1.176	1.175	1.173
.47	1.180	1.179	1.178	1.177
.48	1.184	1.182	1.182	1.180
.49	1.187	1.185	1.185	1.183
.50	1.190	1.188	1.188	1.186
.50	1.190	1.188	1.188	1.186
.52	1.197	1.195	1.194	1.192
.54	1.203	1.201	1.201	1.199
.56	1.209	1.207	1.207	1.205
.58	1.216	1.214	1.213	1.211
.60	1.222	1.220	1.219	1.217
.62	1.228	1.226	1.225	1.223
.64	1.234	1.232	1.231	1.229
.66	1.240	1.238	1.237	1.235
.68	1.246	1.244	1.243	1.241
.70	1.252	1.249	1.249	1.246
.72	1.257	1.255	1.255	1.252
.74	1.263	1.261	1.260	1.258
.76	1.269	1.267	1.266	1.263
.78	1.275	1.272	1.272	1.269
.80	1.280	1.278	1.277	1.274
.82	1.286	1.283	1.283	1.280
.84	1.291	1.289	1.288	1.285
.86	1.297	1.294	1.294	1.291
.88	1.302	1.300	1.299	1.296
.90	1.307	1.305	1.304	1.301
.92	1.313	1.310	1.309	1.307
.94	1.318	1.315	1.315	1.312
.96	1.323	1.321	1.320	1.317
.98	1.329	1.326	1.325	1.322
1.00	1.334	1.331	1.330	1.327
1.00	1.334	1.331	1.330	1.327
1.02	1.339	1.336	1.335	1.332
1.04	1.344	1.341	1.340	1.337
1.06	1.349	1.346	1.345	1.342
1.08	1.354	1.351	1.350	1.347
1.10	1.359	1.356	1.355	1.352
1.12	1.364	1.361	1.360	1.357
1.14	1.369	1.366	1.365	1.362
1.16	1.374	1.371	1.370	1.366
1.18	1.378	1.375	1.375	1.371
1.20	1.383	1.380	1.379	1.376
1.22	1.388	1.385	1.384	1.381
1.24	1.393	1.390	1.389	1.385
1.26	1.397	1.394	1.393	1.390
1.28	1.402	1.399	1.398	1.395
1.30	1.407	1.404	1.403	1.399
1.32	1.411	1.408	1.407	1.404
1.34	1.416	1.413	1.412	1.408
1.36	1.421	1.417	1.416	1.413
1.38	1.425	1.422	1.421	1.417
1.40	1.430	1.426	1.425	1.422
1.42	1.434	1.431	1.430	1.426
1.44	1.438	1.435	1.434	1.430
1.46	1.443	1.439	1.438	1.435
1.48	1.447	1.444	1.443	1.439
1.50	1.452	1.448	1.447	1.443
1.52	1.456	1.452	1.451	1.448
1.54	1.460	1.457	1.456	1.452
1.56	1.464	1.461	1.460	1.456
1.58	1.469	1.465	1.464	1.460
1.60	1.473	1.469	1.468	1.464
1.62	1.477	1.473	1.473	1.468
1.64	1.481	1.478	1.477	1.473
1.66	1.485	1.482	1.481	1.477
1.68	1.490	1.486	1.485	1.481
1.70	1.494	1.490	1.489	1.485
1.72	1.498	1.494	1.493	1.489
1.74	1.502	1.498	1.497	1.493
1.76	1.506	1.502	1.501	1.497
1.78	1.510	1.506	1.505	1.501
1.80	1.514	1.510	1.509	1.505
1.82	1.518	1.514	1.513	1.509
1.84	1.522	1.518	1.517	1.513
1.86	1.526	1.522	1.521	1.517
1.88	1.530	1.526	1.525	1.520
1.90	1.534	1.530	1.529	1.524
1.92	1.538	1.534	1.533	1.528
1.94	1.541	1.537	1.536	1.532
1.96	1.545	1.541	1.540	1.536
1.98	1.549	1.545	1.544	1.539
2.00	1.553	1.549	1.548	1.543

[1]Hydration in g of water/g of protein

[2]Partial specific volumes assumed for calculations:

0.730 Catalase
0.738 Fumarase
0.740 Adenylate kinase
0.749 Hemoglobin

TABLE A-I

CONTRIBUTION OF ASYMETRY TO F/FO FOR ELLIPSOIDS OF REVOLUTION[1]

AXIAL RATIO	F/FO PROLATE	F/FO OBLATE	AXIAL RATIO	F/FO PROLATE	F/FO OBLATE	AXIAL RATIO	F/FO PROLATE	F/FO OBLATE	AXIAL RATIO	F/FO PROLATE	F/FO OBLATE
1.02	1.000	1.000	2.00	1.044	1.042	5.00	1.250	1.223	20.00	1.995	1.783
1.04	1.000	1.000	2.10	1.050	1.048	5.50	1.282	1.251	21.00	2.034	1.809
1.06	1.000	1.000	2.20	1.057	1.054	6.00	1.314	1.277	22.00	2.073	1.835
1.08	1.001	1.001	2.30	1.064	1.060	6.50	1.345	1.302	23.00	2.111	1.860
1.10	1.001	1.001	2.40	1.071	1.067	7.00	1.375	1.326	24.00	2.148	1.885
1.12	1.001	1.001	2.50	1.078	1.073	7.50	1.405	1.350	25.00	2.184	1.909
1.14	1.002	1.002	2.60	1.084	1.079	8.00	1.433	1.373	26.00	2.220	1.932
1.16	1.002	1.002	2.70	1.091	1.086	8.50	1.462	1.395	27.00	2.255	1.955
1.18	1.002	1.002	2.80	1.098	1.092	9.00	1.489	1.416	28.00	2.289	1.977
1.20	1.003	1.003	2.90	1.105	1.098	9.50	1.516	1.437	29.00	2.323	1.999
1.22	1.004	1.003	3.00	1.113	1.105	10.00	1.543	1.458	30.00	2.357	2.020
1.24	1.004	1.004	3.10	1.120	1.111	10.50	1.569	1.477	31.00	2.390	2.041
1.26	1.005	1.005	3.20	1.127	1.117	11.00	1.595	1.497	32.00	2.423	2.061
1.28	1.005	1.005	3.30	1.134	1.123	11.50	1.620	1.516	33.00	2.455	2.081
1.30	1.006	1.006	3.40	1.141	1.130	12.00	1.644	1.534	34.00	2.488	2.101
1.32	1.007	1.007	3.50	1.148	1.136	12.50	1.669	1.552	35.00	2.518	2.120
1.34	1.008	1.008	3.60	1.155	1.142	13.00	1.693	1.569	36.00	2.548	2.139
1.36	1.008	1.008	3.70	1.162	1.148	13.50	1.716	1.587	37.00	2.579	2.158
1.38	1.009	1.009	3.80	1.169	1.154	14.00	1.739	1.603	38.00	2.609	2.176
1.40	1.010	1.010	3.90	1.176	1.160	14.50	1.762	1.620	39.00	2.639	2.194
1.42	1.011	1.011	4.00	1.182	1.166	15.00	1.785	1.636	40.00	2.668	2.212
1.44	1.012	1.012	4.10	1.189	1.172	15.50	1.807	1.652	41.00	2.697	2.229
1.46	1.013	1.013	4.20	1.196	1.178	16.00	1.829	1.667	42.00	2.726	2.246
1.48	1.014	1.014	4.30	1.203	1.184	16.50	1.851	1.683	43.00	2.755	2.263
1.50	1.015	1.014	4.40	1.210	1.190	17.00	1.872	1.698	44.00	2.783	2.280
1.52	1.016	1.015	4.50	1.216	1.195	17.50	1.893	1.712	45.00	2.811	2.296
1.54	1.017	1.016	4.60	1.223	1.201	18.00	1.914	1.727	46.00	2.839	2.313
1.56	1.018	1.017	4.70	1.230	1.207	18.50	1.935	1.741	47.00	2.866	2.328
1.58	1.019	1.018	4.80	1.237	1.212	19.00	1.955	1.755	48.00	2.893	2.344
1.60	1.020	1.019	4.90	1.243	1.218	19.50	1.975	1.769	49.00	2.920	2.360
1.62	1.021	1.020	5.00	1.250	1.223	20.00	1.995	1.783	50.00	2.947	2.375
1.64	1.022	1.021									
1.66	1.023	1.023									
1.68	1.024	1.024									
1.70	1.026	1.025									
1.72	1.027	1.026									
1.74	1.028	1.027									
1.76	1.029	1.028									
1.78	1.030	1.029									
1.80	1.031	1.030									
1.82	1.033	1.031									
1.84	1.034	1.033									
1.86	1.035	1.034									
1.88	1.036	1.035									
1.90	1.038	1.036									
1.92	1.039	1.037									
1.94	1.040	1.038									
1.96	1.041	1.040									
1.98	1.043	1.041									
2.00	1.044	1.042									

[1]Calculated with equations of Perrin (1956):

$$\left(\frac{f}{f_o}\right)_{Asy} = \frac{\gamma^{2/3}}{\sqrt{1-\gamma^2}} \log_e\left(\frac{1+\sqrt{1-\gamma^2}}{\gamma}\right) \qquad \text{for } \gamma < 1$$

$$\left(\frac{f}{f_o}\right)_{Asy} = \frac{\gamma^{2/3}}{\sqrt{\gamma^2-1}} \arctan(\gamma^2 - 1) \qquad \text{for } \gamma > 1$$

where γ is the axial ratio.

TABLE A-II

lated contribution of molecular asymmetry to the observed f/f_o for ellipsoids of revolution.

The relative contributions of hydration and asymmetry to the observed f/f_o can be determined independently for hemoglobin from data on its hydration and axial ratio. Hemoglobin has between 0.3 and 0.4 grams water of hydration per gram of protein (Adair and Adair, 1936; Perutz, 1946; Drabkin, 1950). From Table A-I, this hydration would give $(f/f_o)_h$ between 1.12 and 1.15. The hemoglobin tetramer has an axial ratio of approximately 1.2 (Perutz et al., 1960), which, from Table A-II, would give $(f/f_o)_{asy}$ = 1.003. Thus, the calculated $f/f_o = (f/f_o)_h(f/f_o)_{asy}$ is between 1.12 and 1.15. The f/f_o measured by sedimentation-diffusion for the compact hemoglobin tetramer will be shown to be about 1.15 (Table A-V), in agreement with f/f_o calculated from hydration and molecular asymmetry. Generalizing to the other compact globular proteins used in this study, the measured f/f_o reflects primarily the hydration of the molecule and is rather insensitive to the molecular shape.

The anhydrous molecular weight of a solute can be obtained from sedimentation-diffusion studies with the Svedberg equation (Svedberg and Pedersen, 1940) as follows:

$$M = \frac{\mathcal{R}TS}{D(1 - \bar{v}\rho)} \qquad \text{(A-10)}$$

where S is the sedimentation coefficient and ρ is the solvent density. The density of an aqueous solvent is near 1, and the partial specific volumes of the proteins used in this study are near 0.74. Thus an error in $\bar{v}$ causes roughly a three-fold increased error in the molecular weight. Relatively few determinations of $\bar{v}$ have been made for the proteins used

in this work, and changes in $\bar{v}$ due to dissociation or aggregation of the proteins have not been studied extensively (see Table A-IV).

Experimentally determined values of S and D and experimental or calculated values of $\bar{v}$ are tabulated from the literature in Table A-IV for the proteins used in this work. The data for each protein are segregated according to molecular weight in order to separate data concerning the variously sized subunits and aggregates of each protein. Some data are further divided according to the experimental conditions in order to facilitate comparison. The molecular weights tabulated are those given by the authors and were generally obtained with the Svedberg equation. Molecular weights obtained by other means under conditions similar to those under which S and/or D were determined are also tabulated.

A determination of S or D alone does not provide enough information to determine the molecular weight. Thus, diffusion coefficients that overlap the region 5.5 to 8.5×10^{-7} cm^2/sec have been measured under different conditions for the hemoglobin tetramer, dimer and monomer (Table A-IV, data with molecular weights calculated from S and D). The conditions under which a measurement was made can be used to predict the subunit composition of the solution. Thus, data presented in Table A-IV and in which the molecular weight was not determined have been assigned a molecular weight based on the probable composition of the solution obtained by comparison of the measurement conditions with the measurement conditions of other data in which the molecular weight was determined.

The molecular weights assigned to the intact proteins are those obtained by amino acid analysis or amino acid sequence analysis with the

TABLE A-III. Molecular weights and partial specific volumes assumed in calculations.

Protein	Size	$\bar{v}$[a]	Molecular Weight MW[b]	Method	Reference
Adenylate kinase	monomer	0.74	22028.	Average of values obtained by amino acid analysis	see Table A-IV
	dimer		44056.		
	trimer		66084.		
Hemoglobin	tetramer	0.749	64459.	Amino acid sequence plus hemes	Braunitzer, 1964
	dimer		32230.		
	monomer		16115.		
	octamer		128918.		
Fumarase	tetramer	0.738	194000.	Sedimentation-equilibrium	Kanarek et al., 1964
	dimer		97000.		
	monomer		48500.		
Catalase[c]	Cat/1	0.73	232400.	Preliminary amino acid sequence plus heme	Schroeder et al., 1969
	Cat/2		116200.		
	Cat/4		58100.		
	(Cat/8	apo + heme	28800. 29400.)		
	(Cat/12	apo + heme	19200. 19800.)		

References:

[a] Partial specific volume obtained by calculation from amino acid composition or from measurement on normal protein. The same value was assumed for all subunits and aggregates of each protein. See Table A-IV for references.

[b] Molecular weights of subunits were obtained by assuming that all the polypeptide chains of a protein are of equal weight. See Appendix B for a discussion of the size of the catalase monomer.

[c] Catalase contains four heme groups and dissociates into halves and quarters. The possible further dissociation into subunits one-eighth and one-twelfth the size of the intact molecule is discussed in Appendix B.

addition of heme groups when necessary except for fumarase for which the best available data are from sedimentation-equilibrium (Table A-III). It is possible that the molecular weight used for fumarase is too high owing to reversible aggregation of the protein during measurement. The molecular weights of subunits have been obtained by assuming that all polypeptide chains of a protein are of equal weight. The partial specific volumes employed in calculations were primarily obtained from intact nondissociated molecules but have been applied to all subunits and aggregates of that protein (Table A-III).

If only S was determined by the authors, the expected value of D was calculated with the molecular weight and partial specific volume listed in Table A-III and the density of water at 20°C with the Svedberg equation, and its value is enclosed in parentheses in Table A-IV.

The Stokes-Einstein radii have been calculated from the measured or expected D. Frictional ratios determined by the authors are listed in the table. If the frictional ratio was not reported but both S and D were determined, f/f_o was calculated with the molecular weight determined from S and D and the value of the $\bar{v}$ listed in Table A-III unless the authors measured $\bar{v}$, in which case their value was used. If only S or D was determined, the expected f/f_o was calculated from the assumed M and $\bar{v}$ (Table A-III), and its value is enclosed in parentheses (Table A-IV).

Table A-IV documents the dissociation of hemoglobin, fumarase and catalase into units approximately one-half and one-fourth the size of the intact molecule normally isolated with physiological activity. The possible further dissociation of catalase is considered in Appendix B. Data concerning aggregates of adenylate kinase and hemoglobin are also tabulated. It is evident, however, that a unique Stokes-Einstein radius has not been

TABLE A-IV

Stokes-Einstein radii and frictional ratios of adenylate kinase, hemoglobin, fumarase and catalase subunits, intact molecules and aggregates as estimated from sedimentation and/or diffusion data for mammalian enzymes.

The data have been grouped by protein and by size unit as estimated either by a molecular-weight determination or by comparison of measurement conditions with conditions of experiments in which the molecular weight was determined. Some data have been further divided by conditions of measurement to aid in comparison of the conditions.

Explanation of Headings

Species and conditions	Species from which the protein was isolated and conditions under which the sedimentation coefficient and/or diffusion coefficient were measured. Isolation and purification procedures are not tabulated but may be of importance.
pH	pH at which S and/or D was measured.
Conc.	Protein concentration in percent. $\rightarrow 0$ = extrapolated to infinite dilution.
S	Sedimentation coefficient in units of 1×10^{-13} sec, corrected to water at 20°C, at the protein concentration listed unless otherwise noted.
D	Diffusion coefficient in units of 1×10^{-7} cm^2/sec, corrected to water at 20°C, unless otherwise noted. Values enclosed in parentheses have been calculated from the sedimentation coefficient with the Svedberg equation (A-10) with assumed values for the molecular weight, partial specific volume, and solvent density as described in the text.

$\bar{v}$ — Partial specific volume in units of cm^3/g. Values tabulated were determined experimentally or were calculated from the amino acid composition of the protein. Authors who calculated a molecular weight from S and D but did not determine $\bar{v}$ used one of the tabulated values.

f/f_o — Frictional ratio. Frictional ratios have been quoted from the authors when possible. When not possible, they were calculated from Eq. (A-5) with the authors measured $\bar{v}$ when possible, otherwise with the value from Table A-III and M as determined with the Svedberg equation. If D was measured, M was taken from Table A-III and the value enclosed in parentheses. If S was measured, D was estimated with the Svedberg equation with the value of M and $\bar{v}$ from Table A-III and the density of water at 20°C, and f/f_o enclosed in parentheses.

MW — Molecular weight as determined by the authors from S and D or by other means under conditions similar to those under which S and/or D were measured

R_{SE} — Stokes-Einstein radius in Angstroms as calculated from the measured or estimated diffusion coefficient using Eq. (A-2). Values that have not been used in calculating an average R_{SE} have been enclosed in parentheses. The reasons for omission are indicated as follows (see text for discussion).

Letter References

^{a}Measurement in amide solution

^{c}High protein concentration

^{d}Probable error in data (see Samejima, McCabe, and Yang, 1968).

^{m}Molecular weight not corresponding to an expected size unit.

^{p}Measurement at high or low pH.

^{t}Treatment, modification or reaction of the protein.

TABLE A-IV(1). Stokes-Einstein radii and frictional ratios of adenylate kinase.

Source and conditions	pH	Concn.	S	D	$\bar{v}$	f/f_o	MW	R_{SE}	Reference
Monomer									
Rabbit muscle	6.5	1.0%	1.7				21600	--	Callaghan, 1957
Rabbit muscle, 0.15M KCl	7.0	→0 0.77%	2.30[1]	10.0[1]	0.73	1.15	21000	24.4[1]	Noda and Kuby, 1957b
Rabbit muscle					0.741		21279		Mahowald, Noltmann and Kuby, 1962
Bovine liver mitochondria	7.4 8.5	0.04-0.4	2.49	10.3	0.73	1.11	21500 21744	20.7	Markland and Wadkins, 1966
Rat liver III[2]	7.2	→0	1.23	4.8	0.74	1.1[10]	23000[3] 23404	(44.5)[11]	Criss, Sapico and Litwack, 1970
Pork muscle, 0.15M KCl	7.0	→0	2.30[6]	10.1[6]	0.74 0.736	1.15	21000[4]	21.1[5]	Schirmer, Schirmer, Schultz and Thuma, 1970
Human muscle	7.0	--		9.9[7]	0.74	(1.15)	21686	21.6[7]	Thuma, Schirmer and Schirmer, 1972
Dimer									
Rat liver III[2]	7.2						46000		Criss, Sapico and Litwack, 1970
Rat liver II[2]	7.2 7.2	→0 1.1%	3.02 2.7	5.52[8] 5.34	0.65 0.65	1.81[9] 1.92[9]	38000[9] 35000[9]	38.7 (40.0)[c]	Sapico, Litwack and Criss, 1972
Trimer									
Rat liver III[2]	7.2	→0	3.52	4.8		(1.6)	68000	44.5	Criss, Sapico and Litwack, 1970

TABLE A-IV(1) References:

[1]D and S measured at 25°C in 0.15M KCl and 0.01M phosphate buffer, specific viscosity = 1.003. Stokes-Einstein radius calculated with viscosity of water at 25° = 0.8935 (Rauen and Kuhn, 1964).

[2]No significant difference between the diffusion coefficients, partial specific volumes, and frictional ratios of rat liver adenylate kinase isozymes II and III (Sapico, Litwack and Criss, 1972).

[3]Molecular weight = 46000 and infrequently 21000 and 160000, observed in gel filtration but not sedimentation.

[4]Additional molecular weight determinations: gel filtration, 21000; sedimentation equilibrium, 21600; titration of -SH groups, 21400; amino acid analysis, 21400.

[5]R_{SE} calculated from solvent viscosity given by Schirmer et al. (1970).

[6]Not corrected to water.

[7]Thuma, Schirmer, and Schirmer (1972) determined that the Stokes-Einstein radii of human and rabbit muscle adenylate kinase were the same by gel filtration. They state that the diffusion coefficient of Noda and Kuby (1957b), when corrected to 0% protein and 20°C, is 9.9×10^{-7} cm^2/sec and use this value as the diffusion coefficient. Compare with data of Noda and Kuby above.

[8]Diffusion coefficient used is the average of the two values given by Sapico, Litwack and Criss (1972). Presumably, the extrapolation to zero protein would be the average (Litwack, personal communication).

[9]Calculated from data given. If $\bar{v} = 0.74$ instead of 0.65, the calculated values become:

S	D	$\bar{v}$	f/f_o	MW
3.02	5.52	0.74	1.57	51000
2.7	5.34	0.74	1.67	47000

Sapico, Litwack and Criss (1972) found $f/f_o = 1.3$ and MW = 49000 from these S, D and $\bar{v}$ data and MW = 46000 by gel filtration.

[10]Frictional ratio calculated from S and D is 2.33

[11]Not included on average R_{SE} or f/f_o because R_{SE} is about twice all other monomer R_{SE}.

TABLE A-IV(2). Stokes-Einstein radii and frictional ratios of hemoglobin

Species and conditions	pH	Concn.	S	D	$\bar{v}$	f/f_o	MW	R_{SE}	Reference
Tetramer									
Horse CO-Hb[9]	7.56	1.0%	5.46	8.52	0.7575	0.95	66800	--	Svedberg and Nichols, 1927
Horse CO-Hb					0.749				Svedberg and Fåhraeus, 1926
met-Hb					0.747				
Cattle CO-Hb, 5°C	6.8	2.5%		4.86[1]		(1.64)		(44.0)[c]	Northop and Anson, 1929
Horse CO-Hb	6.8	>0.8%		6.3		(1.27)		(33.9)[c]	Tiselius and Gross, 1934
Sheep CO-Hb					0.752				Adair and Adair, 1936
Human CO-Hb, 0.1M NaCl	6.5	→0	4.50	6.90		1.17	63000	31.0	Lamm and Polson, 1936; Polson, 1939
Horse, reassociated heme + globin	7.0	0.1%	4.0			1.23	69000		Gralén, 1939
		0.8%		6.3				(33.9)[c]	
Human	7.4	--	5.3	6.7		1.13	76000	(31.9)[m]	Moore and Reiner, 1944
Cattle	7.4	--	5.0	5.8		1.26	85000	(36.8)[m]	
Ox CO-Hb					~0.749[8]				Adair and Adair, 1947
Human CO-Hb	7.0	0.1%	4.35	(6.52)		(1.23)		(32.8)[c]	Kegeles and Gutter, 1951
Human CO-Hb, 0.1M KCl	6.3	0.7%	4.1	6.0		1.3	64500	(35.6)[c]	Gutter, Sober and Peterson, 1956
0.1M KCl + 4M urea	6.6	0.7%	3.1	4.3		1.8	69000	(49.7)[a]	
Horse CO-Hb, 0.1M KCl	6.3	0.7%	4.3	5.9		1.3	69000	(36.2)[c]	
Human proto-Hb	7.2	→0	4.69[2]	6.4[2]		1.2	66800	(33.4)[t]	Rossi-Fanelli, Antonini and Caputo, 1959
Protoporphyrin-globin		→0	4.61[2]	6.5[2]		1.19	69000	(32.9)[t]	

TABLE A-IV(2) continued *(Hemoglobin tetramer)*

Species and Conditions	pH	Conc.	S	D	$\bar{v}$	f/f_o	MW	R_{SE}	Reference
Horse	7.0	→0	4.22	6.02		1.31	67800	(35.5)[d]	Kurihara and Shibata, 1960
	10.0	→0	3.48	5.00		1.58	67300	(42.7)[p]	
Human	6.7	1.%		6.6		(1.21)		(32.4)[c]	Ackers and Steere, 1961
Human A and E	7.0	→0	4.53	(6.79)		(1.18)		31.5	Das Gupta et al., 1963
Human F	6.8	→0	4.74[3]	(7.10)		(1.12)		30.1	Ganguly, Das Gupta and Chatterjea, 1963
Human A and E	6.8	→0	4.56[3]	(6.83)		(1.17)		31.3	
Human	--	1.%		6.60		(1.21)		(32.4)[c]	Polson and Potieter, 1964
Human	7.0	→0	4.5	(6.74)		(1.18)		31.7	Bucci et al., 1965
Recombined β-chains	7.0	→0	~4.6	(6.89)		(1.16)		31.0	
Human A, 0.1M NaCl	--	→0	4.44	(6.65)		(1.20)		32.1	Ganguly and Misra, 1965
Human CO-Hb, undissociated	--	0.4%	4.60	6.8		1.17	65500	31.4	Kawahara, Kirshner and Tanford, 1965
Mouse									
IAA = iodoacetamide									
BALB/cJ + IAA	7.0	1.25%	3.93	(5.89)		(1.37)		(36.3)[c]	Riggs, 1965
BALB/cJ - IAA	7.0	1.25%	4.10	(6.14)		(1.30)		(34.8)[c]	
C3H/HeJ + IAA	7.0	1.25%	4.24	(6.35)		(1.26)		(33.6)[c]	
C3H/HeJ - IAA	7.0	1.25%	3.88	(5.81)		(1.37)		(36.7)[c]	
DBA/2J + IAA	7.0	1.25%	3.93	(5.89)		(1.36)		(36.3)[c]	
DBA/2J - IAA	7.0	1.25%	3.98	(5.96)		(1.34)		(35.8)[c]	
Human oxy-Hb	7.0	>0.015%	4.6[2]	(6.89)		(1.16)		31.0	Schachman and Edelstein, 1966
Human met-Hb, 0.154M NaCl	--	→0	4.59	6.96		1.15	63500	30.7	Behlke, Lampe and Scheler, 1970
met-Hb•N_3	--	→0		7.1		(1.12)	62000	30.1	

TABLE A-IV(2) continued

(Hemoglobin tetramer)

Species and conditions	pH	Concn.	S	D	$\bar{v}$	f/f_o	MW	R_{SE}	Reference
Human deoxy-Hb									
0.09M NaCl	7.0	0.002%	4.81	(7.21)		(1.11)	63800	29.6	Kellett, 1971
2.0 M NaCl	7.0	0.002%	4.68	(7.01)		(1.14)	61300	30.5	
1.0 M NaI	7.0	0.002%	4.82	(7.22)		(1.11)	62000	29.6	
Dimer									
Human CO-Hb, NaCl →0	--	--		9.5		(1.06)		22.5	Lamm and Polson, 1936
Horse globin	7.0	~0.5%	2.57	6.5		1.47	37000	(32.9)[t]	Gralén, 1939
Human, reassociated isolated chains	7.0	→0	~2.8	(8.39)		(1.20)		25.5	Bucci et al., 1965
Human met-Hb, NaCl →0	--	→0		2.97	9.26		1.10	31000[4] 27000	23.1	Behlke, Lampe and Scheler, 1970
Dimer in salts									
Horse, 4M NaCl	7.5	1.0%		8.33		(1.21)		25.6	Polson, 1939
Human oxy-Hb, 4M NaCl	--	--		8.9		(1.13)		24.0	Taylor and Van Osdol, 1964
Bovine met-Hb and human CO-Hb, high salt limit	--	→0	2.8	(8.39)	0.748 0.752	(1.20)		25.5	Kirshner and Tanford, 1964
$CaCl_2$ limiting value	--	0.4%	2.6	(7.79)		(1.29)		27.4	Kawahara, Kirshner and Tanford, 1965
Dimer in acetate									
Horse CO-Hb, 0.1% AC^-	4.4	0.5%	2.9[2]	(8.69)		(1.16)		24.6	Levin, 1963
Human oxy-, deoxy- and met-Hb, 0.25M AC^-	4.6	0.5%	2.7	(8.09)		(1.24)	30600[s]	26.4	Banerjee and Sagaert, 1967

TABLE A-IV(2) continued *(Hemoglobin dimer)*

Species and conditions	pH	Concn.	S	D	$\bar{v}$	f/f_o	MW	R_{SE}	Reference
Human A, 0.1M AC^-	4.3	0.5%	2.8[2]	(8.39)		(1.20)		25.5	Misra and Ganguly, 1968
Dimer in acid or base									
Cattle, fast electrophoretic component	3.0	0.5%	3.6	7.7		1.17	45000	(27.7)[m]	Moore and Reiner, 1944
Human CO-Hb	11.0	→0	2.7	7.4		1.27	34000	(28.9)[p]	Hasserodt and Vinograd, 1959
Human, dodecylsulfate	8.6	2.2%	2.2[2]						
globin + dodecyl-sulfate	8.6	2.2%	2.4[2]						Ingram, 1959.
Horse	11.9	→0	2.01	5.51		1.78	35300	(38.8)[d]	Kurihara and Shibata, 1960
Dimer in amide									
Horse CO-Hb, 4M urea	7.0	0.5%	3.23	7.81		1.20	40000	(27.4)[a]	Steinhardt, 1938
6.4 M Acetamide	7.0	0.5%	3.36	7.68		1.20	42000	(27.8)[a]	
Horse, 10M urea	7.0	--	2.0	(5.99)		(1.68)		(35.6)[a]	
3M guanidine·HCl	7.0	--	2.35	(7.04)		(1.43)		(30.3)[a]	Kurihara and Shibata, 1960
Human CO-Hb, 6.4M urea	--	0.4%	3.27	7.5[5]		(1.03)	33000	[6](22.8)[a]	
8M urea	--	0.4%	2.97	7.1[5]		1.16	28000	[6](20.7)[a]	Kawahara, Kirshner,
1M guanidine·HCl	--	0.4%	3.06	9.5[5]		1.12	34000	[6](24.7)[a]	and Tanford, 1965

TABLE A-IV(2) continued *(Hemoglobin monomer)*

Source and conditions	pH	Concn.	S	D	$\bar{v}$	f/f_o	MW	R_{SE}	Reference
Monomer									
Human α and β chains	7.0	→0	~1.8	(10.79)		(1.18)		19.8	Bucci et al., 1965
Human α chains	6.8	0.04%	1.7	(10.19)		(1.24)	17000	21.0	Huehns and Shooter, 1966
Human oxy-Hb	7.0	→0	1.8	(10.79)		(1.18)		19.8	Schachman and Edelstein, 1966
Human azo-Hb	7.0	0.5%	1.35	6.3		2.0	17000	$(33.9)^t$	Salák, 1970
azo-globin	7.0	0.5%	1.00	5.4		2.3	18000	$(39.6)^t$	
Monomer in acid									
Cattle Hb slow	3.0	--	1.8	11.0		1.16	16000	19.4	Moore and Reiner, 1944
globin slow	3.0	0.25%	1.6	(9.59)		(1.32)		$(22.3)^t$	
globin slow	5.0	0.12%	1.8	(10.79)		(1.18)		$(19.8)^t$	
Horse Hb slow	3.0	0.3%	1.9	(11.39)		(1.11)		18.8	
Human Hb slow	4.0	0.1%	2.0	(11.99)		(1.06)		17.8	
Horse Hb	2.0	0.1%	1.6	(9.59)		(1.32)	*	$(22.3)^m$	Reichmann and Colvin, 1956
globin	2.0	1.0%	1.17	(7.01)		(1.81)	*	$(30.5)^t$	
oxidized globin	2.0	1.0%	1.6	(9.59)		(1.32)	*	$(22.3)^t$	
Monomer in amide									
Horse 6M guanidine·HCl	7.0	--	1.2	(7.19)		(1.76)		$(29.7)^a$	Kurihara and Shibata, 1960
Human CO-Hb 6M guanidine·HCl + 0.1M β-mercaptoethanol	--	0.4%	1.08	(6.47)		1.96	15500	$(33.0)^a$	Kawahara, Kirshner, and Tanford, 1965

TABLE A-IV(2) continued *(Hemoglobin)*

Species and conditions	pH	Concn.	S	D	$\bar{v}$	f/f_o	MW	R_{SE}	Reference
Octamer									
Mouse CO-Hb, BALB/cJ	7.0	1.25%[7]	7.45	(5.58)		(1.14)		38.3	Riggs, 1965
C3H/HeJ	7.0	1.25%[7]	6.83	(5.12)		(1.24)		41.7	
DBA/2J	7.0	1.25%[7]	6.32	(4.74)		(1.34)		45.1	
Higher Aggregates									
Human Azo-Hb	7.0	0.5%	4.26	2.9		2.12	141000	(73.7)[t]	Salák, 1970

References:

[1]Corrected to 20°C with $\eta_{5°}/\eta_{20°} = 1.5114$ (Biochemsches Taschenbuch, 1964); $D_{20,w} = 6.97 \times 10^{-7}$ cm²/sec

[2]Not corrected to water.

[3]Corrected to $S^{o}_{20,w} = 4.44$ in Ganguly and Misra, 1965.

[4]Molecular weight from gel filtration.

[5]At 25°C and in amide concentration listed under conditions.

[6]Stokes-Einstein radius calculated with specific viscosity of amide solution from Handbook of Biochemistry, 2nd Edition, p. J-279 (1970), and viscosity of water at 25°C from Biochemisches Taschenbuch, p. 765 (1964).

[7]Total protein concentration; concentration of octamer was lower.

[8]The effects of protein concentration, salt concentration, buffer, pH, and temperature on the partial specific volume of hemoglobin were determined. Consult reference for exact values under various conditions.

[9]All measurements at 30°C; not corrected to water.

TABLE IV-A(2) References continued

*Molecular Weights: Sources and conditions	Archibald method	Osmotic pressure	Light scattering
Horse Hb	23000 50000	20000	
globin	22000	16000	37000
oxidized globin		21000	41000

TABLE A-IV(3). Stokes-Einstein radii and frictional ratios of fumarase.

Source and conditions	pH	Conc.	S	D	$\bar{v}$	f/f_o	MW	R_{SE}	Reference
Tetramer									
Pig heart	7.34	0.7%	8.51	4.05	(0.75)	1.34	204000[1]	52.8	Cecil and Ogston, 1952
Pig heart	6.7	→0	9.09	(4.34)		(1.28)	220000[2]	49.3	Frieden, Bock, and Alberty, 1954
Pig heart	7.4	→0	9.20	(4.39)		(1.27)	220000[2]	48.7	Johnson and Massey, 1957
Pig heart	7.3	0.34%	8.94	(4.27)		(1.30)		(50.1)[c]	Hill and Kanarek, 1964
treated: native	7.3	0.4%	8.80	(4.20)		(1.32)		(50.9)[c]	
p-chloromercuri-benzoate	7.3	0.4%	8.10	(3.87)		(1.44)		(55.3)[t]	
Hg^{++}	7.3	0.4%	8.80	(4.20)		(1.33)		(50.9)[t]	
Ag^{+}	7.3	0.4%	8.69	(4.15)		(1.34)		(51.5)[t]	
N-ethylmaleimide	7.3	0.4%	8.14	(3.88)		(1.43)		(55.0)[t]	
Iodoacetamide	7.3	0.4%	8.17	(3.90)		(1.43)		(54.8)[t]	
2-Mercaptoethanol	7.3	0.4%	8.13	(3.88)		(1.43)		(55.1)[t]	
Mercaptoglycerol	7.3	0.4%	8.12	(3.87)		(1.43)		(55.1)[t]	
Pig heart					0.738				Kanarek and Hill, 1964
Pig heart	7.3	0.3%					194000		Kanarek, Marler, Bradshaw, Fellows, and Hill, 1964
Pig heart	7.3	→0	9.26	(4.42)		(1.26)		48.3	Teipel and Hill, 1971
Dimer									
Pig heart, 0.1M NH_4SCN									
96 hr at pH	7.4	→0	5.9[3]	(5.63)		(1.24)		(37.9)[t]	Johnson and Massey, 1957
1 hr at pH	6.3	→0	5.2[3]	(4.96)		(1.41)		(43.1)[t]	

TABLE A-IV(3) continued *(Fumarase)*

Source and conditions	pH	Conc.	S	D	$\bar{v}$	f/f_o	MW	R_{SE}	Reference
Pig heart, treated:									
Iodoacetate	7.3	0.4%	5.10	(4.87)		(1.44)		(43.9)[t]	Hill and Kanarek, 1964
Ethyleneimine	7.3	0.4%	4.97	(4.74)		(1.48)		(45.0)[t]	
Cystine	7.3	0.4%	4.60	(4.39)		(1.60)		(48.7)[t]	
2-Mercaptoethylamine	7.3	0.4%	5.05	(4.82)		(1.45)		(44.3)[t]	
Mercaptosuccinate	7.3	0.4%	5.56	(5.31)		(1.32)		(40.3)[t]	
Thioglycolate	7.3	0.4%	5.2	(4.96)		(1.41)		(43.1)[t]	
Pig heart									
0.5M guanidine·HCl	7.4	0.35%	~6.5	(6.20)		(1.13)		34.4	Teipel and Hill, 1971
Monomer									
Pig heart, EDTA + mercaptoethanol (not homogeneous, S_{20})	2.6 2.9	0.17%	2.6	(4.96)		(1.78)		(43.1)[p]	Deal, Rutter, Massey, and Van Holde, 1963
Pig heart, 3M urea	7.3	0.34%	1.46	(2.79)		(3.17)		(76.7)[a]	Hill and Kanarek, 1964
Cystine + 3M urea	7.3	0.4%	1.93	(3.68)		(2.40)		(58.0)[a]	
Pig heart									
6M guanidine·HCl	4.5	0.006%			0.72		48500		Kanarek, Marler, Bradshaw, Fellows, and Hill, 1964
Pig heart, AC^-	< 6. >10.	0.6%	<2.5	--		--		--	Teipel and Hill, 1971
1.5M guanidine·HCl	7.4	0.35%	~1.6	(3.05)		(2.89)		(70.0)[a]	

References:

[1] If $\bar{v} = 0.738$ is used with Cecil and Ogston's (1952) S and D values determined at 7 mg/ml fumarase, the calculated molecular weight = 197000 (Hill and Bradshaw, 1969).

[2] Molecular weight calculated with diffusion coefficient of Cecil and Ogston (1952).

[3] Not corrected to water.

TABLE A-IV(4). Stokes-Einstein radii and frictional ratios of catalase.

Source and conditions	pH	Conc.	S	D	$\bar{v}$	f/f_o	MW	R_{SE}	Reference
Catalase									
Horse liver	--	--	11.2[1]	4.3[1]	0.715	1.25	225000	49.7	Agner, 1938
Bovine liver	7-9	--	11.3[1]		0.73	1.25	248000	52.1	Sumner and Gralén, 1938
	--	1.%		4.1[1]					
Horse and beef liver	--	--		4.5		(1.17)		47.5	Sumner, Dounce, and Frampton, 1940
Human RBC in 0.2M NaCl	--	0.5%	11.2	(4.33)		(1.21)		49.3	Cecil and Ogston, 1948
Horse RBC	--	0.6%	11.64	4.11 4.19	0.74	1.17	269000[2]	51.5	Deutsch, 1952
Rat liver		→0	11.8	(4.56)		(1.15)		46.8	Deutsch, 1952
	5.7	0.8%	10.6	(4.10)		(1.28)		52.1	Price and Greenfield, 1954
Bovine liver, major component	--	--	11.0	(4.25)		(1.24)		50.2	Nakatani, 1958
Bovine liver	7.0	→0	11.2	4.1		5.0[6]	248000	52.1	Samejima, 1959
Bovine liver	7.0	→0	11.15	4.1		1.26	244000	52.1	Samejima, Kamata, and Shibata, 1962
Bovine liver, native	7.0	→0	11.40	(4.41)		(1.19)	240000	48.5	Samejima and Yang, 1963
reassociated and crystallized	7.0	→0	11.58	(4.48)		(1.17)	250000	47.7	
Human liver	5.7	0.8%	12.5	(4.83)		(1.09)		44.2	Nishimura, Carson, and Kobara, 1964

TABLE A-IV(4) continued *(Catalase)*

Source and conditions	pH	Conc.	S	D	$\bar{v}$	f/f_o	MW	R_{SE}	Reference
Human RBC	5.7	0.6%	11.3	(4.37)		(1.20)			
Human RBC	7.0	→0	11.1	4.4	0.73	1.17	240000	48.6	Shpitsberg, 1965
Human RBC	6.0	0.5%	11.3	4.52	0.724	1.19	222000[3]	47.3	Stansell and Deutsch, 1965
Human RBC, 0.1M AC^-	--	--	11.8	(4.56)		(1.15)	251000	46.8	Shpitsberg, 1966
Bovine liver, 0.1M AC^-	--	--	11.8				246000		
Bovine liver	7.6	→0	11.29	4.17		1.24	243000	51.2	Sund, Weber, and Mölberg, 1967
Bovine liver, native	--	→0	11.4	(4.41)	0.730	(1.19)	240000	48.5	Samejima, McCabe, and Yang, 1968
reconstituted	--	→0	11.4						
Catalase/2									
Rat liver	5.7	0.8%	6.4	(4.95)		(1.34)		43.2	Price and Greenfield, 1954
Bovine liver, minor component	--	--	8.9[4]	(6.88)		(0.96)		31.0	Nakatani, 1958
Bovine liver, native	3.0	→0	4.25	3.3		2.00	116000	(64.7)[p]	Samejima and Shibata,
7M urea	7.0	→0	6.20	3.7		1.63	151000	(57.7)[a]	1961
Bovine liver	3.0	→0	4.25	3.28		2.01	117000	(65.1)[p]	Samejima, Kamata, and
	2.5	→0	3.22	2.13		2.92	136500	(100.3)[p]	Shibata, 1962
Bovine liver	3.0	→0	4.50	(3.48)		(1.90)	120000	(61.4)[p]	Samejima and Yang, 1963
Human liver	5.7	0.8%	7.9[4]	(6.11)		(1.08)		35.0	Nishimura, Carson, and Kobara, 1964

TABLE A-IV(4) continued *(Catalase)*

Source and conditions	pH	Conc.	S	D	$\bar{v}$	f/f_o	MW	R_{SE}	Reference
Human RBC, 0.7M urea	3.0	0.6%	5.1	(3.94)		(1.68)	118000	(54.2)^p	Shpitsberg, 1966
8M then 4M urea	7.1	0.2%	5.6	(4.33)		(1.53)	122000	(49.3)^a	
Bovine liver, 8M urea	7.5	→0	3.6	2.3		2.70	128000 141000	(92.9)^a	Hiraga, Abe and Anan, 1967
8M urea oxidized with HCO_3H in HCO_2H + 8M urea	2.7	→0	3.0	(2.32)		(2.85)		(92.1)^a	
	7.5	→0	3.5	2.3		2.73	118000 137000	(92.9)^t	
Bovine liver, 8M urea	--	→0	3.3	2.23		2.83	133000	(95.8)^a	Sund, Weber, and
5M guanidine·HCl	7.6	→0	3.50	2.17		2.83	140000	(98.5)^a	Mölbert, 1967
Catalase/4									
Bovine liver	12.0	→0	3.1	3.3		26.0[5]	85000	(64.7)^p	Samejima, 1959
Bovine liver	12.0	--	3.10	3.3		2.23	84000	(64.7)^p	Samejima and Shibata, 1961
Bovine liver, succinylated	7.6	→0	3.2	4.4		1.82	65000	(48.6)^t	Weber and Sund, 1965
Human RBC	11.5	0.4%	3.1	(4.79)		(1.74)	63000	(44.6)^p	Shpitsberg, 1966
Bovine liver	11.5	0.4%	3.1				61800		
+ Na dodecylsulfate + 0.1M AC^-	5.6	0.3%	4.4	--		--	61500	--	
Bovine liver, 6 hr							67000		
at succinylated,	12.6	→0	2.89	(4.47)		1.90	54000	(47.8)^p	Sund, Weber, and
HCO_2H	7.6	→0	3.22	4.43		1.81	65000	(48.2)^t	Mölbert, 1967
HCOOH, then Na dodecylsulfate	7.6	→0	3.8	5.1		1.56	60000	(41.9)^t	
β-mercaptoethanol + 5M guanidine·HCl	7.6	→0	2.10	3.20		2.59	59000	(66.8)^a	

TABLE A-IV(4) continued *(Catalase)*

Source and conditions	pH	Conc.	S	D	$\bar{v}$	f/f_o	MW	R_{SE}	Reference
Bovine liver	12.0	→0	2.85	(4.41)	0.720	(1.89)	60000 65000	(48.5)[p]	Samejima, McCabe, and Yang, 1968
Catalase — possible subunits smaller than catalase/4									
Bovine liver	9.9 2.8	1.% --	1.2 1.6						Sumner and Gralén, 1938
Bovine liver, 13M formamide	7.0	→0	2.13	4.6		2.02	42000	46.4	Samejima and Shibata, 1961
Bovine liver, 6M urea + NaCl	--	--	2.1						Saha, Campbell, and Schroeder, 1964
Bovine liver, performic acid oxidized in 8M urea	2.7	→0	2.1	6.5		1.62	25000 25400 29000	32.9	Hiraga, Abe, and Anan, 1967
Bovine liver, major component after 60 hr at pH	12.5-12.8	0.4%	1.7						Sund, Weber, and Mölbert, 1967

References:

[1] Not corrected to water.

[2] Additional molecular weights: Fe content, 233000; hemin content, 250000.

[3] Molecular weight from hemin content = 228000.

[4] If treated as tetramer: S, 7.9 and 8.9; D, (3.05) and (3.44); f/f_o, (1.72) and (1.53), and R_{SE}, 70.0 and 62.1

[5] Frictional ratio calculated from S and D is 2.2.

[6] Frictional ratio calculated from S and D is 1.26.

determined for each protein size unit but rather a large range of values have been observed.

The calculated Stokes-Einstein radius and frictional ratio are not independent as can be seen by combining Eqs. (A-2) and (A-5) to obtain

$$R_{SE} = \left(\frac{3M\bar{v}}{4\pi N}\right)^{1/3} \frac{f}{f_o} \qquad \text{(A-11)}$$

Because the M and $\bar{v}$ values used for each size unit were the same for all data in which only S or D was determined, if R_{SE} is plotted against f/f_o, these points will all fall on the same line. Data calculated from measurements of both S and D may not fall on this line. Figure A-1 presents the data of Table A-IV as calculated R_{SE} versus f/f_o for each protein size unit and indicates by symbol the conditions of measurement. It is evident that high protein concentrations, extremes of pH, amides, and modification of the protein tend to give large R_{SE} and f/f_o values. Measurements in salt solutions at neutral pH tend to give low R_{SE} and f/f_o values. The increased R_{SE} and f/f_o at high protein concentration is due, in part, to the nonideal behavior of the solution and is an artifact of the simplified calculations employed. Amines and extremes of pH have been shown to modify the native protein configuration as evidenced by a reduction of the α-helix content (Samejima and Kita, 1969; Tanford, 1968). Thus, the nonphysiological conditions employed to dissociate proteins tend to increase R_{SE} and f/f_o above the values for the physiologically compact molecule. There is, however, significant scatter of the data under what can be considered physiological conditions. The extent to which this scatter depends on the species from which the protein was isolated, the method of isolation, and experimental error has not been studied. Thus,

Figure A-1. Stokes-Einstein radius versus frictional ratio for (a) adenylate kinase, (b) hemoglobin, (c) fumarase, and (d) catalase. The data of Table A-IV have been plotted according to the conditions of measurement. Data in which the molecular weight did not correspond to an exacted size unit and data with probable equipment errors were omitted. The lines represent $R_{SE} = (3M\bar{v}/4\pi N)^{1/3} (f/f_o)$ with M and $\bar{v}$ as listed in Table A-III. Arrows indicate the size unit of the protein when the data do not fall near the line calculated for that size. Conditions of measurement are indicated by the following symbols:

×	in water or salt solution at neutral pH and low protein concentration
□	in amide solution
◇	at high or low pH
+	high protein concentration
⊠	treated, modified or reacted protein
*	data omitted when computing average R_{SE} and f/f_o (see Table A-V)

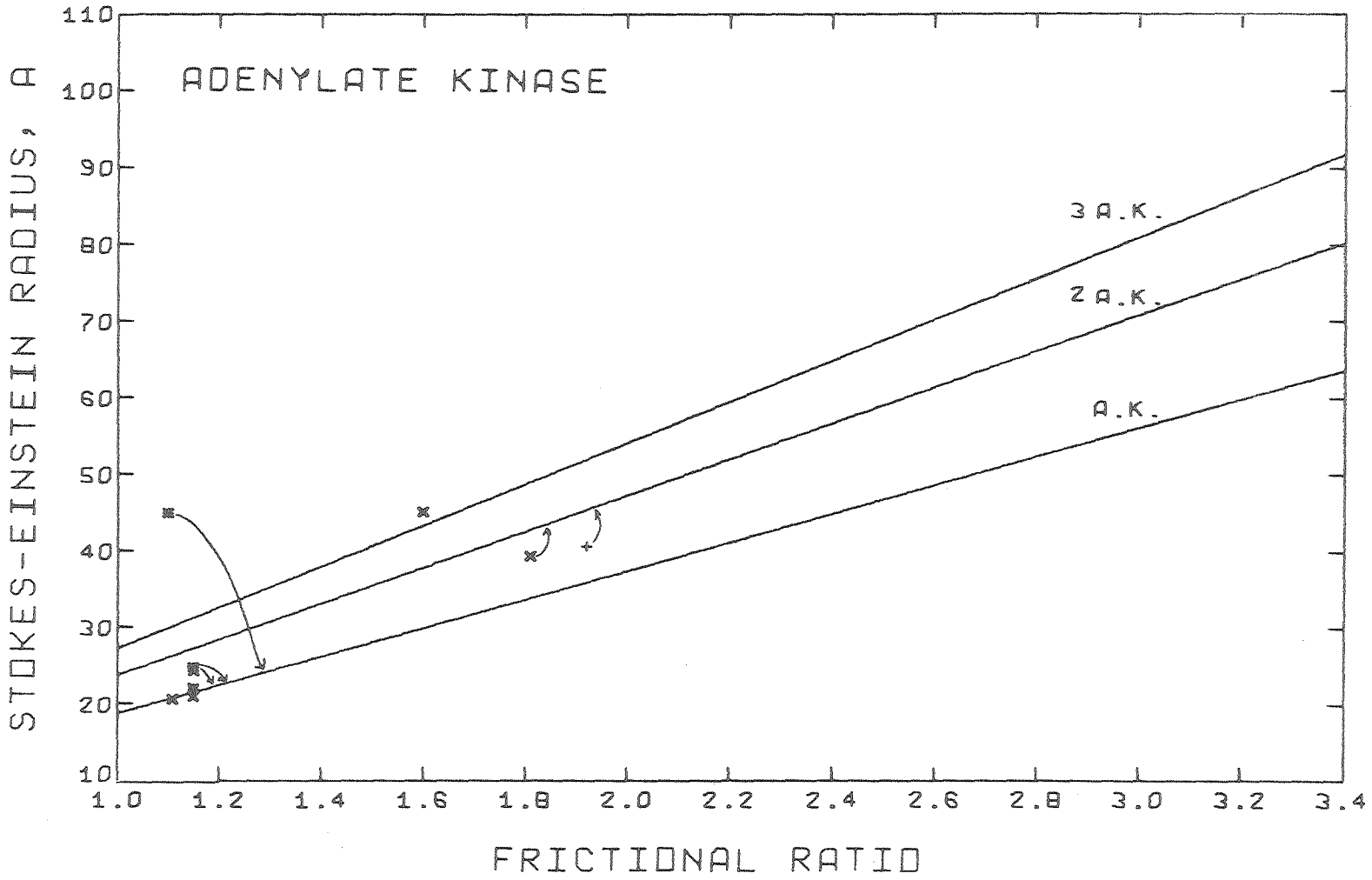

XBL 772-7671

Figure A-1a

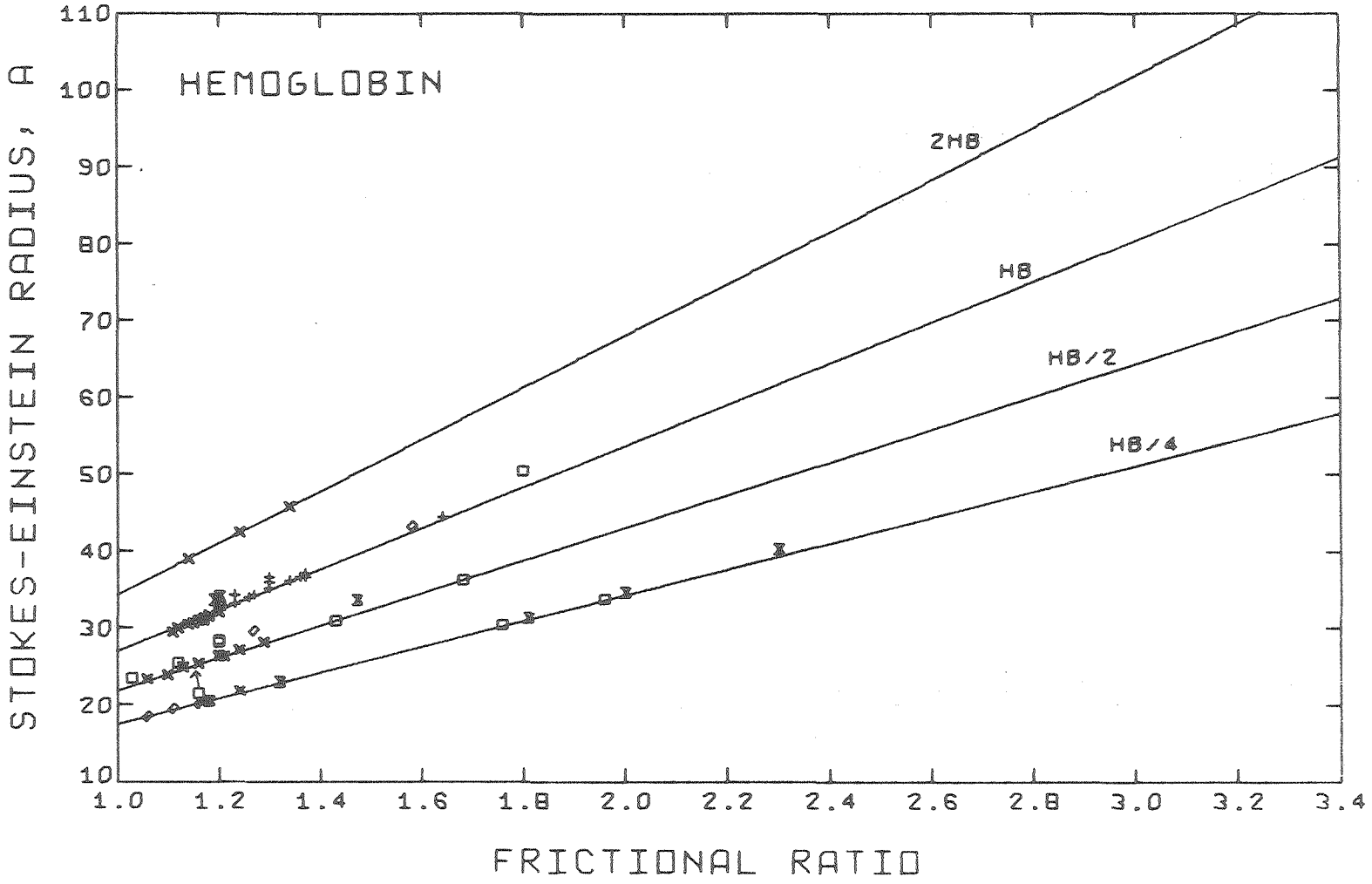

XBL 772-7672

Figure A-1b

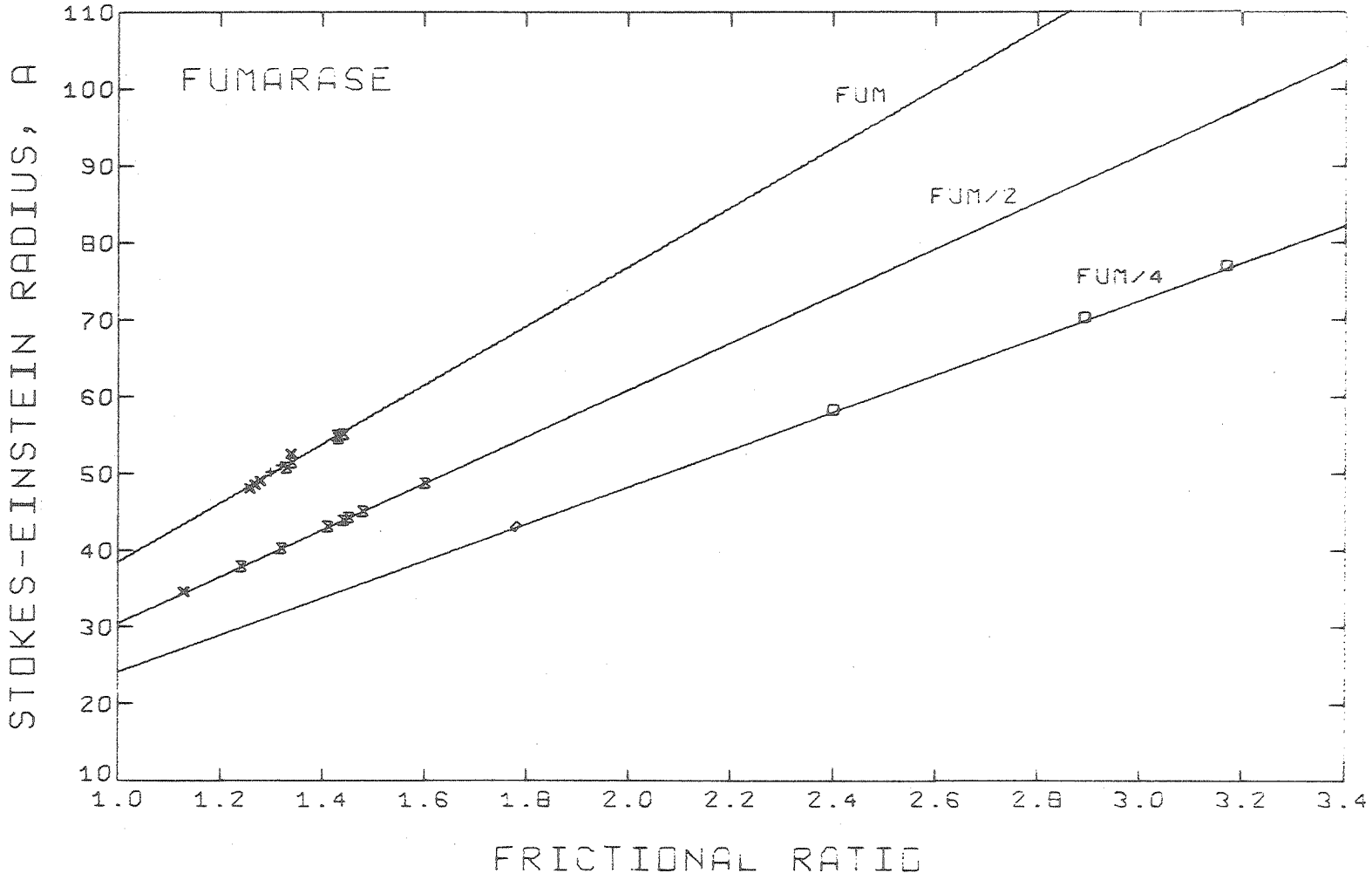

XBL 772-7673

Figure A-1c

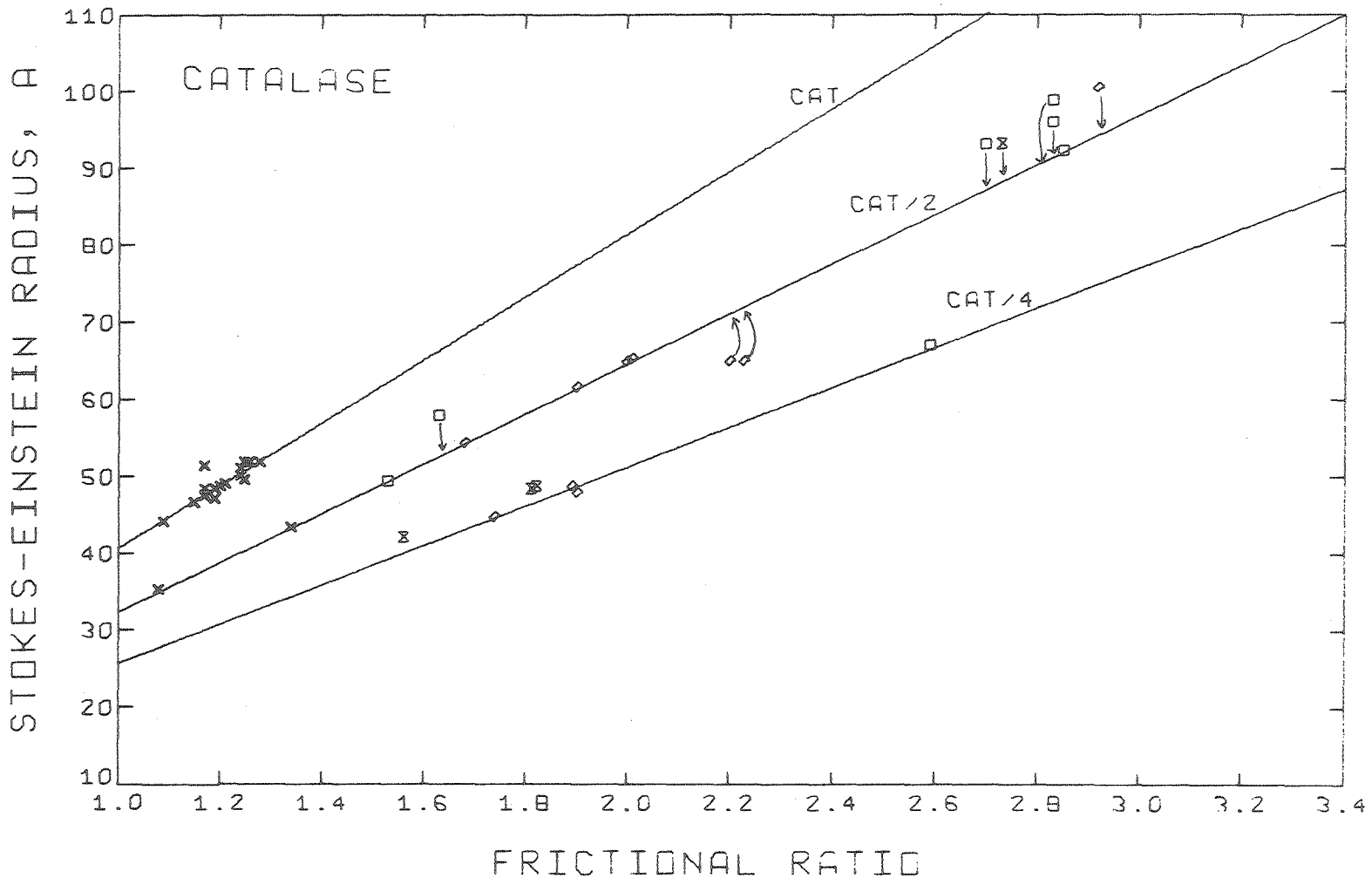

Figure A-1d

XBL 772-7674

if these data are used to select an R_{SE} and an f/f_o to represent the compact physiological molecule, an arbitrary decision must be made regarding the use of the available data. It was decided to eliminate data obtained under conditions that tend to give large values of R_{SE} and f/f_o and to average all of the remaining data. This procedure underweights data extrapolated to zero protein concentration in comparison with data obtained at a single protein concentration but gives equal weight to each reported determination, tending to reduce the effects of instrumental calibration errors. More specifically, data obtained in the presence of amines, at extremes of pH, or on treated, modified or reacted proteins have been omitted in calculating the average R_{SE} and f/f_o. If the molecular weight calculated from S and D does not correspond to an expected molecular weight for that protein or if an equipment calibration error was probable, the data were omitted from the averages. Additionally, if it is evident that S and/or D is markedly concentration-dependent, data at higher concentrations are omitted. Specific comments and exceptions are noted with the averages in Table A-V.

The quality of the R_{SE} and f/f_o estimates in Table A-V varies with the availability of data. The estimates for the hemoglobin tetramer probably correspond closely to the hydrated molecule in solution. The estimates for the hemoglobin octamer, however, were obtained at a high total protein concentration from highly scattered data based on S measurements only, and the fumarase dimer estimates were based on a single S determination at modestly high protein concentrations in dilute amide solution. The adenylate kinase dimer and trimer appear to correspond partially to unfolded proteins. Thus, the R_{SE} and f/f_o listed in Table A-V are tentative and should be considered as upper limits to the physio-

TABLE A-V. Average Stokes-Einstein radii and frictional ratios.[a]

Protein	Size	R_{SE}[b]	f/f_o[b]	N[c]	Data Averaged and Comments[d]
Adenylate kinase	monomer	22.1 ± 2.0	1.14 ± 0.02	3	Data of Thuma, Schirmer, and Schirmer (1972) not used because it used the data of Noda and Kuby (1957b) as standard. Data of Criss, Sapico, and Litwack (1970) not used because its Stokes-Einstein radius is about twice the value of that of all other monomer data.
	dimer	38.7 --	1.81 --	1	One determination: S and D extrapolated to 0 protein.
	trimer	44.5 --	1.6 --	1	One determination: S and D extrapolated to 0 protein.
Hemoglobin	tetramer	30.8 ± 0.8	1.15 ± 0.03	14	Data eliminated at protein concentration $\geqslant$ 0.5% for S and D data and for D only data and at concentrations $\geqslant$ 0.1% for S only data. The relative abundance of hemoglobin tetramer data provides a better estimate of R_{SE} and f/f_o than for other proteins or other size units of hemoglobin.
	dimer	25.0 ± 1.4	1.18 ± 0.07	10	Data averaged include dimers in acetate.
	monomer	19.4 ± 1.1	1.16 ± 0.06	6	Data averaged include dimers in acid.
	octamer	41.7 ± 3.4	1.24 ± 0.10	3	All measurements at 1.25% total protein: S only.
Fumarase	tetramer	49.8 ± 3.4	1.29 ± 0.04	4	Data eliminated at concentrations $\geqslant$ 0.1% protein for S only data.
	dimer	34.4 --	1.13 --	1	One determination in 0.5M guanidine·HCl at 0.35% protein: S only.
	monomer	-- --	-- --		

TABLE A-V (continued)

Protein	Size	R_{SE} [b]	f/f_o [b]	N [c]	Data Averaged and Comments [d]
Catalase	Cat/1	49.2 ± 2.2	1.20 ± 0.05	19	Average all data.
	Cat/2	36.4 ± 6.2	1.13 ± 0.14	3	
	Cat/4	-- --	-- --		
	Cat/x, x > 4	-- --	-- --		

References:

[a] Tabulated Stokes-Einstein radii and frictional ratios were averaged from the remaining data of Table A-IV after data that tended to produce large R_{SE} and f/f_o were arbitrarily eliminated as described in the text. In cases where poor data exist, the tabulated values should be considered as upper limits to the physiological R_{SE} and f/f_o.

[b] Plus or minus standard deviation of data averaged. Deviations from physiological R_{SE} and f/f_o may be caused by isolation procedures and methods used to dissociate proteins.

[c] Number of determinations averaged.

[d] Data obtained in amide solutions, at extremes of pH, or on treated, modified or reacted proteins; data that yields a molecular weight that does not correspond to an expected size unit for the protein, and data that is questioned because of equipment calibration have been eliminated from the average R_{SE} and f/f_o unless specifically noted.

logical R_{SE} and f/f_o in cases where insufficient data are available.

The Stokes-Einstein radii of the compact proteins for which sedimentation and/or diffusion data are not available can be estimated through a consideration of the Stokes-Einstein radius as a function of the molecular weight and hydration of the protein. Such a consideration will also indicate that the Stokes-Einstein radii of the adenylate kinase dimer and trimer listed in Tables A-IV and A-V are unexpectedly large.

The Stokes-Einstein radius of a spherical hydration complex containing w grams of water per gram of protein, in analogy with Eq. (A-3) for the spherical anhydrous molecule, is

$$R_{SE} = \left(\frac{3M(\bar{v} + w\bar{v}_w)}{4\pi N} \right)^{1/3} \qquad \text{(A-12)}$$

where $\bar{v}_w$ is the partial specific volume of water.

It was previously demonstrated that the measured f/f_o for globular proteins is rather insensitive to the shape of the molecule but quite sensitive to the hydration of the molecule. Thus, f/f_o can be used to estimate the hydration w. If it is assumed that the deviation of f/f_o from unity is entirely due to hydration, that is, the molecules are spherical so that asymmetry does not contribute to f/f_o, the hydrations listed in Table A-VI can be obtained from the average f/f_o data of Table A-V and the contribution of hydration to f/f_o given in Table A-I. With the exception of the adenylate kinase dimer and trimer, the hydration of monomers and dimers is near 0.4 grams water per gram protein; this value for tetramers varies from 0.39 for the hemoglobin tetramer to 0.84 for the fumarase tetramer; and the value for the single octamer is 0.68. Thus, there appears to be a trend for the hydration value to be near 0.4 for

one to two polypeptide chains and to be higher for four to eight polypeptide chains. Such a variation hydration with the number of polypeptide chains is plausible from electron microscope and x-ray diffraction studies of hemoglobin and catalase tetramers that indicate central aqueous regions within the molecule between the polypeptide chains.

Because R_{SE} for the hydration complex is dependent on the cube root of $(\bar{v} + w\bar{v}_w)$, it is not highly sensitive to the exact value of $\bar{v}$. The values of $\bar{v}$ assumed for calculations for the proteins employed in this study vary between 0.73 and 0.749 (Table A-III). A partial specific volume of 0.74 will be used to predict the dependence of R_{SE} on the molecular weight and hydration. The average R_{SE} from Table A-V are plotted against the molecular weight assigned to the subunit, molecular or aggregate from Table A-III in Fig. A-2. It is evident that the adenylate kinase dimer and trimer deviate from the other data. The predicted variation of R_{SE} with molecular weight for hydrations of 0.0, 0.4 and 0.7 grams water per gram protein are indicated. The data for the lower number of polypeptide chains are seen to fall on or near the theoretical line for 0.4 gram water per gram protein, and the data for larger numbers of polypeptide chains tend to fall near the line for 0.7 gram water per gram protein.

Three pertinent conclusions can be drawn from these observations. First, the data for the adenylate kinase dimer and trimer either are in error or correspond to a protein that is in some way different from the other proteins used. Such a difference might be due to differences between soluble and membrane-bound adenylate kinase. In rat liver, however, adenylate kinase III is localized in the outer compartments of mitochondria and is thus presumably membrane-bound whereas adenylate kinase II is found

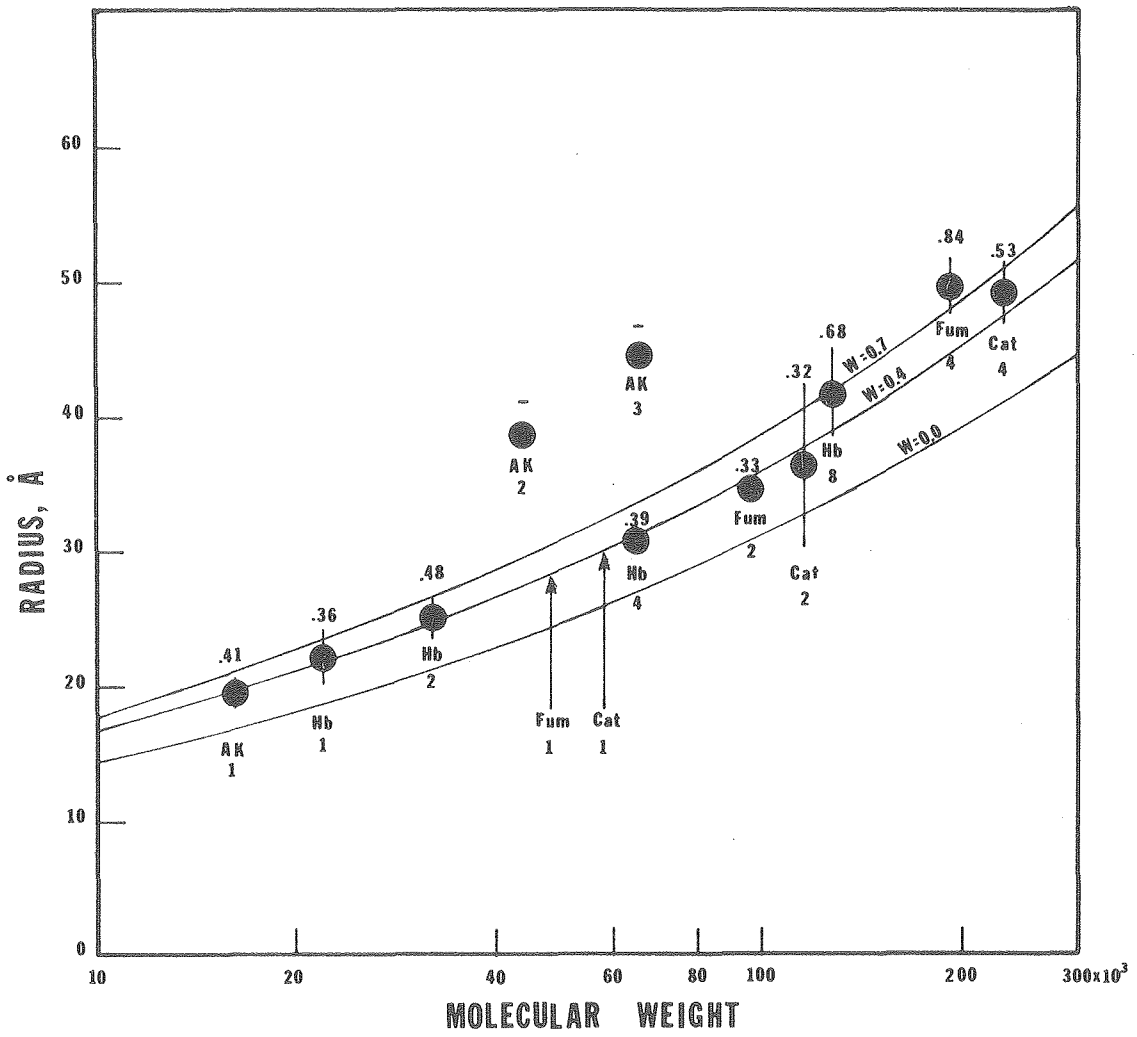

Figure A-2. Stokes-Einstein radius of proteins versus molecular weight. The hydration estimated by assuming that deviation of f/f_o from 1.00 is entirely due to hydration is indicated above each data point. The number of polypeptide chains comprising the protein unit is indicated below each data point. Catalase of molecular weight 232,400 has been assumed to be a tetramer for the purposes of this figure. Error bars indicate the standard deviation of the data averaged to obtain the Stokes-Einstein radius (single data source for AK 2, AK3, and Fum 2; error bar smaller than dot for Hb 4). The significance of the standard deviations is discussed in the text. Theoretical lines were calculated for hydrations of 0.0, 0.4 and 0.7 gram water per gram protein and partial specific volume of 0.74.

primarily in the cytosol (Criss, 1970). Because the size estimates for the dimer and trimer were obtained from isozymes II and III, respectively, it is doubtful that the solubility of the enzyme is responsible for the differences between these proteins and the other proteins indicated in Fig. A-2. The monomer of isozyme III had a Stokes-Einstein radius about twice that of the other monomer data (Table A-IV). Purification of the isozymes by isoelectric focusing in the presence of ampholytes is likely to have caused the increased R_{SE} and f/f_o observed (Table A-IV).

The second conclusion is that the agreement between the hydration values calculated from f/f_o assuming that only hydration contributed to f/f_o and the hydration values that provided a good fit of R_{SE} to the molecular-weight data substantiates the assumption that f/f_o primarily reflects molecular hydration and is relatively insensitive to molecular asymmetry for the proteins used in this study.

The third conclusion is that the Stokes-Einstein radius of a subunit or molecule consisting of a few polypeptide chains can be estimated from its molecular weight if it is assumed that the unit is spherical and has 0.4 gram water of hydration per gram of protein. The radii obtained for the hypothetical Cat/8 and Cat/12 (see Appendix B) are 20.6 and 23.6Å, respectively; values of 28.0 and 29.7Å were obtained for Fum/4 and Cat/4, respectively; and 27.1 and 31.0Å are the values obtained for the compact adenylate kinase dimer and trimer, respectively, when a partial specific volume of 0.74 is assumed.

The estimates of the Stokes-Einstein radii of the subunits, molecules and aggregates used in the text are listed in Table A-VI. It must again be stressed that arbitrary decisions have been made regarding the use of

the available data and that the extrapolations based on assumed shape and hydration have not been proven.

TABLE A-VI. Hydration estimated from f/f_o and the Stokes-Einstein radius to be used in the text.

Protein	Size	Molecular weight[a] (M)	Partial specific volume[a] ($\bar{v}$)	Stokes-Einstein radius[b] (R_{SE})	Frictional ratio[b] (f/f_o)	Hydration[c] (from f/f_o) (w)	Stokes-Einstein radius to be used in text (R_{SE})
Adenylate kinase	monomer	22028	0.74	22.1	1.14	0.36	22.1
	dimer	44056		38.7	1.81	--	27.1[d]
	trimer	66084		44.5	1.6	--	31.1[d]
	tetramer	88112		--	--	--	34.2[d,f]
Hemoglobin	monomer	16115	0.749	19.4	1.16	0.41	19.4
	dimer	32230		25.0	1.18	0.48	25.0
	tetramer	64459		30.8	1.15	0.39	30.8
	octamer	128918		41.7	1.24	0.68	41.7
Fumarase	monomer	48500	0.738	--	--	--	28.0[d]
	dimer	97000		34.4	1.13	0.33	34.4
	tetramer	194000		49.8	1.29	0.84	49.8
Catalase	Cat/12	19200-19800	0.73	--	--	--	20.6[d,e]
	Cat/8	28800-29400		--	--	--	23.6[d,e]
	Cat/4	58100		--	--	--	29.7[d]
	Cat/2	116200		36.4	1.13	0.32	36.4
	Cat/1	232400		49.2	1.20	0.53	49.2

References:

[a] From Table A-III.

[b] From Table A-V.

[c] Deviation of f/f_o from 1.00 assumed to be entirely due to hydration; values taken from Table A-I.

[d] Estimated from assumed molecular weight, hydration of 0.4 gram water per gram protein, and partial specific volume of 0.74.

[e] Hypothetical subunit; see Appendix B.

[f] Stokes-Einstein radii for larger aggregates of adenylate kinase have not been estimated because of uncertainties concerning stable configurations and hydration.

APPENDIX B

THE SIZE OF THE CATALASE MONOMER

The molecular weight of the intact catalase molecule as determined by sedimentation-diffusion is generally between 240,000 and 250,000 (Table A-IV); it was determined to be 232,400 by preliminary amino acid sequencing (Schroeder et al., 1969) and 256,000 by sedimentation-equilibrium (Bonaventura, Schroeder and Fang, 1972) although 232,400 was used in the calculations by these authors.

Schroeder et al. could find no evidence for subunits smaller than Cat/4. Subunits smaller than Cat/4 have been observed by sedimentation-diffusion (Table A-IV(4)). Hiraga, Abe, and Anan (1967) found that catalase oxidized with performic acid to open S-S bonds and suspended in 8M urea at pH 2.7 had a molecular weight of 29,000, 25,400, or 25,000 when determined by sedimentation-diffusion, viscosity-sedimentation, or sedimentation-equilibrium, respectively.

Because catalase has four heme groups, the molecular weight of subunits smaller than Cat/4 depends on the fate of the heme groups after dissociation. If it is assumed that all forms of Cat have the same molecular weight and subunit composition (Aebi, Moerikofer-Zwez and Vaon Wartburg, 1972), that all polypeptide chains are of equal weight, and that all Cat/4 subunits dissociate in the same manner, the molecular weights listed in Table B-I can be hypothesized for the catalase monomer. The sedimentation-diffusion molecular weight of 29,000 determined by Hiraga, Abe and Anan (1967) agrees well with the hypothesized molecular weight of Cat/8 based on the molecular weight of catalase estimated by

TABLE B-I. Molecular weights of possible catalase monomers.

Assumed molecular weight of intact catalase	250,000[a]	232,400[b]
Assumed molecular weight of Cat/4	62,500	58,100
Assumed molecular weight of apo-Cat/4	61,900	57,500
Predicted molecular weight of Cat/8	31,000	28,800
Predicted molecular weight of Cat/8 + heme	31,600	29,400
Predicted molecular weight of Cat/12	20,600	19,200
Predicted molecular weight of Cat/12 + heme	21,200	19,800

References:

[a] A high estimate of the molecular weight of catalase from sedimentation-diffusion; see Table A-IV.

[b] Estimate of the molecular weight of catalase from the preliminary amino acid sequence of Schroeder et al. (1969); this estimate is lower than the molecular weights generally determined by sedimentation-diffusion.

Schroeder et al. The molecular weight estimated by viscosity-sedimentation and sedimentation-equilibrium, however, are intermediate between the hypothesized molecular weights of Cat/8 and Cat/12.

Possible Stokes-Einstein radii and frictional ratios for subunits smaller than Cat/4 have been calculated from the sedimentation coefficients of Table A-IV and are tabulated in Table B-II. The values of f/f_o for Cat/8 and Cat/12 are reasonable although the Cat/8 value is more probable because the f/f_o value of 1.23 for Cat/12 is lower than would be expected for a protein in concentrated amide solution (See Table A-IV).

Hall (1950) and Valentine (1964) reported observing catalase subunits smaller than Cat/4 by electron microscopy. These observations do not appear to be reproducible and will not be discussed here.

If catalase does dissociate further than Cat/4, the smaller subunits appear to be tightly bound together, most likely by S-S bridges. Thus, if catalase dissociates into Cat/8, it would be expected that at least one S-S bond per Cat/4 would be required to bind the monomers into a Cat/4 subunit; dissociation into Cat/12 would require two S-S bonds per Cat/4.

The total number of S groups determined for the catalase molecule is tabulated from literature sources in Table B-III. The early data of Bonnichsen (1947) are subject to larger methodological error than more recent data. The number of S-residues in the preliminary amino acid sequence given by Schroeder et al. (1969) would appear to be low. Aebi, Moerikofer-Zwez and Vaon Wartburg (1972) isolated two forms of catalase from both human and horse RBC's and found 14- and 16-SH groups in type A catalase and 4- and 6-SH groups in type C catalase, respectively. These

TABLE B-II. Frictional ratios and Stokes-Einstein radii calculated from sedimentation-coefficients for possible catalase subunits smaller than Catalase/4.

Source and Conditions	pH	Conc.	S	Assumed Subunits per Catalase — Calculated f/f_o and R_{SE}[a] — 4		8		12		Reference
Bovine liver in 5% NaCl	9.9	1.%	1.2	4.49	115.1	2.83	57.6	2.16	38.4	Sumner and Gralén, 1938
	2.8	--	1.6	3.37	86.3	2.12	43.2	1.62	28.8	
Bovine liver, 13M formamide	7.0	→0	2.13	2.53	64.9	1.60	32.4	1.22	21.6	Samejima and Shibata, 1961[b]
Bovine liver, 6M urea	--	--	2.1	2.57	65.8	1.62	32.9	1.23	21.9	Saha, Campbell, and Schroeder, 1964
Bovine liver, performic acid oxidized in 8M urea	2.7	→0	2.1	2.57	65.8	1.62	32.9	1.23	21.9	Hiraga, Abe, and Anan, 1967[b]
Bovine liver, major component after 60 hrs at pH	12.6	0.4%	1.7	3.17	81.3	2.00	40.6	1.53	27.1	Sund, Weber, and Mölbert, 1967

References:

[a]The molecular weight of catalase was taken as 232,400, and the partial specific volume was taken as 0.73 for the purposes of calculation; see Table A-IV for method of calculation.

[b]Compare with Stokes-Einstein radius determined from diffusion coefficient (Table A-IV).

TABLE B-III. Total number of S groups per catalase.

Total Number of S Groups per grams Catalase[a]		
250,000	232,400	Reference
38 34	36 32	Bonnichsen, 1947
22	21	Schnuchel, 1956
29	27	Schroeder et al., 1962
20	18	Higashi and Shibata, 1964
20-25	19-23	Hermel and Havemann, 1966
(17)[b]	16[b]	Schroeder et al., 1969

References:

[a]The number of S groups per catalase were converted from the molecular weights used by the authors to the tabulated molecular weights of 250,000 and 232,400.

[b]Four S groups are indicated in the preliminary amino acid sequence of Cat/4. The molecular weight for intact catalase obtained from this sequence, plus heme, is 232,400.

low values support the data of Schroeder et al. (1969) and suggest that attempts to treat the catalase of red cells as a single entity might produce erroneous results. The enzymatic activity of catalase depends on the number of free -SH groups (Hermel and Havemann, 1966). Alterations in the number of free -SH groups might account for the range of R_{SE} and f/f_o observed for the Cat/1 data in Table A-IV. The maximum number of tetratable -SH groups observed in 8M guanidine·HCl is 10.26 per 225,000g of catalase (Schütte and Nürnberger, 1959), which converts to 11 per 232,400 or 250,000g of catalase. If it is assumed that the remaining S groups could form S-S bridges, some or all of which join catalase monomers to form the Cat/4 subunits, the maximum number of such bridges is likely to be one per Cat/4 subunit, although two bridges would be permitted by the higher total S residue data (Table B-IV). Thus, if the data of Bonnichsen (1947) is omitted, dissociation into Cat/8, with perhaps an unequal number of S-residues on the different monomeric chains, would appear to be more probable than dissociation into Cat/12.

In summary, no evidence is found in amino acid sequencing for subunits smaller than Cat/4. The molecular weight of performic-acid-oxidized catalase either corresponds to Cat/8 or is intermediate between Cat/8 and Cat/12 depending on the method of measurement. The frictional ratios calculated from the sedimentation coefficients of subunits that may be smaller than Cat/4 suggest dissociation into Cat/8 but are consistent with dissociation into Cat/12. The maximum number of S-S bridges per Cat/4 is sufficient to bind two monomers into a Cat/4 subunit and may be sufficient to bind three monomers together. Thus, definitive evidence regarding the size of the catalase monomer is not available.

TABLE B-IV. Maximum number of S-S bridges per Cat/4.

Assumed molecular weight of intact catalase	250,000	232,400
Total number of S groups per catalase[a]	22 (17-29)	21 (16-27)
Maximum number of free -SH groups per catalase[b]	11	11
Maximum number of S groups that could be involved in structural bridges	11 (6-18)	10 (5-16)
Maximum number of structual S-S bridges per catalase	5 (3-9)	5 (2.5 - 8)
Maximum number of structural S-S bridges per Cat/4	1 (0.8 - 2.3)	1 (0.6 - 2.0)

References:

[a]Average from Table B-III with data of Bonnichsen (1947) omitted. Numbers in parenthesis indicate range of remaining data.

[b]Schütte and Nürnberger, 1959.

Dissociation into subunits smaller than Cat/4 is probable, and, if the monomers are of equal size, dissociation into Cat/8 appears more probable than dissociation into Cat/12. If the molecular weight of catalase is taken to be 232,400, the probable apo-monomer molecular weight is 28,800.

REFERENCES

Ackers, G.K. and R.L. Steere, 1961. Cell for rapidly measuring restriction to diffusion of macromolecules through agar gels of various pore sizes. Nature 192: 436-437.

Adachi, K. and T. Asakura, 1974. Effect of 2,3-diphosphoglycerate and inosital hexaphosphate on the stability of normal and sickle hemoglobins. Biochem. 13: 4976-4982.

Adair, G.S. and M.E. Adair, 1936. Densities of protein crystals and hydration of proteins. Proc. Roy. Soc. (London) Series B 120: 422-446.

Adair, G.S. and M.E. Adair, 1947. The density increments of proteins. Proc. Roy. Soc. (London) Series A, 190: 341-356.

Adams, L.R., 1964. A variant cytophotometric technique and its application to the study of erythropoiesis through measurement of total DNA and hemoglobin in single erythroid cells. Ph.D. Thesis, University of California, Berkeley, UCRL-11459 (Lawrence Radiation Laboratory, May 29, 1964).

Addink, A.D.F., P. Boer, T. Wakabayashi, and D.E. Green, 1972. Enzyme localization in beef heart mitochondria. Biochemical and electron-microscope study. Eur. J. Biochem. 29: 47-59.

Aebi, H., S.Moerikofer-Zwez, and J.P. Vaon Wartburg, 1970. Alternative molecular forms of erythrocyte catalase. Wenner-Gren Cent. Int. Symp. 1970. 18: 345-351, in Chem. Abs. 80: 142365y.

Aebi, H., B. Scherz, Y. Ben-Yoseph, and S.R. Wyss, 1975. Dissociation of erythrocyte catalase into subunits and their reassociation. Experientia 31: 397-399.

Aebi, H., S.R. Wyss, B. Scherz, and F. Skvaril, 1974. Heterogeneity of erythrocyte catalase: II. Isolation and characterization of normal and variant erythrocyte catalase and their subunits. Eur. J. Biochem. 48: 137-145.

Agner, K., 1938. The preparation and properties of a highly active catalase from horse liver. Biochem. J. 32: 1702-1706.

Altman, P.L. and D.S. Dittmer, eds., 1974. Biology Data Book, 2nd Edition, Vol. 3, (Fed. Amer. Soc. Exptl. Brol., Bethesda).

Ambs, E., 1956. Durchmesser und Hämoglobingehalt der Erythrocyten. Acta Haematol. 15: 302-313.

Amidon, G.L., S.H. Yalkowsky, and S. Leung, 1974. Solubility of nonelectrolytes in polar solvents. II. Solubility of aliphatic alcohols in water. J. Pharm. Sci. 63: 1858-1866.

Antonini, E., M. Brunori, and S. Anderson, 1968. Studies on the relations between molecular and functional properties of hemoglobin. VII. Kinetic effects of the reversible dissociation of hemoglobin into single chain molecules. J. Biol. Chem. 243: 1816-1822.

Antonini, E., E. Bucci, C. Fronticelli, E. Chiancone, J. Wyman, and A. Rossi-Fanelli, 1966. The properties and interactions of the isolated α- and β-chains of human hemoglobin. V. The reaction of α- and β-chains. J. Mol. Biol. 17: 29-46

Antonini, E., E. Bucci, C. Fronticelli, J. Wyman, and A. Rossi-Fanelli, 1965. The properties and interactions of the isolated α- and β-chains of human hemoglobin. III. Observations on the equilibria and kinetics of the reactions with gases. J. Mol. Biol. 12: 375-384.

Arpin, M. A.M. Reboud, and J.P. Reboud, 1972. Conformational changes of large ribosomal subunits of rat liver, induced by some monovalent cations. Biochim. Biophys. Acta 277: 134-139.

Austin, J.H. and D.L. Drabkin, 1935. Spectrophotometric studies. III. Methemoglobin. J. Biol. Chem. 112: 67-88.

Awasthi, Y.C., E. Beutler, and S.K. Srivastava, 1975. Purification and properties of human erythrocyte glutathione peroxidase. J. Biol. Chem. 250: 5144-5149.

Bahr, G.F. and E. Zeitler, 1962. Determination of the total dry mass of human erythrocytes by quantitative electron microscopy. Lab. Invest. 11: 912-917.

Baker, R.F., 1967. Ultrastructure of the red blood cell. Fed. Proc. 26: 1785-1801.

Baker, R.F. and N.R. Gillis, 1969. Osmotic hemolysis of chemically modified red blood cells. Blood 33, 170-178.

Banerjee, R. and L. Sagaert, 1967. The dissociation of human hemoglobin in acid media. Biochim. Biophys. Acta 140: 266-273 (French).

Barnes, G.T., T.I. Quickenden, and J.E. Saylor, 1970. Statistical calculation of monolayer permeation by water. J. Colloid Interface Sci. 33: 236-243.

Bechhold, H., 1921. Bau der roten Blutkörperchen und Hämolyse. Münch. Med. Wochensch. 68: 127-130.

Behlke, J., J. Lampe, and W. Scheler, 1970. Zum Elekrolyt-und Liganden-einfluss auf die Quartärstruktur des menschlichen Methämoglobins. Acta. Biol. Med. Ger. 24: 431-444.

Belitsina, N.V., A.V. Rozenblat, and A.S. Spirin, 1971. Effect of different cations on the stability of association of ribosomal subparticles. Mol. Biol. 5(6): 898-907 (Russian), in Chem. Abst. 76: 69217n.

Benesch, R.E., R. Benesch, and M.E.Williamson, 1962. The influence of reversible oxygen binding on the interaction between hemoglobin subunits. Proc. Natl. Acad. Sci. US 48: 2071-2075.

Benjamins, J., J.A. de Feijter, M.T.A. Evans, D.E. Graham, and M.C. Phillips, 1975. Dynamic and static properties of proteins adsorbed at the air/water interface. Disc. Faraday Soc. 59: 218-229.

Ben-Na'im, A., 1974. Water and Aqueous Solutions; Introduction to a Molecular Theory (Plenum Press, New York).

Ben-Na'im, A., 1975. Hydrophobic interaction and structural changes in the solvent. Biopolymers 14: 1337-1355.

Berg, H.C., J.M. Diamond, and P.S. Marfey, 1966. Erythrocyte membrane: chemical modification. Science 150, 64-67.

Bessis, M. and G. Brecher, 1971. Action du plasma conservé sur la forme des globules rouges (transformation discocyte echinocyte). Nuov. Rev. Fr. Hemat. 11: 305-308 (French).

Bessis, M. and P. Mandon, 1972. La microsphérulation et les formes myéliniques des globules rouges. Examen comparé au microscope électronique à balayoge et à transmission. Nuov. Rev. Fr. Hematol. 12: 443-454 (French).

Bielen, T., 1967. Association of hemoglobin, Meded. Vlaam. Chem. Ver. 29(5): 164-167 (Dutch), in Chem. Abst. 68: 84353g.

Biochemisches Taschenbuch, 1964, edited by H.M. Rauen and R. Kuhn (Springer-Verlag, Berlin and New York).

Blais, J.J.B.P. and P.H. Geil, 1969. Deformation behavior of erythrocyte ghost. Biopolymers 8: 275-287.

Blank, M., 1962. Monolayer permeability and the properties of natural membranes. J. Phys. Chem. 66: 1911-1918.

Blank, M., 1964. An approach to a theory of monolayer permeation by gases. J. Phys. Chem. 68: 2793-2800.

Blank, M. and J.S. Britten, 1965. Transport properties of condensed monolayers. J. Colloid Sci. 20, 789-800.

Blank, M. and J.S. Britten, 1973. Comment on the Molecular basis of fluidity in membranes. Chem. Phys. Lipids 10, 286-288.

Blok, M.C., L.L.M. van Deenen, and J. De Gier, 1976. Effect of the gel-to-liquid crystalline phase transition on the osmotic behavior of phosphotidylcholine liposomes. Biochim. Biophys. Acta 433: 1-12.

Blok, M.C., E.C.M. Van der Neut-Kok, L.L.M. Van Deenen, and J. De Gier, 1975. The effect of chain length and lipid phase transition on the selective permeability properties of liposomes. Biochim. Biophys. Acta 406: 187-196.

Bobinski, H. and W.D. Stein, 1966. Isolation of a glucose-binding component from human erythrocyte membranes. Nature 211: 1366-1368.

Bockman, D.O., 1969. Interfacial mass transfer. Ind. Eng. Chem. Fundamentals 8: 77-80.

Bodemann, H. and H. Passow, 1972. Factors controlling the resealing of the membrane of human erythrocyte ghosts after hypotonic hemolysis. J. Membrane Biol. 8(1): 1-26.

Bonaventura, J., W.A. Schroeder, and S. Fang, 1972. Human erythrocyte catalase: an improved method of isolation and a reevaluation of reported properties. Arch. Biochem. Biophys. 150: 606-617.

Bonnichsen, R.K., 1947. A comparative study of the blood and liver catalases from the horse. Arch. Biochem. 12: 83-94.

Boyer, S.H., T.K. Belding, L. Margolet, and A.N. Noyes, 1975. Fetal hemoglobin restriction to a few erythrocytes (F cells) in normal human adults. Science 188: 361-363.

Bramley, T.A. and R. Coleman, 1972. Effects of inclusion of Ca^{++}, Mg^{++}, EDTA or EGTA during the preparation of erythrocyte ghosts by hypotonic hemolysis. Biochim. Biophys. Acta 290: 219-228.

Bramley, T.A., R. Coleman, and J.B. Finean, 1971. Chemical, enzymological and permeability properties of human erythrocyte ghosts prepared by hypotonic lysis in media of different osmolarites. Biochim. Biophys. Acta 241: 752-769.

Branton, D. and D.W. Deamer, 1972. Membrane Structure. Protoplasmatologia IIE1, 70 pp.

Braunitzer, G., 1964. The molecular weight of human hemoglobin. Bibliotheca Haematol. 18: 59-60 (English).

Bretscher, M.S., 1972. Membranes — asymmetrical lipid bilayer structure. Nature (New Biology) 236(61): 11-12.

Bretscher, M.S., 1973. Membrane structure: some general principles. Science 181: 622-629.

Brochard, F. and J.F. Lennon, 1975. Frequency spectrum of the flicker phenomenon in erythrocytes. J. Phys. (Paris) 36: 1035-1047.

Broyles, R.H. and M.J. Deutsch, 1975. Differentiation of red blood cells in vitro. Science 190: 471-473.

Brunori, M., E. Antonini, J. Wyman and S.R. Anderson, 1968. Spectral differences between hemoglobin and isolated hemoglobin chains in the deoxygenated state. J. Mol. Biol. 34: 357-359.

Bucci, E., C. Fronticelli, E. Chiancone, J. Wyman, E. Antonini, and A. Rossi-Fanelli, 1965. The properties and interactions of the isolated α- and β-chains of human hemoglobin. I. Sedimentation and electrophoretic behavior. J. Mol. Biol. 12, 183-192.

Bull, T.E., J. Andrasko, E. Chiancone, and S. Forsén, 1973. Pulsed nuclear magnetic resonance studies on ^{23}Na, ^{7}Li, and ^{35}Cl binding to human oxy- and carbon-monoxyhaemoglobin. J. Mol. Biol. 73(2): 251-259.

Burton, A.C., 1969. The stretching of "pores" in a membrane, in Permeability and Function of Biological Membranes; Third Int. Conf. Biol. Membrane Stress, Italy, June 15, 1969.

Butler, K.W., 1975. Effects of a myelin apoprotein on lipid structure. Spin probe study. Can J. Biochem. 53: 758-767.

Cabantchik, Z.I., T. Ostwald, P.A. Knauf, and A. Rothstein, 1975. The relationship between permeation of an anionic photoreactive probe and its binding to red blood cell membrane proteins. Biophys. J. 15: 209a, Abstract.

Calissano, P., S. Alemà, and G. Rusca, 1972. Effect of hemoglobin on liposome permeability of Rb^+ and other solutes. Biochim. Biophys. Acta 255: 1009-1013.

Callaghan, O.H., 1957. The purification and properties of rabbit-muscle myokinase. Biochem. J. 67: 651-657.

Canham, P.B. and A.C. Burton, 1968. Distribution of size and shape in populations of normal human red cells. Circ. Res. 22: 405-422.

Canham, P.B. and D.R. Parkinson, 1970. The area and volume of single human erythrocytes during gradual osmotic swelling to hemolysis. Can. J. Physiol. Pharmacol. 48: 369-376.

Capaldi, R.A., 1973. A cross-linking study of the beef erythrocyte membrane: extensive interaction of all the proteins of the membrane except for the glycoproteins. Biochem. Biophys. Res. Commun. 50(3): 656-661.

Carraway, K.L., D. Kobylka, J. Summers, and C.A. Carraway, 1972. Chemical modification of erythrocyte membranes: double labeling with acetic anhydride. Chem. Phys. Lipids 8: 65-81.

Carraway, K.L., D. Kobylka, and R.B. Triplett, 1971. Surface proteins of erythrocyte membranes. Biochim. Biophys. Acta 241: 934-940.

Carraway, K.L. and B.C. Shin, 1972. Specific modification, isolation and partial characterization of an erythrocyte membrane protein. J. Biol. Chem. 247: 2102-2108.

Carraway, K.L., R.B. Triplett, and D.R. Anderson, 1975. Calcium-promoted aggregation of erythrocyte membrane proteins. Biochem. Biophys. Acta 379: 571-581.

Carrell, R.W. and H. Lehmann, 1969. The unstable haemoglobin haemolytic anaemias. Seminar Hematol. 6: 116-132.

Cecil, R. and A.G. Ogston, 1948. Examination of crystalline catalases in the ultracentrifuge. Biochem. J. 43: 205-206.

Cecil, R. and A.G. Ogston, 1952. Sedimentation and Diffusion, in a paper by Massey, V., "The crystallization of fumarase," Biochem. J. 51: 490-494.

Cerletti, P. and G. De Ritis, 1962. Enzymes of the red blood cell membrane: adenylate kinase activity. Clin. Chim. Acta 7: 402-405.

Chandrasekhar, S., R. Shashidhar, and N. Tara, 1970. Theory of melting of molecular crystals: the liquid crystalline phase. Molec. Crystals Liquid Cryst. 10: 337-358.

Chapman, D., 1975. Phase transitions and fluidity characteristics of lipids and cell membranes. Quart. Rev. Biophys. 8: 185-235.

Chapman, D., K.M. Keough, and J. Urbina, 1974. Biomembrane phase transitions: studies of lipid water systems using differential scanning calorimeter. J. Biol. Chem. 249, 2512-2521.

Charaches, S., C.L. Conley, D.F. Waugh, R.J. Ugoretz, J.R. Spurrell, and E. Gayle, 1967. Pathogenesis of hemolytic anemia in homozygous hemoglobin C disease. J. Clin. Invest. 46: 1795-1811.

Chau-Wong, M. and P. Seeman, 1971. The control of membrane-bound Ca^{2+} by ATP. Biochim. Biophys. Acta 241: 473-482.

Chua, C.G. and R.W. Carrell, 1974. Three cysteine residues in the α chain of rat hemoglobin. Biochim. Biophys. Acta 365: 328-334.

Clarke, M., 1971. Isolation and characterization of a water soluble protein from bovine erythrocyte membranes. Biochem. Biophys. Res. Commun. 45: 1063-1070.

Cohen, B.E., 1975a. The permeability of liposomes to nonelectrolytes. I. Activation energies for permeation. J. Membr. Biol. 20: 205-234.

Cohen, B.E., 1975b. The permeability of liposomes to nonelectrolytes. II. The effect of nystatin and gramicidin A. J. Membr. Biol. 20: 235-268.

Cohen, B.E. and A.D. Bangham, 1972. Diffusion of small nonelectrolytes across liposome membranes. Nature 236: 173-174.

Cohen, G. and P. Hochstein, 1963. Glutathione peroxidase: the primary agent for the elimination of hydrogen peroxide in erythrocytes. Biochem. 2: 1420-1428.

Colacicco, G., 1969. Applications of monolayer techniques to biological systems: symptoms of specific lipid-protein interactions. J. Colloid Interface Sci. 29: 345-364.

Colacicco, G., 1970. Lipid monolayers: mechanism of protein penetration with regard to membrane models. Lipids 5: 636-649.

Colacicco, G. and M.M. Rapport, 1968. Lipid monolayers. Effect of phosphatidyl choline and cholesterol on the interaction of dihydroceramide lactoside with rabbit γ-globulin. Adv. Chem. Series 84: 157-168.

Coldman, M.F., M. Gent, and W. Good, 1970. Identical effect of electrolyte and nonelectrolyte on the osmotic fragility of mammalian erythrocytes. Comp. Biochem. Physiol. 33: 157-165.

Coldman, M.F. and W. Good, 1967. The distribution of sodium, potassium and glucose in the blood of some mammals. Comp. Biochem. Physiol. 21: 201-206.

Colombe, B.W. and R.I. Macey, 1974. Effects of calcium on potassium and water transport in human erythrocyte ghosts. Biochim. Biophys. Acta 363: 226-239.

Comandon, J. and P. De Fonbrune, 1929. Contribution a l'etude du mecanisme de l'hemolyse. Arch. Anat. Microsc. 25: 555-570.

Connerty, H.V. and A.R. Briggs, 1962. New method for the determination of whole-blood iron and hemoglobin. Clin. Chem. 8: 151-157.

Cooper, R.A., 1970. Lipids of human red cell membrane: normal composition and variability in disease. Semin. Hematol. 7: 296-322.

Cooper, R.A. and J.H. Jandl, 1969. The selective and conjoint loss of red cell lipids. J. Clin. Invest. 48: 906-914.

Craig, L.C. and W. Konigsberg, 1961. Dialysis studies. III. Modification of pore size and shape in cellophane membranes. J. Phys. Chem. 65: 166-172.

Criss, W.E., 1970. Rat liver adenosine triphosphate: adenosine monophosphate phosphotransferase activity. II. Subcellular localization of adenylate kinase isozymes. J. Biol. Chem. 245: 6352-6356.

Criss, W.E., V. Sapico, and G. Litwack, 1970. Rat liver adenosine triphosphate: adenosine monophosphate phosphotransferase activity. I. Purification and physical and kinetic characterization of adenylate kinase III. J. Biol. Chem. 245(23): 6346-6351.

Dan, M. and A. Hagiwara, 1967. Detection of two types of hemoglobin (HbA and HbF) in single erythrocytes by fluorescent antibody technique. Exp. Cell Res. 46: 596-598.

Danon, D., 1961. Osmotic hemolysis by a gradual increase in the ionic strength of the surrounding medium. J. Cell. Comp. Physiol. 57: 111-117.

Danon, D., A. Nevo, and Y. Marikovsky, 1956. Preparation of erythrocyte ghosts by gradual haemolysis in hypotonic aqueous solution. Bull. Research Council Israel 6E: 36-39.

Darke, A., E.G. Finer, A.G. Flook, and M.C. Phillips, 1972. Nuclear magnetic resonance study of lecithin-cholesterol interactions. J. Mol. Biol. 63: 265-278.

Das Gupta, N.N., D.N. Misra, P. Ganguly, A.B. Sanyal, and J.B. Chatterjea, 1963. Electron microscopic and sedimentation studies on human hemoglobins A, F, and E. Aspects Protein Struct., Proc. Symp., Madras: 301-305.

Davies, H.G., N.V.B. Marsden, S.G. Östling, and A.M.M. Zade-Oppen, 1968. The effect of some neutral macromolecules on the pattern of hypotonic hemolysis. Acta Physiol. Scand. 74: 577-593.

Davies, J.T. and E.K. Rideal, 1961. Interfacial Phenomena (Adacemic Press, New York and London).

Davson, H., 1939. Studies on the permeability of erythrocytes. VI. The effect of reducing the salt content of the medium surrounding the cell. Biochem. J. 33: 389-401.

Davson, H. and J.F. Danielli, 1938. Studies on the permeability of erythrocytes. V. Factors in cation permeability. Biochem. J. 32: 991-1001.

Davydova, S. Ya., V.S. Shapot, and G.A. Drozdova, 1970. Heterogeneity of catalase in rat liver and experimental hepatomas of rats and mice. Biochim. Biophys. Acta 220, 206-212.

Dawson, R.M.C. and P.J. Quinn, 1971. The interaction of soluble proteins with lipid interfaces. Adv. Expth. Med. Biol. 14: 1-17.

Deal, W.C., W.J. Rutter, V. Massey, and K.E. Van Holde, 1963. Reversible alteration of the structure of enzymes in acidic solution. Biochim. Biophys. Res. Comm. 10: 49-54.

Deamer, D.W. and D. Branton, 1967. Fracture planes in an ice-bilayer model membrane system. Science 158: 655-657.

de Gier, J. and L.L.M. van Deenen, 1964. A dietary investigation on the variations in phospholipid characteristics of red-cell membranes. Biochim. Biophys. Acta 84: 294-304.

De Kruyff, B., P.W.M. Van Dijck, R.A. Demel, A. Schuijff, F. Brants, and L.L. M. van Deenen, 1974. Non-random distribution of cholesterol in phosphatidyl choline bilayers. Biochem. Biophys. Acta 356: 1-7.

Demel, R.A., W.S.M. Geurts van Kessel, R.F.A. Zwaal, B. Roelofsen, and L.L.M. Van Deenen, 1975. Relation between various phospholipase actions on human red cell membranes and the interfacial phospholipid pressure in monolayers. Biochim. Biophys. Acta 406: 97-107.

Deutsch, H.F., 1952. The properties of various crystalline horse erythrocyte catalase preparations. Acta Chem. Scand. 6: 1516-1521.

Dick, D.A.T., 1966. An approach to the molecular structure of the living cell by water flux studies. Phys. Bases Circ. Transp., Regul. Exch. Proc. Conf., Denver. pp. 217-234.

Diezel, W., S. Liebe, G. Kopperschlaeger, and E. Hofmann, 1970. Aggregation forms of bovine liver catalase. FEBS Lett. 6: 166-170 (German).

Diezel, W., S. Liebe, G. Kopperschlaeger, and E. Hofmann, 1972. Bovine liver catalase: microheterogeneity and enzyme association. Acta Biol. Med. Ger. 28: 715-725 (German).

Dodge, J.T., C. Mitchell, and D.J. Hanahan, 1963. The preparation and chemical characteristics of hemoglobin-free ghosts of human erythrocytes. Arch. Biochem. Biophys. 100: 119-130.

Donlon, J.A. and A. Rothstein, 1969. The cation permeability of erythrocytes in low ionic strength media of various tonicities. J. Membr. Biol. 1(1): 37-52.

Drabkin, D.L., 1950. Spectrophotometric studies. XV. Hydration of macro sized crystals of human hemoglobin and osmotic concentrations in red cells. J. Biol. Chem. 185: 231-245.

Duchon, G. and H.B. Collier, 1971. Enzyme activities of human erythrocyte ghosts: effects of various treatments. J. Membr. Biol. 6: 138-157.

Dupont, Y., A. Garbriel, M. Chabre, T. Gulik-Krzywicki, and E. Schechter, 1972. Use of a new detector for x-ray diffraction and kinetics of the ordering of the lipids in *E coli* membranes and model systems. Nature 238: 331-333.

Duprez, A. and A. Vignes, 1967. Détermination ponctuelle du potassium intracellulaire d'hématies humaines. Analyse à la microsonde electronique de Castaing. C. R. Soc. Biol. 161: 1358-1360.

Edidin, M., 1974. Rotational and translational diffusion in membranes. Ann. Rev. Biophys. Bioeng. 3: 179-201.

Edidin, M., Y. Zagyansky, and T.J. Lardner, 1976. Measurement of membrane protein lateral diffusion in single cells. Science 191: 466-468.

Edzes, H.T. and H.J.C. Berendsen, 1975. The physical state of diffusible ions in cells. Annul. Rev. Biophys. Bioeng. 4: 265-285.

Einstein, A., 1926. Investigations on the Theory of the Brownian Movement, edited by F. Fürth, translated by A.D. Cowper. (Methuen & Co., Ltd., London).

Elbaum, D., J. Harrington, and R.L. Nagel, 1975a. Surface activity of different human hemoglobins. Biophys. J. 15: 82a. Abstract.

Elbaum, D., J. Harrington, and R.L. Nagel, 1975b. Surface Activity of Hemoglobin S in Erythrocyte Structure and Function, edited by G.J. Brewer, (A. R. Liss, Inc., New York), pp. 311-324.

Elgsaeter, A. and D. Branton, 1974. Intramembrane particle aggregation in erythrocyte ghosts. I. Effects of protein removal. J. Cell. Biol. 63: 1018-1036.

Elgsaeter, A., D.M. Shotton, and D. Branton, 1976. Intramembrane particle aggregation in erythrocyte ghosts. II. The influence of spectrin aggregation. Biochim. Biophys. Acta 426: 101-122.

Emmelot, P. and R.P. Van Hoeven, 1975. Phospholipid unsaturation and plasma membrane organization. Chem. Phys. Lipids 14: 236-246.

Enoki, Y., S. Tomita, and M. Sato, 1966. Presence of multiple hemoglobins in rats. Jap. J. Physiol. 16: 702-709 (English).

Evans, E.A., 1973a. A new material concept for the red cell membrane. Biophys. J. 13: 926-940.

Evans, E.A., 1973b. New membrane concept applied to the analysis of fluid shear- and micropipette-deformed red blood cells. Biophys. J. 13: 941-954.

Evans, E. and Y.-C. Fung, 1972. Improved measurements of the erythrocyte geometry. Microvas. Res. 4: 335-347.

Evans, E.A. and P.L. La Celle, 1975. Intrinsic material properties of the erythrocyte membrane indicated by mechanical analysis of deformation. Blood 45: 29-43.

Evans, E.A. and P.F. Leblond, 1973. Geometric properties of individual red blood cell discocyte-spherocyte transformations. Biocheology 10: 393-404.

Fairbanks, G., T.L. Steck, and D.F.H. Wallach, 1971. Electrophoretic analysis of the major polypeptides of the human erythrocyte membrane. Biochem. 10: 2606-2617.

Farmer, R.E. and R.I. Macey, 1972. Perturbation of red cell volume: constancy of membrane transport parameters for certain slow penetrants. Biochim. Biophys. Acta 255: 502-516.

Féo, C., 1972. Transformation discocyte-échinocyte. Rôle de la formation de lysolécithine dans le plasma. Nuov. Rev. Fr. Hemat. 12: 455-463.

Feo, C.J. and P.F. Leblond, 1974. Discocyte-echinocyte transformation. Comparison of normal and ATP-enriched human erythrocytes. Blood 44: 639-647.

Fischer, S., R.L. Nagel, R.M. Bookchin, E.F. Roth, Jr., and I. Tellez-Nagel, 1975. Binding of hemoglobin to membranes of normal and sickle erythrocytes. Biochim. Biophys. Acta 375: 422-433.

Fisher, K.A., 1976. Analysis of membrane halves: cholesterol. Proc. Nat. Acad. Sci. U.S. 73: 173-177.

Forslind, E. and R. Kjellander, 1975. Structure model for the lecithin-cholesterol-water membrane. J. Theor. Biol. 51: 97-109.

Forstner, J. and J.F. Manery, 1971. Calcium binding by human erythrocyte membranes. Biochem. J. 124: 563-571.

Franks, F., editor, 1972-1975. Water, A Comprehensive Treatise (Plenum Press, New York and London).

Franks, F., 1973. The Solvent Properties of Water, in Water, Vol. 2 (Plenum Press, New York and London), pp. 1-54.

Frieden, C.F., R.M. Bock, and R.A. Alberty, 1954. Studies of the enzyme fumarase. II. Isolation and physical properites of crystalline enzyme. J. Am. Chem. Soc. 76: 2482-2484.

Frisch, H.L. and R. Simha, 1957. Statistical mechanics of flexible high polymers at surfaces. J. Chem. Phys. 27: 702-706.

Fromherz, P., 1971. New technique for investigating lipid protein films. Biochim. Biophys. Acta 225: 382-387.

Fromherz, P., J. Peters, H.G. Müldner, and W. Otting, 1972. An infrared spectroscopic study on the lipid protein interaction in an artificial lamellar system. Biochim. Biophys. Acta 274: 644-648.

Fujii, T. and M. Sato, 1975. Possible adsorption of aldalase and glyceraldehyde 3-phosphate dehydrogenase to erythrocyte ghosts prepared under hypotonic conditions. Rinsho Kagaku 3: 453-459, in Chem. Abs. 84: 175715y.

Gabrio, B.W., D.M. Donohue, and C.A. Finch, 1955. Erythrocyte preservation. V. Relationship between chemical changes and viability of stored blood treated with adenosine. J. Clin. Invest. 34: 1509-1512.

Gaffney, F.M., 1957. Experimental haemolytic anaemia with particular reference to the corpuscular haemoglobin concentration of the erythrocytes. Brit. J. Haemat. 3: 311-319.

Gaines, G.L., Jr., 1966. Insoluble Monolayers at Liquid-Gas Interfaces (Interscience, New York, London and Sydney).

Ganguly, P., N.N. Das Gupta, and J.B. Chatterjea, 1963. Sedimentation characteristics of the human hemoglobins, A, F, and E. Nature 199: 919-920.

Ganguly, P and D.N. Misra, 1965. II. Interaction of phosphotungstate with haemoglobin. J. Mol. Biol. 12: 385-393.

Garrick, M.D., M. Reichlin, M. Mattoli, and R. Manning, 1973. Anemia-induced reversible switch from hemoglobin A to hemoglobin C in caprine ruminants. Immunochemical evidence that both hemoglobins are found in the same cell. Develop. Biol. 30(1): 1-12.

Gary-Bobo, C.M. and A.K. Solomon, 1968. Properties of hemoglobin solutions in red cells. J. Gen. Physiol. 52: 825-853.

Gazitt, Y., A. Loyter, Y. Reichler, and I. Ohad, 1976. Correlation between changes in the membrane organization and susceptibility to phospholipase C attack induced by ATP depletion of rat erythrocytes. Biochim. Biophys. Acta 419: 479-492.

Ginzburg, B.Z., T. Friedlander, and E. Pouchovsky, 1967. Specific binding of sodium and potassium ions in erythrocyte membranes. Nature 216: 1185-1188.

Gō, N, 1976. Statistical mechanics of protein folding, unfolding and fluctuation. Adv. Biophys. 9: 65-113.

Gould, R.M. and Y. London, 1972. Specific interaction of central nervous system myelin basic protein with lipids. Effects of basic protein on glucose leakage from liposomes. Biochim. Biophys. Acta 290: 200-218.

Grahm, J.M. and D.F.H. Wallach, 1971. Protein conformation transitions in the erythrocyte membrane. Biochim. Biophys. Acta 241: 180-194.

Gralén, N., 1939. The splitting of haemoglobin by acids. Biochem. J. 33: 1907-1912.

Gratzer, W.B. and G.H. Beaven, 1975. Properties of the high-molecular weight protein (spectrin) from human erythrocyte membranes. Eur. J. Biochem. 58: 403-409.

Greenquist, A.C. and S.B. Shohet, 1975. Phosphorylation and dephosphorylation in the erythrocyte membrane. Prog. Clin. Biol. Res. 1: 515-534.

Groom, A.C. and J.C. Anderson, 1972. Measurement of the size distribution of human erythrocytes by a sedimentation method. J. Cell. Physiol. 79(1): 127-138.

Grover, N.B., J. Naaman, S. Ben-Sasson, and F. Doljanski, 1972. Electrical sizing of particles in suspension. III. Rigid spheroids and red blood cells. Biophys. J. 12: 1099-1117.

Guidotti, G., 1967. Studies of hemoglobin. II. The effect of salts on the dissociation of hemoglobin into subunits. J. Biol. Chem. 242: 3685-3693.

Guidotti, G. and L. Craig, 1963. Dialysis Studies. VII. The behavior of solutes which associate. Proc. Nat. Acad. Sci. U.S. 50: 46-54.

Gulik-Krzywicki, T., E. Schecter, V. Luzzati, and M. Faure, 1969. Interactions of proteins and lipids: structure and polymorphism of protein-lipid-water phases. Nature 223: 1116-1121.

Gunn, R., J.O. Wieth, and D.C. Tosteson, 1973. Kinetics of bromide and iodide fluxes in human red blood cells. 17th Annual Meeting Biophysical Society, Columbus, Ohio, February 27-March 3, 1973, p. 258a. Abstract.

Gutter, F.J., H.A. Sober, and E.A. Peterson, 1956. The effect of mercaptoethanol and urea on the molecular weight of hemoglobin. Arch. Biochem. Biophys. 62: 427-434.

Hall, C.E., 1950. Electron microscopy of crystalline catalase. J. Biol. Chem. 185: 749-754.

Hamasaki, N. and Z.B. Rose, 1974. The binding of phosphorylated red cell metabolites to human hemoglobin A. J. Biol. Chem. 249: 7896-7901.

Hanahan, D.J., J.E. Ekholm, and M.G. Luthra, 1974. Is lipid lost during preparation of erythrocyte membranes? Biochim. Biophys. Acta 363: 283-286.

Handbook of Biochemistry. Selected Data for Molecular Biology, 2nd Edition. Edited by H.A. Sober, 1970 (The Chemical Rubber Co., Cleveland, Ohio).

Harris, E.J. and B.C. Pressman, 1967. Obligate cation exchanges in red cells. Nature 216: 918-920.

Harris, M.J., T. Higuchi, and J.H. Rytting, 1973. Thermodynamic group contributions from ion pair extraction equilibria for use in the prediction of partition coefficients. Correlation of surface area with group contributions. J. Phys. Chem. 77: 2694-2703.

Harrison, D.G. and C. Long, 1968. The calcium content of human erythrocytes. J. Physiol. 199: 367-381.

Hasserodt, U. and J. Vinograd, 1959. Dissociation of human carbonmonoxyhemoglobin at high pH. Proc. Nat. Acad. Sci. U.S. 45: 12-15.

Heedman, P.A., 1958. Hemolysis of individual red blood cells. An interferometer microscopic investigation. Exptl. Cell Res. 14: 9-22.

Helfrich, W., 1974. The size of bilayer vesicles generated by sonication. Phys. Lett. 50A: 115-116.

Heller, M. and D.J. Hanahan, 1972. Erythrocyte membrane-bound enzymes: ATPase, phosphatase and adenylate kinase in human, bovine and porcine erythrocytes. Biochim. Biophys. Acta 255(1): 239-250.

Heller, P. and U. Yakulis, 1969. The distribution of hemoglobin A_2. Ann. N.Y. Acad. Sci. 165: 54-59.

Henderson, R., 1975. The structure of the purple membrane from *Halobacterium halobium:* Analysis of the x-ray diffraction pattern. J. Mol. Biol. 93: 123-138.

Henderson, R. and N. Unwin, 1976. Three-dimensional structure of purple membrane. Biophys. J. 16, 1a. Abstract.

Hendrikx, Y. and L. Ter-Minassian-Saraga, 1975. Thermodynamics of penetration of soluble constituents into spread insoluble monolayers. Adv. Chem. Series 144: 177-191.

Hermann, R.B., 1971. Theory of hydrophobic bonding. I. The solubility of hydrocarbons in water within the context of the significant structure theory of liquids. J. Phys. Chem. 75: 363-368.

Hermann, R.B., 1972. Theory of hydrophobic bonding. II. The correlation of hydrocarbon solubility in water with solvent cavity. J. Phys. Chem. 76: 2754-2759.

Hermel, H. and R. Havemann, 1966. Über den Mechanismus der Katalase-Wasserstoffperoxid-Reaktion. I. Der Disulfid- und Sulfhydrylgehalt der Rinderleber-Katalase. Biochim. Biophys. Acta 128: 272-282.

Heusinkveld, R.S., 1973. Studies of erythrocyte membrane rigidity. Ph.D. Thesis, The University of Rochester, 141 pp. (Dissertation Abstract 34: 2263-B. Xerox University Miesbiling, Order No. 73-26, 544.)

Higashi, T. and Y. Shibata, 1964. Studies on rat liver catalase. III. Amino acid composition of rat liver catalase. J. Biochem. (Tokyo) 56(4): 361-363.

Hill, R.L. and R.A. Bradshaw, 1969. Fumarase, pp. 91-99 in, Methods in Enzymology, Vol. XIII, edited by J.M. Lowenstein (Academic Press, New York).

Hill, R.L. and L. Kanarek, 1964. The subunits of fumarase, pp. 80-97 in, Subunit Structure of Proteins: Biochemical and Genetic Aspects. Symposium June 1-3, 1964. (U.S. Atomic Energy Comm., BNL-869-(C-40)).

Hill, T.L., 1956. Statistical Mechanics (McGraw-Hill, New York, Toronto, and London).

Hiraga, M., K. Abe, and F.K. Anan, 1967. The subunit structure of catalase: estimation of the molecular weight of performic acid-oxidized catalase. Bull. Tokyo Med. Dent. Univ. 14: 293-307 (English).

Hjelm, M., S.G. Ostling, and A.E.G. Persson, 1966. The loss of certain cellular components from human erythrocytes during hypotonic hemolysis in the presence of dextran. Acta. Physiol. Scand. 67: 43-49.

Höber, R. and S.L. Ørskov, 1933. Untersuchungen über die Permeiergeschwindig Keit von Anelektrolyten bei den roten Blutkörperchen verschiedener Tierarten. Pfluegers Arch. Gesamte Physiol. Menchen Tiere 231: 599-615.

Hoffman, J.F., 1954. Re-hemolytic characteristics of human erythrocyte ghosts and the mechanism of hemolysis. J. Cell. Comp. Physiol. 44: 335. Abstract.

Hoffman, J.F., 1958. Physiological characteristics of human red blood cell ghosts. J. Gen. Physiol. 42: 9-28.

Hoffman, J.F., 1962. The active transport of sodium by ghosts of human red blood cells. J. Gen. Physiol. 45: 837-859.

Hoffman, J.F., 1975. Ionic transport across the plasma membrane. pp. 95-103 in, Cell Membranes, edited by G. Weissmann and R. Claiborne (HP Publishing, New York).

Hoffman, J.F., M. Eden, J.S. Barr, and R.H.S. Bedell, 1958. The hemolytic volume of human erythrocytes. J. Cell Comp. Physiol. 51: 405-414.

Holmes, R.S., 1972. Catalase multiplicity in normal and acatalasemic mice. FEBS Lett. 24(2): 161-164.

Holzwarth, G., J. Yu, and T.L. Steck, 1976. Heterogeneity in the conformation of different protein fractions from human erythrocyte membrane. J. Supramol. Struc. 4: 161-168.

Horne, R.A., editor, 1972. Water and Aqueous Solutions. Structure, Thermodynamics, and Transport Processes (Wiley-Interscience, New York, London, Sydney and Toronto).

Hsia, C. and L. Spero, 1972. Quoted by P. Seeman in discussion of paper of B.G. McFarland: Molecular basis for fluidity in membranes. Chem. Phys. Lipids 8: 303-313.

Huehns, E.R. and E.M. Shooter, 1966. Further studies on the isolation and properties of α-chain subunits of hemoglobin. Biochem. J. 101: 843-851.

Huestis, W. and H.M. McConnell, 1973. Quoted as work in progress in M.G. McNamee and H.M. McConnell: Transmembrane potentials and phospholipid flip-flop in excitable membrane vesicles. Biochem. 12: 2951-2958.

Huhn, D., G.D. Pauli, and D. Grassman, 1970. Die Erythrocytenmembran. Feinstruktur der gefriergeätzten Membran nach Einwirkung von hypotonen Lösungen und Suponen. Klin. Wochschr. 48: 939-943.

Hui, S.W. and D.F. Parsons, 1974. Electron diffraction of wet biological membranes. pp. 198-199 in, Electron Microscopy, Vol. II, edited by J.V. Sanders and D.J. Goodchild. 8th Intern. Congr. Electron Microscopy, Canberra, Australia, August 25-31, 1974.

Ihler, G.M., R.H. Glew, and F.W. Schnure, 1973. Enzyme loading of erythrocytes. Proc. Nat. Acad. Sci. U.S. 70: 2663-2666.

Ikai, A. and H. Noda, 1968. Partially helical conformation of hemoglobin in aqueous 2-chloroethanol. J. Biol. Chem. 234: 5028-5034.

Ingram, V.M., 1959. Separation of the peptide chains of human globin. Nature 183: 1795-1798.

Jacob, H.S., 1970. Mechanisms of Heinz body formation and attachment to red cell membrane. Seminars Hematol. 7: 341-354.

Jacob, H.S., 1975. Pathologic States of the Erythrocyte Membrane in Cell Membranes, edited by G. Weissmann and R. Claiborne (HP Publishing, New York) pp. 249-255.

Jacob, H., T. Amsden, and J. White, 1972. Membrane microfilaments of erythrocytes: Alteration in intact cells reproduces the hereditary spherocytosis syndrome. Proc. Nat. Acad. Sci. U.S. 69: 471-474.

Jacob, H.S. and H.K. Winterhalter, 1970. Role of hemoglobin heme loss in Heinz body formation; studies with a partially heme-deficient hemoglobin and with genetically unstable hemoglobins. J. Clin. Invest. 49: 2008-2016.

Jacobs, M.H. and A.K. Parpart, 1931. Osmotic properties of the erythrocyte. II. The influence of pH, temperature and oxygen tension on hemolysis by hypotonic solutions. Biol. Bull. 60: 95-119.

Jacobs, M.H. and A.K. Parpart, 1933. Osmotic properties of the erythrocyte. VI. The influence of the escape of salts on hemolysis by hypotonic solutions. Biol. Bull. 65: 512-528.

Jacobs, M.H. and D.R. Stewart, 1947. Osmotic properties of the erythrocyte. XII. Ionic and osmotic equilibria with a complex external solution. J. Cell. Comp. Physiol. 30: 79-103.

Jain, M.K., 1975. Role of cholesterol in biomembranes and related systems. Curr. Top. Membr. Transp. 6: 1-57.

Jain, M.K., N.Y.M. Wu, and L.V. Wray, 1975. Drug-induced phase change in bilayer as possible mode of action of membrane-expanding drugs. Nature 255: 494-496.

James, V. and D.G. Goldstein, 1974. Hemoglobin content of individual erythrocytes in normal and abnormal blood. J. Haematol. 28: 89-102.

Jay, A.W.L., 1973. Viscoelastic properties of the human red blood cell membrane. I. Deformation, volume loss, and rupture of red cells in micropipettes. Biophys. J. 13: 1166-1182.

Jay, A.W.L., 1975. Geometry of the human erythrocyte. I. Effect of albumin on cell geometry. Biophys. J. 15: 205-222.

Jensen, W.N. and L.S. Lessin, 1970. Membrane alterations associated with hemoglobinpathies. Sem. Hematol. 7: 409-426.

Jirgensons, B., 1966. Effect of anionic detergents in the optical rotatory dispersion of proteins. J. Biol. Chem. 241: 4855-4860.

Jirgensons, B. and S. Capetillo, 1970. Effect of sodium dodecyl sulfate on circular dichroism of some nonhelical proteins. Biochim. Biophys. Acta 214: 1-5.

Johnson, P. and V. Massey, 1957. Sedimentation studies on fumarase. Biochim. Biophys. Acta 23: 544-550.

Jones, G.L. and C.J. Masters, 1972. On the differential inhibition of the multiple forms of catalase in mouse tissue. FEBS Lett. 21(2): 207-210.

Joos, P., 1968. Constitution of protein films adsorbed from their solutions, pp. 513-519 in, Chim. Phys. Appl. Prat. Ag. Surface, C. R. Congr. Int. Deterg. 5th, Vol. 2, Part 1, Barcelona, Spain, September 9-13, 1968 (published 1969).

Jost, P., U.J. Brooks, and O.H. Griffith, 1973. Fluidity of phospholipid bilayers and membranes after exposure to osmium tetroxide and gluteraldehyde. J. Mol. Biol. 76(2): 313-318.

Jost, P.C., O.H. Griffith, R.A. Capaldi, and G. Vanderkooi, 1973. Evidence for boundary lipid in membranes. Proc. Nat. Acad. Sci. U.S. 70: 480-484.

Juliano, R.L., H.K. Kimelberg, and D. Papahadjopoulos, 1971. Synergistic effects of a membrane protein (spectrin) and Ca^{2+} on the Na^{+} permeability of phospholipid vesicles. Biochem. Biophys. Acta 241: 894-905.

Kahlenberg, A. and C. Walker, 1976. Partial purification of a membrane protein from human erythrocytes involved in glucose transport. J. Biol. Chem. 251: 1582-1590.

Kanarek, L. and R.L. Hill, 1964. The preparation and characterization of fumarase from swine heart muscle. J. Biol. Chem. 239: 4202-4206.

Kanarek, L., C. Marler, R.A. Bradshaw, R.E. Fellows, and R.L. Hill, 1964. The subunits of fumarase. J. Biol. Chem. 239: 4207-4211.

Kashket, S. and O.F. Denstedt, 1958. The metabolism of the erythrocyte. XV. Adenylate kinase of the erythrocyte. Can. J. Biochem. Physiol. 36: 1057-1064.

Katchalsky, A., O. Kedem, C. Klibansky, and A. De Vries, 1960. Rehological considerations of the haemolysing red blood cell, pp. 155-171 in, Flow Properties of Blood and Other Biological Systems, edited by A.L. Copley and G. Stainsky (Pergamon Press, New York).

Kawahara, K., A.G. Kirshner, and C. Tanford, 1965. Dissociation of human CO-hemoglobin by urea, quanidine hydrochloride, and other reagents. Biochem. 4: 1203-1213.

Kegeles, G. and F.J. Gutter, 1951. The determination of sedimentation constants from Fresnel diffraction patterns. J. Am. Chem. Soc. 73: 3770-3777.

Kellett, G.L., 1971. Dissociation of hemoglobin into subunits. Ligand-linked dissociation at neutral pH. J. Mol. Biol. 59: 401-424.

Kimelberg, H.K. and D. Papahadjopoulos, 1971a. Phospholipid-protein interactions: membrane permeability correlated with monolayer "penetration." Biochim. Biophys. Acta 233: 805-809.

Kimelberg, H.K. and D. Papahadjopoulos, 1971b. Interactions of basic proteins with phospholipid membranes. Binding and changes in the sodium permeability of phosphatidylserine vesicles. J. Biol. Chem. 246: 1142-1148.

King, E.J., 1932. The colorimetric determination of phosphorus. Biochem. J. 26: 292-297.

Kirkpatrick, F.H., G.M. Woods, and P.L. La Celle, 1975. Absence of one component of spectrin adenosine triphosphatase in hereditary spherocytosis. Blood 46: 945-954.

Kirkpatrick, F.H., G.M. Woods, P.L. La Celle, and R. I. Weed, 1975. Calcium and magnesium ATPases of the spectrin fraction of human erythrocytes. J. Supramol. Struc. 3: 415-425.

Kirshner, A.G. and C. Tanford, 1964. Dissociation of hemoglobin by inorganic salts. Biochem. 3: 291-296.

Klethi, J. and P. Mandel, 1968. Tissue determined variations of adenylate kinase. Nature 218: 467-468.

Klibansky, C., A. de Vries, and A. Katchlsky, 1960. La pénétration de l'albumine et de l'hémoglobine dans les érythrocytes au cours de l'hemolyse. Path. Biol. 8: 2005-2014.

Klipstein, F.A. and H.M. Ranney, 1960. Electrophoretic components of the hemoglobin of red cell membranes. J. Clin. Invest. 39: 1894-1899.

Klotz, I.M., D.W. Darnall, and N.R. Langerman, 1975. Quaternary structure of proteins, pp. 293-411 in, The Proteins, Vol. 1, edited by H. Neurath, R.L. Hill, and C.-L. Boeder (Academic Press, New York).

Kochen, J.A., 1964. The surface precipitation reaction in the hemolyzing red cell. Proc. IX Cong. Int. Soc. Hematol. 1: 19-24.

Kornberg, R.D. and H.M. McConnell, 1971. Inside-outside transitions of phospholipids in vesicle membranes. Biochem. 10: 1111-1120.

Krainev, S.I., 1970. Forms of catalase in human erythrocytes. Biokhimiya 35: 662-669 (Russian).

Krizan, J.E. and A.R. Williams, 1973. Biological membrane rupture and a phase transition model. Nature New Biol. 246: 121-123.

Kuby, S.A., L. Noda, and H.A. Lardy, 1954. Adenosinetriphosphate-creatine transphosphorylase. I. Isolation of the crystalline enzyme from rabbit muscle. J. Biol. Chem. 209: 191-201.

Kumins, C.A. and T.K. Kwei, 1968. Free volume and other theories, pp. 107-140 in, Diffusion in Polymers, edited by J. Crank and G.S. Park (Academic Press, New York and London).

Kurihara, K. and K. Shibata, 1960. Dissociation of horse hemoglobin at high pH. Arch. Biochem. Biophys. 88: 298-301.

Kusumoto, S. and T. Nakajima, 1968. The constitution of Heinz bodies. Naunyn-Schmiedebergs Arch. Pharmakol Exp. Pathol. 259: 266-275, in Chem. Abs. 68: 85469m.

Kwant, W.O. and P. Seeman, 1969. The membrane concentration of a local anesthetic (chlorpromagine). Biochim. Biophys. Acta 183: 530-543.

La Celle, P.L., 1970. Alteration of membrane deformability in hemolytic anemias. Seminars Hematol. 7: 355-371.

La Celle, P.L., 1973. Microbiology of individual sickle cells. 17th Ann. Meeting Biophysical Soc., Columbus, Ohio, February 27-March 3, 1973. p. 225a.

La Celle, P.L. and F.H. Kirkpatrick, 1975. Determinants of erythrocyte membrane elasticity. Prog. Clin. Biol. Res. 1975: 535-557.

La Celle, P.L., F.H. Kirkpatrick, M.P. Udkow, and B. Arkin, 1972. Membrane fragmentation and Ca^{++} membrane interaction: potential mechanisms of shape change in the senescent red cell. Nouv. Rev. Fr. Hematol 12: 789-798.

La Celle, P.L. and R.I. Weed, 1969. Reversibility of abnormal deformability and permeability of the hereditary spherocyte. Blood 34: 858. Abstract.

Ladbrooke, B.D. and D. Chapman, 1969. Thermal analysis of lipids, proteins, and biological membranes. A review and summary of some recent studies. Chem. Phys. Lipids 3: 304-367.

Lajeunie, R., 1974. Dispositif de dosage de l'ATP contenu dans une cellule isolée per bioluminscence. [Description of the opta-electronics of a device for measurement of ATP in a single cell by bioluminescence.] Nouv. Rev. Fr. Hematol. 14: 771-782.

Lamm, O. and A. Polson, 1936. The determination of diffusion constants of proteins by a refractometric method. Biochem. J. 30, 528-541.

Landau, L.D. and E.M. Lifshitz, 1958. Statistical Physics, translated by E. Peierls and R.F. Peierls (Pergamon Press Ltd, London and Paris, and Addison-Wesley, Reading, Massachusetts).

Langley, G.R. and M. Axell, 1968. Changes in erythrocyte membrane and autohemolysis during in vitro incubation. Brit. J. Haematol. 14: 593-603.

Lankisch, P.G. and W. Vogt, 1972. Direct hemolytic activity of phospholipase A. Biochim. Biophys. Acta 270: 241-247.

Lauffer, M.A., 1975. Entropy-Driven Processes in Biology. Polymerization of Tobacco Mosaic Virus Protein and Similar Reactions (Springer-Verlag, New York, Heidelberg, Berlin) and Mol. Biol. Biochem. and Biophys. 20.

Lawaczeck, R., M. Kainosho, J.-L. Girardet, and S.I. Chan, 1975. Effects of structural defects in sonicated phospholipid vesicles on fusion and ion permeability. Nature 256: 584-586.

Leblond, P., 1972. The discocyte-echinocyte transformation of the human red cell: deformability characteristics. Nouv. Rev. Fr. Hematol. 12: 815-824.

LeFevre, P.G., K.I. Habich, H.S. Hess, and M.R. Hudson, 1964. Phospholipid-sugar complexes in relation to cell membrane monosaccharide transport. Science 143: 955-957.

Lepke, S. and H. Passow, 1972. Effect of pH at hemolysis on the reconstitution of low cation permeability in human erythrocyte ghosts. Biochim. Biophys. Acta 255: 696-702.

Lessin, L.S., 1972. Membrane ultrastructure of normal, sickled and Heinz-body erythrocytes by freeze-etching. Nouv. Rev. Fr. Hematol. 12: 871-888.

Lessin, L.S., W.N. Jensen, and P. Klug, 1972. Ultrastructure of the normal and hemoglobinopathic red blood cell membrane. Arch. Intern. Med. 129: 306-319.

Levin, O, 1963. Electron microscopic investigations of the subunit of hemoglobin and the myoglobin molecule. J. Mol. Biol. 6: 158-163.

Leyko, W. and Z. Jozwiak, 1970. Effect of ATP on the stability of the hemoglobin molecule, in Int. Symp. Strukt. Funkt. Erythrocyten, 6th, edited by S. Rapoport (Akad-Verlag, Berlin, E. Germany), in Chem. Abs. 77: 57704b.

Lidgard, G.P. and M.N. Jones, 1975. D-glucose permeability of block lipid membranes modified by human erythrocyte membrane functions. J. Membr. Biol. 21: 1-10.

Lichtman, M.A. and R.I. Weed, 1972. Divalent cation content of normal and ATP-depleted erythrocytes and erythrocyte membranes. Nouv. Rev. Fr. Hematol. 12: 799-814.

Lieb, W.R. and W.D. Stein, 1969. Biological membranes behave as non-porous polymeric sheets with respect to the diffusion of non-electrolytes. Nature 224: 240-243.

Lieb, W.R. and W.D. Stein, 1971. The molecular basis of simple diffusion within biological membranes, pp. 1-39 in Current Topics in Membranes and Transport, Vol. 2, edited by F. Brouner and A. Kleinzeller (Academic Press, New York).

Linden, C.D., K.L. Wright, H. M. McConnell, and C.F. Fox, 1973. Lateral phase separations in membrane lipids and the mechanism of sugar transport in *Escherichia coli*. Proc. Nat. Acad. Sci. U.S. 70: 2271-2275.

Ling, G.N., 1962. A Physical Theory of the Living State (Blaesdell Publishing Co., New York and London).

Lionetti, F.J., J. McKay, and H. Gendron, 1968. Relation of shape and metabolism in human erythrocytes. I. Volume, ATP, and monovalent cation interdependence of cells incubated at 37°C. Microvos. Res. 1: 196-209.

Lippert, J.L., L.E. Gorczyca, and G. Meiklejohn, 1975. Laser Raman spectroscopic investigations of phospholipid and protein configurations in hemoglobin-free erythrocyte ghosts. Biochim. Biophys. Acta 382: 51-57.

Litster, J.D., 1975. Stability of lipid bilayers and red blood cell membranes. Phys. Lett. 53A: 193-194.

Livne, A. and A. Raz, 1971. Erythrocyte fragility and potassium efflux as affected by temperature and hemolyzing rate. FEBS Lett. 16: 99-101.

Lossen, O., R. Brennecke, and D. Schubert, 1973. Electrical properties of block membranes from oxidized cholesterol and a strongly bound protein fraction of human erythrocyte membranes. Biochim. Biophys. Acta 330: 132-140.

Lowenstein, L.M., 1960. The effect of albumin on osmotic hemolysis. Exptl. Cell Res. 20: 56-65.

Lucy, J.A., 1975. The fusion of cell membranes , pp. 75-83 in Cell Membranes, edited by G. Weissmann and R. Claiborne (HP Publishing, New York).

Lundstrom, J.E., 1973. A statistical model for diffusion in polymers. Trans. N.Y. Acad. Sci., Series II, 35: 95-111.

Lushbaugh, C.C., N.J. Bassman, and B. Glascock, 1962. Electronic measurement of cellular volumes: 2. Frequency distribution of erythrocyte volumes. Blood 20: 241-248.

Luy, S.E., R. Hirz, R.I. Shrager, and A.M. Gotto, 1972. The influence of lipid on the conformation of human plasma high density apolipoproteins. J. Biol. Chem. 247: 2598-2606.

Macey, R.I. and R.E. Farmer, 1970. Inhibition of water and solute permeability in human red cells. Biochim. Biophys. Acta 211: 104-106.

MacFate, R.P., 1964. Measurement of hemoglobin in blood, pp. 31-39 in Hemoglobin: Its Precursors and Metabolites, edited by F.W. Sunderman and F.W. Sunderman, Jr. (J.B. Lippencott, Philadelphia).

MacGregor, R.D. II and C.A. Tobias, 1972. Molecular sieving of red cell membranes during gradual osmotic hemolysis. J. Membr. Biol. 10: 345-356.

MacRitchie, F. and A.E. Alexander, 1963. Kinetics of adsorption of proteins at interfaces. Part II. The role of pressure barriers in adsorption. J. Colloid Sci. 18: 458-463.

Maddy, A.H. and B.R. Malcolm, 1965. Protein conformations in the plasma membrane. Science 150: 1616-1618.

Mahowald, T.A., E.A. Noltmann, and S.A. Kuby, 1962. Studies on adenosine triphosphate transphosphorylases. I. Amino acid composition of adenosine triphosphate-adenosine 5'-phosphate transphosphorylase (myokinase). J. Biol. Chem. 237: 1138-1145.

Makowski, L., 1976a. A physical basis for red cell membrane elasticity. J. Theor. Biol. 61: 27-45.

Makowski, L., 1976b. A phase transition model for hemolysis. J. Theor. Biol. 61: 47-53.

Malassez, M.L., 1873. Sur la numération des globules sanguins. Thesis, Paris. Quoted in M.L. Malassez Les premières recherches sur la résistance des globules rouges du sang. Mem Soc. Biol. 47: 2-5 (1895).

Marcelja, S., 1974. Chain ordering in liquid crystals. II. Structure of bilayer membranes. Biochim. Biophys. Acta 367: 165-176.

Marchesi, V.T., 1975. The structure and orientation of a membrane protein pp. 45-53 in, Cell Membranes, edited by G. Weissmann and R. Claiborne (HP Publishing, New York).

Marchesi, V.T., E. Steers, T.W. Tillack, and S.L. Marchesi, 1969. Some properties of spectrin, a fibrous protein isolated from red cell membranes. pp. 117-130 in Red Cell Membrane, edited by G.A. Jamieson and T.J. Greenwalt, (Lippencott, Philadelphia and Toronto).

Marinetti, G.V. and R. Love, 1974. Extent of crosslinking of amino phospholipid neighbors in the erythrocyte membrane as influenced by the concentration of difluorodinitrobenzene. Biochem. Biophys. Res. Commun. 61: 30-37.

Marinkovic, D.V. and L.F. Smith, 1970. Fractionation studies of the α and β chains from rat hemoglobin. Bull. Boris Kidric Inst. Nucl. Sci., Biol. 1970, 21(1): 1-6 (English), in Chem. Abs. 75: 94624e.

Markland, F.S. and C.L. Wadkins, 1966. Adenosine triphosphate-adenosine 5'-monophosphate phosphotransferase of bovine liver mitochondria. I. Isolation and chemical properties. J. Biol. Chem. 241: 4124-4135.

Marsden, N.V.B. and G.G. Hall, 1973. Some theoretical considerations on the measurement of the kinetics of hemolysis in individual red cells. Uppsala J. Med. Sci. 78: 12-18.

Marsden, N.V.B. and S.G. Östling, 1959. Accumulation of dextran in human red cells after hemolysis. Nature 184: 723-724.

Marsden, N.V.B., M. Zade-Oppen, and L.P. Johansson, 1957. The effect of dextran on the dry mass distribution in osmotic hemolysis. Exp. Cell Res. 13: 177-181.

Martinek, R.G., 1966. A simple spectrophotometric method for quantitating hemoglobin in serum or plasma. J. Am. Med. Technologists 28: 42-58.

McBride, J.A. and H.S. Jacob, 1968. Cholesterol loading of acanthocytic red cell membranes causing hemolytic anemia in experimental and genetic abetalipoproteinemia. J. Clin. Invest. 47: 67a. Abstract.

McConnell, H.M., K.L. Wright, and B.G. McFarland, 1972. The fraction of the lipid in a biological membrane that is in a fluid state: a spin label assay. Biochem. Biophys. Res. Commun. 47: 273-281.

McFarland, B.G., 1972. Molecular basis for fluidity in membranes. Chem. Phys. Lipids 8: 303-313.

McGregor, M.A. and G.T. Barnes, 1974. The equilibrium penetration of monolayers. J. Colloid Interface Sci. 49: 362-367.

Mel, H.C. and J.P. Yee, 1975. Erythrocyte size and deformability studies by resistive pulse spectroscopy. Blood Cells 1: 391-399.

Meryman, H.T., 1972. The modification of water structure by divalent cations as a mechanism of membrane permeability control. pp. 341-348 in, Passive Permeability of Cell Membranes, edited by F. Kreuzer and J.F.G. Siegers (Plenum Publishing, New York).

Meryman, H.T., 1973. Influence of certain neutral solutes on red cell membrane area and permeability during hypotonic stress. Amer. J. Physiol. 225: 365-371.

Metz, E.N., W.N. Jensen, N. R. Larrimer, and S.P. Balcerzak, 1971. Irreversible changes in the red blood cell membrane during hypotonic swelling. Arch. Internal Med. 127: 273-277.

Misra, D.N. and P. Ganguly, 1968. Negative staining of human hemoglobin molecules with uranyl acetate. Arch. Biochem. Biophys. 124: 349-357.

Mitchell, C.D., W.B. Mitchell, and D.J. Hanahan, 1965. Enzyme and hemoglobin retention in human erythrocyte stroma. Biochim. Biophys. Acta 104: 348-358.

Moore, D.H. and L. Reiner, 1944. Electrophoretic and ultracentrifugal analysis of globin components. J. Biol. Chem. 156: 411-420.

Morris, R. and R.D. Wright, 1954. On the interaction of haemoglobin with sodium and potassium. Aust. J. Exp. Biol. Med. Sci. 32: 669-676.

Morselt, A.F.W. and N.T. Tijmes, 1974. Hemoglobin content and projected area of erythrocytes as an indication of cell age. Blut 29: 277-279.

Murayama, M., 1966. Molecular mechanism of sickling. Science 153: 145-149.

Murphy, J.R., 1962. Erythrocyte metabolism. III. Relationship of energy metabolism and serum factors to the osmotic fragility following incubation. J. Lab. Clin. Med. 60: 86-109.

Nagel, J.F., 1973. Theory of biomembrane phase transitions. J. Chem. Phys. 58: 252-264.

Nakao, M., T. Nakao, and S. Yamazoe, 1960. Adenosine triphosphate and maintenance of shape of human red cells. Nature 187: 945-946.

Nakao, M., T. Nakao, S. Yamazoe, and H. Yoshikawa, 1961. Adenosine triphosphate and shape of erythrocytes. J. Biochem (Tokyo) 49: 487-492.

Nakatani, M., 1958. A chromatographic study of crystalline catalase from bovine liver. Bull. Agr. Chem. Soc. Japan 22: 308-313.

Nathan, D.G. and S.B. Shohet, 1970. Erythrocyte ion transport defects and hemolytic anemia: "Hydrocytosis" and desiccytosis. Seminars Hematol. 7: 381-408.

Nelson, G. J., 1967. Lipid composition of erythrocytes in various mammalian species. Biochim. Biophys. Acta 144(2): 221-232.

Nicolson, G.L., V.T. Marchesi, and S.J. Singer, 1971. The localization of spectrin on the inner surface of human red blood cell membranes by ferritin-conjugated antibodies. J. Cell Biol. 51: 265-272.

Nicolson, G.L. and R.G. Painter, 1973. Anionic sites of human erythrocyte membranes. II. Antispectrin-induced transmembrane aggregation of the binding sites for positively charged colloidal particles. J. Cell Biol. 59: 395-406.

Niemi, M., 1958. Cytophotometry by silver analysis photomicrographs. Description of a new method and its application to the study of corpuscular haemoglobin. Acta Anatom. Suppl. 34: 1-92.

Nienhuis, A.W. and H.F. Bunn, 1974. Hemoglobin switching in sheep and goats: occurrence of hemoglobins A and C in the same red cell. Science 185: 946-948.

Nilsson, O. and G. Ronquist, 1969. Enzyme activities and ultrastructure of a membrane fraction from human erythrocytes. Biochim. Biophys. Acta 183: 1-9.

Nishimura, E.T., S.N. Carson, and T.Y. Kobara, 1964. Isozymes of human and rat liver catalases. Arch. Biochem. Biophys. 108: 452-459.

Nisioka, K., 1969a. Catalase activity in the red cell ghost of hypocatalasemia and normal subject. I. Catalase in the red cell ghost of hypocatalasemic and normal subject. Acta Med. Okayama 23: 413-420, in Chem. Abs. 72: 40964k.

Nisioka, K., 1969b. Catalase activity in the red cell ghost of hypocatalasemia and normal subjects. II. Isolation of catalase in the red cell ghost by electrophoresis. Acta. Med. Okayama 23: 553-558 (English), in Chem. Abs. 73: 33154p.

Noda, L. and S.A. Kuby, 1957a. Adenosine triphosphate-adenosine monophosphate transphosphorylase (myokinase). I. Isolation of the crystalline enzyme from rabbit skeletal muscle. J. Biol. Chem. 226: 541-549.

Noda, L. and S.A. Kuby, 1957b. Adenosine triphosphate-adenosine monophosphate transphosphorylase (myokinase). II. Homogeneity measurements and physicochemical properties. J. Biol. Chem. 226: 551-558.

Northop, J.H. and M.G. Anson, 1929. A method for the determination of diffusion constants and the calculation of the radius and weight of the hemoglobin molecule. J. Gen. Physiol. 12: 543-554.

Ohki, S. and O. Aono, 1970. Phospholipid bilayer-micelle transformation. J. Colloid Interface Sci. 32: 270-281.

Oldfield, E., 1973. Are cell membranes fluid? Science 180: 982-983.

Oldfield, E. and D. Chapman, 1972. Dynamics of lipids in membranes: heterogeneity and the role of cholesterol. FEBS Lett. 23: 285-297.

Op den Kamp, J.A.F., M.Th. Kauerz, and L.L.M. Van Deenen, 1975. Action of pancreatic phospholipase A_2 on phosphatidylcholine bilayers in different physical states. Biochim. Biophys. Acta 406: 169-177.

Palek, J., W.A. Curby, and F.J. Lionetti, 1971. Effects of calcium and adenosine triphosphate on volume of human red cell ghosts. Am. J. Physiol. 220: 19-26.

Palek, J., G. Stewart, and F.J. Lionetti, 1974. The dependence of shape of human erythrocyte ghosts on calcium, magnesium, and adenosine triphosphate. Blood 44: 583-597.

Papahadjopoulos, D., 1968. Surface properties of acitic phospholipids: interaction of monolayers and hydrated crystals with uni- and bi-valent metal ions. Biochim. Biophys. Acta 163: 240-254.

Papahadjopoulos, D., M. Cowden, and H. Kimelberg, 1973. Role of cholesterol in membranes. Effects on phospholipid-protein interactions, membrane permeability and enzymatic activity. Biochim. Biophys. Acta 330: 8-26.

Papahadjopoulos, D., M. Moscarello, E.H. Eylar, and T. Isac, 1975. Effects of proteins on thermotropic phase transitions of phospholipid membranes. Biochim. Biophys. Acta 401: 317-335.

Papahadjopoulos, D. and G. Poste, 1975. Calcium-induced phase separation and fusion in phospholipid membranes. Biophys. J. 15: 945-948.

Parker, J.C., H.G. Welt, 1972. Pathological alterations of cation movements in red blood cells. Arch. Intern. Med. 129: 320-332.

Parpark, A.K. and A.J. Dziemian, 1940. The chemical composition of the red cell membrane. Cold Spring Harbor Symp. Quant. Biol. 8: 17-24.

Parrish, R.G. and R.J. Kurland, 1975. Effect of some general anesthetics on water near lipid bilayer surfaces. Biophys. J. 15: 303a.

Passow, H., 1969. Passive ion permeability of the red blood cell. An assessment of the scope and limitations of the fixed charge concept. Progr. Biophys. Mol. Biol. 19(II): 423-467.

Paysant, M. and J. Polonovski, 1971. Phospholipase A activity from rat erythrocytes. Phospholipase release during hemolysis. C.R. Soc. Biol. 165: 1847-1853 (French).

Pennell, R.B., 1964. Composition of normal human red cells, pp. 29-69 in, The Red Blood Cell, edited by C. Bishop and D.M. Surgenor (Academic Press, New York and London).

Perk, K., 1966. Osmotic hemolysis of camel's erythrocytes. I. A micro-cinematographic study. J. Exptl. Zool. 163: 241-246.

Perk, K. and D. Danon, 1965. Comparative structure analysis of foetal and adult type red cells in newborn and adult cattle. Res. Vet. Sci. 6: 442-446.

Perrin, F., 1936. Mouvement Brownien d'un ellipsoide (II). Rotation libre et dépolarisation des fluorescences. Translatiou et diffusion de molécules ellipsoidales. J. Phys. Radium [7] 7: 1-11.

Perutz, M.F., 1946. Composition and swelling properties of hemoglobin crystals. Trans. Faraday Soc. 42B: 187-195.

Perutz, M.F., 1969. The Croonian Lecture, 1968. The haemoglobin molecule. Proc. Roy. Soc. B. 173: 113-140.

Perutz, M.F. and H. Lehmann, 1968. Molecular pathology of human haemoglobin. Nature 219: 902-909.

Perutz, M.F., M.G. Rossman, A.F. Cullis, H. Muirhead, G. Will, and A.C.T. North, 1960. Structure of haemoglobin. A three-dimensional Fourier synthesis at 5.5Å resolution, obtained by x-ray analysis. Nature 185: 416-422.

Peters, R., J. Peters, K.H. Tews, and W. Bähr, 1974. A microfluorometric study of translational diffusion in erythrocyte membranes. Biochim. Biophys. Acta 367: 282-294.

Pethica, B.A., 1955. The thermodynamics of monolayer penetration at constant area. Trans. Faraday Soc. 51: 1402-1411.

Pfister, H. and H. Pauly, 1972. Chemical potential of potassium chloride and its ion constituents in concentrated protein salt solutions. J. Polym. Sci., Part C, 39: 179-189.

Phillips, M.C., 1972. The physical state of phospholipids and cholesterol in monolayers, bilayers, and membranes. Prog. Surface Memb. Sci. 5: 139-221.

Phillips, M.C., M.T.A. Evans, D.E. Graham, and D. Oldani, 1975. Structure and properties of protein films adsorbed at the air-water interface. Colloid Polym. Sci. 253: 424-427.

Phillips, M.C., M.T.A. Evans, and H. Hauser, 1975. Interaction of proteins with phospholipid monolayers. Adv. Chem. Series 144: 217-230.

Phillips, M.C. and E.G. Finer, 1974. The stoichiometry and dynamics of lecithin-cholesterol clusters in bilayer membranes. Biochim. Biophys. Acta 356: 199-206.

Phillips, M.C., E.G. Finer, and H. Hauser, 1972. Differences between conformations of lecithin and phosphatidyl ethanolamine polar groups and their effects on interactions of phospholipid bilayer membranes. Biochem. Biophys. Acta 290: 397-402.

Phillips, M.C., D.E. Graham, and H. Hauser, 1975. Lateral compressibility and penetration into phospholipid monolayers and bilyaer membranes. Nature 254: 154-156.

Phillips, M.C., H. Hauser, and F. Paltauf, 1972. The inter- and intra-molecular mixing of hydrocarbon chains in lecithin/water systems. Chem. Phys. Lipids 8: 127-133.

Phillips, M.C., V.B. Kamat, and D. Chapman, 1970. The interaction of cholesterol with the sterol free lipids of plasma membranes. Chem. Phys. Lipids 4: 409-417.

Pinder, J.C., D. Bray, and W.B. Gratzer, 1975. Actin polymerization by spectrin. Nature (London) 258: 765-766.

Pinto da Silva, P., 1972. Translational mobility of the membrane intercolated particles of human erythrocyte ghosts: pH dependent, reversible aggregation. J. Cell Biol. 53: 777-787.

Polson, A., 1939. Untersuchungen über die Diffusions konstanten der Proteine. Kolloidzschr. 87: 149-181.

Polson, A. and G.M. Potieter, 1964. Diffusion constants of proteins determined by a multi-unit analytical method. Nature 204: 379.

Ponder, E., 1933. Osmotic behavior of red cells. II. Cold Spring Harbor Symposium Quant. Biol. 1: 178-183.

Ponder, E., 1934. The mammalian red cell and the properties of haemolytic systems. Protoplasma-Monographier 6: 311 pp.

Ponder, E., 1948a. A method for determining the form of the distribution of red cell resistance to simple hemolysis. Blood 3: 556-565.

Ponder, E., 1948b. Hemolysis and Related Phenomena (Grune & Stratton, New York).

Ponder, E., 1955. Red cell structure and its breakdown. Protoplasmatologia, X(2), 123 pp.

Ponder, E. and D. Barreto, 1955. The variation in the corpuscular hemoglobin concentration in the human red cell, as measured by densitometry. J. Gen. Physiol. 39: 23-29.

Porte, D., Jr. and R.J. Havel, 1961. The use of cholesterol-4-C^{14}-labeled lipoproteins as a tracer for plasma cholesterol in the dog. J. Lipid Res. 2: 357-362.

Pressman, B.C., 1973. Properties of ionophores with broad range cation selectivity. Fed. Proc. 32: 1698-1703.

Price, V.E. and R.E. Greenfield, 1954. Liver catalase. II. Catalase functions from normal and tumor-bearing rats. J. Biol. Chem. 209: 363-376.

Princen, H.M. and S.G. Mason, 1965. The permeability of soap films to gases. J. Colloid Sci. 20: 353-375.

Putzeys, P. and H. Reijnaers, 1966. Hemoglobin association and the sigmoid O equilibrium curve. Nature 212: 506- .

Quickenden, T.I. and G.K. Tan, 1974. Random packing in two dimensions and the structure of monolayers. J. Colloid Interface Sci. 48: 382-393.

Quinn, P.J. and R.M.C. Dawson, 1969a. Interactions of cytochrome C and carboxymethylated cytochrome C with monolayers of phosphatidylcholine, phosphatidic acid, and cardiolipin. Biochem. J. 115: 65-75.

Quinn, P.J. and R.M.C. Dawson, 1969b. The interaction of cytochrome C with monolayers of phosphatidylethanolamine. Biochem. J. 113: 791-803.

Ralston, G.B., 1975. Isolation of aggregates of spectrin from bovine erythrocyte membranes. Aust. J. Biol. Sci. 28: 259-266.

Rand, R.P., 1964. Mechanical properties of the red cell membrane. II. Viscoelastic breakdown of the membrane. Biophys. J. 4(4): 303-316.

Rand, R.P., 1967. Some biophysical considerations of the red cell membrane. Fed. Proc. 26: 1780-1784.

Rand, R.P., 1968. The structure of a model membrane in relation to the viscoelastic properties of the red cell membrane. J. Gen. Physiol. 52: 173s-186s.

Rand, R.P., 1971. Structural studies by x-ray diffraction of model lipid-protein membranes of serum albumin-lecithin-cardiolipin. Biochim. Biophys. Acta 241: 823-834.

Rand, R.P. and A.C. Burton, 1963. Area and volume changes in hemolysis of single erythrocytes. J. Cell Comp. Physiol. 61: 245-253.

Rand, R.P. and A.C. Burton, 1964a. Mechanical properties of the red cell membrane. I. Membrane stiffness and intracellular pressure. Biophys. J. 4(2): 115-135.

Rand, R.P. and A.C. Burton, 1964b. The pressure inside red cells and the "metabolic pump." Biophys. J. 4: 491-495.

Rand, R.P. and V. Luzzati, 1968. X-ray diffraction study in water of lipids extracted from human erythrocytes. The position of cholesterol in the lipid lamellae. Biophys. J. 8: 125-137.

Rand, R.P. and S. SenGupta, 1972. Structural studies by x-ray diffraction of model phospholipid-insulin membranes. Biochem. 11: 945-949.

Rauen, H.M. and R. Kuhn, editors, 1964. Biochemisches Taschenbuch (Springer-Verlag, Berlin and New York).

Raz, A. and A. Livne, 1973. Differential effects of lipids on the osmotic fragility of erythrocytes. Biochim. Biophys. Acta 311: 222-229.

Reboud, A.M., M. Buisson, and J.P. Reboud, 1972. Ribosomal subunits from rat liver. 2. Effect of cations on isolated subunits. Eur. J. Biochem. 26: 354-359.

Reed, C.F., 1968. Phospholipid exchange between plasma and erythrocytes in man and the dog. J. Clin. Invest. 47: 749-760.

Reed, C.F. and S.N. Swisher, 1966. Erythrocyte lipid loss in hereditary spherocytosis. J. Clin. Invest. 45: 777-781.

Reichmann, M.E. and J.R. Colvin, 1956. The number of subunits in the molecule of horse hemoglobin. Can. J. Chem. 34: 411-425.

Rentsch, G., 1968. Genesis of Heinz bodies and methemoglobin formation. Biochem. Pharmacol. 17: 423-427.

Reynaers, H., 1966. Molecular properties of hemoglobin. Vehr. Kon. Vlaam. Acad. Wetensch. Belg., Kl. Wetensch. 28(85), 31 pp. (Dutch), in Chem. Abs. 66: 26076s.

Reynolds, J.A., D.B. Gilbert, and C. Tanford, 1974. Empirical correlation between hydrophobic free energy and aqueous cavity surface area. Proc. Nat. Acad. Sci. U.S. 71: 2925-2927.

Rigas, D.A., R.D. Koler, and E.E. Osgood, 1956. Hemoglobin H: clinical, laboratory, and genetic studies of a family with a previously undescribed hemoglobin. J. Lab. Clin. Med. 47: 51-64.

Riggs, A., 1965. Hemoglobin polymerization in mice. Science 147: 621-623.

Riggs, A. and M. Rona, 1969. Oxygen equilibria and aggregation behavior of polymerizing mouse hemoglobins. Biochim. Biophys. Acta. 175: 248-259.

Ronquist, G., 1969. Enzyme activities at the surface of intact human erythrocytes. Acta Physiol. Scand. 76: 312-320.

Rosano, H.L. and V.K. La Mer, 1956. The rate of evaporation of water through monolayers of esters, acids and alcohols. J. Phys. Chem. 60: 348-353.

Rose, B. and W.R. Loewenstein, 1971. Junctional membrane permeability. Depression by substitution of lithium for extracellular sodium, and by long-term lack of calcium and magnesium. Restoration by cell repolarization. J. Membr. Biol. 5: 20-50.

Rossi-Fanelli, A., E. Antonini, and A. Caputo, 1959. Studies on the structure of hemoglobin. II. Properties of reconstituted protohemoglobin and protoporphyrin-globin. Biochim. Biophys. Acta 35: 93-101.

Rothman, J.E., 1973. The molecular basis of mesomorphic phase transitions in phospholipid systems. J. Theor. Biol. 38: 1-16.

Rubinstein, D., P. Ottolenghi, and O.F. Denstedt, 1956. The metabolism of the erythrocyte. XIII. Enzyme activity in the reticulocyte. Can. J. Biochem. 34: 222-235.

Saari, J.T. and J.S. Beck, 1974. Probability density function of the red cell membrane permeability coefficient. Biophys. J. 14: 33-45.

Saari, J.T., A.W.G. Jay, and J.S. Beck, 1972. Effect of cytochalasin B on the osmotic fragility of human erythrocytes. 16th Ann. Meeting Biophys. Soc., February 24-27, 1972, p. 105a.

Saha, A., D.H. Campbell, and W.A. Schroeder, 1964. Immunochemical studies on liver and erythrocyte catalases from cattle, horse, rabbit, and human. Biochim. Biophys. Acta 85: 38-49.

Sakagami, T., O. Minari, and T. Orii, 1965. Behavior of plasma lipoproteins during exchange of phospholipids between plasma and erythrocytes. Biochim. Biophys. Acta 98: 111-116.

Salák, J., 1970. On the conformation of human hemoglobin and globin in aqueous solutions. Chemical modification of the proteins and specifications of the reacted regions. Collect. Czech. Chem. Commun. 35: 3092-3100.

Samejima, T., 1959. Splitting of catalase molecules by alkali treatment. J. Biochem. (Tokyo) 46: 155-159; 1101.

Samejima, T., M. Kamata, and K. Shibata, 1962. Dissociation of bovine liver catalase at low pH. J. Biochem (Japan) 51: 181-187.

Samejima, T. and M. Kita, 1969. Conformational changes of the catalase molecule caused by ligand molecules. Biochim. Biophys. Acta 175: 24-30.

Samejima, T., W.J. McCabe, and J.T. Yang, 1968. Reconstitution of alkaline-denatured catalase. Arch. Biochem. Biophys. 127: 354-360.

Samejima, T. and K. Shibata, 1961. Denaturation of catalase by formamide and urea related to the subunit make-up of the molecule. Arch. Biochem. Biophys. 93: 407-412.

Samejima, T. and J.T. Yang, 1963. Reconstitution of acid-denatured catalase. J. Biol. Chem. 238: 3256-3261.

Sapico, V., G. Litwack, and W.E. Criss, 1972. Purification of rat liver adenylate kinase isozyme II and comparison with isozyme III. Biochim. Biophys. Acta 258(2): 436-445.

Savitz, D., V.W. Sidel, and A.K. Solomon, 1964. Osmotic properties of human red cells. J. Gen. Physiol. 40: 79-94.

Schachman, H.K. and S.J. Edelstein, 1966. Ultracentrifuge studies with absorption optics. IV. Molecular weight determinations at the microgram level. Biochem. 5: 2681-2705.

Schatzmann, H.J., 1973. Dependence on calcium concentration and stoichiometry of the calcium pump in human red cells. J. Physiol. 235: 551-569.

Schedel, I., K. Fischer, and H. Suter, 1974. Demonstration of erythrocytic catalase with indirect immunofluorescence technique. Z. Immunitaetsforsch Exp. Klin. Immuno 146: 396-404 (German), in Bio. Abs. 58: 51474.

Schirmer, I., R.H. Schirmer, G.E. Schultz, and E. Thuma, 1970. Purification, characterization, and crystallization of pork myokinase. FEBS Lett. 10: 333-338.

Schnuchel, G., 1956. Untersuchungen an Rinderleberkatalase. II. Mitteil: die Aminosauren des Proteins. Z. Physiol. Chem., Hoppe-Seyleir 303: 91-93.

Schroeder, W.A., A. Saha, W.D. Fenninger, and J.T. Cua, 1962. Preliminary chemical investigation of the structure of beef liver and horse liver catalase. Biochim. Biophys. Acta 68: 611-613.

Schroeder, W.A., J.R. Shelton, J.B. Shelton, B. Robberson, and G. Apell, 1969. The amino acid sequence of bovine liver catalase: a preliminary report. Arch. Biochem. Biophys. 131: 653-655.

Schroeter, W. and H. Bodemann, 1968. Effect of monoiodoacetic acid plus ferricyanide on the 2,3-diphosphoglycerate content and cation permeability of red cells. Folia Haematol. 90: 204-209 (German).

Schütte, H.R. and H. Nürnberger, 1959. Untersuchungen über Rinderleber-katalase, I. Zur Kenntnis der Sulfhydryl-und Disulfidgrupden des proteins. Z. Physiol. Chem., Hoppe-Seyler's 315: 13-19.

Scott, H.L., 1974. A model for phase transitions in lipid bilayers and biological membranes. J. Theor. Biol. 46: 241-253.

Scott, H.L., 1975. A theoretical model for lipid monolayer phase transitions. Biochim. Biophys. Acta 406: 329-346.

Sears, D.A., 1973. Prehemolytic changes in membrane protein of incubated human erythrocytes. J. Lab. Clin. Med. 82: 719-726.

Seeman, P., 1967. Transient holes in the erythrocyte membrane during hypotonic hemolysis and stable holes in the membrane after lysis by saponin and lysolecithin. J. Cell Biol. 32: 55-70.

Seeman, P., 1973. Macromolecules may inhibit diffusion of hemoglobin from lysing erythrocytes by exclusion of solvent. Can. J. Physiol. Pharmacol. 51: 226-229.

Seeman, P., 1974. Ultrastructure of membrane lesions in immune lysis, osmotic lysis, and drug-induced lysis. Fed. Proc. 33: 2116-2124.

Seeman, P., 1975. The actions of nervous system drugs on cell membranes. pp. 239-247 in, Cell Membranes, edited by G. Weissmann and R. Claiborne (HP Publishing, New York).

Seeman, P., M. Chau-Wong, and S. Moyyen, 1973. Membrane expansion by vinblastine and strychnine. Nature, New Biol. 241, 22.

Seeman, P., D. Cheng, and G.H. Iles, 1973. Structure of membrane holes in osmotic and saponin hemolysis. J. Cell Biol. 56: 519-527.

Seeman, P. and W.O. Kwant, 1969. Membrane expansion of the erythrocyte by both the neutral and ionized forms of chlorpromozine. Biochim. Biophys. Acta 183: 512-519.

Seeman, P., W.O. Kwant, T. Sauks, and W. Argent, 1969. Membrane expansion of intact erythrocytes by anesthetics. Biochim. Biophys. Acta 183: 490-498.

Seeman, P., T. Sauks, W. Argent, and W.O. Kwant, 1969. The effect of membrane-strain rate and of temperature on erythrocyte fragility and critical hemolytic volume. Biochim. Biophys. Acta 183: 476-489.

Segrest, J.P. and R.J. Feldmann, 1974. Membrane proteins: amino acid sequence and membrane penetration. J. Mol. Biol. 87: 853-858.

Segrest, J.P., T. Gulik-Krzywicki, and C. Sardet, 1974. Association of the membrane penetrating polypeptide segment of the human erythrocyte MN glycoprotein with phospholipid bilayers. I. Formation of freeze-etch intramembranous particles. Proc. Nat. Acad. Sci. U.S. 71: 3294-3298.

Segrest, J.P., R.L. Jackson, J.D. Morrisett, and A.M. Gotto, Jr., 1974. A molecular theory of lipid-protein interactions in the plasma lipoproteins. FEBS Lett. 38: 247-253.

Shapiro, S.I., S.A. Landaw, H.S. Winchell, and M.C. Williams, 1969. Independence of mechanical fragility and red blood cell age in the rat. Proc. Soc. Exptl. Biol. Med. 131: 1206-1209.

Shaw, A.R.E. and N. MacLean, 1971. A Reevaluation of the haemoglobin electrophoretogram of the Wistar rat. Comp. Biochem. Physiol. B 40: 155-163.

Shechter, E., T. Gulik-Krzywicki, R. Azerad, and C. Gros, 1971. Correlations between structure and spectroscopic properties in membrane model systems. Fluorescence of dansylated protein and dansylated lipid in protein-lipid-water phases. Biochim. Biophys. Acta 241: 431-442.

Sheetz, M.P. and S.I. Chan, 1972. Proton magnetic resonance studies of whole human erythrocyte membranes. Biochem. 11: 548-555.

Shepard, M.K., D.J. Weatherall, and C.L. Conley, 1962. Semi-quantitative estimation of the distribution of fetal hemoglobin in red cell populations. Bull. Johns Hopkins Hosp. 110: 293-310.

Shibata, Y., T. Higashi, H. Hirai, and H.B. Hamilton, 1967. Immunochemical studies on catalase. II. An anticatalase reacting component in normal, hypocatalasic, and acatalasic human erythrocytes. Arch. Biochem. Biophys. 118(1): 200-209.

Shipley, G.G., 1973. Recent x-ray diffraction studies of biological membranes and membrane components. pp. 1-89 in, Biological Membranes, Vol. 2, edited by D. Chapman and D.H.F. Wallach (Academic Press, New York and London).

Shohet, S.B. and J.E. Haley, 1972. Red cell membrane shape and stability: relation to cell lipid renewal pathways and cell ATP. Nouv. Rev. Fr. Hematol. 12: 761-770.

Shpitsberg, V.L., 1965. Isolation and investigation of some properties of catalase from human erythrocytes. Biokhimiya 30: 801-804 (Russian).

Shpitsberg, V.L., 1966. Dissociation and reassociation of catalase of human erythrocytes. Biofizika 11: 766-772 (Russian), also Biophys. 11: 881-889.

Sieberth, H.G., 1971. Affect of trapped plasma on the determination of intraerythrocyte electrolyte values. Med. Welt 4: 134-140 (German), in Chem. Abs. 74: 72739y.

Sillén, L.G. and A.E. Martell, 1964. Stability Constants of Metal-Ion Complexes. (The Chemical Society, London, Special Publication No. 17).

Simmons, N.L. and R.J. Naftalin, 1976. Membrane and intracellular modes of sugar-dependent increments in red cell stability. Biochim. Biophys. Acta 419: 493-511.

Singer, S.J., 1971. The molecular organization of biological membranes, pp. 145-222 in, Structure and Function of Biological Membranes, edited by L.I. Rothfield (Academic Press, New York and London).

Singer, S.J., 1974. The molecular organization of membranes. Ann. Rev. Biochem. 43: 805-833.

Singer, S.J. and G.L. Nicolson, 1972. The fluid mosaic model of the structure of cell membranes. Science 175: 720-731.

Sober, H.A., editor, 1968. Handbook of Biochemistry, 2nd Edition. (The Chemical Rubber Co., Cleveland, Ohio).

Spector, W.S., editor, 1956. Handbook of Biological Data (W.B. Saunders, Philadelphia and London).

Srivastava, S.K. and E. Beutler, 1974. Formation and cleavage of mixed disulfide of hemoglobin-glutathione in intact erythrocytes. Haematologia 8: 121-125.

Stamatoff, J.B., S. Krimm, and N.R. Harvie, 1975. X-ray diffraction studies of the human erythrocyte membrane. Prog. Clin. Biol. Res. 1: 507-514.

Stansell, M.J. and H.F. Deutsch, 1965. Preparation of crystalline erythrocuprein catalase from human erythrocytes. J. Biol. Chem. 240(11): 4299-4305.

Starodub, N.F. and I.M. Shur'yan, 1973. Problem of hemoglobin dissociation under the effect of p-chloromercuribenzoate. Dopov. Akad. Nauk. Ukr. RSR., Ser. B. 35(5): 454-456 (Ukraine), in Chem. Abs. 80: 23934y.

Staros, J.V., B.E. Haley, and F.M. Richards, 1974. Human erythrocytes and resealed ghosts: a comparison of membrane topology. J. Biol. Chem. 249: 5004-5007.

Steck, T.L., 1972. Cross-linking the major proteins of the isolated erythrocyte membrane. J. Mol. Biol. 66(2): 295-305.

Steers, E. Jr., and V.T. Marchesi, 1969. Protein component of guinea pig erythrocyte membranes. J. Gen. Physiol. 54: 65s-71s.

Stein, S., 1971. Heterogeneity of rat hemoglobin, Thesis, the University of New York, 62 pp. Univ. Microfilms 72-1011 (Diss. Abs. Int. B 32: 3177).

Stein, S., M.G. Cherian, and A. Mazur, 1971. Preparation and properties of six rat hemoglobins. Nonuniform biosynthesis in marrow erythroid cells. J. Biol. Chem. 246: 5287-5293.

Stein, W.D., 1967. The Movement of Molecules Across Cell Membranes. (Academic Press, New York and London).

Steinhardt, J., 1938. Properties of hemoglobin and pepsin in solutions of urea and other amides. J. Biol. Chem. 123: 543-575.

Sterling, W.R., R.E. Greenfield, and V.E. Price, 1958. Erythrocytes of tumor-bearing animals. Fed. Proc. 17: 316.

Suess, J., D. Limentani, W. Dameshek, and M.J. Dolloff, 1948. A quantitative method for the determination and charting of the erythrocyte hypotonic fragility. Blood 3: 1290-1303.

Sumner, J.B., A.L. Dounce, and V.L. Frampton, 1940. Catalase. III. J. Biol. Chem. 136: 343-356.

Sumer, J.B. and N. Gralén, 1938. The molecular weight of crystalline catalase. J. Biol. Chem. 125: 33-36.

Sund, H., K. Weber, and E. Mölbert, 1967. Dissoziation der Rinderleber-Katalase in ihre Untereinheiten. Eur. J. Biochem. 1(4): 400-410 (German).

Svedberg, T. and R. Fåhraeus, 1926. A new method for the determination of the molecular weight of the proteins. J. Am. Chem. Soc. 48: 430-438.

Svedberg, T. and J.B. Nichols, 1927. The application of the oil turbine type of ultracentrifuge to the study of the stability region of carbon monoxide-hemoglobin. J. Am. Chem. Soc. 49: 2920-2934.

Svedberg, T. and K.O. Pedersen, 1940. The Ultracentrifuge (Clarendon Press, Oxford).

Sweet, C. and J.E. Zull, 1969. Activation of glucose diffusion from egg lecithin liquid crystals by serum albumin. Biochim. Biophys. Acta 173: 94-103.

Sweet, C. and J.E. Zull, 1970. Interaction of the erythrocyte-membrane protein, spectrin, with model membrane systems. Biochem. Biophys. Res. Commun. 41: 135-141.

Tanaka, K. and S. Ohnishi, 1976. Heterogeneity in the fluidity of intact erythrocyte membrane and its homogenization upon hemolysis. Biochim. Biophys. Acta 426: 218-231.

Tanford, C., 1968. Protein denaturation. Adv. Protein Chem. 23: 121-282.

Tanford, C., 1970. Protein denaturation. Part C. Theoretical models for the mechanism of denaturation. Adv. Protein Chem. 24: 1-95.

Tanford, C., 1972. Hydrophobic free energy, micelle formation, and the association of proteins with amphiphiles. J. Mol. Biol. 67: 59-74.

Tanford, C., 1973. The Hydrophobic Effect: Formation of Micelles and Biological Membranes. (John Wiley & Sons, New York), 200 pp.

Tanford, C., 1974a. Thermodynamics of micelle formation: prediction of micelle size and size distribution. Proc. Nat. Acad. Sci. U.S. 71: 1811-1815.

Tanford, C., 1974b. Theory of micelle formation in aqueous solutions. J. Phys. Chem. 78: 2469-2479.

Tarlov, A.R. and E. Mülder, 1967. Phospholipid metabolism in rat erythrocytes: quantitative studies of lecithin biosynthesis. Blood 30: 853- . Abstract.

Taupin, C., M. Dvolaitzky, and C. Sauterey, 1975. Osmotic pressure-induced pores in phospholipid vesicles. Biochem. 14: 4771-4775.

Taylor, J.F. and B. Van Osdol, 1964. Quoted in A. Rossi-Fanelli, E. Antonini, and A. Caputo, Hemoglobin and myoglobin. Adv. Protein Chem. 19: 121.

Taylor, N.F. and G.L. Gagneja, 1975. Model for the mode of action of cytochalasin B inhibition of D-glucose transport in the human erythrocyte. Can. J. Biochem. 53: 1078-1084.

Teipel, J.W. and R.L. Hill, 1971. Subunit interactions of fumarase. J. Biol. Chem. 246: 4859-4865.

Teitel, P., 1969. A heamorheological view on molecular interactions between red blood cell constituents in the pathogenesis of constitutional haemolytic anaemias. Internat. Soc. Haemorheology, 2nd Int. Conf., Heidelberg, Germany, 1969. Abstract, p. 30.

Theodore, J. and E.D. Robin, 1965. The holiness of ghosts. Clin. Res. 13: 283. Abstract.

Thomas, J.O. and S.J. Edelstein, 1972. Dissociation of unliganded hemoglobin. J. Biol. Chem. 247: 7870-7874.

Thompson, T.E., C. Huang, and B.J. Litman, 1974. Bilayers and biomembranes: compositional asymmetries induced by surface curvature, pp. 1-16 in, The Cell Surface in Development, edited by A.A. Moscona (John Wiley & Sons, New York).

Thuma, E., R.H. Schirmer, and I. Schirmer, 1972. Preparation and characterization of a crystalline human ATP: AMP phosphotransferase. Biochim. Biophys. Acta 268: 81-91.

Tillack, T.W., S.L. Marchesi, V.T. Marchesi, and E. Steers, Jr., 1970. A comparative study of spectrin: a protein isolated from red blood cell membranes. Biochim. Biophys. Acta 200: 125-131.

Tilney, L.G. and P. Detmers, 1975. Actin in erythrocyte ghosts and its association with spectrin. Evidence for a nonfilamentous form of these two molecules in situ. J. Cell Biol. 66: 508-520.

Tiselius, A. and D. Gross, 1934. Messungen der Diffusion von Eiweisskorpern. Kolloidzschr. 66: 11-20.

Tolberg, A.B. and R.I. Macey, 1972. The release of membrane-bound calcium by radiation and sulfhydryl reagents. J. Cell Physiol. 79: 43-51.

Tosteson, D.C., 1955. Effects of sickling on ion transport. II. The effect of sickling on sodium and cesium transport. J. Gen. Physiol. 39: 55-67.

Tosteson, D.C., E. Carlsen, and E.T. Dunham, 1955. The effects of sickling on ion transport. I. Effect of sickling on potassium transport. J. Gen. Physiol. 39: 31-53.

Toyoshima, Y. and T.E. Thompson, 1975. Chloride flux in bilayer membranes. Chloride permeability in aqueous dispersions of single-walled bilayer vesicles. Biochem. 14: 1525-1531.

Träuble, H., 1971. The movement of molecules across lipid membranes: a molecular theory. J. Membr. Biol. 4: 193-208.

Travnicek, T., J. Borova, and K. Sule, 1971. Subunit composition of polymorphic rat hemoglobins. Physiol. Bohemoslov., 20: 27-31.

Travnicek, T., Z. Vodrazka, J. Borova, J. Cejka, J. Salak, and K. Sule, 1967. The structural basis of polymorphism of rat hemoglobin. Physiol. Bohemoslov. 16: 543-547.

Trayer, H.R., Y. Nozaki, J.A. Reynolds, and C. Tanford, 1971. Polypeptide chains from human red blood cell membranes. J. Biol. Chem. 246: 4485-4488.

Triplett, R.B., J.M. Wingate, and K.L. Carraway, 1972. Calcium effects on erythrocyte membrane proteins. Biochem. Biophys. Res. Commun. 49: 1014-1020.

Turner, S.R. M. Litt, and W.S. Lynn, 1975. Permeation of water vapor through lipid monolayers. J. Colloid Interface Sci. 50: 181-193.

Urry, D.W., 1972. Conformation of protein in biological membranes and a model transmembrane channel. Ann. N.Y. Acad. Sci. 195: 108-125.

Usami, S., S. Chien, and M.I. Gregersen, 1969. Viscometric behavior of young and aged erythrocytes. pp. 266-270 in, Int. Soc. Hemorheology, 2nd Int. Conf., Heidelberg, Germany.

Valentine, R.C., 1960. The shapes of protein molecules. Proc. European Regional Conf. Electron Microscopy 2: 708-711. Delft, The Netherlands.

Valet, G., H. Metzger, V. Kachel, and G. Ruhenstroth-Bauer, 1972. Demonstration of different erythrocyte populations in the rat. Blut 24: 42-53.

van Deenen, L.L.M. and J. de Gier, 1964. Chemical composition and metabolism of lipids in red cells of various animal species, pp. 243-307 in The Red Blood Cell, edited by C. Bishop and D.M. Surgenor (Academic Press, New York).

van Deenen, L.L.M., R.A. Demel, W.S.M. Geurts van Kessel, H.H. Kamp, B. Roelofsen, A.J. Verkleij, K.W.A. Wirtz, and R.F.A. Zwaal, 1976. Phospholipases and monolayers as tools in studies on membrane structure, pp. 21-38 in, Structural Basis of Membrane Function, edited by Y. Hatefi and L. Djavadi-Ohaniance (Academic Press, New York, San Francisco and London).

van Deenen, L.L.M., U.M.T. Houtsmuller, G.H. de Haas, and E. Mulder, 1962. Monomolecular layers of synthetic phosphatides. J. Pharm. Pharmocol. 14: 429-444.

Vanderkooi, G. and R.A. Capaldi, 1972. Discussion paper: a comparative study of the amino acid compositions of membrane proteins and other proteins. Ann. N.Y. Acad. Sci. 195: 135-138.

van Gastel, C., D. van den Berg, J. de Grier, and L.L.M. van Deenen, 1965. Some lipid characteristics of normal red blood cells of different age. Brit. J. Haemat. 11: 193-199.

Verdery, R.B. III and A.V. Nichols, 1975. Arrangement of lipid and proteins in human serum high density lipoproteins: a proposed model. Chem. Phys. Lipids 14: 123-134.

Verkleij, A.J. and P.H.J.Th. Ververgaert, 1975. The architecture of biological and artificial membranes as visualized by freeze etching. Annul. Rev. Physical Chem. 26: 1011-1022.

Verkleij, A.J., R.F.A. Zwaal, B. Roelofsen, P. Comfurius, D. Kastelijn, and L.L. van Deenen, 1973. The asymmetric distribution of phospholipids in the human red cell membrane: a combined study using phospholipases and freeze-etch electron microscopy. Biochim. Biophys. Acta 323: 178-193.

von Hippel, P.H. and T. Schleich, 1969. The effects of neutral salts on the structure and conformational stability of macromolecules in solution, pp. 417-574 in, Structure and Stability of Biological Macromolecules, edited by S.N. Timasheff and G.D. Fasman (Marcel Dekker, Inc., New York), 694 pp. (Biological Membranes, Vol. 2).

Wada, A., 1976. The α-helix as an electric macro-dipole. Adv. Biophys. 9: 1-63.

Wallach, D.F.H. and A.S. Gordon, 1968. Lipid-protein interactions in cellular membranes, pp. 87-98 in, Regulatory Functions of Biological Membranes II, edited by J. Järnefelt (Elsevier, Amsterdam).

Walter, H. and E.J. Krob, 1976. Hydrophobic affinity partition in aqueous two-phase systems containing poly(ethylene glycol)-palmitate of right-side-out and inside-out vesicles from human erythrocyte membranes. FEBS Lett. 61: 290-293.

Wang, K. and F.M. Richards, 1974. Approach to nearest neighbor analysis of membrane proteins. Application to human erythrocyte membrane of a method employing cleanable crosslinkages. J. Biol. Chem. 249: 8005-8018.

Wang, K. and F.M. Richards, 1975. Reaction of dimethyl-3,3'-dithiobispropionimidate with intact human erythrocytes. Cross-linking of membrane proteins and hemoglobin. J. Biol. Chem. 250: 6622-6626.

Ward, A.F.H. and L. Tordai, 1952. Time dependence of boundary tensions of solutions. IV. Kinetics of adsorption at liquid-liquid interface. Rec. Trav. Chim. 71: 572-584.

Wasemiller, G., A. Abrams, and S. Bakerman, 1968. Fluorescence studies on components of human erythrocyte membrane. Biochem. Biophys. Res. Commun. 30: 178-184.

Weast, R.C., editor in chief, 1965. Handbook of Chemistry and Physics, 46th Edition (The Chemical Rubber Co., Cleveland, Ohio).

Weber, K. and H. Sund, 1965. Zur Quartärstraktur ker Katalase aus Rinderleber. Angew. Chem. 77: 621.

Weber, R.E. and C. Tanford, 1959. The configuration of ribonuclease at low pH in 2-chloroethanol and in 2-chloroethanol-water mixtures. J. Am. Chem. Soc. 81: 3255-3260.

Weed, R.I. and M. Bessis, 1974. Mesure de l'adénosine triphosphate (ATP) contenu dans une cellule isolée. C.R. Acad. Sci. (Paris) D278: 545-547.

Weed, R.I. and A.J. Bowdler, 1966. Metabolic dependence of the critical hemolytic volume of human erythrocytes: relationship to osmotic fragility and autohemolysis in hereditary spherocytosis and normal red cells. J. Clin. Invest. 45: 1137-1149.

Weed, R.I. and A.J. Bowdler, 1967. The influence of hemoglobin concentration on the distribution pattern of the volumes of human erythrocytes. Blood 29: 297-312.

Weed, R.I., P.L. La Celle, and E.W. Merrill, 1969. Metabolic dependence of red cell deformability. J. Clin. Invest. 48: 795-809.

Weed, R.I. and C.F. Reed, 1964. The structural role of hemoglobin in the erythrocyte membrane. IX Congress Internat. Soc. Hematology 1: 3-8.

Weidekamm, E. and D. Brdiczka, 1975. Extraction and localization of a (calcium-magnesium ion)-stimulated ATPase in human erythrocyte spectrin. Biochim. Biophys. Acta 401: 51-58.

Werner, E. and H. Heider, 1963. Katalseaktivitätsbestimmung im Blut. Z. Klin. Chem. 1: 115-117.

Wessels, J.M.C. and J.H. Veerkamp, 1973. Aspects of the osmotic lysis of erythrocytes. II. Differences in osmotic behavior of erythrocytes after treatment with electrolyte and nonelectrolyte solutions. Biochim. Biophys. Acta 291: 178-189.

Westerman, M.P., L.E. Pierce, and W.N. Jensen, 1963. Erythrocyte lipids: a comparison of normal young and normal old populations. J. Lab. Clin. Med. 62: 394-400.

Whitaker, T.R., G.S. Sartiano, L.J. Hamelly, Jr., W.L. Scott, and R.H. Glew, 1974. Hypotonic exchange loading of human erythrocytes with ^{59}Fe-labeled rabbit hemoglobin. J. Lab. Clin. Med. 84: 879-888.

White, R.A. and T.H. Ji, 1973. The characterization of a high molecular weight protein from red blood cell membranes. 17th Ann. Meeting Biophysical Soc., Columbus, Ohio, February 27-March 3, 1973. p.256a.

White, S.L., 1972. Differential effects of 2,3-diphosphoglyceric acid upon human hemoglobin aggregation. Thesis, Temple University, Philadelphia, Pennsylvania. 285 pp. University microfilms 72-17723. (Dissert. Abs. Int. B, 32: 7214).

Wilkins, M.H.F., A.E. Blaurock, and D.M. Engelman, 1971. Bilayer structure in membranes. Nature New Biol. 230: 72-76.

Williams, L.A. and B. Zak, 1957. Standardization of hemoglobin. Amer. J. Clin. Path. 28: 195-199.

Williams, T.F., C.C. Fordham, W. Hollander, and L.G. Welt, 1959. A study of the osmotic behavior of the human erythrocyte. J. Clin. Invest. 38: 1587-1598.

Wilson, L. and J. Bryan, 1974. Biochemical and pharmacological properties of microtubules. Adv. Cell Molec. Biol. 3: 22-72.

Wintrobe, M.M., 1967. Clinical Hematology (Lea and Febiger, Philadelphia).

Wong, W.M. and P.H. Geil, 1975. Ultrastructural deformation studies on biological membranes. J. Supramol. Struct. 3: 401-414.

Woodward, C.B. and R.F.A. Zwaal, 1972. The lytic behavior of pure phospholipases A_2 and C towards osmotically swollen erythrocytes and resealed ghosts. Biochim. Biophys. Acta 274: 272-278.

Yakulis, V.J. and P. Heller, 1964. An elution test for the visualization of hemoglobin S in blood smears. Blood 24: 198-201.

Yu, J., D.A. Fischman, and T.L. Steck, 1973. Selective solubilization of proteins and phospholipids from red blood cell membranes by nonionic detergents. J. Supramol. Struct. 1: 233-248.

Yu, J. and T.L. Steck, 1975. Associations of band 3, the predominant polypeptide of human erythrocyte membrane. J. Biol. Chem. 250: 9176-9184.

Zade-Oppen, A.M.M and T.C. Laurent, 1963. On a possible mode of action of polymers on hypotonic hemolysis. Acta Physiol. Scand. 59, Suppl. 213: 168. Abstract.

Zahler, P., 1972. Lipid binding of membrane proteins. Biomembrn. 3: 193-195.

Zala, C.A. and M.N. Jones, 1974. Detection of the enthalpy of binding of D-glucose of human red blood cell membranes by microcalorimetry. FEBS Lett. 48: 196-199.

Zimmer, G., H. Schirmer, and P. Bastian, 1975. Lipid-protein interactions at the erythrocyte membrane. Different influence of glucose and sorbose membrane lipid transition. Biochim. Biophys. Acta 401: 244-255.

Zwaal, R.F.A., B. Roelofsen, P. Comfurius, and L.L.M. van Deenen, 1971. Complete purification and some properties of phospholipase C from *Bacillus cereus*. Biochim. Biophys. Acta 233: 474-479.